Investigating chromatin remodelling by the Swi-Snf and Tup1-Cyc8 complexes

Investigating chromatin remodelling by the Swi-Snf and Tup1-Cyc8 complexes

A dissertation presented for the degree of Doctor of Philosophy,
in Faculty of Science, University of Dublin, Trinity college.

February 2020 by

Mohamed Alhussain

Department of Microbiology

The Moyne Institute of Preventive Medicine

Trinity College

University of Dublin

Declaration

I, Mohamed Alhussain, certify that the experimentation recorded herein represents my own work, unless otherwise stated in the text and has not been previously presented for a higher degree at this or any other University. This thesis may be lent at the discretion of the Librarian.

……

Mohamed Alhussain

Summary

Swi-Snf is an ATP-dependent chromatin remodelling complex which generally acts as a co-activator of gene transcription via its removal of promoter nucleosomes. Conversely, Tup1-Cyc8 (Ssn6) is a co-repressor complex which acts to repress transcription by positioning nucleosomes at gene promoters. The antagonistic activity of these two complexes has been investigated at only a handful of genes, including the *FLO1* and *SUC2* genes. We have identified all of the genes in *Saccharomyces cerevisiae* which are subject to co-regulation by these two complexes and have mapped the Snf2 and Tup1 proteins across the genome to identify genes directly under the control of Swi-Snf and Tup1-Cyc8. The impact upon chromatin structure of target genes by Tup1-Cyc8 and Swi-Snf has also been shown. The co-regulated genes are enriched for stress-response genes, and 30% of these genes reside in subtelomeric regions. Furthermore, the co-regulated subtelomeric genes are the most robustly regulated genes under the control of these two complexes. The data has revealed two potential models for the chromatin remodelling activities by Swi-Snf and Tup1-Cyc8 at co-regulated genes. In one model, Swi-Snf is recruited to Tup1-Cyc8 repressed genes in the absence of the co-repressor to activate transcription. In the second model, Snf2 and Tup1 both occupy the repressed gene, whilst gene activation correlates with an enrichment of Snf2 at target genes in the absence of Tup1. Thus, this study has identified (i) which genes are under control of the Swi-Snf activator and the Tup1-Cyc8 co-repressor, (ii) where Snf2 and Tup1 are located across the genome, and (iii) how these complexes remodel the chromatin at target genes.

Acknowledgements

In honour of The King Salman Bin Abdulaziz Al Saud and The Crown Prince Mohammad Bin Salman Al Saud

Foremost, words just cannot express my gratitude and appreciation for my supervisor Dr. Alastair Fleming for his advice and support over the past four years. I would like to thank my past and recent lab members Dr. Michael Church, Dr. Conor Young and Brenda Lee for their great company. A huge thanks for Dr. Karsten Hokamp (School of Genetics, Trinity college Dublin) and Dr. Nicholas A. Kent (School of Bioscience, Cardiff University) for their excellent cooperation and help throughout this work.

Special thanks for Professor Khalid Alfarhan (Chemistry Department, King Saud University, Raiyah, KSA) for his frequent amazing help and advice. A great thanks to Professor Abdullah M. Aldhelaan (Saudi Cultural Attache in Ireland) and the academic advisor Mourad Jemli (Saudi Cultural Bureau, Ireland). I would like here to thank my master supervisor Professor Mohamed Hani Mubasher (Since College, Cairo University, Egypt).

Thanks to the current and past members of the Moyne Institute, especially Amy, Aisling, Michelle, Daniela, Elaine, Dara, Laura, Chandie, Mark, Aalap, German, Eoin, Marty, Thaina, Chanelle, Mary, Isa, Roberto, Stefani, Niamh, Leanne, Orla and Joanna. Special thanks to Michael and Marina for the best company, encouragement and the great scientific and non-scientific chat. Huge thanks to my committee Dr. Ursula Bond, Dr. Sinead Corr and Dr. Ciaran Finn for their great suggestions. Thanks to the Moyne departmental office and technical staff Jayne and Caroline, Stephen and Ronan.
My sincere thanks to my friends in Saudi Arabia Aziz Alremethy, Dhafer Alahmari, Abdullah Alharbi and Salah Alharbi whom offer to me the help and smiles.

My family, My Father/ Mubarak Alhussain and My Mother/ Esha Alyosef, this was your harvest and you planted it, there is no way words can express my gratitude. Thanks also to my brother Eng. Major/ Marwan Mubarak and my sisters Enas and Dr. Hanan Alhussain. Thanks to my sisters' husband Bader Almoutari and my uncle Khalid Alyosef. My deepest thanks to my wife Hadel Aljaeed.

To my daughter and my son Sarah and Khalid Alhussain

Table of Contents

List of figures

List of Table

Appendix

Appendix I

Table S1	RNA-Seq Fold change =2, FDR=0.01 and Location.
Table S2	List of genes up-regulated in *cyc8*.
Table S3	List of genes down-regulated in *cyc8*.
Table S4	List of genes up-regulated in *cyc8* gene ontology.
Table S5	List of genes down-regulated in *cyc8* gene ontology.
Table S6	List of genes down-regulated in *snf2*.
Table S7	List of genes up-regulated in *snf2*.
Table S8	List of genes down-regulated in *snf2* gene ontology.
Table S9	List of genes up-regulated in *snf2* gene ontology.
Table S10	List of genes down-regulated in *snf2K798A*.
Table S11	List of genes up-regulated in *snf2K798A*.
Table S12	Tup1-Cyc8 and Swi-Snf co-regulated genes.
Table S13	Tup1-Cyc8 and Swi-Snf co-regulated gene ontology
Table S14	Tup1-Cyc8 and Swi-Snf co-regulated genes in *snf2K798A* mutant

Appendix II

Table S1	Snf2 occupancy.
Table S2	Tup1 occupancy.
Table S3	The genes up-regulated in *cyc8* and occupied by Tup1.
Table S4	Snf2 occupancy in absence of Tup1 (Tup1-AA).

Chapter 1

Introduction

1.1 Overview

Investigation of gene regulation in micro-organisms has contributed greatly to our understanding of the mechanisms of eukaryotic gene expression. *Saccharomyces cerevisiae*, commonly known as baker's yeast, has been widely used for genetic research since the mid-twentieth century. The experimental value of this single-celled eukaryote lies in its simple life cycle and short generation time (Johnston, 1987; Mell & Burgess, 2001).

Eukaryotic DNA is usually not accessible for the transcriptional machinery because DNA is compressed into a structure called chromatin. Chromatin is a nucleoprotein complex that forms the structure of chromosomes. The fundamental repeating unit of chromatin is the nucleosome which is composed of two each of the histone proteins, H2A, H2B, H3 and H4, around which is wrapped 146 bp of DNA (Andrews & Luger, 2011).

Chromatin is generally repressive to transcription of genes. However, this repressive structure can be altered by ATP-dependent chromatin remodelling complexes, the first example of which was the Swi-Snf complex which was discovered in *Saccharomyces cerevisiae*. Subsequent work showed that the SWItch/Sucrose Non-Fermentable (Swi-Snf) complex was evolutionary conserved from yeasts to human cells (Wang *et al*. 1996). This complex can slide, disassemble or even evict nucleosomes in an ATP-dependent manner to promote gene transcription. The Swi-Snf complex consists of 12 subunits, each with a specific role. Importantly, abnormalities in this complex are estimated to be the cause of 20% of human cancers (Roberts & Orkin, 2004).

Conversely, the Tup1-Cyc8 (Ssn6) complex was the first global repressor of transcription that was characterized in yeast (Keleher *et al*. 1992). The Tup1-Cyc8 complex represses numerous genes in *S. cerevisiae,* including the stress response genes, carbohydrate utilization genes and cell wall proteins, such as those of the *FLO* gene family that are involved in the cellular aggregation or flocculation phenotype.

The two best characterised genes whose expression is regulated by the antagonistic mechanism of the repressor, Tup1-Cyc8, and the activator, Swi-Snf, are the *FLO1* gene, encoding a product which is responsible for cell to cell adhesion and the invertase-encoding *SUC2* gene that is involved in glucose repression (Fleming and Pennings 2001; Fleming and Pennings 2007). However, the total number of genes subject to the antagonistic regulation of transcription by Swi-Snf and Tup1-Cyc8 is not known.

1.2 The process of gene transcription

When yeast are grown in a nutrient-rich medium, it is estimated to synthesise nearly 13,000 proteins per second (Dever *et al*. 2016; von der Haar 2008). There are several steps in a gene's expression, starting from the DNA and ending in the production of the protein. The first step in the transcription of a gene, termed transcription initiation, is where RNA polymerase II (Pol II) binds to a region in the gene promoter called the TATA box which often resides within the nucleosome free region (NFR). Pol II binds the promoter in collaboration with the general transcription factors (TFs) such as TFIIA, TFIIB, TFIID, TFIIE, TFIIF and TFIIH. When Pol II and the various TFs interact, they form the pre-initiation complex (PIC) and RNA synthesis begins (Smolle & Workman, 2013). The TFs act in the NFR, a region in which the DNA is resistant to nucleosome-binding, and is flanked by two well-positioned nucleosomes that are referred to as nucleosome -1 and +1, respectively (Sekinger *et al*. 2005). The second step of transcription is elongation, in which the RNA polymerase progresses along the gene, synthesizing RNA transcript (mRNA). The Pol II then dissociates from the DNA in a step called transcriptional termination (Nechaev & Adelman, 2011). The mRNA is then exported out of the nucleus to the cytoplasm to the ribosome, where it is translated to form a protein (Dever *et al*. 2016) (Fig. 1.1).

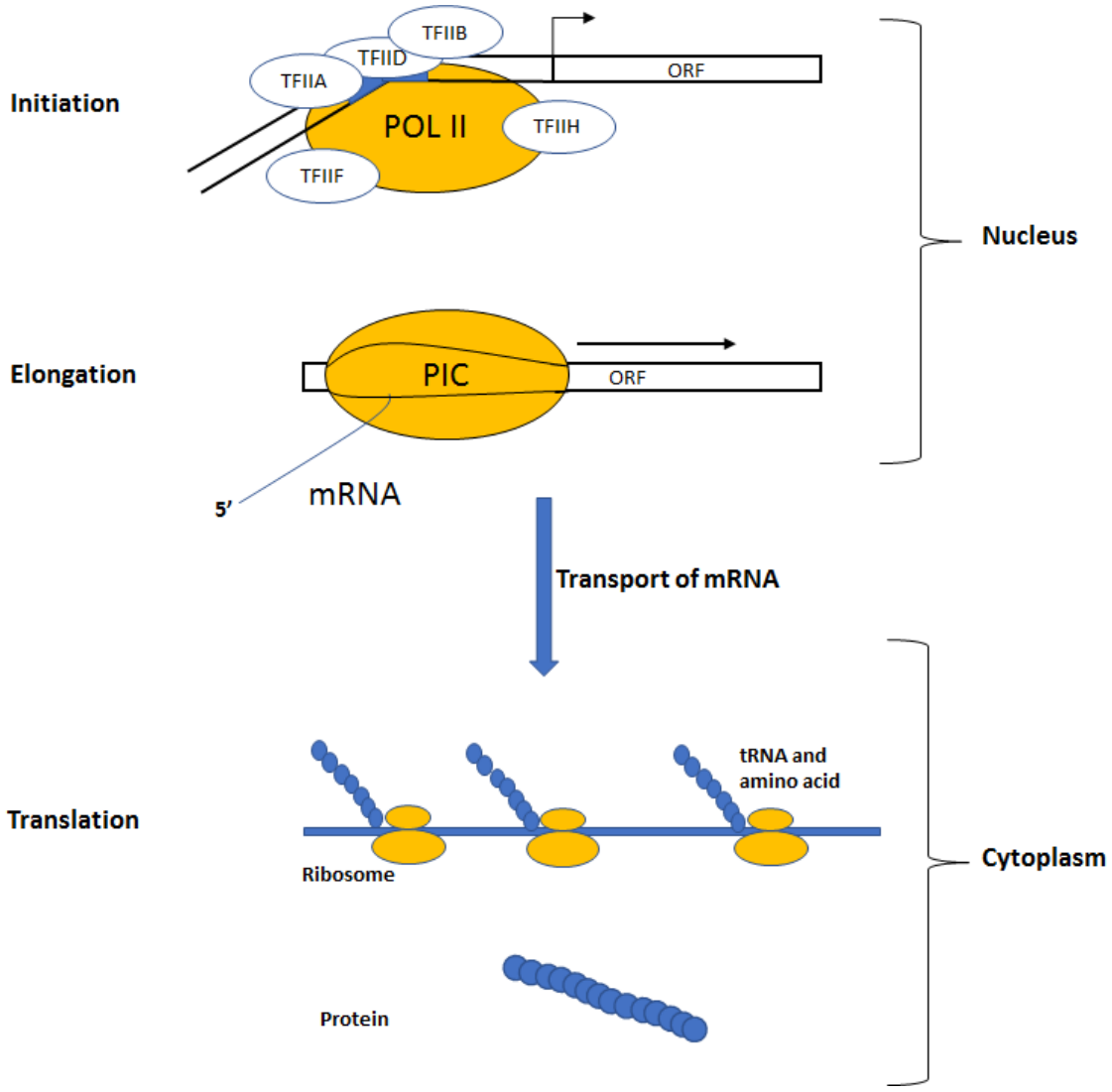

Figure 1.1 The transcription and translation pathway. The RNA polymerase II (Pol II) is recruited to the promoter with the general transcription factors (TFs) forming the pre-initiation complex (PIC). The RNA polymerase II then elongates across the gene body (ORF) generating the mRNA, which is then transported from the nucleus to the cytoplasm and is translated at the ribosome, to form the protein. This figure is adapted from (Turner, 2001).

1.3 Chromatin is considered repressive for transcription

The yeast genome is relatively large (22.7 Mbp) (León-Medina *et al*. 2016), and must be compacted into a nucleus which measures about 6 µm, in a manner which allows timely expression of genes. To achieve this, the genome is packaged with proteins in a structure known as chromatin. However, this packaging of the DNA is considered to be generally repressive to the process of transcription and all other processes that need to access the DNA (Turner, 2001).

The fundamental subunit of chromatin is the nucleosome (Li *et al*. 2007). The nucleosome is composed of four core histone proteins; two each of histones H2A, H2B, H3 and H4 around which approximately 146 base-pairs of DNA is coiled (Fig. 1.2) (Cooper 2000; Li *et al*. 2007). The *S. cerevisiae* genome also contains the linker histone H1 that also regulates chromatin structure, and can affect the transcriptional activation (Georgieva *et al*. 2012; Georgieva *et al*. 2015; Hellauer *et al*. 2001) . The nucleosome was first identified by using a nuclease enzyme Micrococcal nuclease (MNase) isolated from bacteria that cleaves DNA into a regular repeating unit. Upon this discovery, the author suggested that the chromatin has fundamental repeating subunits with repetitive sites sensitive to nuclease digestion (Hewish & Burgoyne, 1973) (Fig. 1.3). This initial experimental evidence for the nucleosome suggested that a protein bound to DNA protected the DNA from digestion by the nuclease, while unbound DNA was accessible to the nuclease (Turner, 2001). Further evidence for nucleosome structure came following electron micrographs of nuclear spreads which revealed a chain of 'beads' along the DNA (Olins and Olins 1974; Thoma *et al*. 1979).

Nucleosomes can form higher order structures by compacting the genome into distinct chromosomes. The yeast's nucleus contains 16 differently-sized chromosomes (J. Luo *et al*. 2018). The eukaryotic genome has two types of chromatin. The first, heterochromatin, is highly compacted and is prohibitive to gene expression. It is prevalent in the eukaryotic genome and makes the genome more stable. The second type of chromatin is euchromatin, which is considered open to gene expression (Grewal & Jia, 2007).

The transcriptional silencing mediated by heterochromatin in yeast is limited to the telomeres and the mating type loci. However, subtelomeric regions, which are defined as being located over 25 Kb from the end of the chromosome are also considered

genomic regions of interest since genes in this region often from a specific gene families, such as the stress response genes (Hocher *et al*. 2018; Louis and Becker 2014; Tashiro *et al*. 2017).

As mentioned previously, the chromatin structure is generally repressive to any process that requires access to the DNA, including transcription, replication, recombination and DNA damage repair (Becker and Workman 2013). However, chromatin structure can be altered, or remodelled, via the action of post-translational modifications (PTMs) made to the histone proteins themselves or via the ATP-dependent chromatin remodelling complexes.

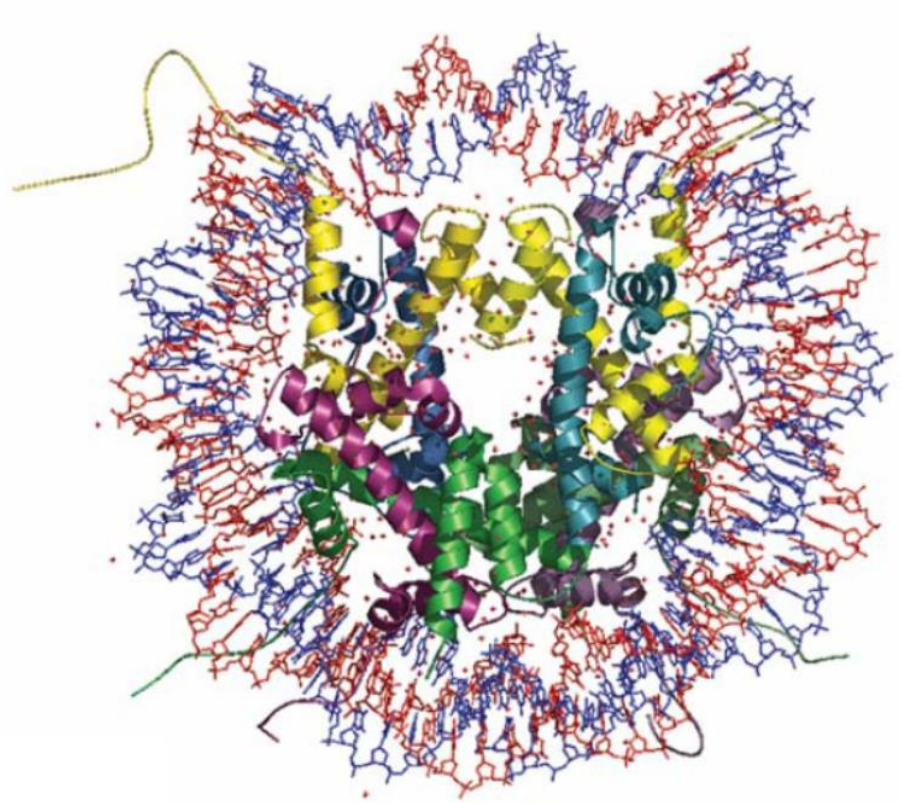

Figure 1.2 The structure of the core nucleosome. High-resolution crystal structure of the nucleosome (Bradbury, 2002) showing the DNA duplex (red and blue) wrapped around the tetramer of H3 (yellow) and H4 (dark green) and two dimers of H2A (purple) and H2B (green). Histone tails can be seen protruding from the nucleosome.

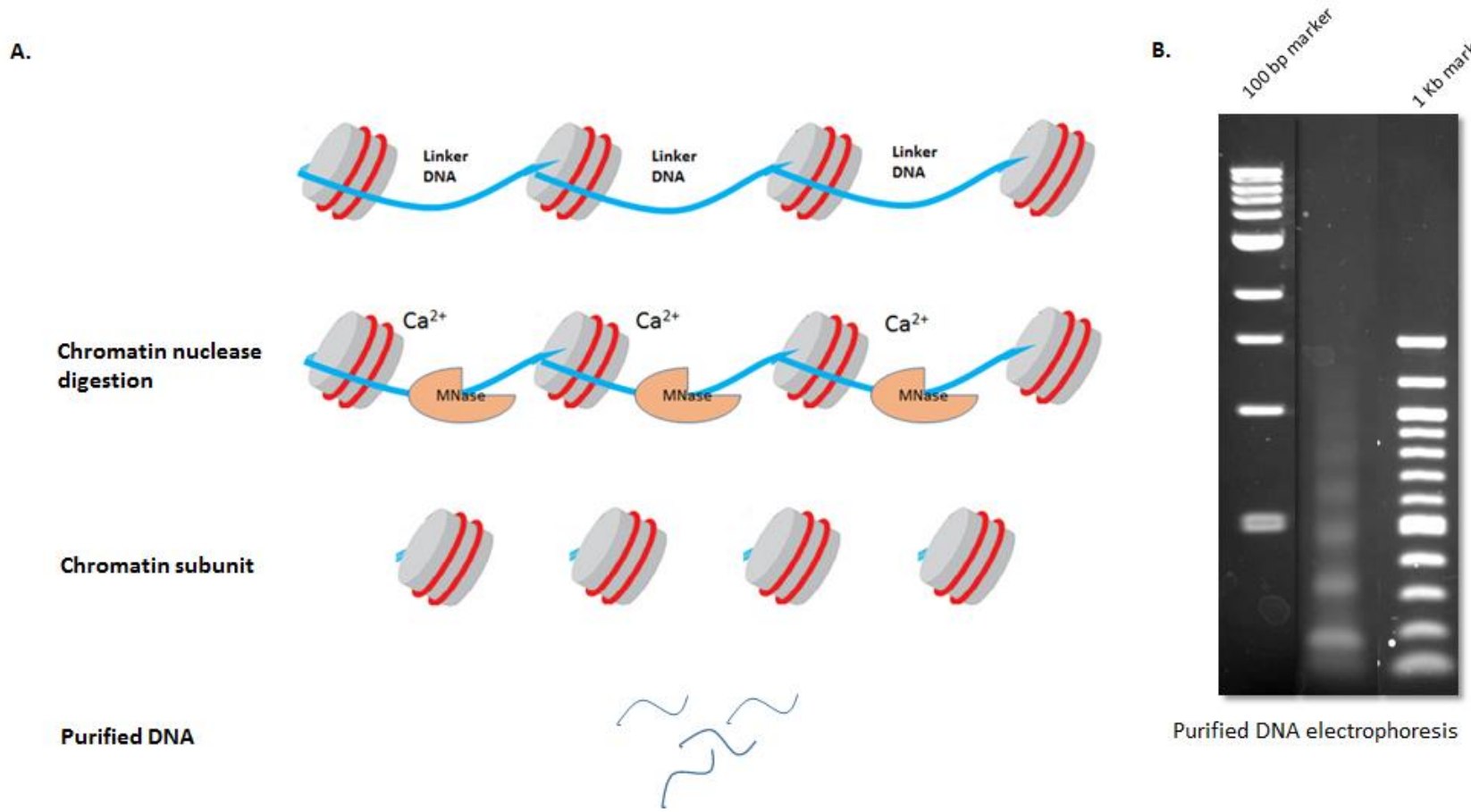

Figure 1.3 Micrococcal nuclease digestion (MNase). A: The MNase cuts the linker DNA in the presence of calcium, resulting in predominantly mono-nucleosomal length DNA. **B:** The DNA as visualised after gel electrophoresis to reveal a chromatin 'ladder'.

1.4 Post-translational modification of histones

The four core histone proteins—H3 (15.3 kDa), H4 (11.3 kDa), H2A (15.3 kDa) and H2B (14 kDa) —around which 147 bp of the DNA is wrapped, form the nucleosome. Histones H2A and H2B form two dimers, whereas histone H3 and H4 form a tetramer (Kornberg, 1974), and the histone tails protrude from this structure. Most post translational modifications (PTMs) takes place in the N-terminal histone tails, such as methylation and acetylation, where they can alter chromatin structure and function (Berger 2001; Narlikar *et al*. 2002).

Histone acetylation is the best characterised post modification that takes place on the lysine residues in the N-terminal tails of each of the histones. Indeed, acetylation was first proposed to activate genes by displacement of the nucleosome over 55 years ago (Allfrey *et al*. 1964). Histone acetylation neutralises the positive charge on the histone octamer surface making the DNA more accessible to the recruitment of l transcription factors (Narlikar *et al*. 2002; Sewack *et al*. 2001). Two enzymes work antagonistically to regulate histone acetylation; lysine (K) acetyl-transferases (KATs), also known as histone acetyltransferase (HATs), add the acetyl modification, while histone deacetylases (HDAC) remove the acetyl modification (Reid *et al*. 2000). Histone H3 is acetylated at lysine residues K4, K9, K14, K18, K23 and K56, whereas histone H4 is acetylated at lysine residues K5, K8, K12, K16 and K20 (Fig. 1.4) (Rando & Winston, 2012). Histones H2A and H2B can also be acetylated. One of the best-characterised HATs is Gcn5, which is the catalytic subunit of three HAT complexes: ADA, SAGA and SLIK. These complexes' catalytic activity is very important for modifying N-terminal lysines on histones H2B and H3, and these complexes have also been found to post-translationally modify the ATP-dependent chromatin remodeller Swi-Snf, which plays a role in regulating the nucleosome remodelling of target gene promoters (Kim *et al*. 2010; Lee & Workman, 2007). This interaction between Gcn5 and Swi-Snf has been studied at genes including *PHO8*, *SUC2*, and *HO*, which require this machinery to activate their gene expression (Mitra *et al*. 2006; Reinke *et al*. 2001). Dutta *et al*. (2017) showed a high level of histone acetylation at target gene promoters may be sufficient to recruit Snf2, the catalytic subunit of Swi-Snf. The *FLO1* gene also requires the Sas3 and Gcn5 (Ada2) containing HAT complexes and Swi-Snf for transcription (Church *et al*. 2017).

In contrast to the transcriptional activation activity of Swi-Snf and histone acetylation, a recent study showed that Tup1-Cyc8 cooperates with HDACs to repress *FLO1* (Fleming *et al*. 2014). Thus, the regulation of *FLO1* gene transcription involves the antagonistic action of the Swi-Snf and Tup1-Cyc8 complexes working in a histone acetylation dependent manner.

Histone methylation is another histone modification that is generally associated with active gene transcription. Only the lysine (K) residues -4, -36 and -79 of histone H3 can be methylated in yeast (Fig. 1.4) (Kouzarides, 2007). However, each lysine can be either mono-, di- or tri-methylated, suggesting each state of modification may play a distinct role. In order to establish these methylation states, cells have enzymes that both add (lysine methyltransferases (KMTs)) and remove (lysine demethylases (KDMs)) from the specific lysine residues of histone H3 (Shilatifard, 2006).

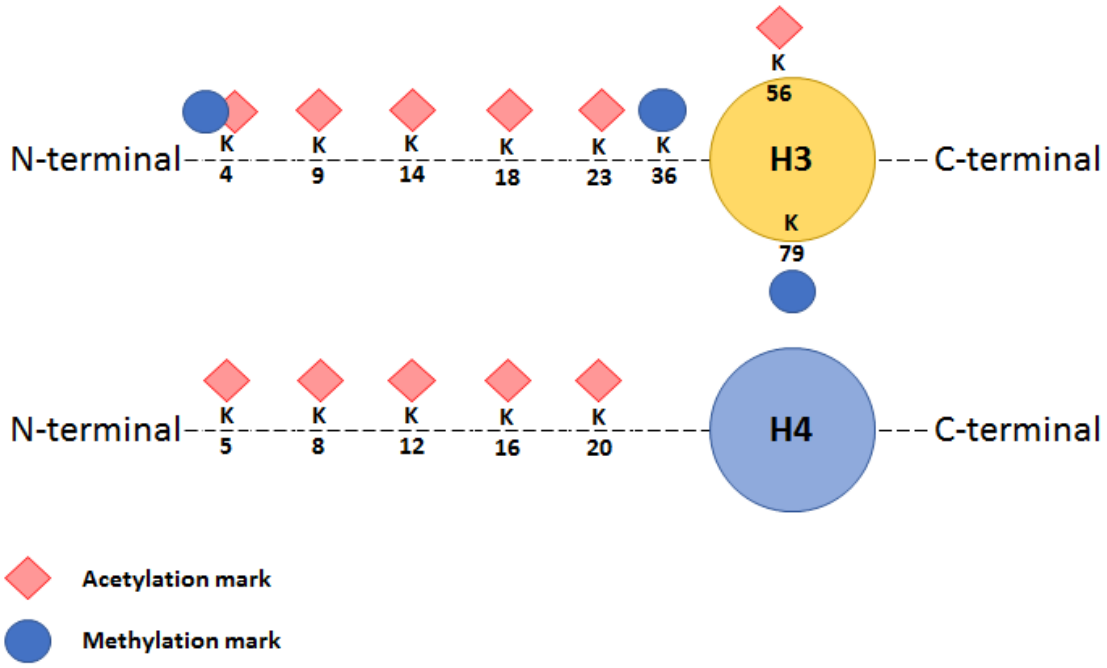

Figure 1.4 Acetylation and methylation of histones H3 and H4. Post translational modification in the N-terminal and globular domains of histones H3 and H4. Only lysines (K) 4, 36 and 79 of H3 are methylated in *S. cerevisiae*, whereas multiple lysines within H3 and H4 are acetylated (Rando and Winston 2012).

Based on their catalytic domains, the lysine methyltransferases (KMTs) are divided into two classes. The first class contains an evolutionarily conserved SET {Su(var)3- 9, Enhancer of Zeste ½E(Z), and Trithorax (trx)} domain (Jenuwein *et al*. 1998). In contrast, the second class consists of an evolutionarily conserved protein named the disruptor of telomeric silencing (Dot1; also called Kmt4) (Singer *et al*. 1998). In yeast, Set1 and Set2 catalyse the methylation of histone H3 lysine -4 and -36, respectively, whereas Dot1 has been identified as the enzyme responsible for H3K79 methylation (van Leeuwen *et al*. 2002).

1.5 ATP-dependent chromatin remodelling

Chromatin remodelling carried out by ATP-dependent chromatin remodelling complexes (remodelling complexes) is an essential process in eukaryotes. The cellular machinery cannot access regulatory regions if they are tightly wrapped around nucleosomes. Remodelling complexes can slide or remove nucleosomes to allow access to such regulatory regions (Clapier & Cairns, 2009). ATP-dependent chromatin remodelling can be brought about by sliding, disassembling or completely removing histone proteins (Clapier *et al*. 2017). Chromatin remodelling complexes have various roles, where they can remove or slide nucleosomes from a region to allow for transcription and DNA repair.

Remodelling complexes use the energy from ATP hydrolysis to disrupt histone-DNA interactions. There are four families of remodelling complexes which are defined by their ATPase subunits; switch/ sucrose non-fermentable (Swi-Snf), imitation switch (ISWI), chromodomain helicase DNA-binding (CHD), and INO80 (Mohrmann and Verrijzer, 2005; Eberharter and Becker, 2004; Becker and Hörz, 2002). It is proposed that all remodelling complexes have a common mechanism which uses a histone-anchored ATPase that brings about directional DNA translocation around a nucleosome. DNA translocation breaks histone-DNA contacts and propels DNA along the histone surface (Fig. 1.5) (Clapier *et al.* 2017).

The ATPase domain, known as the translocase domain (Tr) is the catalytic subunit of remodelling complexes and is split into two RecA-like lobes which are used to bring about DNA translocation. Both lobes sequentially bind to and release the same strand of DNA. The Tr is anchored to a fixed position on the histone octamer and the strand of

DNA moves 1-2 bp of DNA per cycle of ATP hydrolysis. Both lobes sequentially bind and release to the same strand of DNA, one slightly ahead of the other.

The remodelling complex first binds and anchors to a fixed position on the histone octamer through its histone binding domain (HBD). The HBD of Swi-Snf is located at carboxyl terminus of Snf2, and is known as the Snf2 ATP coupling (SnAC) domain (Sen *et al*. 2013). For Imitation SWitch (ISW1) and Chromodomain Helicase DNA binding (CHD) containing remodelling complexes, the HBD resides within the translocase domain on the amino termini of these subunits, while the mechanism in Ino80 is still unknown (Clapier *et al*. 2017).

Once anchored to the octamer there is a conformational change in the Tr, which is an ATP binding-hydrolysis dependent conformational change. This causes the DNA on the proximal side of the Tr to be under-twisted and lack sufficient DNA, whereas the DNA on the distal side is now over-twisted. The conformational change in the Tr breaks histone-DNA contacts, allowing linker DNA to be pulled into the area from the 5' end of the complex-bound DNA strand from the proximal side of the nucleosome, and pushes it towards the distal side of the nucleosome. This results in a loop of excess DNA in the distal region of the nucleosome. This passes through the Tr domain, with histone DNA contacts breaking and then reforming across the second half of the nucleosome. This movement of DNA resolves DNA twist and the final result is the sliding of the DNA 1-2bp along the surface of the histone proteins. Continuous repetition of this cycle eventually leads to the sliding of the nucleosome along a region of DNA.

Two mechanisms have been proposed to describe how the Swi-Snf complex can eject nucleosomes using DNA translocation. One model suggests that the histones may be lost simply due to the breaking of DNA-histone contacts. Eviction could be supported by the action of histone chaperone proteins. Another model proposes that as linker DNA is drawn onto the nucleosome with the remodelling complex attached this will eventually draw DNA from an adjacent nucleosome, which leads to eviction of the adjacent nucleosome.

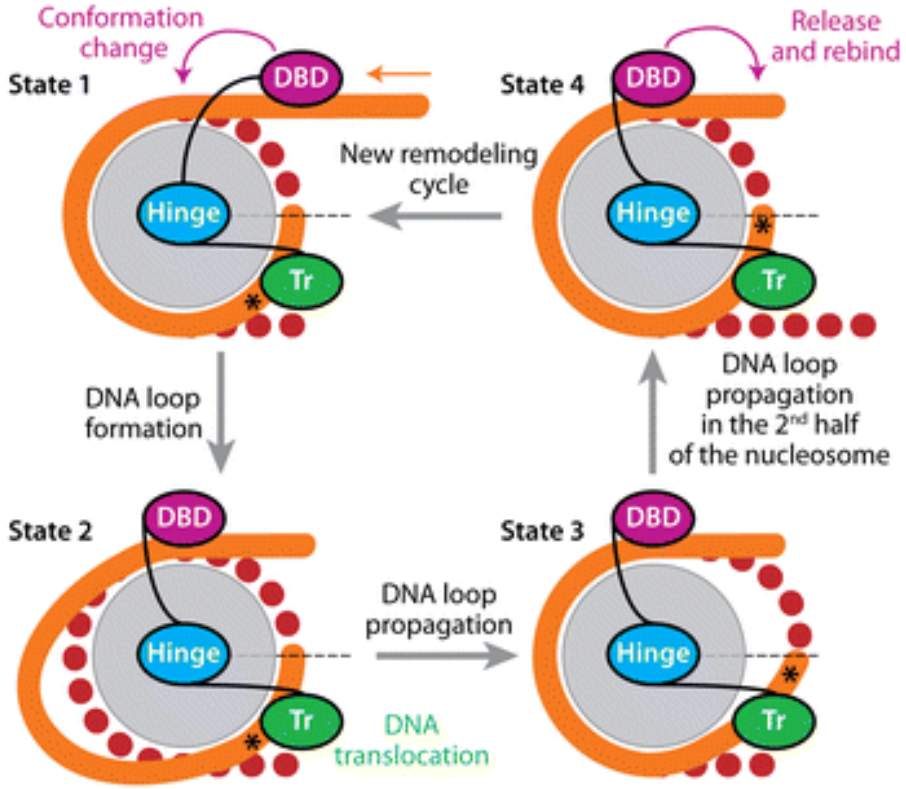

Figure 1.5 Mechanism of the ATP-dependent chromatin remodelling. In State one the Tr is anchored to a fixed region on the histone octamer and the DNA binding domain is attached to linker DNA. A conformational change occurs in the translocation domain (Tr) which leads to DNA-histone contacts breaking apart. This allows linker DNA to be pulled along the surface of the histone octamer and new DNA-histone contacts are created. In State two a loop of excess DNA is created, with this DNA in an over-twisted state. State three demonstrates how the excess DNA passes through the Tr, with DNA-histone contacts in the distal region being broken and new ones formed along the DNA that is moved along the histone surface. State four shows that the Tr is still anchored to the fixed position on the histone octamer, and the DBD can now be released and rebind to linker DNA. This cycle can be then be repeated (Clapier & Cairns, 2009).

1.5.1 The Swi-Snf complex

Swi-Snf, also known in humans as the BAF complex, is a transcriptional co-activator complex that was first identified in *S. cerevisiae*, and is evolutionarily conserved from yeast to humans (Winston & Carlson, 1992). Swi-Snf consists of 12 subunits in yeast and 11–15 subunits in humans and is about 1.5-2 MDa in size (Becker and Workman 2013; Dutta *et al*. 2014; Sudarsanam and Winston 2000). The subunits have different sizes and distinct roles which are summarised in (Table 1.1) (Muchardt and Yaniv 1999; Peterson *et al*. 1994). The genes encoding the subunits were first identified in screens for yeast strains that were defective in their ability to ferment sucrose (sucrose non-fermenting or *snf* mutants) and in mating-type switching (*swi* mutants), hence the name Swi-Snf. The Snf2 subunit contains the ATPase activity of Swi-Snf which is essential for the complex's function (Laurent *et al*. 1993). Current models have concentrated on Swi-Snf function in the gene promoter which is where the most apparent Swi-Snf dependent changes to chromatin occur. As stated previously the complex disrupts chromatin structure by either sliding nucleosomes along the DNA, or via the complete eviction of nucleosomes. It has been proposed that this ATP-dependent activity 'opens' up the promoter chromatin to allow for increased binding of transcription factors to their binding sites so as to activate transcription (Fig. 1.6) (Becker and Workman, 2013; Clapiera and Cairns, 2009; Sudarsanam and Winston, 2000; Kingston and Narlikar, 1999; Cairns, 1998).

Subunit	Function	Size (kDa)	Position within complex
Snf2	Catalytic subunit (ATPase)	194	Catalytic module
Snf11	Promotes Snf2 activity	19	
Snf5	Complex assembly	102.5	Snf5-Swp82- Taf14 module
Taf14	Not essential for stability, unknown function	274.3	
Swp82	Not essential for stability, unknown function	82	
Swi3	Complex assembly	93	Snf6-Snf12-Swi3 module
Snf6	DNA-binding and complex assembly	37	
Snf12	Complex stability	73	
Swi1	DNA binding	148	Swi1 module
Rtt102	peripheral member	177.9	Arp module
Arp9	Promotes Snf2 ATPase activity	53	
Arp7	Promotes Snf2 ATPase activity	54	

Table 1.1 The yeast Swi-Snf subunits. The 12 protein subunits of the Swi-Snf complex in yeast and their size and function (Dutta *et al*. 2017; Sudarsanam and Winston 2000).

The complex is thought to cooperate with high Mobility Group B (HMGB) proteins and histone chaperones in *S. cerevisiae*, including Nhp6B and Hmo1 which have been shown to be important for Swi-Snf activity at the promoters of several genes (Hepp *et al*. 2017; Stillman, 2010). The Swi-Snf complex is required for activation of 2–10% of all yeast genes, including the *SUC2* and *FLO1* genes (Dutta *et al*. 2014; Shivaswamy and Iyer 2008; Yen *et al*. 2012). *SUC2* encodes the invertase enzyme, which is required for sucrose hydrolysis and utilisation, while *FLO1* encodes the cell wall protein responsible for cell-cell aggregation, or flocculation (Fleming and Pennings 2001; Sudarsanam and Winston 2000). In human cells, Swi-Snf (BAF) has been linked to many human diseases, and the aberrant activity of Swi-Snf has been linked to 20% of all cancers and many neurological diseases (Sen *et al*. 2017). Indeed, it was proposed that the loss of *SNF5* (*SMARCB1*) is heavily implicated with childhood malignant rhabdoid tumours and breast cancer (Lu *et al*. 2017; Sen *et al*. 2017).

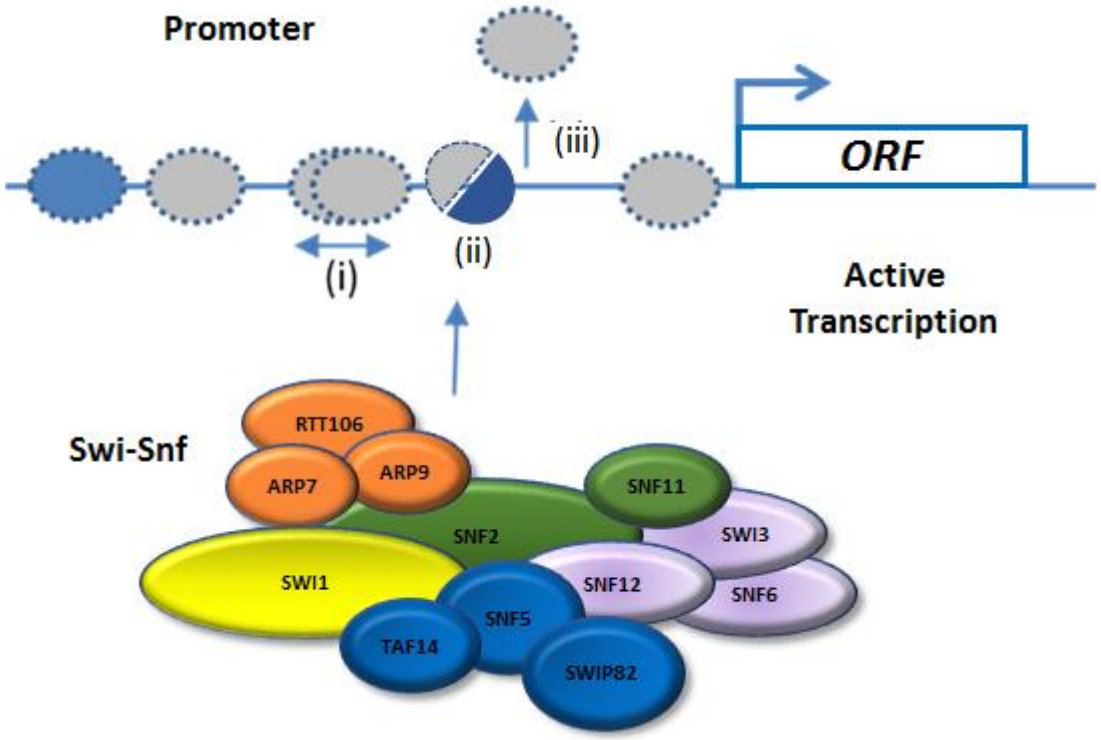

Figure 1.6 ATP-dependent chromatin remodelling Swi-Snf mechanism. The three mechanisms of gene activation by the Swi-Snf complex: (i) change in position of the nucleosome by sliding, (ii) exchange of the standard histone for a variant, and (iii) complete nucleosome removal (Becker and Workman 2013).

The yeast Swi-Snf complex contains four modules: (1) the Swi-Snf-RSC shared Arp module, made of Arp7, Arp9 and Rtt102; (2) the catalytic module, containing Snf2 and Snf11; (3) the Snf5/Swi3 module, consisting of two submodules (a Snf6-Snf12-Swi3 and a Snf5-Swp82-Taf14); and (4) the Swi1 module. In addition, the Snf6-Snf12-Swi3 submodule requires the Snf5-Swp82-Taf14 submodule to interact with Snf2 (Fig. 1.7) (Dutta *et al*. 2017). Regarding the stability of the Swi-Snf complex (Dutta *et al*. 2017), it has been shown that the loss of Snf2 significantly decreased association of Snf6, Swp82 and Taf14 with Swi1. Loss of Snf6 decreased association of Swi3, Snf12, Snf5, Swp82, Taf14 and Swi1 with Snf2, Arp7, Arp9 and Rtt102. These observations indicate that Snf2 and Snf6 are important for the complex's stability. On the other hand, loss of Snf11, Swp82, Taf14 and Rtt102 had no effect on complex stability (Szerlong *et al*. 2003), suggesting that these subunits are peripheral members of the complex and are not essential for complex structure; the loss also did not affect gene expression (Dutta *et al*. 2017). Not surprisingly, deletions of the catalytic subunits, like Snf2, were shown to have the most significant changes in gene expression, whereas *SWP82*, *SNF11* and *RTT102* gene deletions showed the least change (Dutta *et al*. 2017).

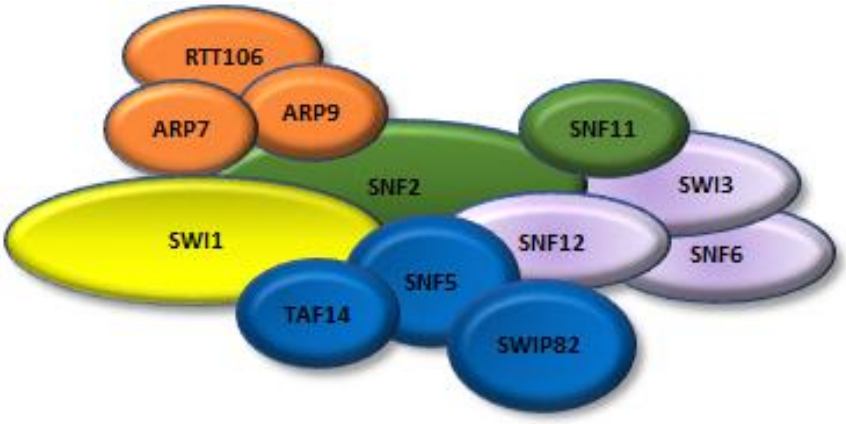

Figure 1.7 The five modules of the yeast SWI-SNF complex. Five submodules identified in Swi-Snf (1) Arp7-Arp9-Rtt102 (orange); (2) Snf11-Snf12 (green); (3) Snf12-Snf6-Swi3, (4) Taf14-Snf5-Swp82 (purple) and (5) Swi1 (yellow) (Dutta *et al*. 2017).

1.6 The Tup1-Cyc8 (Ssn6) complex

The Tup1-Cyc8 (Ssn6) complex is a general co-repressor of transcription in yeast. The complex is comprised of one Cyc8 (Ssn6) subunit and four Tup1 subunits that form a complex 1.2 MDa in size (Fig. 1.8) (Varanasi *et al*. 1996). The Tup1-Cyc8 complex represses numerous types of genes in *S. cerevisiae,* including genes involved in glucose repression and various stress responses (Gounalaki *et al*. 2000). Orthologous complexes are also found in worms, flies and some mammals (Jiménez *et al*. 1997; Mukai *et al*. 1999; Smith and Johnson 2000). Tup1-Cyc8 has four mechanisms by which it may repress target genes that include the following: (i) the inhibition of the general transcription machinery, (ii) the interaction with histone deacetylases (HDACs), (iii) the positioning of nucleosomes over gene promoters and (iv), blocking the activation domain of coactivator proteins (Fig. 1.9) (Treitel & Carlson, 1995). These mechanisms are not necessarily mutually exclusive and may be gene specific (Smith & Johnson, 2000). The Tup1-Cyc8 complex has no DNA binding activity but is recruited to target gene promoters via DNA-binding factors such as α2-Mcm1p, Crt1p, Rox1p, Sfl1p and Mig1p (Malavé and Dent 2006). The loss of Cyc8 in yeast causes slow growth, cell aggregation (flocculation) and the loss of glucose repression (Smith & Johnson, 2000). As mentioned previously, the Tup1-Cyc8 complex represses numerous types of genes including those involved in glucose repression and various stress responses, regulating about 150 genes or 3% of all *S. cerevisiae* genes (Smith & Johnson, 2000). The Tup1-Cyc8 complex was also identified as a transcription co-activator for tryptophan transporter genes *TAT1* and *TAT2,* loss of transcription of which causes a slow growth phenotype in the *Cyc8* mutant (Tanaka & Mukai, 2015).

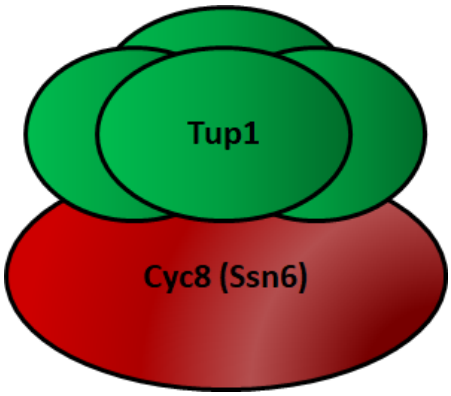

Figure 1.8 Two types of protein reside within the Tup1-Cyc8 complex. The complex consists of four Tup1 protein subunits and one Cyc8 (Ssn6) subunit.

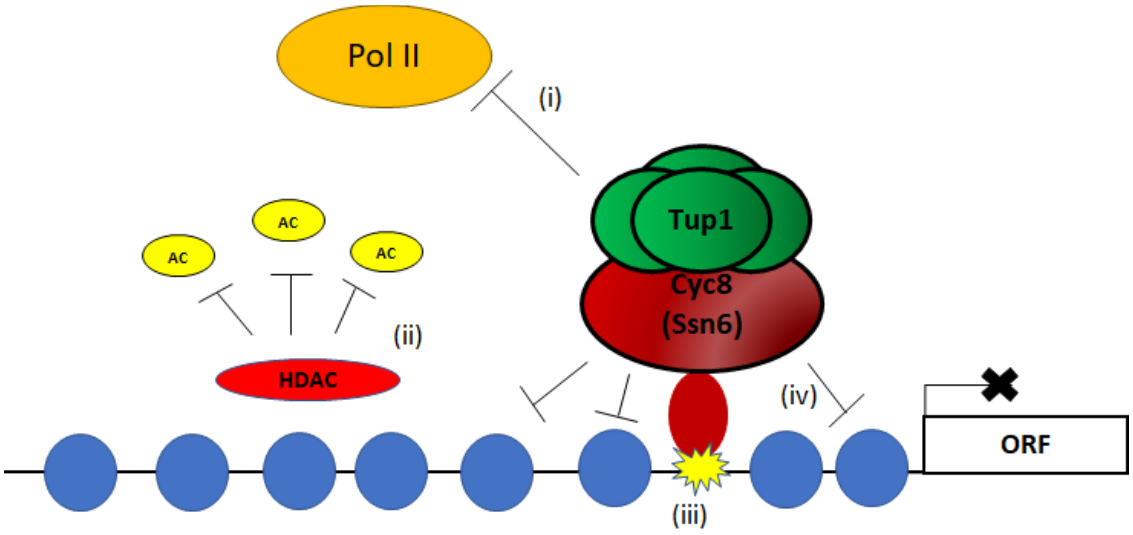

Figure 1.9 Tup1-Cyc8 repressor complex function. The Tup1-Cyc8 represses the transcription of genes by four mechanism (i) preventing binding of RNA polymerase II, (ii) interacting with histone deacetylase (HDAC) to reduce histone acetylation, (iii) positioning of nucleosomes at target promoters and (iv) masking the activator domain of transcription activator proteins.

1.7 The antagonistic mechanism of the repressor Tup1-Cyc8 and the activator Swi-Snf

The best-characterised genes under the antagonistic control of Swi-Snf as an activator and Tup1-Cyc8 as a repressor are the *FLO1* and *SUC2* genes. The expression of *FLO1* causes a flocculation phenotype, which is the non-sexual aggregation between cells that depends on the expression of lectin-like cell wall proteins that bind mannose residues in adjacent cell walls (Church *et al*. 2017; Soares 2011). *SUC2* encodes the enzyme invertase and is required for sucrose utilisation. *FLO1* is repressed in wild-type *S. cerevisiae* laboratory strains by the action of Tup1-Cyc8 that positions nucleosomes across the promoter. In the absence of Tup1-Cyc8, transcription is de-repressed, which correlates with the loss of nucleosomes from the promoter (Treitel & Carlson, 1995). This de-repression is Swi-Snf dependent, as in a *snf2 cyc8* double deletion mutant, nucleosome loss and expression of *FLO1* are abolished (Fleming and Pennings 2001) (Fig. 1.10). However, the total number of genes co-regulated by these complexes is unknown.

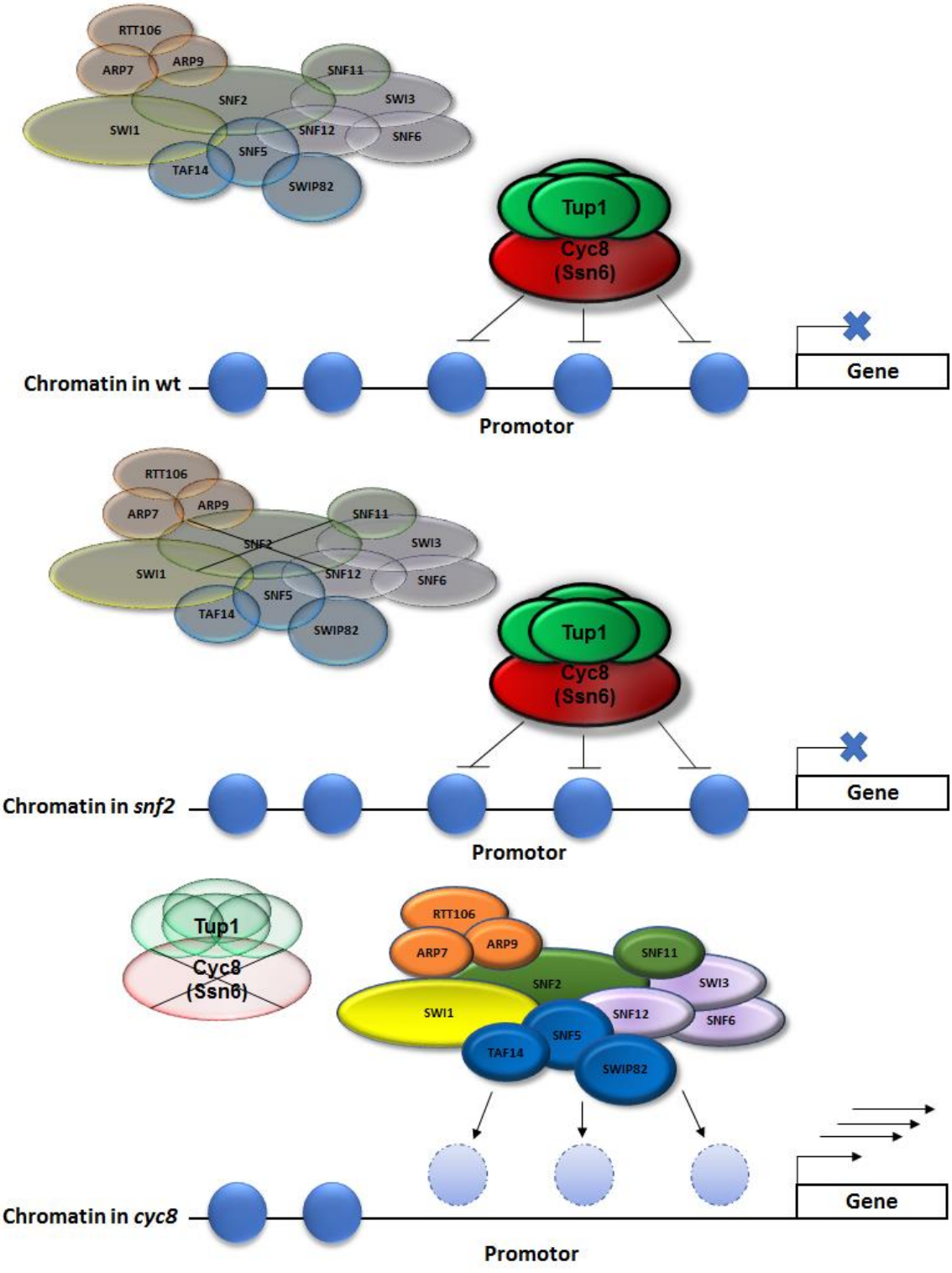

Figure 1.10 The co-regulation of genes by Tup1-Cyc8 and Swi-Snf. The example is of Tup1-Cyc8 repressing the co-regulated gene, *FLO1,* resulting in no flocculation in wild-type *S. cerevisiae*. With the deletion of *cyc8*, Swi-Snf activates the *FLO1* gene that leads to flocculation.

1.7.1 Flocculation and *FLO1* gene transcription

The non-sexual aggregation phenotype of yeast cells is termed flocculation (Soares, 2011; Teunissen & Steensma, 1995). The expression of the *FLO* family of genes, which encode lectin-like proteins which protrude from the cell wall, are responsible for the flocculation phenotype. These proteins contact the mannose residues of adjacent cells in a calcium dependent manner, allowing them to aggregate and sediment out of solution (Ca^{2+})(Fig. 1.11) (Stewart, 2009). This flocculation phenotype protects the cells from external stresses, and is important for the brewing industry and in biofilm formation (Deed *et al*. 2017; Liu *et al*. 1996).

The *FLO* gene family consists of five genes: *FLO1*, *FLO5*, *FLO9*, *FLO10* and *FLO11* (Caro *et al*. 1997; Van Mulders *et al*. 2009; Soares 2011). The *FLO1* gene is located in the subtelomeric region of chromosome I and is robustly repressed by the Tup1-Cyc8 complex which binds within -700 base pairs upstream of the transcription start site and strongly positions hypoacetylated nucleosomes across the promoter and upstream gene region (Fleming *et al*. 2014). Conversely, *FLO1* transcription depends upon the activity of the Swi-Snf complex which disrupts this extensive chromatin region (Church *et al*. 2017; Fleming and Pennings 2001). Thus, regulation of *FLO1* gene transcription via the antagonistic chromatin remodelling activities by Swi-Snf and Tup1-Cyc8 occurs within the context of a 32 nucleosomes array found upstream of the *FLO1* gene (Fleming and Pennings 2001; Fleming *et al*. 2014).

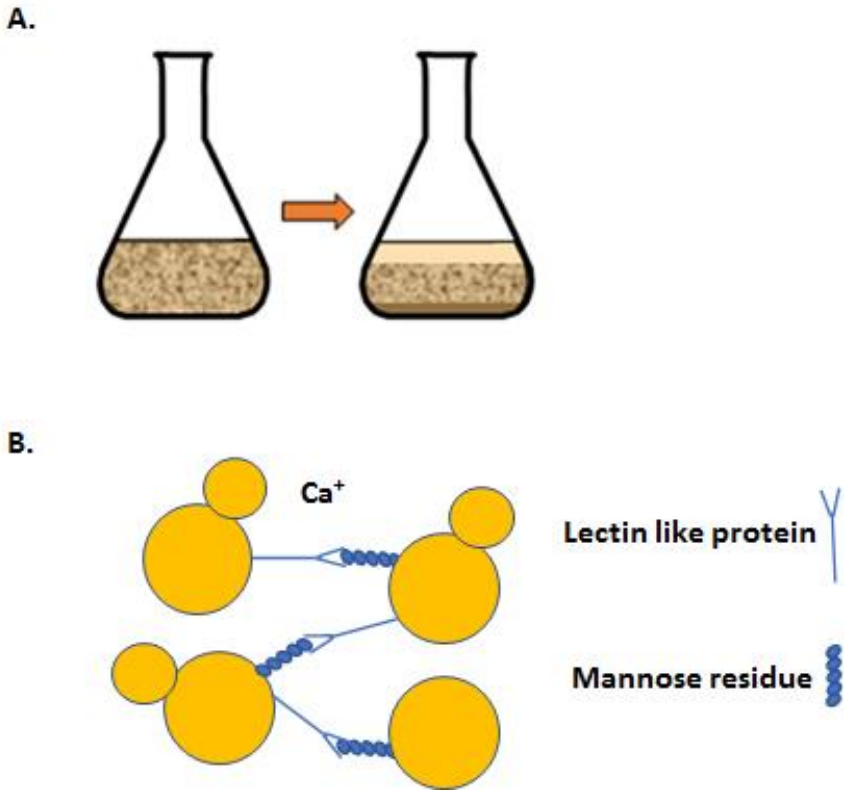

Figure 1.11 The yeast flocculation phenotype. (A) Non-flocculent cells remain in suspension (left hand flask), while flocculant cells aggregate and sediment to the bottom of the flask (right hand flask). (B) The Ca^{+} ions activate the lectin-like proteins to bind to the mannose residues in neighbouring cells. When enough cells accumulate, the flocculant cells precipitate (Soares, 2011).

1.7.2 *SUC2* gene transcription

The *SUC2* gene encodes the enzyme invertase which is responsible for the hydrolysis of the disaccharide, sucrose. The Swi-Snf complex, is named according to the SWItch/Sucrose Non-Fermentable phenotype attributable to mutations in the Swi-Snf complex subunits which are not able to ferment sucrose due to loss invertase activity. Invertase hydrolyses sucrose into the monosaccharides fructose and glucose; *SUC2* can also hydrolyse the trisaccharide raffinose, producing fructose and melibiose (Neuaia and Oliver 1967; Oezcan *et al*. 1997; Taussig and Carlson 1983). The *SUC2* gene is located at the subtelomeric region of chromosome IX and is also under the antagonistic activity of the remodelling complexes Swi-Snf and Tup1-Cyc8. These complexes remodel chromatin over the *SUC2* gene promoter and 5Kb upstream region to regulate *SUC2* transcription (Fleming and Pennings 2007).

1.8 The aim of this research

The objectives of this study were to identify the total number of genes in yeast which are co-regulated by the Tup1-Cyc8 and Swi-Snf chromatin remodelling complexes, and to identify the mechanism of Swi-Snf and Tup1-Cyc8 action at the co-regulated genes.

Chapter 2

Material and Methods

2.1. Strains and growth conditions:

2.1.1 Yeast strain and growth condition

Saccharomyces cerevisiae strains used in this research are listed in (Table 2.1). Yeast extract peptone with dextrose (YEPD or YPD) broth (1% (w/v) yeast extract, 2% (w/v) peptone & 2% (w/v) glucose) and YEPD agar by adding 2% (w/v) agar were used for routine growth, yeast cells were incubated at 30°C in a shaking incubator at 200rpm. 10 ml overnight cultures in YEPD media were inoculated with a single yeast colony, incubated overnight at 30°C in a shaking incubator at 200 rpm, and then sub-cultured in larger volume of YEPD media (25-50ml in conical flask).

For growth of mutants with auxotrophic markers, synthetic complete (SC) medium was prepared using 0.19% (w/v) yeast nitrogen base, 0.059% (w/v) complete supplement medium (Formedium), 0.5% (w/v) $(NH_4)_2SO_4$, adding 2% (w/v) agar for solid media. Remaining amino acids were included or omitted at appropriate concentrations, depending on the desired auxotrophic selection and strain genotype (Mell & Burgess, 2001).

2.1.2 Bacterial strain growth condition

The bacteria, *Escherichia coli* was used for plasmid reproduction and maintenance, and were grown in Lysogeny broth (LB) (10% (w/v) tryptone, 5% (w/v) yeast extract and 10% (w/v) NaCl) containing ampicillin (50 µg/ml). Overnight cultures of *E. coli* were sub-cultured into LB broth and grown at 37°C, at 200 rpm for further use.

Strain	Lab ID	Genotype	Source
wt	BY4741	Mat a his3Δ1 leu2Δ0 met15Δ0 ura3Δ0	ResGen library
cyc8	YAFTCD4	BY4741 parent: Mat a; his3Δ1; leu2Δ0; met15Δ0; ura3Δ0; *cyc8::KAN*	ResGen library
snf2	FY2083	MATa, his3-Δ200, ura3Δ0, trp1-Δ63, lys2Δ0, met15Δ0, *snf2::KAN*	F. Winston
snf2 cyc8	YDB1.7	MATa, his3-Δ200, ura3Δ0, trp1-Δ63, lys2Δ0, met15Δ0, *snf2::KAN*, *cyc8::URA3*	This study
snf2K798A	FY2084	MATa, ura30 snf2-798	F. Winston
snf2K798A cyc8	YMM2	MATa, ura30 snf2-798, *cyc8::URA3*	This study
snf5	*snf5*::*KAN*	MATa, his3-Δ200, ura3Δ0, trp1-Δ63, lys2Δ0, met15Δ0, *snf5::KAN*	ResGen library
cyc8	*cyc8*::*URA3*	MATa, his3-Δ200, ura3Δ0, trp1-Δ63, lys2Δ0, met15Δ0, *snf5::KAN*, *cyc8::URA3*	This study
snf5 cyc8	YMM3	MATa, his3-Δ200, ura3Δ0, trp1-Δ63, lys2Δ0, met15Δ0, *snf5::KAN*, *cyc8::URA3*	This study
swi3	*swi3*::*KAN*	MATa, his3-Δ200, ura3Δ0, trp1-Δ63, lys2Δ0, met15Δ0, *swi3::KAN*	ResGen library
swi3 cyc8	YMM4	MATa, his3-Δ200, ura3Δ0, trp1-Δ63, lys2Δ0, met15Δ0, *swi3::KAN*, *cyc8::URA3*	This study
snf6	*snf6*::*KAN*	MATa, his3-Δ200, ura3Δ0, trp1-Δ63, lys2Δ0, met15Δ0, *snf6::KAN*	ResGen library
snf11	*snf11*::*KAN*	MATa, his3-Δ200, ura3Δ0, trp1-Δ63, lys2Δ0, met15Δ0, *snf11::KAN*	ResGen library

Table 2.1: Yeast strains used in this research.

2.1.3 Detecting the growth rate of yeast

Yeast growth was monitored by measuring the optical cell density with a spectrophotometer (OD_{600}), and also by measuring the colony formation unit in ml (CFU/ml) using the counting champers hemocytometer under a light microscope. All the experiments were performed in mid-log phase for each strain.

The yeast growth rate was measured by perform a growth curve. The yeast strains were inoculated into YEP liquid culture containing 2% (w/v) of different carbon sources, then incubated at 30°C, at 200 rpm. 200 µl from the yeast culture were added in triplicate wells in a 96 well plate, and the growth were monitored by the plate reader (Synergy H1, Biotek) with wave length of 600 nm (OD_{600}), and the increase in optical density was monitored over time. The CFU/ml was measured every 2 hours by using the hemocytometer under a light microscope (LEICA).

2.1.4 Morphological images of the yeast cells

Yeast strains were grown in YEPD at 30°C to the mid-log phase, the cells then washed with distilled water and 20µl spotted onto a glass slide. Light microscopy was performed under 100X oil immersion magnification. Leica Application Suite (LAS) software was used for the images provides and visualisation.

2.1.5 stress response by spot test

Yeast cells were resuspended to the same cell density and 10-fold serial dilutions were prepared from which equal numbers of cells were spotted onto YEP plates containing different reagents or different incubation temperatures.

2.2 Molecular experiment

2.2.1 Plasmid extraction

Plasmids were isolated from *E. coli* by following the manufacturing guidelines of Qiaprep spin miniprep Kit (Qiagen) using a 5ml overnight culture grown at 37ºC at 200 rpm.

2.2.2 DNA Extraction

The yeast genomic DNA extraction protocol was modified from (Hoffman & Winston, 1987). 10 ml overnight yeast culture was centrifuged at 376 g for 5 min. The supernatant was discarded, and the cell pellet was resuspended in 1 ml H_2O then transfer to a 1.5 ml

tube followed by short centrifugation for 2 min at 16,363 g. To breakdown the cell wall and remove protein, the yeast cell pellet was resuspended in 200µl cells lysis buffer (2 % (v/v) Triton X-100, 1 % (w/v) SDS, 100 mM NaCl, 10 mM Tris-Cl [pH 8.0], 1 mM EDTA [pH 8.0]), 200µl (0.3g) by volume 400 µm -600 µm glass beads (Sigma), and 200µl 25:24:1 (V/V/V) phenol/chloroform/isoamyl alcohol were added. The sample was mixed by vertexing for 5 min. 200µl Tris-EDTA (TE) buffer (pH 7.5) was added, the samples were mixed by pipetting, and centrifuged at 16,363 g for 5 min. The upper aqueous layer was transferred to a new 1.5 ml tube and 400 µl chloroform was added. This was mixed by inversion and subjected to centrifugation for 5 min at 16,363 g. The upper aqueous layer was transferred to a new 1.5 ml tube and 1ml 100 % ethanol was added. DNA was pelleted by centrifugation at 16,363 g for 5 min. Supernatant was discarded and the DNA pellet was resuspended in 500 µl 70 % ethanol. DNA was pelleted by centrifugation at 16,363 g for 5 min. The DNA pellet was dried by heat block at 37°C and resuspended in 400 µl TE (pH 7.5) and 25 µg RNase A was added. Samples were incubated at 37°C for 1 hour. 5µl 20mg/ml proteinase k was added and incubated at 50°C for 1 hour. The mix was extracted with 400µl 25:24:1 (V/V/V) phenol/chloroform/isoamyl alcohol as described above. DNA was precipitated with ethanol and resuspended in 50 µl TE (pH 7.5). DNA concentration was determined using a NanoDrop ND-100 spectrophotometer (Thermo Scientific) measured at an absorbance wavelength of 260 nm (A260nm).

2.2.3 RNA Extraction

The RNA extraction protocol was the Hot Phenol method adapted from Current Protocols (Collart & Oliviero, 2001). Cells were grown to log phase and a 10 ml volume of culture was pelleted by centrifugation for 3 minutes at 453 g. The pellet was resuspended in 1 ml H_2O then transferred to new 1.5 ml tube pelleted by short centrifugation. The cells pellet was resuspended in 400ml TES (10 mM Tris-Cl pH 7.5, 10 mM EDTA, 0.5% (w/v) SDS) and 400 µl saturated phenol, pH 4.3 (Fisher). The mix was incubated at 65°C for 1 h with occasional vortexing every 15 min. The sample was incubated on ice for 5 min, followed by centrifugation for 5 min at 16,363 g. The upper aqueous layer was transferred to new 1.5ml tube and 400 µl chloroform was added, and centrifuged at 16,363 g for 5 min. The upper aqueous layer was transferred to new 1.5 tube and 40 µl 4M sodium acetate, pH 5.3 and then 1 ml ice cold 100 % (v/v) ethanol

were added to precipitate the RNA. The mix was subjected to centrifugation at 16,363 g for 5 min at 4°C. the pellet was washed by 70% (v/v) ethanol and centrifugated as before to pellet the RNA. The pellet was dried before being resuspended in 50 µl nuclease free water. RNA concentration was determined using a NanoDrop ND-100 spectrophotometer (Thermo Scientific) measured at an absorbance wavelength of 260 nm (A260nm).

2.2.3.1 Purified RNA quality control

2.2.3.1.1 RNA preparation under denaturing conditions in an agarose-formaldehyde gel

To visualize the extracted mRNA, 1% (w/v) agarose was made by dissolved 1.8 g agarose in 86.4 ml water boiled and cooled to 60°C in a water bath. 12 ml of 10× MOPS running buffer (0.4 M MOPS [3-(*N*-morpholino)-propanesulfonic acid], pH 7.0, 0.5 M sodium acetate and 0.01 M EDTA) and 21.6 ml of 40% formaldehyde were added. The gel was poured and allowed to solidify for 30 min. The gel was placed in a gel tank. 1× MOPS running buffer was added until the gel was immersed. A total of 10 µg of RNA was loaded per lane post sample preparation. The volume of each RNA sample was adjusted up to 10 µl with nuclease free water then 25 µl MMF (500µl formamide, 162 µl formaldehyde (40%) and 100µl 10X MOPS), and 2 µl EtBr was added to each sample. The samples were mixed and incubated at 60°C for 15 min then left on ice. 5 µl loading dye was added to each sample and loaded on the prepared gel.

2.2.3.1.2 RNA quality assessment by Bioanalyzer

The 2100 Bioanalyzer system provides assessment of sizing, quantitation, integrity and purity for RNA. 12 RNA samples with concentration of 0.5 µg was prepared for each chip, the RNA was denaturing at 70°C for 2 min, and cooled in ice for 5 min in advance of loading to the bioanalyzer chip. The chip was prepared according to the manufacturing of bioanalyzer Aligent RNA 6000 Nano Reagent Part I (Kit No. 5067-151). The 2100 Bioanalyzer software setup at Eukaryotic RNA to provide RNA integrity number (RIN) value for 10 being the best RNA quality (Fig.2.1).

A.

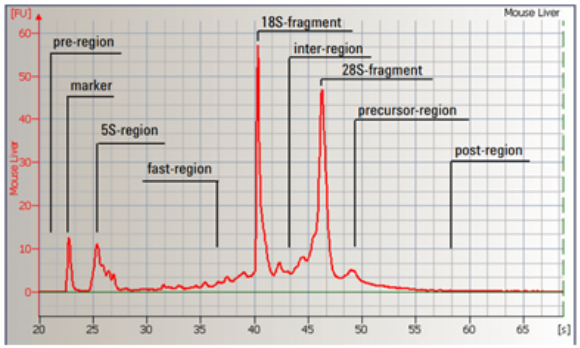

B.

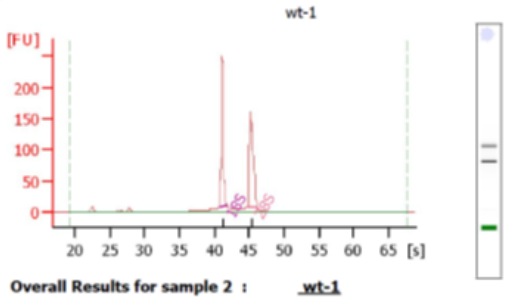

Overall Results for sample 2 : wt-1

RNA Area:	622.8
RNA Concentration:	441 ng/µl
rRNA Ratio [28s / 18s]:	1.2
RNA Integrity Number (RIN):	8.1 (B.02.07, Anomaly Threshold(s) manually adapted)
Result Flagging Color:	
Result Flagging Label:	RIN: 8.10

Fragment table for sample 2 : wt-1

Name	Start Time [s]	End Time [s]	Area	% of total Area
18S	40.80	41.76	180.5	29.0
28S	44.75	46.18	218.2	35.0

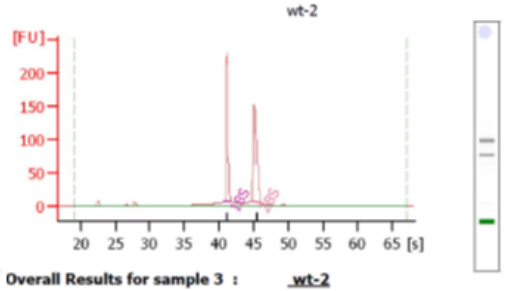

Overall Results for sample 3 : wt-2

RNA Area:	556.9
RNA Concentration:	394 ng/µl
rRNA Ratio [28s / 18s]:	1.2
RNA Integrity Number (RIN):	8.1 (B.02.07, Anomaly Threshold(s) manually adapted)
Result Flagging Color:	
Result Flagging Label:	RIN: 8.10

Fragment table for sample 3 : wt-2

Name	Start Time [s]	End Time [s]	Area	% of total Area
18S	40.74	41.75	164.4	29.5
28S	44.71	46.12	192.8	34.6

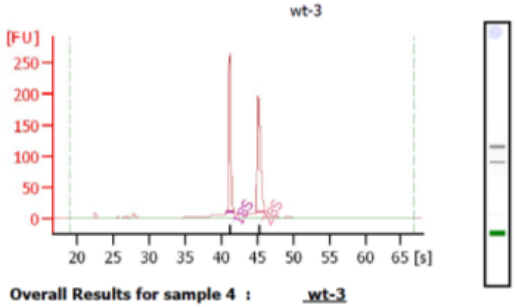

Overall Results for sample 4 : wt-3

RNA Area:	670.8
RNA Concentration:	475 ng/µl
rRNA Ratio [28s / 18s]:	1.3
RNA Integrity Number (RIN):	7.9 (B.02.07, Anomaly Threshold(s) manually adapted)(
Result Flagging Color:	
Result Flagging Label:	RIN: 7.90

Fragment table for sample 4 : wt-3

Name	Start Time [s]	End Time [s]	Area	% of total Area
18S	40.70	41.70	185.5	27.7
28S	44.76	46.08	242.7	36.2

Figure 2.1 RNA quality assessment by RNA integrity number (RIN). Chromatograms showing RNA integrity (RIN) using RNAnano bioanalyzer 2100. (A) schematic showed the details of the regions were indicated by the machine to estimate the RIN value. (B) triplicate samples for wt as an example of the result indicated by the machine which the RIN value was ~ 8.

2.2.4 Protein extraction

Protein was extracted by using 20% (v/v) trichloroacetic acid (TCA) following the protocol obtained from (Szymanski & Kerscher, 2013). The cells were grown to mid-log phase, 10 OD units were harvested then subjected to centrifugation at 376 g for 5 min. The supernatant was discarded, and the pellet was resuspended in 1 ml 20% TCA and transferred to new 1.5 ml tube. The mix was centrifuged at 16,363 g for 15 s, and the supernatant was discarded. The pellet resuspended in 250 µl 20% TCA and approximately 500 mg 400 µm-600 µm glass beads (sigma) were added. The cells were agitated in a vortex (Genie II) mixer at maximum speed at 4°C for 15 min. The post vortexed lysate was transferred to new 1.5 ml tube, the glass beads were washed by adding 5% TCA, mixed, and transferred to the same 1.5 ml containing lysate. The lysate incubated on ice for 3 min followed by centrifugation at 16,363 g for 1 min. The supernatant was discarded, and the pellet resuspended in fresh 300 µl 1X laemmli (0.1 % 2-mercaptoethanol, 10 % glycerol, 2 % SDS & 63 mM Tris-Cl [pH 6.8]). The mix was boiled at 95°C for 5 minutes. The mix subjected to centrifugation at 16,363 g for 1 min. The supernatant was transferred to new 1.5 ml tube.

The concentration of the protein was monitored by Bradford assay according to manufacturer's instructions (Sigma). Protein samples and bovine serum albumin (BSA) standards of 2, 4, 6, 8 and 10 µg/ml were prepared and diluted in H2O with Bradford reagent (Sigma). Absorbance (A595) was measured using a spectrophotometer, where BSA standards were used to generate a standard curve, and sample concentration was calculated by comparing sample absorbance values to those of the standard curve. Working stocks of protein samples were adjusted to a volume of 2 mg/ml and it was stored at -80°C.

2.2.5 SDS Polyacrylamide gel electrophoresis (PAGE)

By using the BioRad Mini cell system 10% (v/v), 12% (v/v) and 15% (v/v) polyacrylamide resolving gels were prepared (10 % (v/v), 12% (v/v) and 15 % (v/v) acrylamide [Protogel, National Diagnostics], 0.38 M Tris-Cl [pH8.8], 0.001 % (w/v) SDS, 0.001 % (w/v) ammonium persulfate [APS] & 0.001% (v/v) TEMED), depending on the required resolution for the protein. These resolving gels were immediately overlaid with 1 ml of isopropanol to allow for polymerization. The isopropanol was discarded after 20 min,

6% (v/v) stacking gel (6 % (v/v) acrylamide, 78 mM Tris-Cl [pH 6.8], 0.001% (w/v) SDS, 0.001% (w/v) APS & 0.001% (v/v) TEMED) was poured, and a plastic comb containing 10 wells sealed in the stacking gel anaerobically to allow for polymerisation. 30 µg of protein was boiled for 5 min at 95°C and loaded into each well and gels were run at 100V for 120 min in running buffer (25 mM Tris, 190 mM glycine, 0.1 % (w/v) SDS).

2.2.6 Western blotting

The western blotting protocol was adapted from Current Protocols (Gallagher *et al*., 2008). The protein was transferred from the SDS-PAGE gel to the polyvinylidene fluoride (PVDF) membrane (Immobilon) in transfer buffer (25 mM Tris, 190 mM glycine & 20% (v/v) methanol) at 300 mA for 40 minutes (Bio-rad, Mini trans-blot, 153BR). The 4X sponges and the SDS-PAGE gel were soaked in transfer buffer, and the PVDF membrane was soaked in methanol for 20 s, followed by ddH2O for 2 minutes in advance of use. When the protein has been transferred to the membrane, it was incubated for 1 hour, rocking at room temperature in blocking buffer (5% (w/v) dried skimmed milk in Tris-buffered saline with 0.05% (v/v) Tween 20 [TBST, Sigma]). Then the PVDF membrane was incubated in the primary antibody diluted to an appropriate concentration (Table 2.2) overnight at 4°C. Post-incubation, the membrane was washed 4 time for 5 minutes by (TBST (Tris-buffered saline, 0.1% Tween 20), Sigma). Secondary HRP-Conjugation antibodies were diluted 1:10,000 in blocking buffer and incubated with the membrane for 90 min at room temperature. After incubation, the membrane was washed for 10 min in TBST followed by 3 washes of 10 min in TBS (TBS, Sigma). Bound antigens were detected using enhanced chemiluminescent (ECL) Western Blotting Substrate (Pierce) according to manufacturers' guidelines before being developed using Imagequant las 4000 imager.

Antibody	dilution	Species	Source
β- Actin	1:3000	Mouse	Abcam
α-Cyc8	1:500	Goat	Santa Cruz Biotechnology
α-Snf2	1:2000	Rabbit	J. Reese
α-Snf5	1:1000	Rabbit	Upstate
α-Snf6	1:2000	Goat	J. Reese
α-Swi3	1:1500	Rabbit	J. Reese
α-Tup1	1:50000	Rabbit	Santa Cruz Biotechnology

Table 2.2: Antibodies used in western blotting: All antibodies were diluted in 5% (w/v) Milk powder in TBST

2.2.7 Yeast transformation

Yeast were transformed with exogenous DNA using the lithium acetate procedure following (Gietz and Woods, 2002) protocol (Fig. 2.2). Yeast cells overnight cultures were counted on a haemocytometer (Fisher) and adjusted to a cell density of 5 x 10^6 cells/ml in YEPD. These cells were incubated at 30°C, 200 rpm until its equivalent to 2 x 10^7 cells/ml. The cells then were harvested by centrifugation at 453 g for 3 min. The supernatant was discarded, and the cells were washed with 25 ml distilled water, and subjected to centrifugation at 453 g for 3 min. The water was discarded, and the cells resuspended in 1 ml 0.1 M lithium acetate (LiAc) and transferred to the 1.5 ml tube. The cells were pelleted by centrifugation at 19745 g for 15 s. The cells were resuspended in 400 µl 0.1 M LiAc and 50 µl was aliquoted into 1.5 ml tube to each transformation mix. Salmon sperm DNA (2 mg/ml, Sigma) was heated to 95°C for 10 min and then quickly chilled on ice. The cells were resuspended in 240 µl 50% (v/v) polyethylene glycol (PEG) v/v. 36 µl 1M LiAc, 50 µl salmon sperm DNA and 34 µl of PCR fragment DNA (or plasmid) giving the final volume of 360 µl. The mix was vortexed vigorously until resuspended. The mix then incubated at 42ºC for 40 min. Post-incubation, samples were centrifugated at 4,600 g for 15 s, and the supernatant was discarded. Cells were then resuspended in 200 µl sterile H_2O. For transformations involving auxotrophic markers, cells were plated directly onto selective media. For transformations involving antibiotic markers, cells were first plated onto YEPD and incubated overnight at 30°C. Following recovery, cells were replica-plated onto selective media and incubated at 30°C. Transformants were verified by PCR.

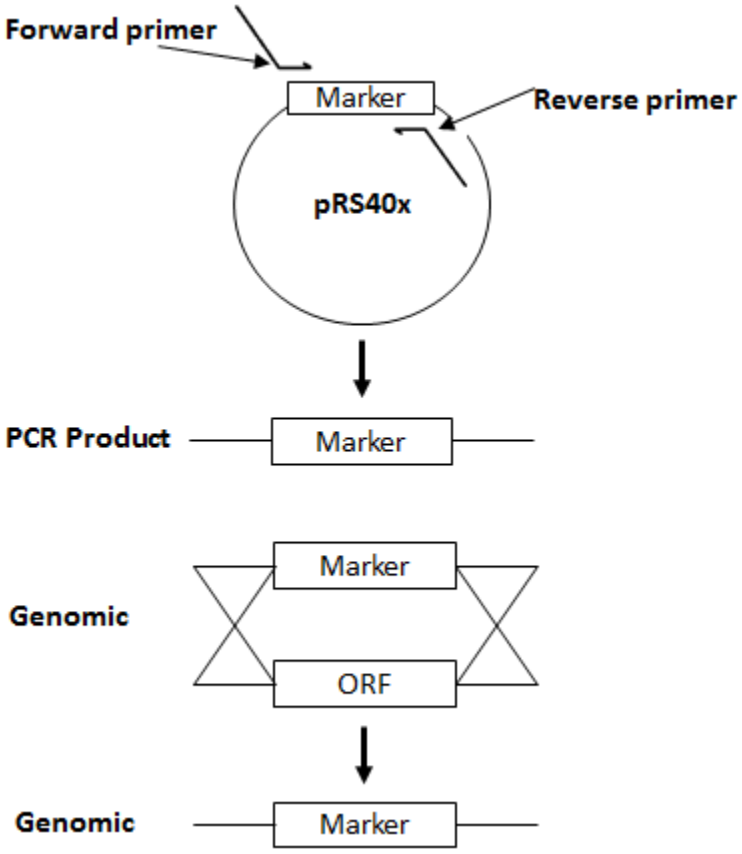

Figure 2.2 Overview of gene deletion and transformation process. Disruption fragments were generated by using primers complementary to the template plasmid. These fragments contained sequences that were homologous to DNA flanking the gene targeted for deletion (Brachmann *et al*. 1998). The selectable marker thus replaced the target ORF by homologous recombination.

2.2.8 DNase treatment and cDNA generation

To remove any DNA contamination in prior to use the RNA subjected to DNase I enzyme (Promega). 10 µg RNA was incubated with 1 unit of DNase in reaction buffer at 37°C for 1 hour. Then, 1 µl stop solution was added and samples were incubated at 65°C for 10 minutes.

For the RNA-Seq, the RNA was DNase treated using the Rneasy minelute cleanup kit (Ref: 74204) Quiagen. RNA concentration was determined using a NanoDrop ND-100 spectrophotometer (Thermo Scientific) measured at an absorbance wavelength of 260 nm (A260nm). The purified RNA was stored at -80 to be used for sequencing.

The cDNA was generated using a High-capacity RNA to cDNA kit (Applied Biosystems). 1 µg of DNase-treated RNA was incubated with 1 unit of reverse transcriptase in reaction buffer at 37°C for 1 hour, and this reaction was stopped by incubation at 95°C for 5 min.

2.2.9 Real time RT-qPCR

The qPCR was adapted from Current Protocols (Bookout *et al*. 2006). cDNA was generated from mRNA, Reverse transcription was carried out using the High Capacity RNA-cDNA kit (Applied Biosystems) according to manufactures instructions for transcription analysis. 9 µl of DNase I treated total RNA was incubated for 37°C for 60 min in the presence of 10 µl 2X RT buffer and 1 µl 20 x Enzyme Mix. Negative RT controls were carried out by replacing Enzyme Mix with DEPC-treated water. The reaction was stopped by heating samples to 95°C for 5 min. For transcription analysis, a 20 µl reaction contained 1X Applied Biosystems Power SYBR Green (Thermo), 150nM of each primer, 2 µl template DNA and dH_2O to 20 µl. qPCR was analysed by relative quantification using a standard curve on an Applied Biosystems Step One Plus real-time PCR system. The relative amount of target gene was compared with *ACT1* which is a reference gene chosen based on previously published data (Pathan *et al*. 2017), and it is stable on all the mutants in log phase.

2.2.10 PCR amplification from yeast colony (colony PCR)

One small colony of yeast were resuspended in 50 µl 25 mM NaOH and samples were boiled at 95°C for 10 min and used for DNA template.

2.2.11 Polymerase chain reaction (PCR)

PCR was performed using the MyTaq HS (Bioline) DNA polymerase mix unless otherwise stated, and the reactions were carried out according to manufacturer's guideline. For amplification of DNA, Plasmid, lysate colony template or confirmation of mutants, each 50µl reaction contained 200 ng DNA template, 400 µM Primers, 25 µl MyTaq Hs Mix 2X and H_2O up to 50 µl. This was mixed and incubated on a thermocycler. The initial denaturation was one cycle at 95ºC for 1 min, followed by 30 cycles 95ºC for 15 second, annealing temperature was based on the primer composition, for 15 second and extension at 72ºC for 10 second for amplicons under 1 Kb. Then final extinction at 72ºC for 5 minutes.

PCR primers were designed using specificity of primers was determined using NCBI's BLAST.

2.2.12 Chromatin digestion

2.2.12.1 Spheroplast preparation and lysis

The spheroplast preparation and lysis method was adapted from the protocols (Dunn & Wobbe, 1993). The yeast cells were grown in 1000 ml YEPD media in 2000 ml conical flasks with 200 rpm shaking at 30°C to a density of 3 - 4.0x10^7 nucleated cells/ml (mid-log phase). cells then were harvested by centrifugation in a sorvall rotor (SLA-1500 and SS-34 rotor) at 1500 g for 5 minutes at 4°C. The weight of the yeast cell pellet was determined in gram (~4 g)

The cells were resuspended by adding 1 vol zymolyase buffer (50 mM Tris Cl, pH 7.5, 10 mM $MgCl_2$, 1 M sorbitol and 30 mM DTT) and incubate 15 minutes at room temperature. When the incubation has done, centrifuge 5 minutes at 1500 g at 4°C and resuspend in 3 vol zymolyase buffer and add 2 mg yeast lysatic enzyme (YLE). Incubate at 30°C for 40 minutes. Centrifuge spheroplasts 5 min at 1500 g and decant the supernatant carefully. resuspending the pellet in 2 vol ice-cold zymolyase buffer and centrifuging 5 min at 1500 g. the washing step repeat two times.

The spheroplasts were resuspended in 1.2 ml Sphaeroplast Digestion Buffer (SDB) (1 M sorbitol, 50mM NaCl, 10mM Tris-HCl (pH 7.5), 5mM $MgCl_2$, 1mM $CaCl_2$, 1mM 2-mercaptoethanol, 0.5 mM spermidine and 0.075% (v/v) Nonidet P40 (Sigma)) by

pipetting. 200 µl aliquots (containing $2x10^8$ nucleated cells) were transferred to six 1.5 ml microfuge tubes containing MNase (Micrococcal nuclease (USB/Pharmacia) dissolved in 10 mM Tris HCl (pH 7.5), 10 mM NaCl, 100 µg/ml bovine serum albumin at 15 units/µl) or Stop solution (5% (w/v) SDS/250 mM EDTA made fresh by mixing equal volumes of 10% (w/v) SDS and 500 mM EDTA stocks) and mixed by pipetting. The tubes incubated at 37°C for 4 min. Of the six aliquots of cells, three were digested with MNase, and the other three were treated with Stop solution. The three undigested samples were later used to prepare marker digests and DNA for "naked DNA" controls. The digests terminated by adding of 20 µl Stop solution and mixed vigorously. The lysate was processed immediately to DNA purification described in (2.2.2 section) (Hoffman & Winston, 1987) .

2.2.12.2 Rapid Micrococcal nuclease digestion for MNase-Seq

This procedure was adapted from (Kent & Mellor, 1995)The yeast cells were grown to mid-log phase in YEPD at 32°C. 1 x 10^9 Yeast cells were harvested at 453 g for 2 min. Media was completely removed, and the cells were resuspended in 20mM EDTA and transferred to 2 ml tube. Samples were centrifuged at 1500 g, the supernatant was discarded, and the pellet was resuspended in 1 ml of spheroplasting solution containing 1 M sorbitol, 20 mg/ml yeast lytic enzyme (ICN, 20000 U/g) and 0.5 mM β-Mercaptoethanol by pipetting. The cells are incubated for 2-2.5 min at room temperature with constant gentle inversion of the tube. Spheroplasts are harvested by centrifugation at 13523 g for 10S and the spheroplasting solution pipetted off for re-use. The spheroplast pellet was washed twice in 1 ml 1 M sorbitol.

The sorbitol washes were aspirated after centrifugation at 13523 g for 5 S. The spheroplast pellet is then quickly resuspended in 1200 µl of digestion buffer (1 M sorbitol, 50 mM NaCl, 10 mM Tris-HCl (pH 7.4), 5 mM $MgCl_2$, 1 mM $CaCl_2$, 1 mM β-Mercaptoethanol, 0.5 mM spermidine, 0.075% (v/v) NP-40 and the appropriate nuclease). 3 µl MNase was added to the mix and incubated for 3 min at 37°C, followed by centrifugation at 17115 g. for 20 S. The supernatant then was added directly to termination solution (20 pl 250 mM EDTA/5% (w/v) SDS) on ice and mixed immediately.

2.3 Bioinformatic analysis

2.3.1 RNA-Seq data

The sequencing of pair end reads was performed by Eurofins, who used the Illumina Sequencing, HiSeq 2500 instrument. The software used was HiSeq Control Software 2.2.58, with the kit version HiSeq SBS Kit V4. The Mapping of reads to reference sequences was performed using BWA-MEM (version 0.7.12-r1039) (H. Li, 2013), and the coverage was 95% of the reference. Raw read counts were created using featureCounts version 1.5.1. The distributions of raw read counts, (raw) normalized to counts-per-million (CPM) values for all samples. Dr. Karsten Hokamp (Trinity College Dublin, Dublin, Ireland) analysed the differential transcription of genes between WT vs mutants, which was calculated from CPM values. Heatmaps were in general clustered in R using the heatmap function, which uses hierarchical clustering the transcription value vs the mutants (Metsalu & Vilo, 2015).

2.3.2 Gene ontology analysis

The gene ontology analyses were performed using tow software, the provided from *S. cerevisiae* database system (SGD)(Cherry *et al*. 1998). A second gene ontology analysis was performed using the panther gene ontology software (Mi *et al*. 2017). The use of each software was dependent on specific pathways to be analysed. The data was then presented by using Microsoft excel.

2.3.2 Preparation of Venn diagrams

The Venn diagrams was used in this research were prepared using FunRich software (M. Pathan *et al*. 2015).

2.3.3 Cluster dendrograms

The cluster dendrograms were in general clustered in R using ggplot2 packages (Galili, 2015).

2.3.4 ChIP-Seq analysis

The data of the ChIP-Seq experiment was provided from Wong and Struhl, (2011), the chromatin was prepared from the protocol described in Fan *et al*. (2008). The Tup1 was epitope tagged with FRB (Tup1-FRB), and Snf2 was epitope tagged with HA (Snf2-HA).

Antibody concentrations of 2 µl of anti-FRB (Alexis), and 2 µg of anti-HA (Santa Cruz Biotechnology) were used to immunoprecipitate protein-DNA complexes. The Anchor Away (AA) technique allows the creation of a conditional mutant of any nuclear protein (Haruki *et al*. 2008). The Tup1 protein is C-terminally tagged with an 11 kDa epitope which is the FKBP12-rapamycin-binding (FRB) domain of human mTOR to form the "target". The "anchor" is the ribosomal protein RPL13A, C-terminally fused to the human 12 kDa FK506 binding protein (FKBP12), which will bind to FRB in the presence of rapamycin (final concentration of 1 µg/ml). Ribosomal proteins naturally transit the nucleus during assembly of the 40S and 60S ribosome subunits (Köhler & Hurt, 2007). These abundant proteins, when tagged with FKBP12, will bind FRB in the presence of rapamycin. The target protein is then shuttled from the nucleus bound to the anchor, creating a rapamycin-induced conditional mutant. Because rapamycin is toxic to wild type yeast, Haruki *et al*. constructed host a strain containing a mutated TOR1 and deleted FPR1 gene which confers resistance to rapamycin, and allows for successful anchor-target interaction upon addition of rapamycin (Fig. 2.3).

The sequencing libraries were constructed according to Illumina's protocol (Illumina, 2012). Raw sequence reads were saved in (NCBI accession no. SRA044839.1) and were separated according to their bar codes. Dr. Karsten Hokamp (Trinity College Dublin, Dublin, Ireland) was responsible for the data merging of replicates, calculation of $\log_{10}$-ratios of the P-value (the lower P-value the higher peak score), and annotated to their closest promoter according to distance from the transcription start sited (TSS). Further analyses were done by myself.

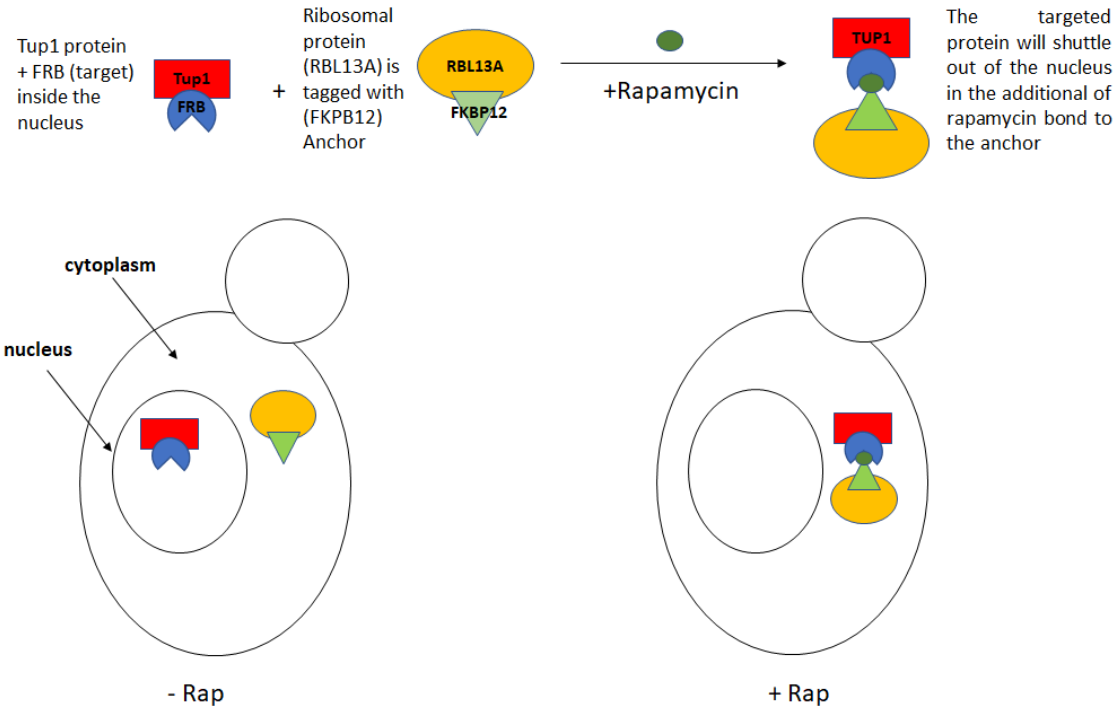

Figure 2.3 Anchor away technique. The Tup1 protein was epitope tagged by FRB in the nucleus, the ribosomal protein RBL13A was tagged by FKBP12. The addition of the rapamycin shuttled the Tup1 protein out from the nucleus.

2.3.5 Nucleosome Mapping

This work has done by Dr. Nicholas A. Kent (School of Biosciences, Cardiff University, Cardiff, Kingdom of Britain). Nucleosome DNA was sequenced by an Illumina-Solexa system, using paired ends. Sequencing reads were aligned using *S. cerevisiae* genome data base (Cherry *et al*. 1998) using the ELAND algorithm. A list of yeast transcription start sites were identified in David *et al*. (2006), and used in this study. The nucleosomes were annotated based on their closest promoter according to distance from TSS. The closest nucleosome upstream of each TSS, dyad within 500 bp, was annotated as −1, with the second closest as −2, and third as −3, and so forth.

Chapter 3

Characterisation of mutants deficient for Swi-Snf subunits

3.1. Introduction:

The Swi-Snf complex is an ATP-dependent chromatin remodelling complex that is required for the regulation of transcription of up to ~ 6% of all yeast genes (Yen *et al*. 2012). It most commonly plays a role in gene activation, although it has also been shown to negatively regulate a few genes. The yeast Swi-Snf complex contains 12 different subunits, with the Snf2 subunit being the catalytic heart of the complex which contains the ATPase activity (see Table 1.1). It is now becoming clear that the different subunits might make distinct contributions to Swi-Snf complex structure and function (Dutta *et al*. 2017). However, the relative contribution of each of the subunits to Swi-Snf activity has not been fully characterised.

I therefore analysed the phenotypes of different strains of yeast each defective for a particular Swi-Snf sub-unit. Specifically, I examined *snf2, swi3, snf5, snf6* and *snf11* gene deletion mutants, as well as a 'catalytically dead' *snf2* mutant strain (*snf2K798A*). This latter strain contains a lysine (K) to alanine (A) amino acid substitution at position 798, which cripples ATPase activity (Martens & Winston, 2002). Together, analysis of these mutants should yield phenotypes of strains deficient for three of the five proposed Swi-Snf sub-modules (see Table 1.1). Mutants deficient for Arp7, Arp9 and Rtt102 were not included in this analysis, as these subunits are also shared with the RSC chromatin remodelling complex (Monahan *et al*. 2008).

Overall, the aim was to examine strains deficient for Swi-Snf complex subunits for various phenotypes to determine which subunit is the most important for complex function. The prediction was that the different mutants might display phenotypes of varying severity depending on the importance of each subunit to Swi-Snf complex function. The Swi-Snf subunit with the greatest role would be combined with an *CYC8* gene deletion mutant and used in the transcriptome analysis to define the Tup1-Cyc8 and Swi-Snf co-regulated genes.

3.2. Results:

3.2.1. Analysis of growth in liquid media containing different carbon sources:

To investigate the growth of the mutants, the strains were individually inoculated into liquid culture containing either glucose (YPD), galactose (YPGal), sucrose (a glucose-fructose disaccharide) or raffinose (a trisaccharide of galactose, glucose and fructose), and the increase in optical density was monitored over time. Next, I examine the doubling time in each strain for each carbon source, when the cells entering to log phase to rise to maximum growth rate the time require for the strains to double in size and value is the doubling time.

3.2.1.1 Growth in glucose-containing broth:

In glucose-containing media (Fig. 3.1A), the *snf11* mutant showed no significant defect in growth, and actually grew to a higher optical density (OD) than wt. The *snf6* mutant showed a delay before maximum growth rate started, after which it achieved a maximum OD similar to wt. The *swi3* and *snf2K798A* mutants showed an even longer lag phase before reaching exponential phase after which the maximum ODs they achieved were half that of wt. The *snf5* mutant behaved in a similar manner to the *Swi3* and *snf2K798A* mutants but grew at a slightly slower rate than these strains. The *snf2* mutant showed the poorest growth on YPD. This strain showed the greatest delay before rapid growth started and achieved the lowest final optical density. Interestingly, the growth of the *snf2* mutant in which the Swi-Snf complex is lost (Dutta *et al*. 2017) and the *snf2K798A* mutant which has the intact complex but without ATPase activity (Martens & Winston, 2002) showed a difference in the growth rate which suggests that the complex itself, without the ATPase activity, is playing a role in the cell growth.

In doubling time which were used to measure the effect of the mutation in each strain compared with wt (Fig. 3.1B), the *snf11* growth rate similar to the wt with about 200 min to double in value and size. *snf2K798A* significant different than wt with about 380 minutes to duplicate in size and value, *snf6* different than wt took about 280 minutes to double, the *swi3* showed an increased in doubling time by about 300 minutes, *snf5* was

delayed in time to double by 400 minutes, *snf2* showed the most delayed in the growth with about 450 minutes doubling time. This suggest the *snf2* deletion has a more severe impact on cell growth.

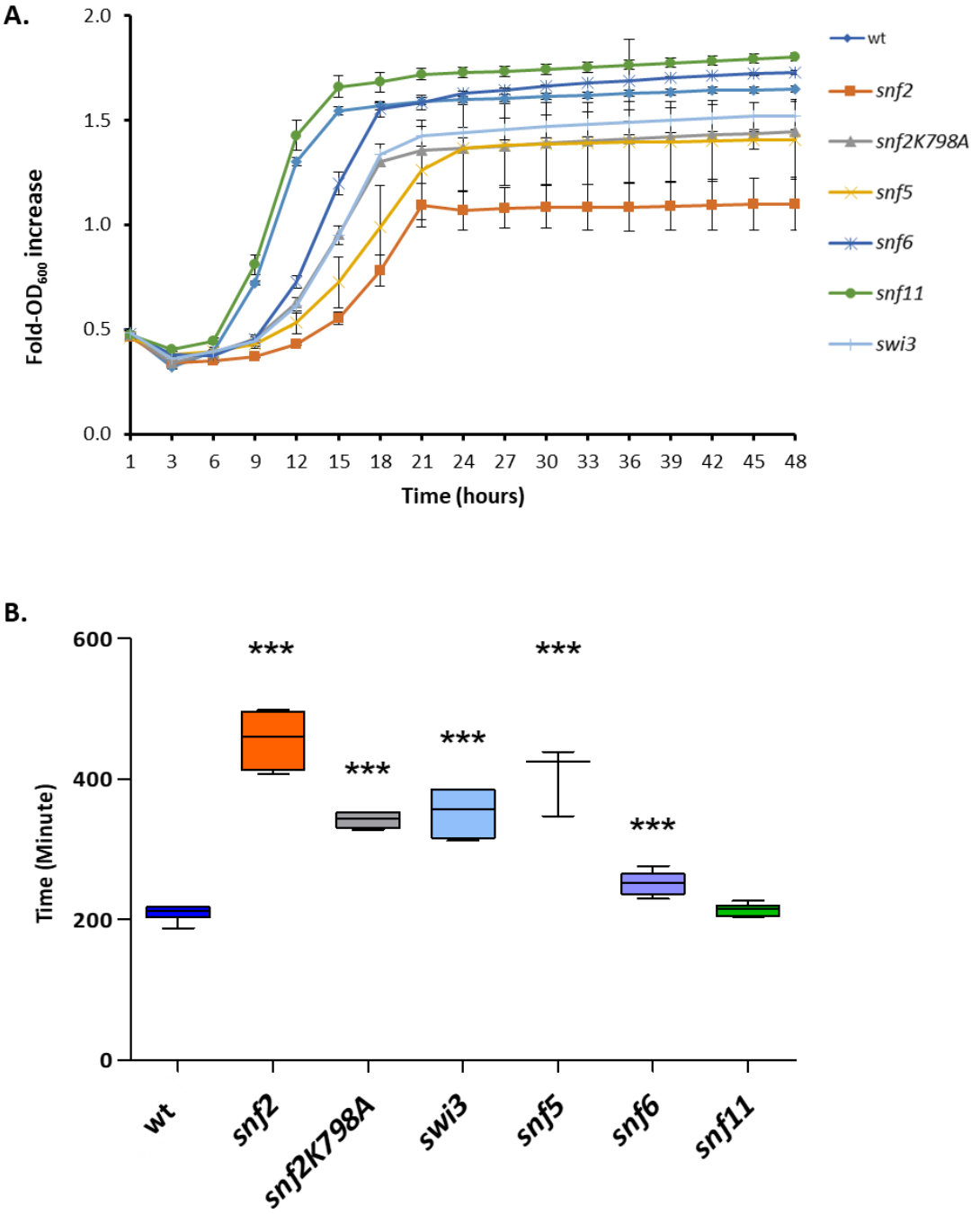

Figure 3.1 Analysing growth of Swi-Snf mutants on glucose. Wild type (wt) and Swi-Snf single mutants were grown at 30°C for 48 hours and (A) OD_{600} readings were taken at regular intervals. Cells were grown in YP-Glu. The experiment was performed in triplicate, and error bars represent standard deviation (SD). (B) Doubling time measurement compared with wt (BY4741). Standard student T-test determines significance (* p = 0.05, ** p = 0.01, *** p = 0.005).

3.2.1.2 Growth in sucrose-containing broth:

In sucrose-containing media (Fig 3.2A) each mutant showed a distinct difference in the time it took them to enter into exponential growth compared to wt. The *snf11* showed no significant defect than wt and grew to higher optical cells density (OD) than wt, *snf2K798A*, *swi3* and *snf6* showed a delayed in in lag phase and reached to the similar optical cell density (OD) as wt, whilst, *snf5* showed increasingly longer lag periods than wt prior to exponential growth eventually reach to similar OD as wt. overall, *snf2* showed the poorest growth in this media. In doubling time, compared with wt the *snf11* showed no different in doubling time with about 300 min to double. *snf2K798A* was taken 390 min to double, *swi3* and *snf6* were significantly delayed than wt with more than 400 min to double, *snf2* and *snf5* were the most delayed in doubling time with about 500 min (Fig. 3.2B).

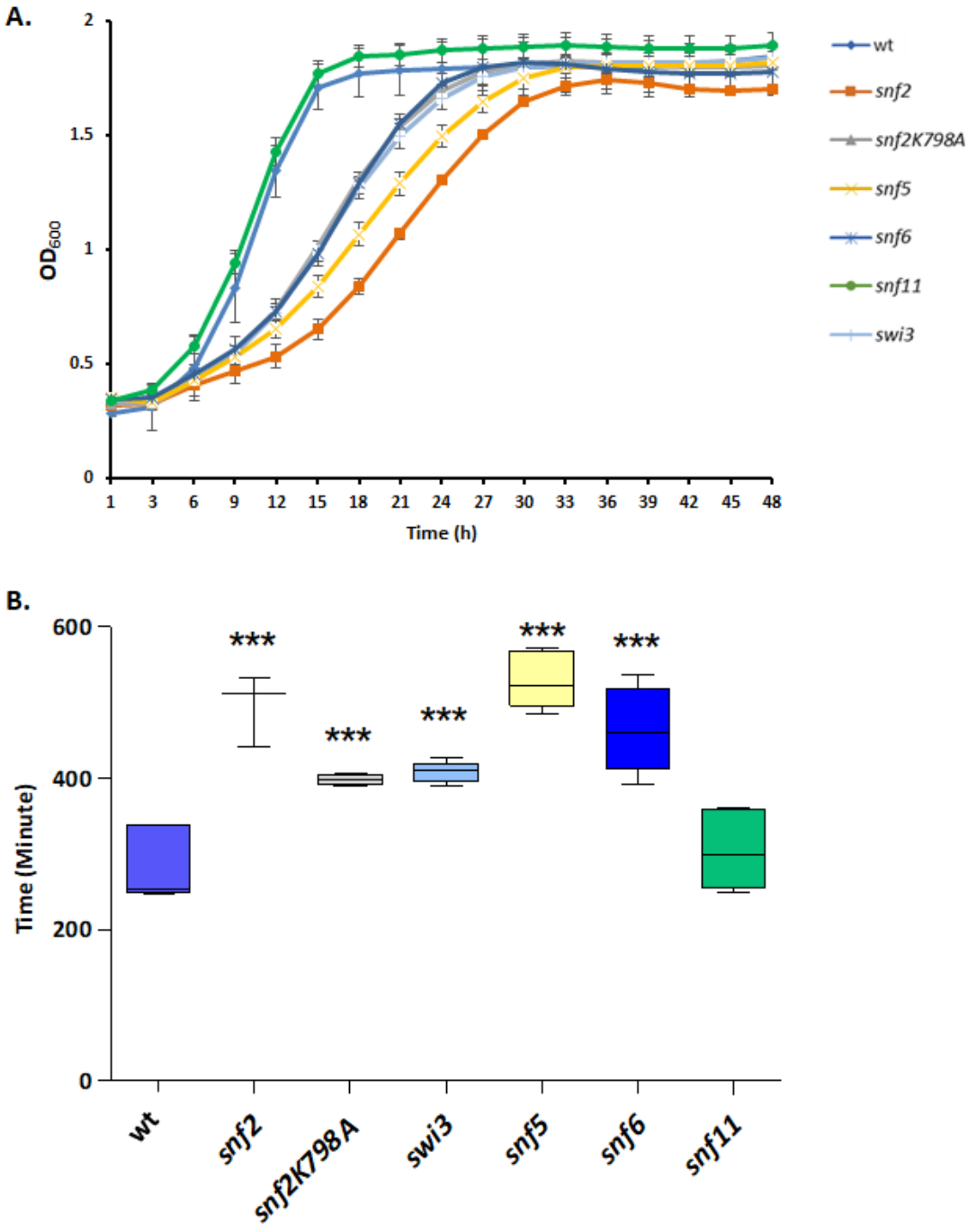

Figure 3.2 Analysing growth of Swi-Snf mutants on sucrose. Wild type (wt) and Swi-Snf single mutants were grown at 30°C for 48 hours (A) OD_{600} readings were taken at regular intervals. Cells were grown in YEP broth containing sucrose (a disaccharide of glucose and fructose). The experiment was performed in triplicate, and error bars represent standard deviation (SD). (B) Doubling time measurement compared with wt (BY4741). Standard student T-test determines significance (* p = 0.05, ** p = 0.01, *** p = 0.005).

3.2.1.3 Growth in galactose-containing broth:

In galactose-containing media, the differences in growth between the mutant strains was much more apparent (Fig. 3.3A). Growth of *snf11* was similar to wt, whereas *snf6* showed a delay before rapid growth started, and then grew at a slightly slower rate. The *snf2K798A* and *swi3* mutants showed a greater delay before rapid growth started compared to the *snf6* mutant. These strains growth also levelled off much later than wt, and at a lower OD. Interestingly, whereas the *snf2* mutant showed the greatest growth defect on glucose- and raffinose containing media, it was the *snf5* mutant that showed the greatest defect in growth on galactose. In doubling time, *snf11* was similar to wt with about 400 minutes, *snf2K798A* mutants slower than wt with about 750 minutes, *snf6* and *swi3* showed a delay with about 500 minutes to multiply, *snf2* and *snf5* showed the poorest growth with about 1000 minutes to multiply. In galactose media doubling time *snf5* sharing *snf2* mutants which they were the severely affected mutants (Fig. 3.3B).

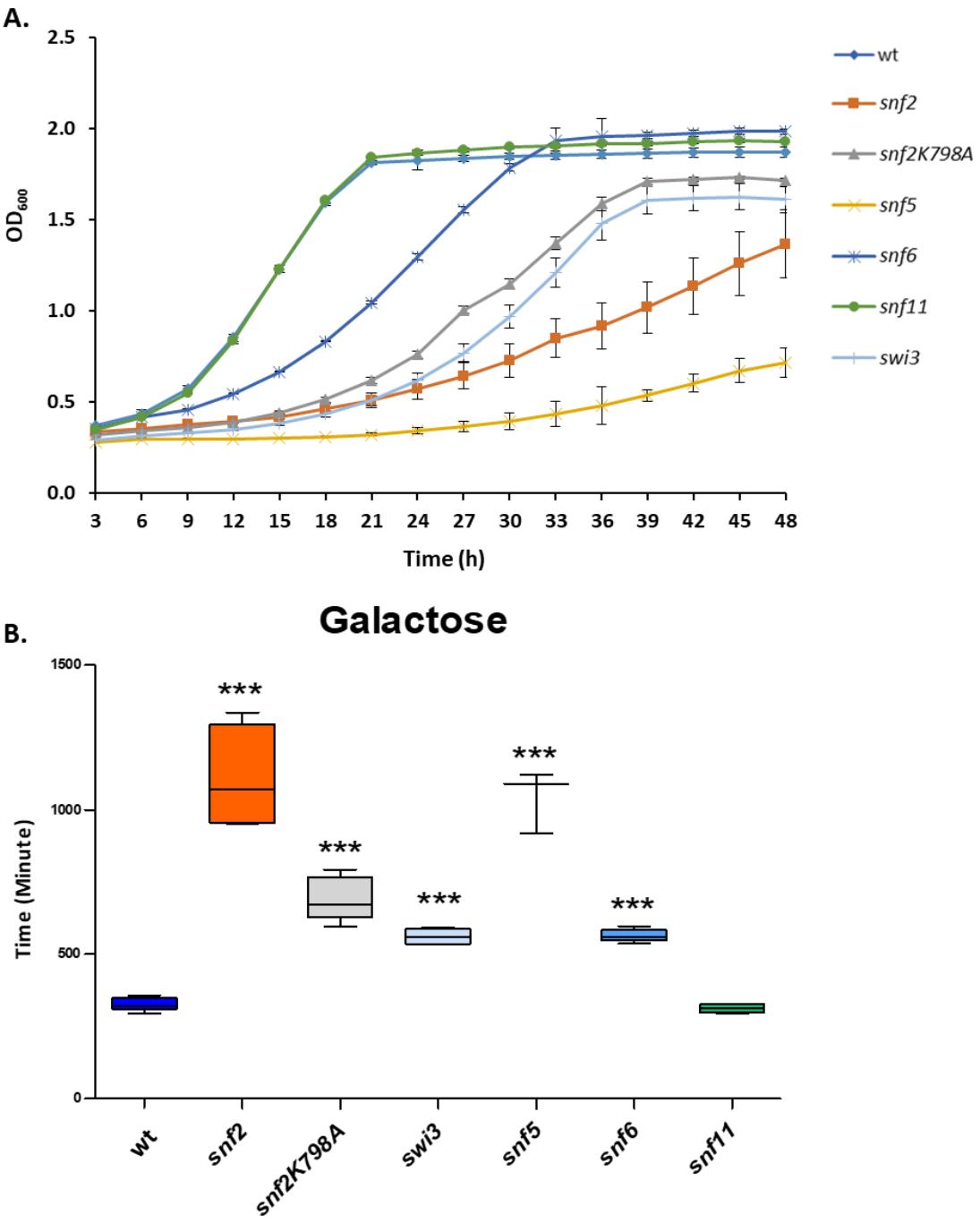

Figure 3.3 Analysing growth of Swi-Snf mutants on galactose. Wild type (wt) and Swi-Snf single mutants were grown at 30°C for 48 hours and (A) OD_{600} readings were taken at regular intervals. Cells were grown in YP-Gal. The experiment was performed in triplicate, and error bars represent standard deviation (SD). (B) Doubling time measurement compared with wt (BY4741). Standard student T-test determines significance (* p = 0.05, ** p = 0.01, *** p = 0.005).

3.2.1.4 Growth in raffinose-containing broth:

I next examined cell growth on media containing raffinose which is a trisaccharide consisting of galactose, glucose and fructose (Fig. 3.4A). The *snf11* mutant again showed a reduced lag phase compared to wt, and consistently yielded higher OD readings than wt throughout the growth period. The growth phenotypes of the *swi3*, *snf5* and *snf6* mutants were similar to wt. Conversely, the *snf2K798A* and *snf2* mutants showed the greatest growth defects. In doubling time, *snf6* and wt are similar with about 1000 minutes to double, *snf2K798A* delayed with about 1400 minutes, in *snf11* are slightly different than wt with about 1200 minutes to double, *swi3* and *snf5* showed a delayed with about 1500 minutes, *snf2* showed the poorest doubling time with about 1700 minutes (Fig. 3.4B).

Together, these data show that the different Swi-Snf subunits make different contributions to cell growth on different carbon sources in liquid culture. In general, the *snf11* mutant showed the least difference in growth, the *snf2* mutant strains grew worst in glucose and raffinose whilst the *snf5* mutant grew the worst in sucrose and galactose-containing media.

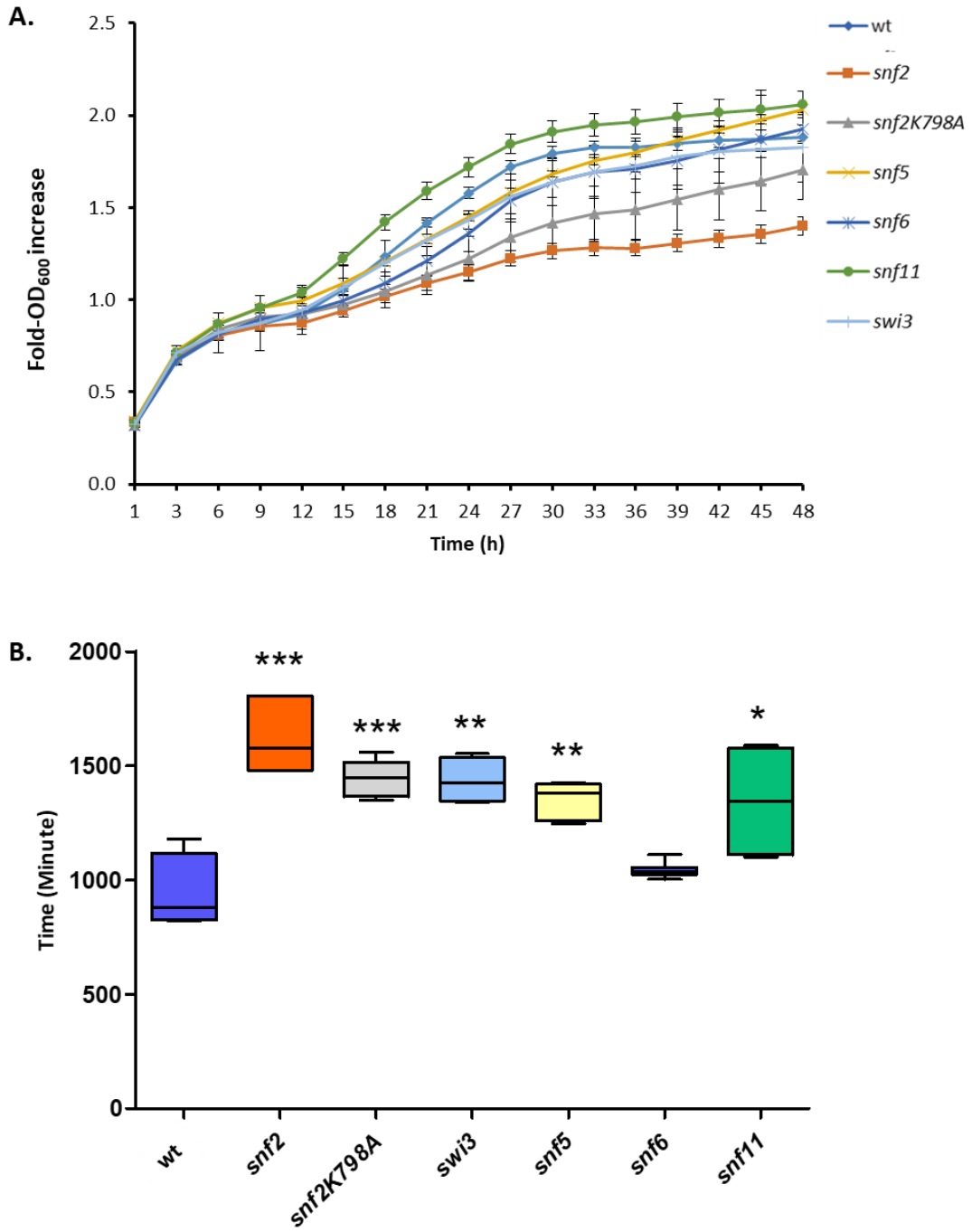

Figure 3.4 Analysing growth of Swi-Snf mutants on raffinose. Wild type (wt) and Swi-Snf single mutants were grown at 30°C for 48 hours and (A) OD_{600} readings were taken at regular intervals. Cells were grown in YP-Raf. The experiment was performed in triplicate, and error bars represent standard deviation (SD). (B) Doubling time measurement compared with wt (BY4741). Standard student T-test determines significance (* p = 0.05, ** p = 0.01, *** p = 0.005).

3.2.2. Analysis of fermentation ability during growth on solid media containing different carbon sources:

I next examined the various Swi-Snf mutants for their ability to perform fermentation when grown on solid media containing different carbon sources. Cells were resuspended to the same cell density and serial dilutions were prepared from which equal numbers of cells were spotted onto YEP plates containing Antimycin A and either glucose, raffinose or galactose. Antimycin A was used as a drug to block respiration thereby allowing us to examine the ability of the cells to metabolise solely via fermentation (Breitenbach-Schmitt *et al*. 1984). When cells were challenged to undergo fermentation when grown on galactose, the *snf11* mutant showed no difference in the ability to grow on the galactose-containing plate as compared to wt (Fig. 3.5, compare growth on YPGal and YPGlu (+Anti A)). The *snf6* and *snf2K798A* mutants showed a mild growth retardation on the galactose plates containing antimycin A. Conversely, the *swi3* and *snf5* deletion strains showed a more severe growth defect, whilst fermentative growth of the *snf2* deletion mutant was completely abolished on galactose.

When the experiment was repeated to assess fermentative growth on raffinose-containing plates, the *snf2* mutant showed the greatest growth defect, which was similar to the growth defect of this mutant when challenged to undergo fermentation on glucose plates. Thus, the *snf2* mutant showed the greatest defect in fermentative growth upon galactose, raffinose and glucose-containing agar plates.

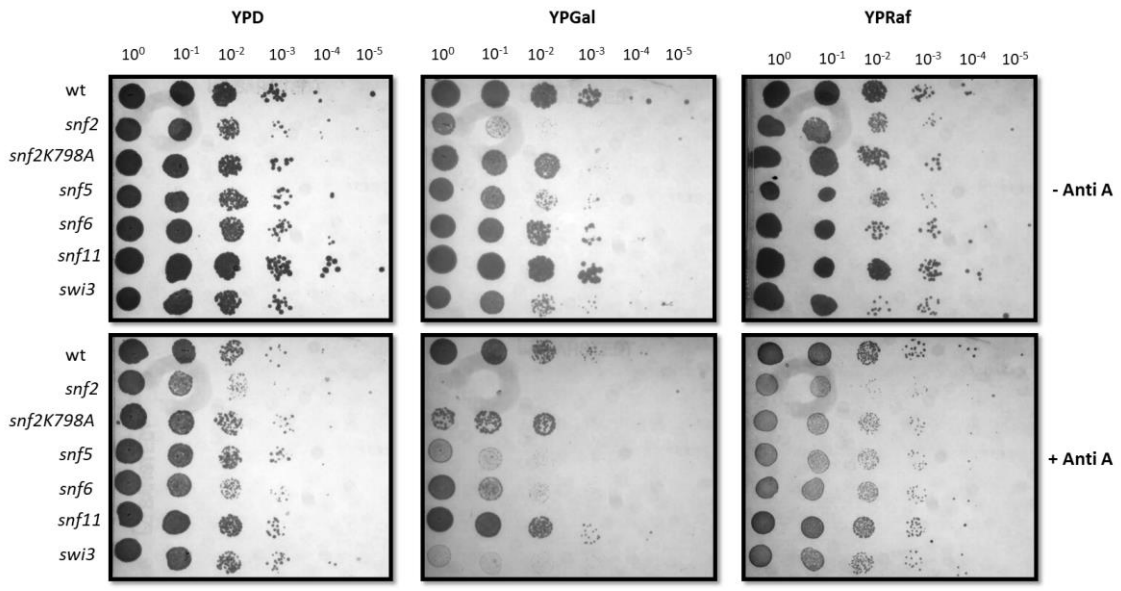

Figure 3.5 Fermentative growth capacity of Swi-Snf mutants on different carbon sources. Spot tests of yeast cells from each of the strains indicated were plated as 10-fold serial dilutions starting from 1 x 10^7 cells/ml. Strain were spotted onto YP media containing glucose (YPD), Raffinose (YPRaf) and Galactose (YPGal) with (+) and without (-) antimycin A (Anti A) as an electron transport inhibitor and incubated at 30°C.

3.2.3. Analysing Swi-Snf mutant cell morphology:

The Swi-Snf mutants were examined under the microscope to reveal diverse cell morphologies (Fig. 3.6). Compared to wt cells, the *snf2* and *snf2K798A* mutants appeared as small clumps of between 4 to 8 cells. These clumps were not dispersed by the addition of EDTA suggesting this cell aggregation was not due to flocculation (data not shown) (Soares, 2011). There was no obvious difference between *swi3* and *snf5* cell morphology compared to wt. However, the *snf6* cells showed a high frequency of elongated cells, a phenotype also apparent in the *snf11* mutant, but to a lesser extent.

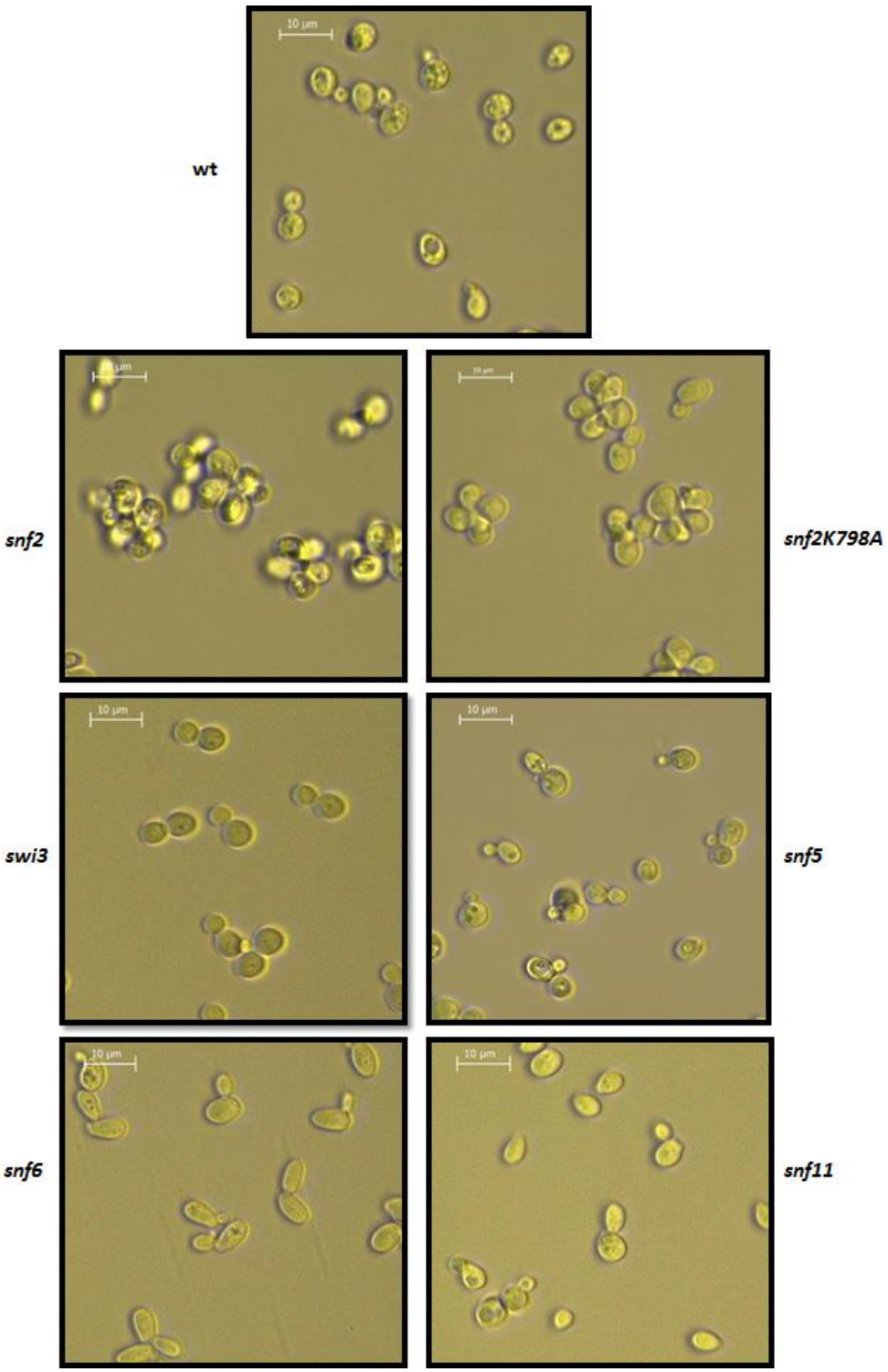

Figure 3.6 Swi-Snf mutant cell morphology. The Swi-Snf mutant strains indicated were grown on YPD, and cells from exponentially growing cultures were examined under the microscope. Microscopy was performed under 100X oil immersion magnification. White scale bar represents 10 µm.

3.2.4. Analysing Swi-Snf mutants for cell wall stress:

Here, I investigated the Swi-Snf mutants for their response to cell wall stress by exposing cells to caffeine (Fig. 3.8). Caffeine has pleiotropic effects on yeast, but is commonly used to evaluate the function of the Mpk1p-mediated cell wall integrity pathway and thus assess resistance of yeast to cell wall stress (Kuranda *et al*. 2006; Levin, 2005). Cells were normalised to an equal cell density and serial dilutions were prepared from which aliquots were spotted onto YPD plates containing caffeine at the concentrations shown.

The results showed that each of the *snf2*, *snf2K798A, snf6*, and *swi3* mutants grew slower than wt. Conversely the *snf5* mutant strain grew better than wt, whilst the *snf11* strain growth was unaffected by the presence of Caffeine. Overall, the Swi-Snf mutants showed a variety of sensitivities to the presence of caffeine in the growth media with *snf2* mutant being the most sensitive and *snf11* showing no sensitivity.

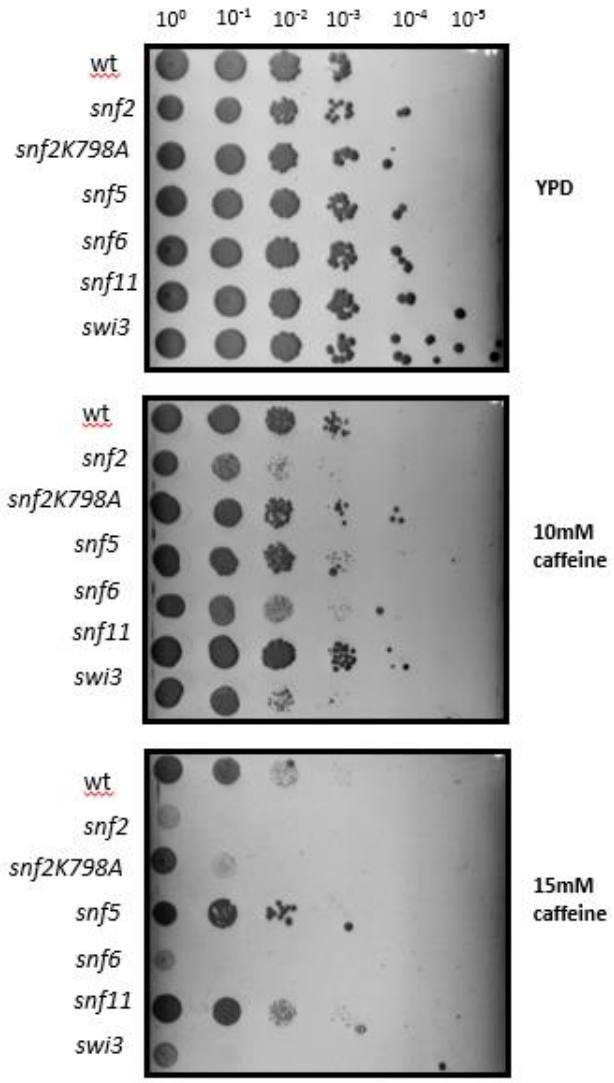

Figure 3.7 Testing cell sensitivity to caffeine. Comparison between wild type and the Swi-Snf mutant strains indicated for sensitivity to growth on YPD plus caffeine. 5 µl of each of the strains at the dilution indicated were plated onto the plates shown and photographed following 48 h of growth.

3.2.5. Analysing Swi-Snf mutants for DNA damage sensitivity:

Swi-Snf was first characterised as a positive regulator of gene transcription (Dutta *et al*. 2017). However, studies have revealed it also plays a role in DNA damage repair pathways (Chai *et al*. 2005). We therefore tested the various Swi-Snf mutants for their response to the DNA damaging agents methyl methanesulfonate (MMS) and hydroxyurea (HU). MMS is a DNA alkylating agent that causes DNA fragmentation following the inhibition of DNA replication (Lundin *et al*. 2005). HU acts to inhibit the enzyme ribonucleotide reductase to reduce dNTPs levels which also initially inhibits DNA replication leading to replication fork collapse and DNA double strand break formation (Koç *et al*. 2004).

Cells were grown until exponential phase in YPD, normalised to an equal cell density, and serial dilutions were prepared from which equal volumes were spotted onto YPD plates containing either MMS or HU at the concentrations shown (Fig. 3.7 A and B).

Surprisingly, when cells were challenged with MMS, all of the Swi-Snf mutants, with the exception of *snf6*, showed an increased resistance to growth in the presence of this reagent compared to wt (Fig. 3.7A). Only the *snf6* mutant was more sensitive to MMS than wt.

When the experiment was repeated using HU, the Swi-Snf mutants showed a much more diverse growth response to the presence of this reagent (Fig. 3.7B). Whereas *snf11* mutants showed no sensitivity to HU, *snf2* and *swi3* mutants were extremely sensitive to HU, with growth of *swi3* almost totally abolished in the presence of 50 mM HU. *snf5* and *snf6* mutants showed an intermediate sensitivity to HU. Interestingly, although the *snf2K798A* mutant did show a sensitivity to HU, this sensitivity was significantly less than that observed in the *snf2* deletion mutant where growth was severely inhibited compared to wt.

Together, these data show that mutants in the different subunits of Swi-Snf show varying responses to the presence of DNA damage inducing agents suggesting distinct roles for the subunits in the DNA damage response.

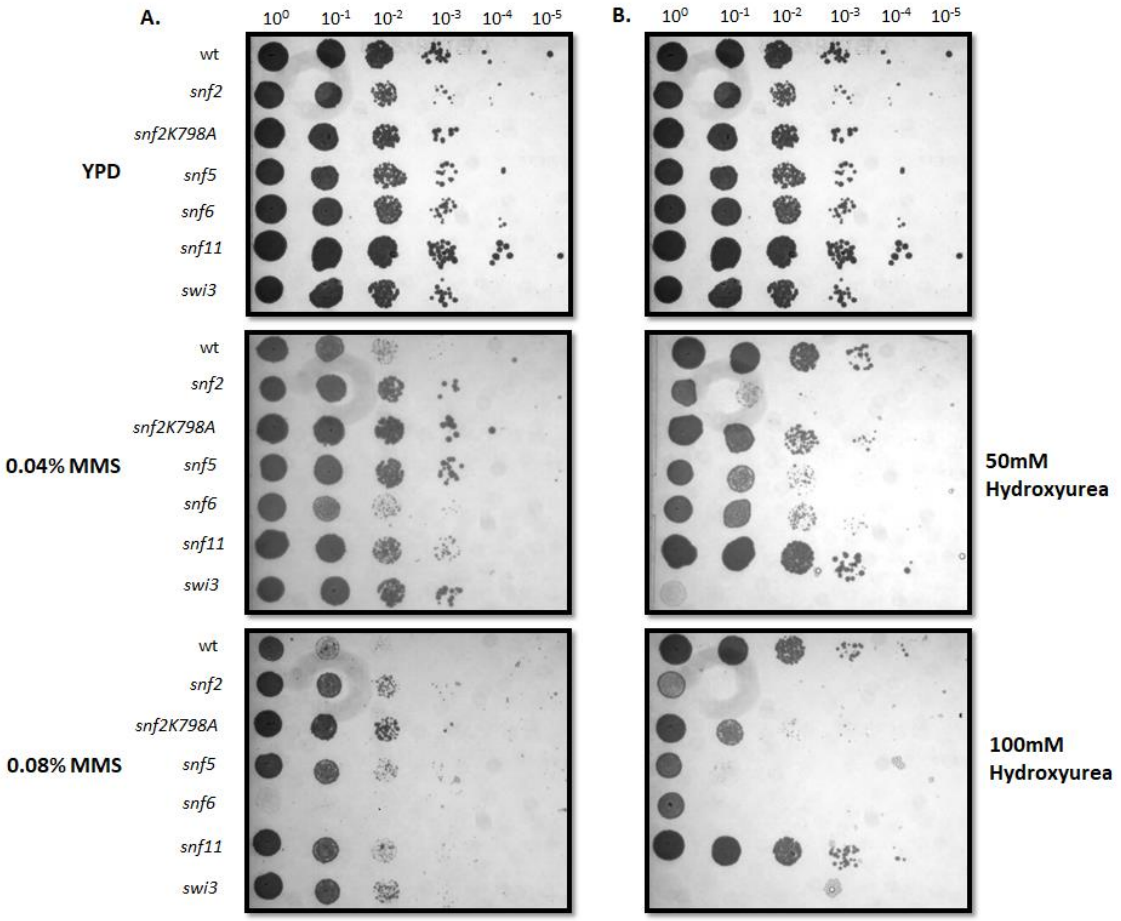

Figure 3.8 Testing cell sensitivity to DNA damaging reagents: Cells from each of the strains indicated were plated as 6-fold serial dilutions starting from 1 x 10^7 cells/ml. 5 µl of culture was spotted on YPD. YPD containing different concentration of methyl methanesulfonate (MMS) (A). YPD media containing different concentration of hydroxyurea (HU)(B).

3.3 Discussion:

Initial experiments aimed to establish which Swi-Snf subunit would be the best to delete in order to determine and analyse the genes co-regulated by Swi-Snf and Tup1-Cyc8. Recent work had suggested that different Swi-Snf sub modules exist which may perform specialist functions within the Swi-Snf complex (Dutta *et al*. 2017). We therefore tested mutant strains deleted for the various Swi-Snf sub units to determine if they had different phenotypes or showed differing severity of phenotypes. It was hoped such an approach would identify whether the different Swi-Snf sub units made differing contributions to complex activity and cell function. Interestingly, we did observe that the strains containing different Swi-Snf sub unit mutations did show a range of different phenotypes, suggesting the different sub units did indeed make distinct contributions to complex function

For example, when these mutants were grown in broth on different carbon sources, whereas the *snf11* mutant showed no significant defect in growth on any carbon source and often grew to a higher optical density (OD) than wt (Fig. 3.1), other mutants did not grow as well as wt. Indeed, the *snf2* mutant showed the poorest growth on glucose (Fig. 3.1), Sucrose and raffinose, whilst the *snf5* mutant showed the poorest growth on galactose. The growth difference in *snf5* mutants in galactose may suggest that other Swi-Snf subunits do not have the ability to degrade the galactose via the enzymes of the Leloir pathway (Sellick *et al*. 2008). The Snf5 subunit is a member of Snf5/Swi3 module which consist of two submodules: a Snf6-Snf12-Swi3 sub-module and a Snf5-Swp82-Taf14 sub-module, the loss of Snf5, the Swp82 and Taf14 subunits no longer associated with Swi1, Snf2 or Snf6 associated complexes (Dutta *et al*. 2017).

Furthermore, the other mutants tested showed various intermediate defects in growth on these carbon sources.

In galactose-containing media, the differences in growth between the mutant strains were the most apparent (Fig. 3.3). Growth of *snf11* was again similar to wt, whereas *snf6* showed a delay before rapid growth started, and then grew at a slightly slower rate. The *snf2K798A* and *swi3* mutants showed a greater delay before rapid growth started compared to the *snf6* mutant. These strains growth levelled off much later than wt, and

at a lower OD. Interestingly, whereas the *snf2* mutant showed the greatest growth defect on glucose-, sucrose- and raffinose-containing media, it was the *snf5* mutant that showed the greatest defect in growth on galactose.

In doubling time *snf11* showed no different than wt in all different carbon source media, whereas, the *snf2* mutants showed the poorest doubling time in glucose-, sucrose and raffinose-containing media. Indeed, the *snf5* sharing *snf2* with the poorest doubling time in galactose-containing media.

When the mutants were investigated for fermentation-dependent growth on solid media with different carbon sources, the *snf2* mutant again showed the greatest growth defect on galactose and raffinose containing media (Fig. 3.5). However, the *swi3* mutant also grew very poorly on the galactose plates. Together, it showed the different subunits made different contributions to cell metabolism and growth, albeit with the *snf2* gene deletion often making the greatest contribution.

The mutants also showed varying cell morphologies. Whereas the *snf2* and *snf2K798A* mutants existed mainly in small clumps of 4 to 8 cells, the *snf6* mutants showed an elongated cell phenotype. Since the clumps of *snf2* and *snf2K798A* cells could not be dispersed by EDTA, the clumpy phenotype does not appear to be a flocculation phenotype and could be due to inefficient cell separation. The elongated cell phenotype in the *snf6* mutant could also be due to aberrant cell wall regulation (Fig. 3.6). Together, the data suggest that Swi-Snf may have important roles in cell wall architecture and regulation and that different Swi-Snf sub units play distinct roles in regulating the cell wall structure and function. This conclusion is further supported by the results from exposing the mutants to the cell wall stress agent, caffeine. Indeed, the strains most sensitive to caffeine were the *snf2* and *snf6* mutants which displayed cell morphologies consistent with defects in cell separation and cell shape, respectively (Fig. 3.7). Conversely, although the *swi3* mutant showed great sensitivity to caffeine, it displayed no apparent cell morphology defects. It would therefore be interesting to expose the Swi-Snf mutants, and *swi3* in particular, to other cell wall stressing agents to determine if the distinct Swi-Snf subunits contribute to a specific aspect of cell wall metabolism or not.

I also examined the abilities of the different mutants to grow in the presence of the DNA damaging agents, methyl methanesulfonate (MMS) and hydroxyurea (HU) (Fig. 3.8). Although MMS and HU inhibit DNA replication by different mechanisms, both reagents lead to double strand DNA breaks (DSBs). When cells were grown in the presence of MMS, the *snf6* mutant showed the greatest sensitivity to its presence compared to wt. Most surprisingly however, the other Swi-Snf mutants grew even better than wt in the presence of this reagent. This is consistent with research that shows Swi-Snf plays a role in the DNA damage response (Chai *et al*. 2005). The increased growth of the mutants in the presence of this drug might suggest that the normal cell cycle arrest and repair mechanisms which should occur in response to double-stranded DNA breaks (dsDSBs), do not occur in these mutants (J. Chen, 2016). Thus, it might be predicted these mutants would continue replication and accrue DNA damage which goes unrepaired. However, the decreased growth of the *snf6* mutant in the presence of MMS suggests this sub unit plays a distinct role in response to replication stress and DSBs compared to the other Swi-Snf sub units.

When the cells were grown in the presence of HU (Fig. 3.7), the *swi3* mutant showed the greatest sensitivity, and was most inhibited for growth compared to wt and the other Swi-Snf sub unit mutants. This again highlights that the different sub units make different contributions to the DNA damage response.

The aim of these experiments was to determine which Swi-Snf sub unit would be the best one to delete in combination with a gene deletion for either Tup1 or Cyc8 so that I could eventually identify the cohort of genes regulated by both Swi-Snf and Tup1-Cyc8. Interestingly, no single mutant showed a consistently severe phenotype under all of the conditions used. Instead, there was considerable diversity of phenotypes in the different Swi-Snf subunit mutants. Perhaps not surprisingly, the *snf2* gene deletion mutant did show severe defects under many of the conditions used, and it was therefore taken forward for further analysis, together with the *snf2K798A* mutant. However, the *snf5* mutant had the most severe growth defects for growth in sucrose and galactose-containing liquid media and the *swi3* mutant was most resistant to fermentative growth on galactose plates and was also most sensitive to exposure to HU. Thus, the *snf5* and *swi3* mutants were also taken forward to be combined with *cyc8* gene deletions.

Chapter 4

Characterisation of mutants deficient for both Swi-Snf and Tup1-Cyc8

4.1. Introduction:

The aim of this project is to identify those genes co-regulated by Swi-Snf and Tup1-Cyc8. To achieve this, I required a mutant deficient for both Swi-Snf and Tup1-Cyc8. Thus, the next experiments aimed to characterise double mutants deficient for various Swi-Snf sub units and *cyc8* in order to determine which mutant would be best to use in the transcriptome analysis.

I chose to delete the *CYC8* gene, and not *TUP1*, since the evidence suggests that Tup1 occupancy should be abolished at Tup1-Cyc8 target genes in an *cyc8* mutant, whereas Cyc8 might persist in a *tup1* mutant (Fleming *et al*. 2014). Thus, a *cyc8* mutant should be representative of a strain totally deficient in Tup1-Cyc8 activity. I therefore analysed *cyc8* mutants in combination with the *snf2*, *snf2K798A*, *swi3* and *snf5* mutants. Together, these combinations enabled comparison of the phenotypes of mutants defective for Tup1-Cyc8 and three of the five sub-modules of Swi-Snf (Dutta *et al*. 2017).

Using the *snf2* and *snf2K798A* mutants also allowed me to test whether there were any differences in phenotype between when Swi-Snf is crippled by the complete absence of *snf2*, which has also been shown to perturb Swi-Snf structural integrity, or when the activity of Swi-Snf is crippled by an amino acid sub in which complex integrity should remain intact (Dutta *et al*. 2017; Martens & Winston, 2002). Considering the aim of this project is to identify and investigate the genes co-regulated by Swi-Snf and Tup1-Cyc8, use of these two different *snf2* mutants which both cripple Swi-Snf activity but have opposite effects on complex integrity might elucidate whether steric hindrance between Swi-Snf and Tup1-Cyc8 plays a role their gene regulatory function.

4.2. Results:

4.2.2. Examining the role of Swi-Snf subunits upon flocculation:

In wt laboratory strains the *FLO1* gene is repressed by the Tup1-Cyc8 complex (Fleming *et al*. 2014). In the absence of *CYC8*, *FLO1* transcription is de-repressed and cells become flocculent. This *FLO1* de-repression is considered Swi-Snf dependent, since an additional *snf2* deletion in the *cyc8* mutant background abolishes *FLO1* transcription and flocculation (Fleming & Pennings, 2001). I therefore analysed the flocculation phenotype

in *cyc8* mutants additionally deleted for either *snf2*, *swi3*, *snf5*, or containing the *snf2K798A* mutation. If the different Swi-Snf mutants all play the same role in *FLO1* transcription, then flocculation should be abolished in all of the double mutants.

Cells were grown to the same cell density and visualised to look for flocculation (Fig. 4.1). As expected, the wt and the Swi-Snf single mutants showed no flocculation. Conversely, and consistent with previous results, the *cyc8* single mutant cells exhibited a strong flocculation (clumpy) phenotype (Fig. 4.1, bottom row). However, the *snf2 cyc8, snf2K798A cyc8,* and *swi3 cyc8* double mutants showed a vast decrease in flocculation compared to the *cyc8* single mutant, showing the requirement of flocculation upon *snf2* and *swi3*. Interestingly, the *snf5 cyc8* double mutant did not show a significant decrease in flocculation suggesting the role of Swi-Snf in transcription of *FLO1* does not require the Snf5 sub unit.

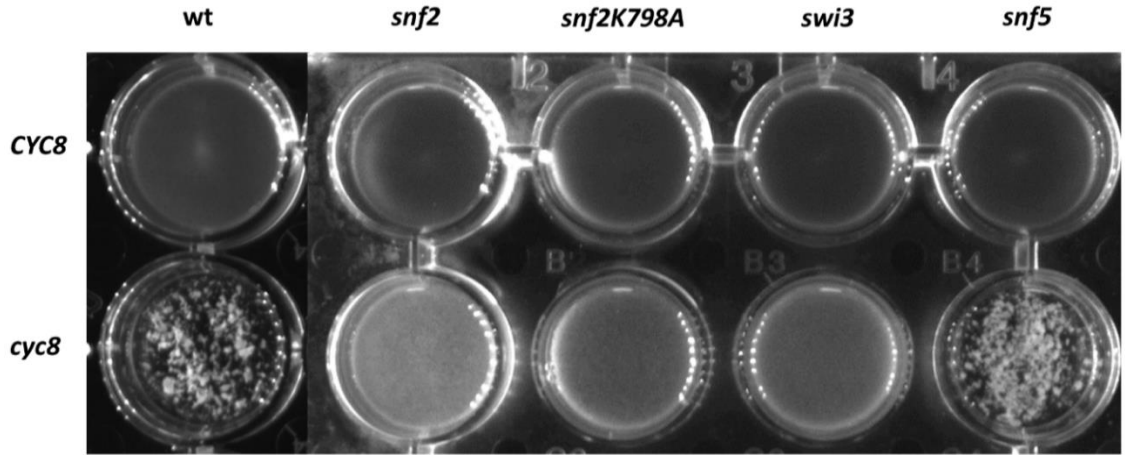

Figure 4.1 Flocculation phenotype. wt, *snf2*, *snf2K798A*, *swi3* and *snf5* mutants were assayed for flocculation in the presence (*CYC8*), and absence (*cyc8*), of the *CYC8* gene. Cells were grown to log phase and normalized to $2x10^7$ cells/ml and flocculation visualised in tissue culture plate.

4.2.3 Examining the role of Swi-Snf subunits upon *FLO1* and *SUC2* transcription:

I next analysed transcription of the *FLO1* and *SUC2* genes which were both previously shown to be under control of Swi-Snf and Tup1-Cyc8 (Fleming and Pennings 2007; Fleming and Pennings 2001). As expected, the data showed that the *SUC2* and *FLO1* genes are repressed in the wt, *snf2*, *snf2K798A, swi3* and *snf5* mutant strains, where Tup1-Cyc8 is present (Fig 4.2). However, in the absence of *cyc8*, both *FLO1* and *SUC2* are de-repressed and the mRNA production was detected. When *snf2* is additionally deleted in the *cyc8* mutant background (*snf2 cyc8* double mutant), both *FLO1* and *SUC2* transcription are significantly reduced. I also prepared double mutants deleted for *cyc8* and containing either the *snf2K798A* mutation or the *swi3* and *snf5* gene deletions, to look at the impact of the loss of *swi3*, *snf5* and the catalytic activity of *snf2*, upon *SUC2* and *FLO1* de-repression. The results showed the *snf2K798A* and *swi3* mutations, when combined with the *cyc8* deletion (*snf2K798A cyc8 and swi3 cyc8*), largely abolished the *FLO1* mRNA levels seen in the *cyc8* single mutant. The same double mutants also reduced *SUC2* levels compared to the *cyc8* single mutant, but not to the same low levels observed in the *snf2 cyc8* double mutant. When *snf5* was deleted together with *cyc8*, the *SUC2* and *FLO1* mRNA levels in these strains were only about 2-fold lower than the levels in the *cyc8* single mutants, suggesting that the other Swi-Snf subunit may have a greater impact on the transcription of *FLO1* and *SUC2*.

I also analysed the constitutively transcribed *PMA1* gene which is not known to be under Swi-Snf or Tup1-Cyc8 control. No significant difference in mRNA levels from this gene was observed in any of the mutants compared to wt (Fig 4.2, C). Together, this suggests that Snf2 plays the greatest role in transcription of both *FLO1* and *SUC2* when the Tup1-Cyc8 repressor is absent, whilst Snf5 is only partially required for transcription (Fig. 4.2).

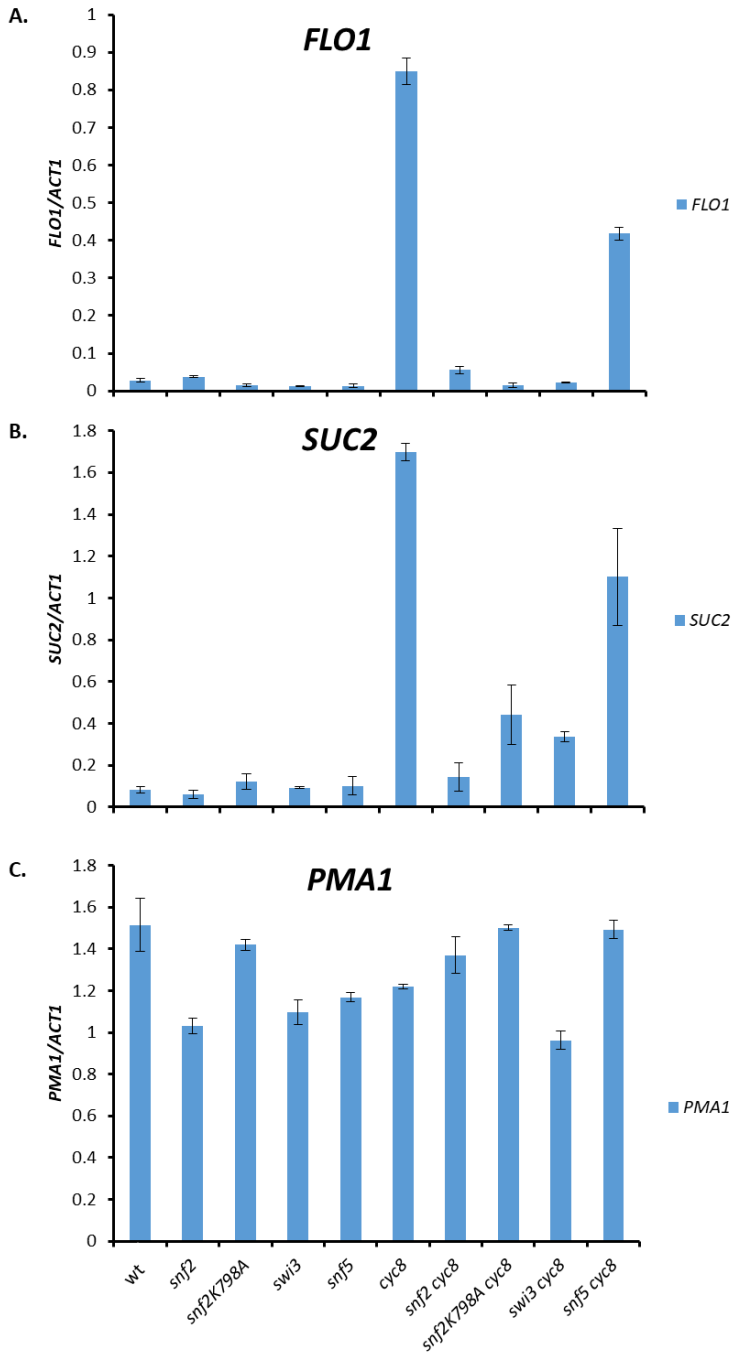

Figure 4.2 *FLO1* and *SUC2* transcription in the absence of *CYC8* and Swi-Snf subunits. (A) *FLO1,* (B) *SUC2* and (C) *PMA1* gene transcription was analysed by RT-qPCR in wt, *snf2, snf2K798A, snf5* and *cyc8* single mutant, *snf2 cyc8, snf2K798A cyc8* and *snf5 cyc8* double mutants. Transcript levels of *PMA1*, *FLO1* and *SUC2* were measured in triplicate and normalised to transcript levels of *ACT1*. Error bars represent standard error of the mean (SEM).

4.2.4 Investigating whether Tup1-Cyc8 and Swi-Snf regulate transcription of each other:

I also examined *CYC8*, *SNF2, SWI3* and *SNF5* mRNA levels in each of the strains to determine if the complexes regulated transcription of their own subunits or transcription of each other's subunits. Interestingly, the level of the *CYC8* transcription was significantly high in *swi3* mutants relative to wt, while other mutants showed no significant different (Fig. 4.3 A). in the *SWI3* transcription it was significantly low in *cyc8*, *snf2 cyc8* and *snf2K798A cyc8* while it was no change in the level of mRNA with other mutants (Fig. 4.3 B), in *SNF2* transcription there was no dramatic change for all the mutants except *swi3* which was highly transcribed than wt (Fig. 4.3 C). In *SNF5* transcription *swi3 cyc8* was significantly high than wt other mutants showed no dramatically different than wt (Fig. 4.3 D).

Overall, no such regulation of transcription was observed, although *SNF2*, *SWI3* and *SNF5* mRNA levels were consistently lower in the *cyc8* mutant (Fig. 4.3).

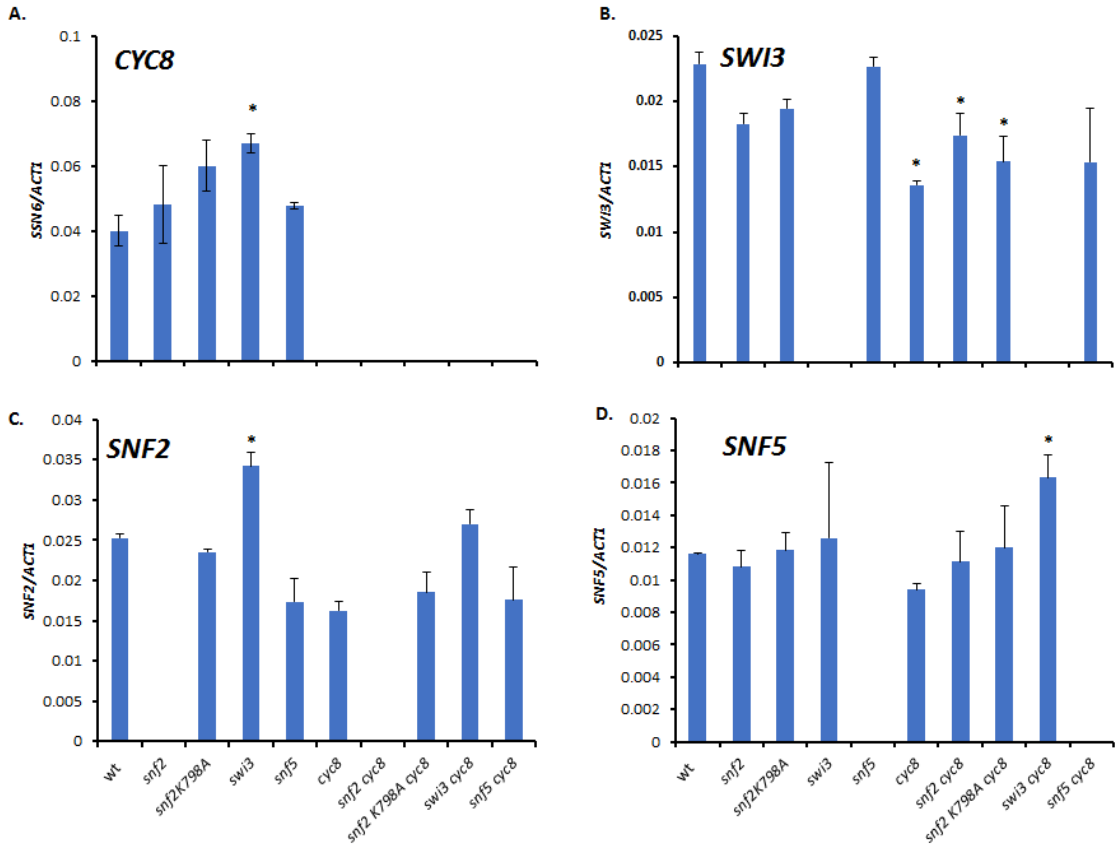

Figure 4.3 Transcription of *CYC8*, *SNF2*, *SWI3* and *SNF5* genes in the absence of *cyc8* and Swi-Snf subunits. (A) *TUP1*, (B) *CYC8* and (C) *SNF2* gene transcription was analysed by RT-qPCR in wt, *snf2, snf2K798A, snf5* and *cyc8* single mutant, *snf2 cyc8, snf2K798A cyc8* and *snf5 cyc8* double mutant. Transcript levels of were normalised to transcript levels of *ACT1*. Error bars represent standard error of the mean (SEM). Asterisks indicate the student's t-test a significance level of $p < 0.05$.

4.2.5 Investigating Swi-Snf protein levels in *cyc8* and Swi-Snf mutants:

To complement the previous mRNA analysis, western blot analysis was performed to determine Snf2, Swi3, Snf5, Snf6, Snf11, Tup1 and Cyc8 protein levels in the various single mutants (Fig. 4.4 and 4.5). Indeed, the formal possibility exists that Swi-Snf might influence Tup1 and Cyc8 protein levels and vice-versa, and that Tup1 and Cyc8 might also impact each other's stability.

The data showed that the Snf2 protein levels were slightly reduced in the *cyc8* and *snf2K798A* mutants (Fig. 4.4). Swi3 levels were also reduced in the *cyc8* and both *snf2* mutants, whereas Snf5 protein levels were reduced compared to wt in the *cyc8* strain. Finally, Snf6 levels were lower than wt in the *cyc8* and *swi3* mutants. Together, this showed that there were slight reductions in the protein levels of all the Swi-Snf proteins tested in an *CYC8* gene deletion mutant, which was similar to the decrease in transcription seen for these genes of the Swi-Snf gene transcription levels tested in the *cyc8* mutant (see Fig. 4.3). Furthermore, the absence of Snf2 and Swi3 subunits led to a slight reduction in the remaining Swi-Snf sub unit protein levels.

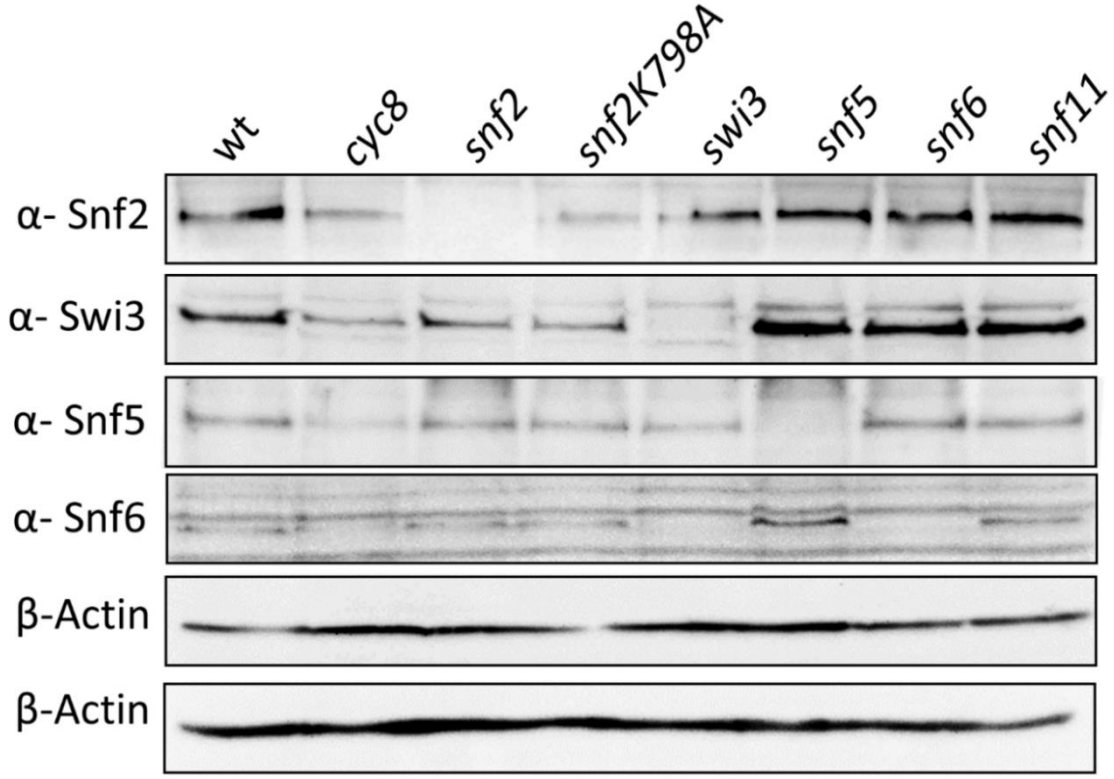

Figure 4.4 Swi-Snf sub unit protein levels in the different Tup1-Cyc8 and Swi-Snf mutants. Western blot analysis of TCA extracted protein in log phase from wild type (wt), *cyc8* and Swi-Snf complex single mutants. Antibodies were specific to Snf2, Swi3, Snf5 and Snf6. Representative β-Actin blots are shown which was used as a loading control.

4.2.6 Investigating Tup1 and Cyc8 protein levels in Tup1-Cyc8 and Swi-Snf mutants:

I next examined Cyc8 and Tup1 protein levels in *tup1*, *cyc8* and the various Swi-Snf single mutants to determine whether either sub unit was affected by loss of the other Tup1-Cyc8 complex component, or by loss of Swi-Snf sub units (Fig. 4.5). The results showed that Tup1 protein levels were unaffected in either the *cyc8* mutant, or in any of the Swi-Snf mutants. Similarly, Cyc8 levels were largely unaffected in the *tup1* mutant. However, Cyc8 levels were almost completely abolished in a *swi3* mutant. Thus, the absence of the Swi3 component of the Swi-Snf complex, affects Cyc8 protein levels in the cell.

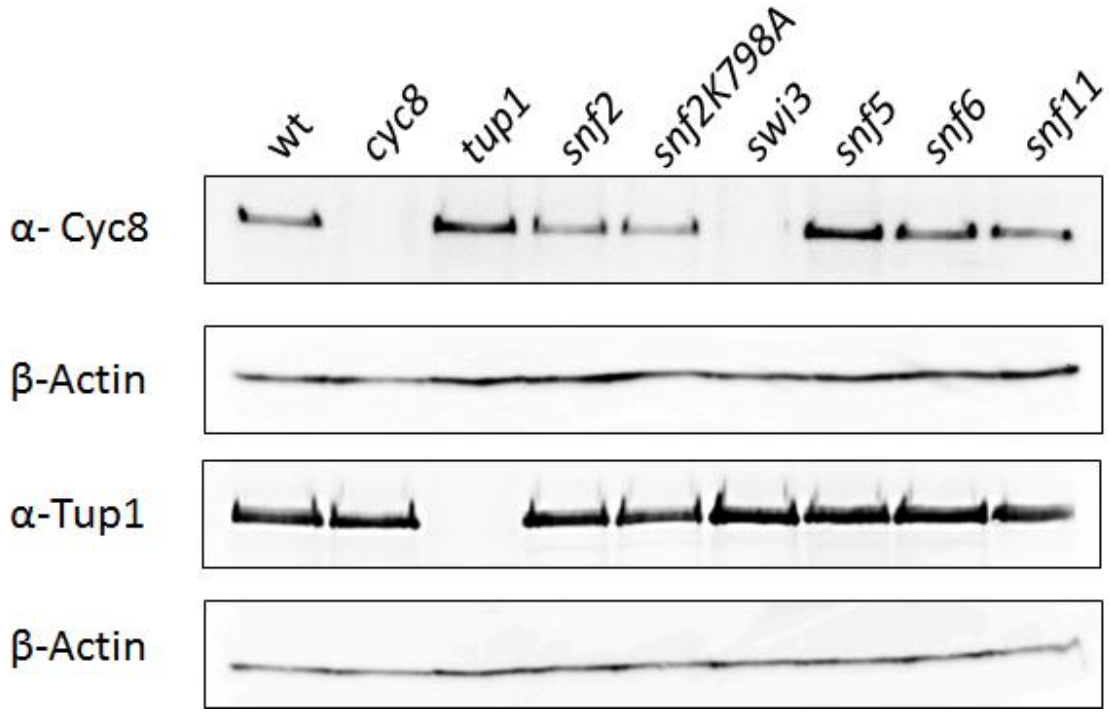

Figure 4.5 Tup1 and Cyc8 protein levels in the different Tup1-Cyc8 and Swi-Snf single mutants. Western blot analysis of Cyc8 and Tup1 in wild type (wt), *cyc8* and the Swi-Snf complex single mutants shown. β-Actin was used as a loading control.

4.2.7 Measuring cell growth on YPD of *snf2* and *cyc8* single and double mutants:

In the next series of experiments, I focussed on characterisation of *snf2* and *cyc8* single and double mutants only, since the *snf2* mutant was looking like the best candidate to take forward for my global transcription analysis. I ruled out taking the *snf5* and *swi3* mutants further since Snf5 only played a partial role in *FLO1* transcription, and Cyc8 levels were greatly reduced in a *swi3* mutant. To investigate the effect of the gene deletion mutations, I analysed cell growth of the four strains in YPD broth batch culture. Wild type (wt), *cyc8, snf2* and *snf2 cyc8* mutants were inoculated into YPD and cell density was measured over time (Fig. 4.6 A). Each of the *snf2*, *cyc8* and *snf2 cyc8* mutants did not show as robust growth on YPD as wt. However, the *cyc8* mutant had the greatest growth defect, showing the longest lag before exponential growth occurred. In doubling time, the wt took~90 minutes to double, *snf2* showed significantly delayed with about 300 minutes to double, there was dramatically increased in doubling time in *cyc8* mutants with about ~180 minutes, *snf2 cyc8* double mutants showed no significant different than wt with~110 minutes doubling time (Fig. 4.6B).

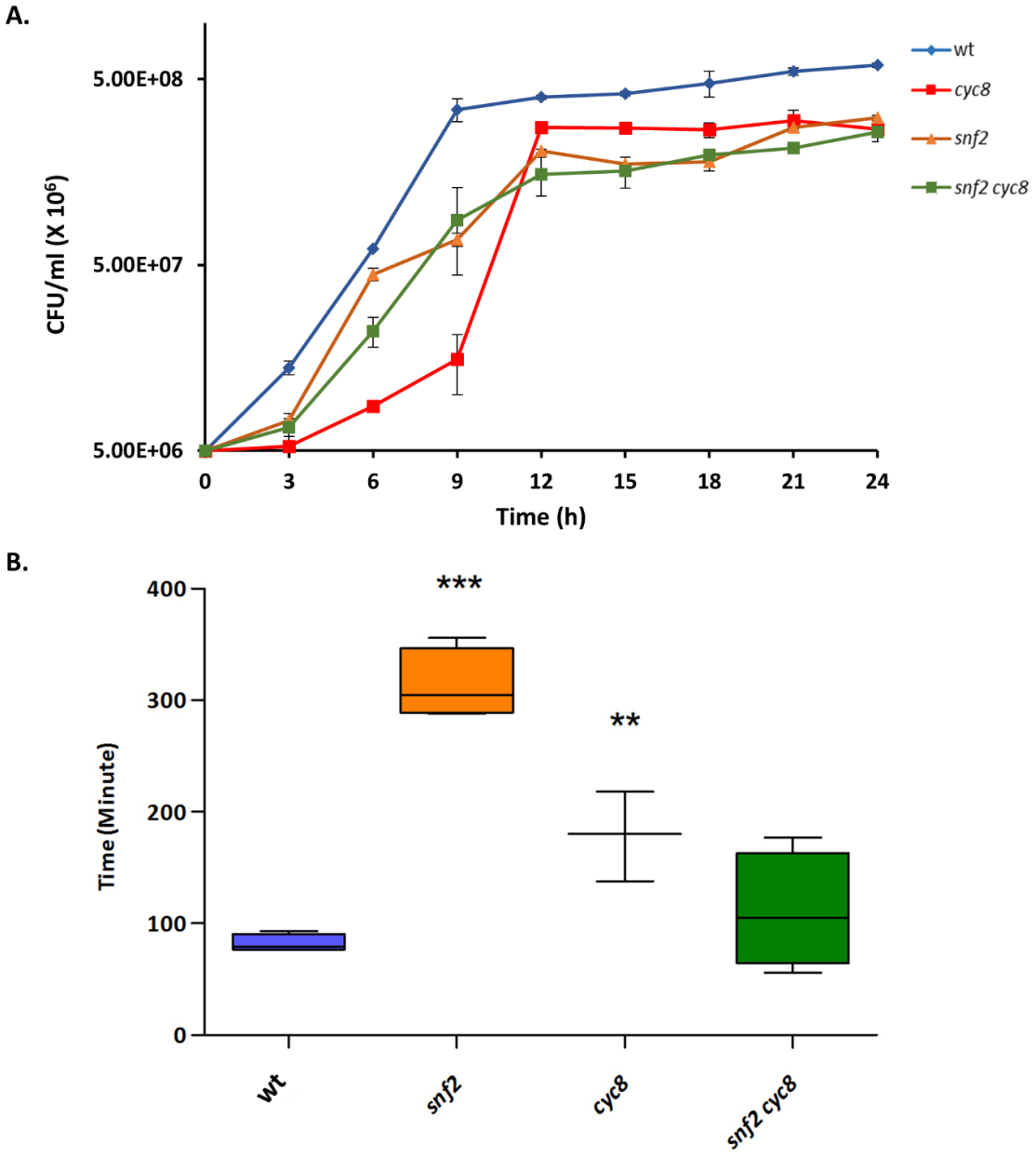

Figure 4.6 Comparison of growth in batch culture of wt and *snf2*, *cyc8* and *snf2 cyc8* mutants. Yeast were cultured in YPD at 30°C. Cell density is expressed as cell number per ml (cell no./ml). Cells were counted at the intervals indicated over a 24 h period using a haemocytometer.

4.2.8 Analysing Tup1-Cyc8 mutants cell morphology:

Cells were examined under the microscope to reveal diverse cell morphologies (Fig. 4.7). Cells were visualised in the absence and presence of EDTA to look at flocculating and dispersed cell morphology, respectively. Consistent with the data in Chapter 3, the *snf2* mutants formed clumps of between 4 to 8 cells. These clumps were not dispersed in the persence of EDTA suggesting this phenotype is not flocculation. Conversely, and consistent with data shown in (Fig. 4.7), the *cyc8* mutant formed large cell aggregations as a result of flocculation. When the *cyc8* cells were dispered by EDTA, there were a high number of *cyc8* cells displaying a large cell phenotype compared to wt. The *snf2 cyc8* double mutants also exhibited a flocculation phenotype which upon EDTA treatment dispersed cells to smaller clumps of cells similar to that seen in the *snf2* mutant. Thus, the *snf2 cyc8* mutant exhibited morphological traits found in both the *cyc8* and *snf2* single mutants.

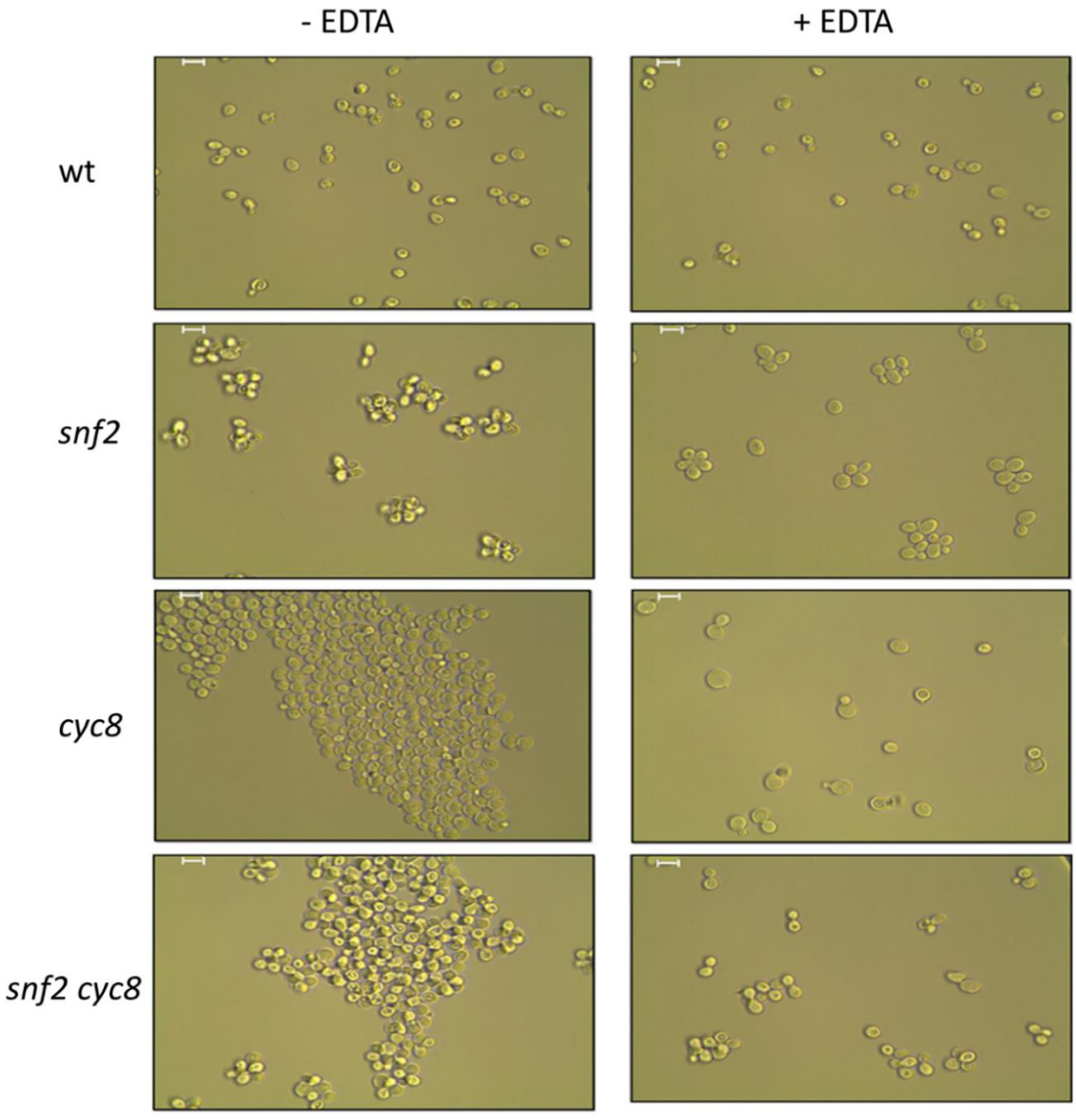

Figure 4.7 Cell morphology. Microscopy was performed using oil immersion under 100x magnification. Cells were treated with and without 20mM EDTA prior to visualisation. Scale bar represents 10µm.

4.2.9 Measuring cell sedimentation rates:

The cell aggregation phenotypes visualised by microscopy in the *snf2* and *cyc8* mutants were further investigated by measuring cell sedimentation rates (Fig 4.8). Cells were grown to log phase in YPD, normalised to a similar cell density in a cuvette, and the rate of sedimentation measured over time by monitoring the decrease in absorbance. The experiment was performed in the presence and absence of EDTA.

The results showed that in the absence of EDTA the *cyc8* strain showed the fastest sedimentation rate, consistent with its previously observed flocculation phenotype. The *snf2* and *snf2 cyc8* double mutant strains showed an equal sedimentation rate attributable to calcium independent cell aggregation and flocculation phenotypes in the *snf2* and *snf2 cyc8* mutants respectively. In the presence of EDTA the high sedimentation rate previously observed in the *cyc8* mutant was abolished, whilst the *snf2* mutant now showed the greatest sedimentation rate, consistent with its calcium-independent cell aggregation phenotype.

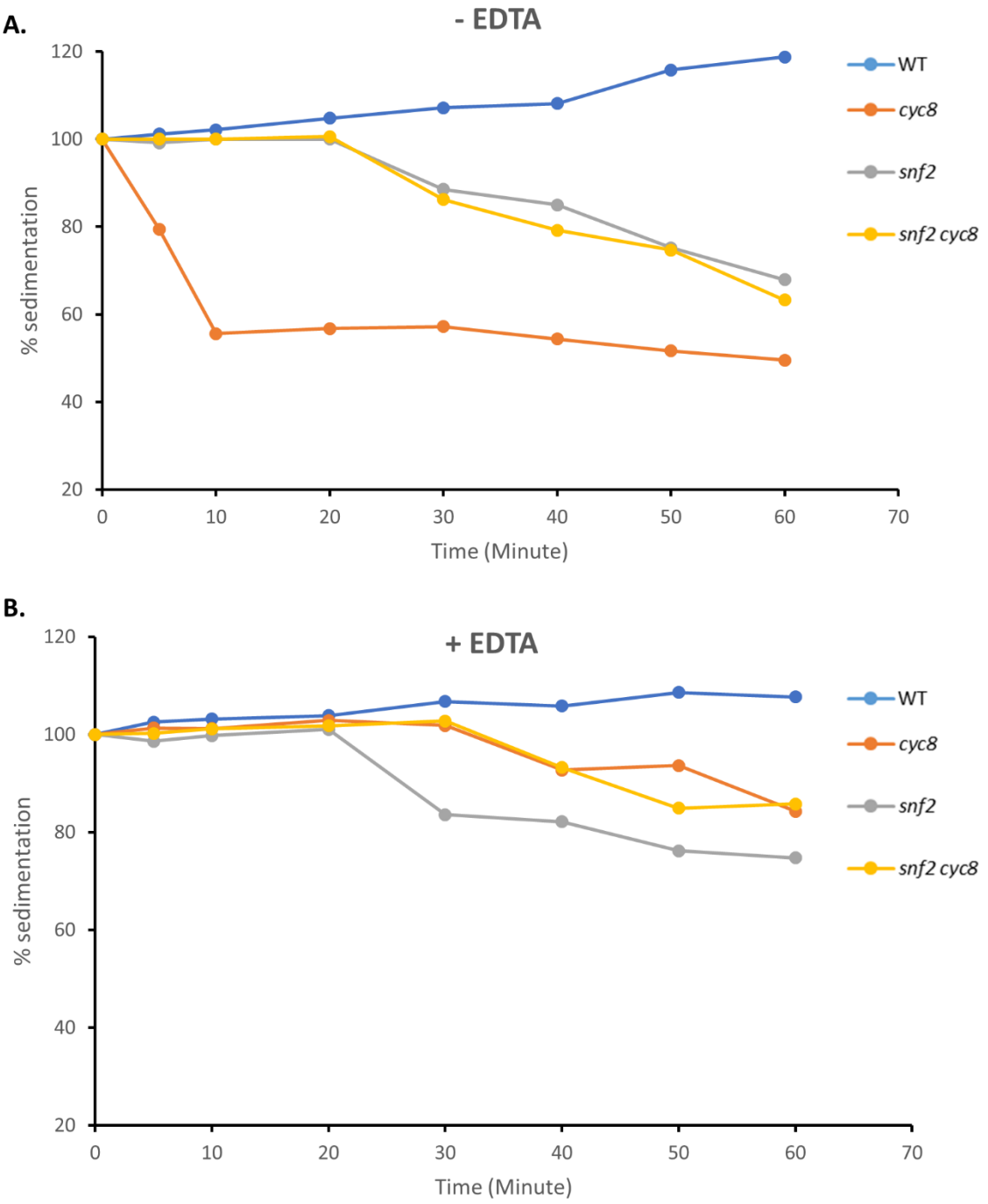

Figure 4.8 Sedimentation rates in wt, *snf2*, *cyc8* and *snf2 cyc8* mutant strains. Sedimentation assay cells were measured by spectrophotometer (OD_{600}) the values are normalized to the optical OD_{600} number in the absence of EDTA (A). sedimentation assay was repeated with the addition of 20mM EDTA (B).

4.2.10 Measuring the sensitivity of the mutants to temperature:

I next measured the ability of the mutants to grow at high (37°C) and low (15°C) temperature (Fig. 4.9). At low temperature, the *snf2* mutant showed the greatest sensitivity and grew the least well. However, this phenotype was rescued by the additional depletion of *cyc8* in the *snf2* mutant background. Indeed, the double mutant grew slightly better than wt at this temperature. When the strains were challenged to grow at 37°C, all of the mutant strains showed weaker growth than wt, although the *cyc8* was the most sensitive to growth at this temperature and grew the least.

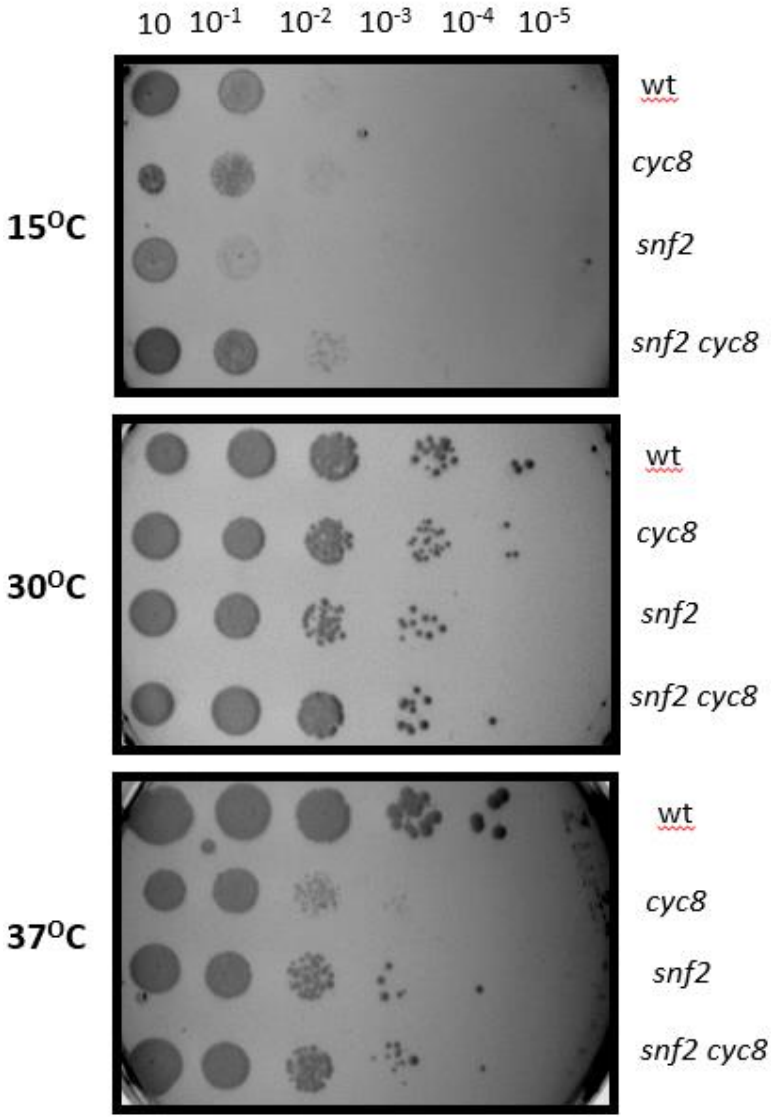

Figure 4.9 Testing temperature sensitivity. Strains were spotted onto plates containing glucose (YPD) and incubated at either 15°C, 30°C or 37°C as indicated.

4.2.11 Measuring the ability to perform fermentation on galactose and raffinose:

To examine the fermentation abilities of the strains, I performed 'spot tests' of the strains on rich media containing either glucose, galactose or raffinose, in the presence or absence of Antimycin A, which was used to block respiration. Consistent with earlier results, the *snf2* mutant grew poorly on the galactose and raffinose plates as compared to wt and the other mutant strains. The growth defect in the *snf2* mutant was even worse when grown on these carbon sources in the presence of Antimycin A. The *cyc8* and *snf2 cyc8* mutants showed only a slight growth defect in the presence of galactose or raffinose and antimycin A. Thus, the additional deletion of *CYC8* in the *snf2* mutant background rescued the *snf2* defect for growth on galactose and raffinose (Fig. 4.10).

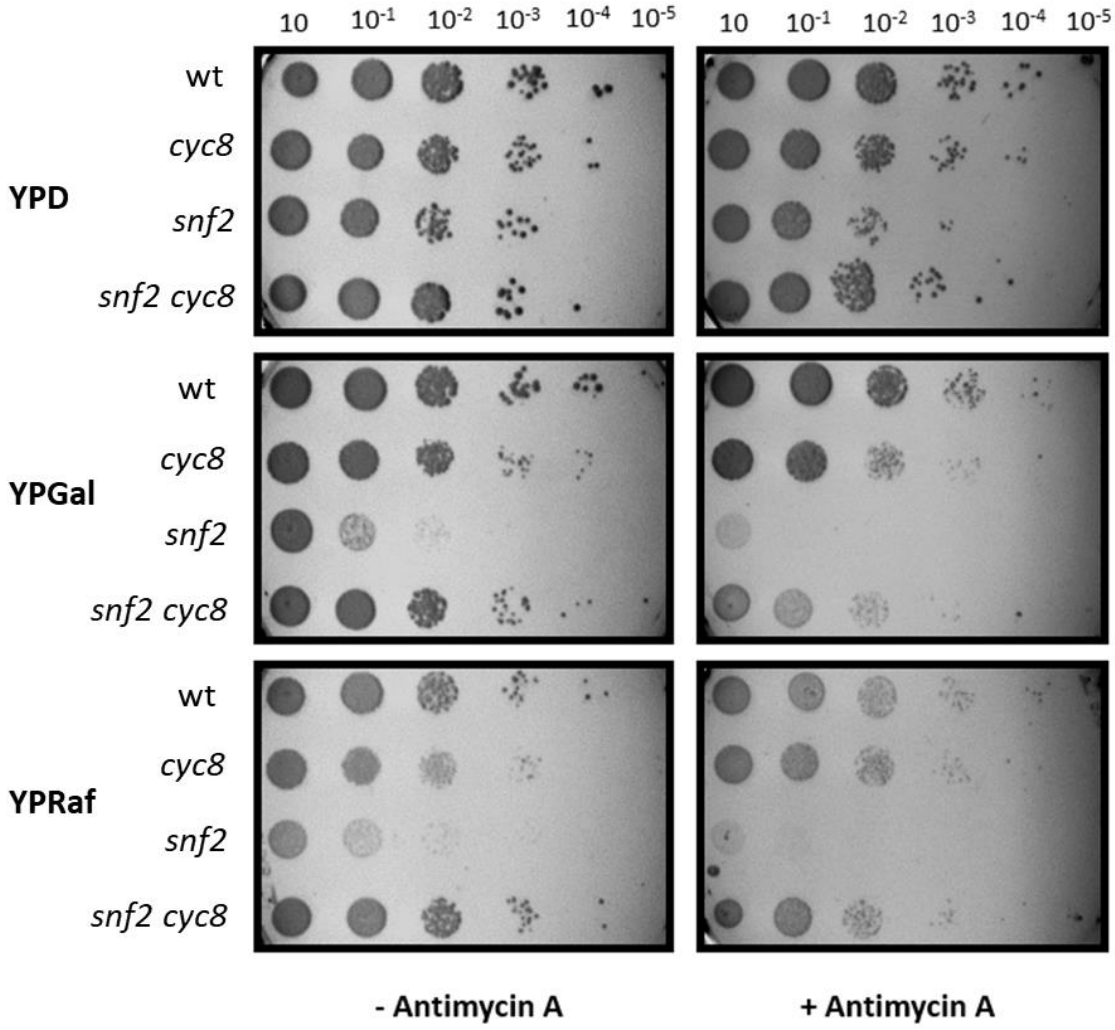

Figure 4.10 Testing fermentative capacity. Strains were spotted onto plates containing either glucose (YPD), galactose (YPGal), or raffinose (YPRaf) and with or without Antimycin-A.

4.2.12 Measuring the sensitivity to DNA damage:

I next measured the sensitivity of the mutant strains to the DNA damaging agent, hydroxyurea (HU) and methane methoxysulphonate (MMS). The hydroxyurea inhibit the enzyme ribonucleotide reductase to reduce dNTPs levels which also initially inhibits DNA replication leading to replication fork collapse and DNA double strand break formation (Koç *et al*. 2004). MMS is a DNA alkylating agent that causes DNA fragmentation following the inhibition of DNA replication (Lundin *et al*. 2005).

Cells were grown until exponential phase in YPD, normalised to an equal cell density, and serial dilutions were prepared from which equal volumes were spotted onto YPD plates containing either MMS or HU at the concentrations shown (Fig. 4.11 A and B).

In hydroxyurea the cells showed different response *cyc8* and *snf2 cyc8* were abolished, *snf2* was severely sensitive to HU than wt (Fig. 4.11 A). Interestingly, the results showed that each of the *snf2*, *cyc8* and *snf2 cyc8* mutant strains showed a greater resistance to growth in the presence of MMS as compared to wt (Fig. 4.11 B).

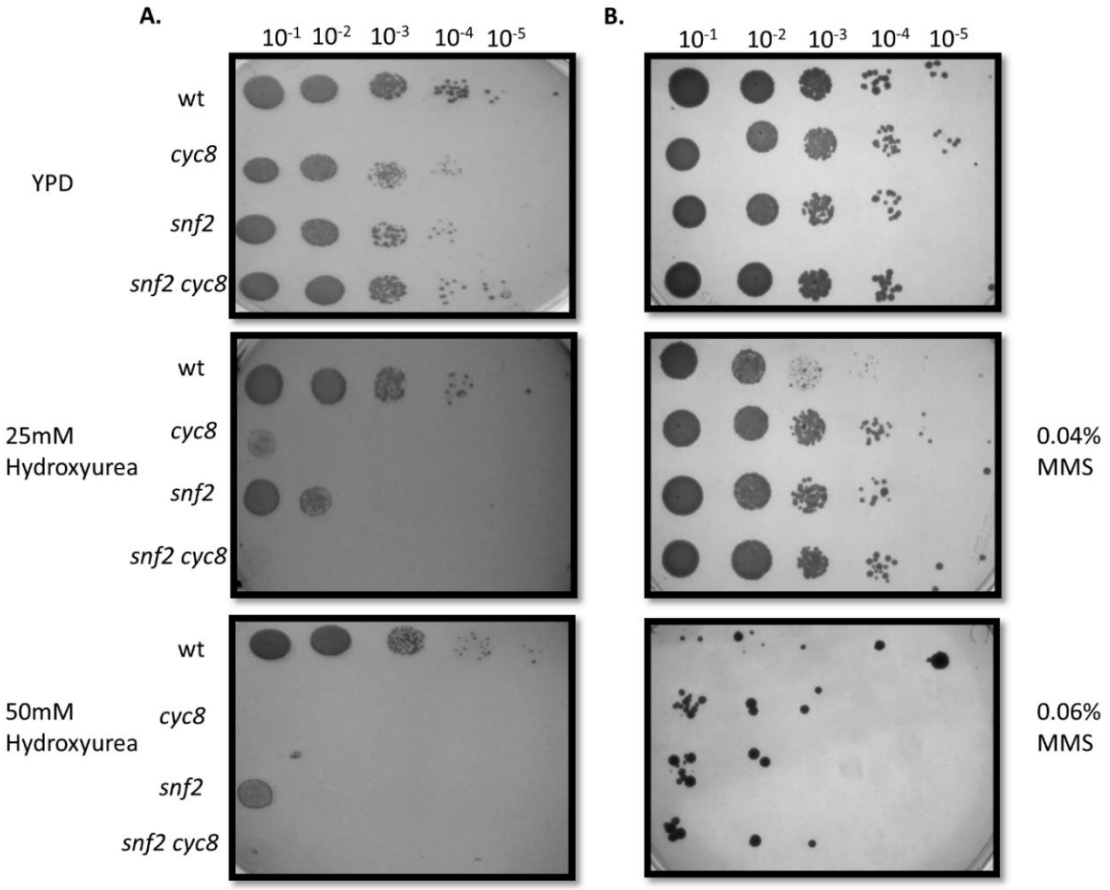

Figure 4.11 Testing cell sensitivity to DNA damaging reagents. Cells from each of the strains indicated were plated as 5-fold serial dilutions starting from 1 x 10^7 cells/ml. 5 µl of culture was spotted on YPD. YPD containing different concentration of hydroxyurea (HU) (A). YPD media containing different concentration of methyl methanesulfonate (MMS) (B).

4.2.13 Measuring the sensitivity to cell wall stress:

To measure the sensitivity of cells to cell wall stress, I challenged the cells to grow in the presence of caffeine. Which is commonly used to evaluate the function of the Mpk1p-mediated cell wall integrity pathway and thus assess resistance of yeast to cell wall stress (Kuranda *et al*. 2006; Levin, 2005).

Cells were grown until exponential phase in YPD, normalised to an equal cell density, and serial dilutions were prepared from which equal volumes were spotted onto YPD plates containing caffeine at the concentrations shown (Fig. 4.12).

The *snf2*, *cyc8* and *snf2 cyc8* double mutants all grew slower than wt, with *cyc8* being the most sensitive to this drug.

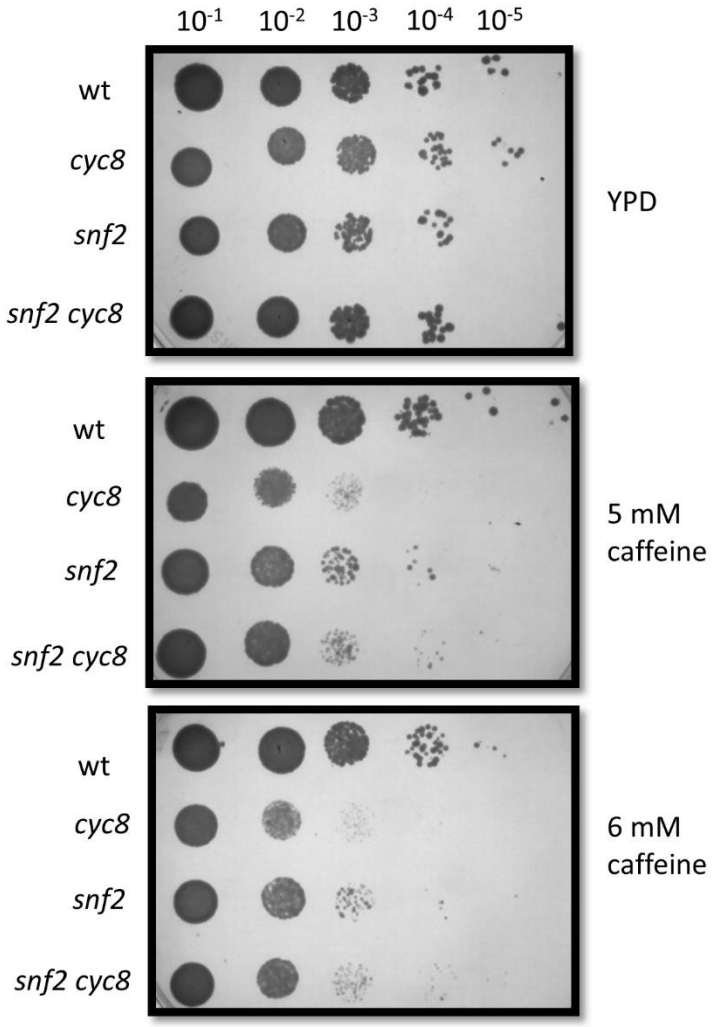

Figure 4.12 Testing cell sensitivity to caffeine. Comparison between wild type, *cyc8*, *snf2* and *snf2 cyc8* mutant strains for sensitivity to growth on YPD plus either caffeine.

4.2.14 *snf2* and *cyc8* mutants display different levels of *SUC2* transcription:

The *SUC2* gene, which encodes the enzyme invertase, is an example of a gene which is known to be under the control of the antagonistic action of Swi-Snf and Tup1-Cyc8 (Fleming and Pennings 2007; Treitel and Carlson 1995). *SUC2* is repressed by Tup1-Cyc8 in the presence of high glucose concentrations and is transcribed in response to low glucose (Oezcan *et al*. 1997). I therefore monitored transcription of *SUC2* in *cyc8, snf2* and *snf2 cyc8* mutants following growth in media containing either high or low glucose concentrations (Figure 4.13). when wt grew in high glucose (2%), *SUC2* transcription was repressed, while in *cyc8* was significantly high. In *snf2* and *snf2 cyc8* the *SUC2* gene was repressed.

When wt cells were grown in low glucose (0.05%) the *SUC2* mRNA was de-repressed. However, it was dramatically high in *cyc8* compared with wt with similar level of *cyc8* grew in high glucose level. In *snf2* the mRNA level was repressed. furthermore, in *snf2 cyc8* transcription was lower than the *SUC2* transcription in wt.

Overall, the *SUC2* transcription in *cyc8* was very highly de-repressed under high and low glucose while it was repressed in *snf2* in both high and low glucose. This data suggests the role of Tup1-Cyc8 in *SUC2* repression and Swi-Snf activation.

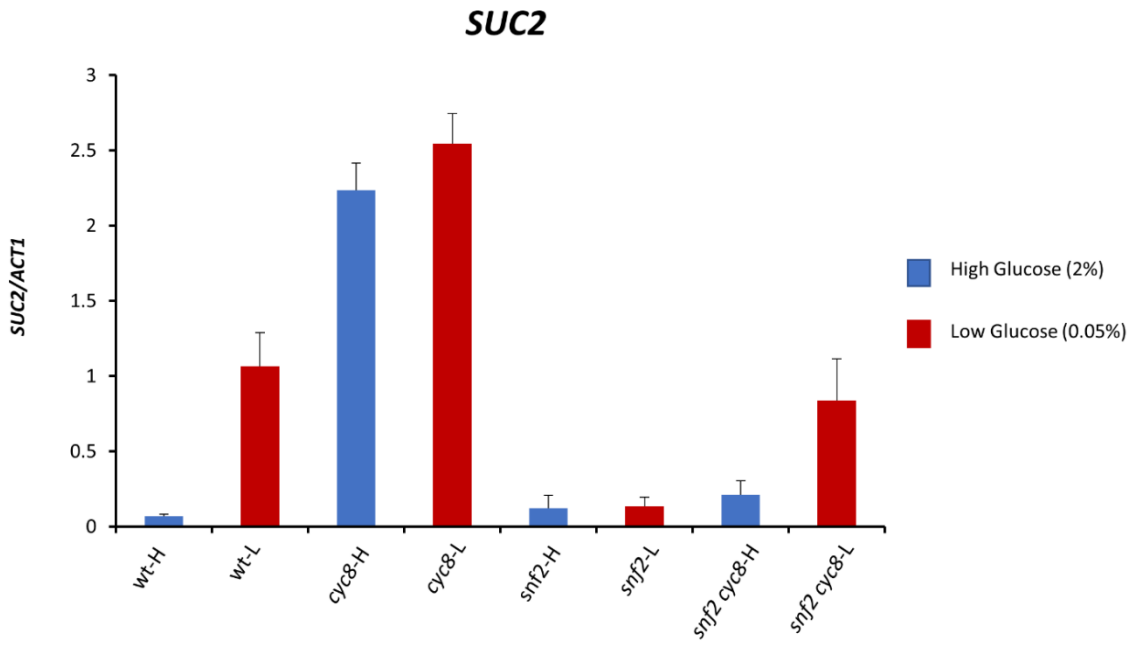

Figure 4.13 *SUC2* transcription in *snf2*, *cyc8* and *snf2 cyc8* mutants. *SUC2* transcription was monitored in wild type, *snf2* and *cyc8* single mutants and a *snf2 cyc8* double mutant grown in 2% glucose (H) (repressed) and 0.05% glucose (L) (de-repressed), by RT-qPCR. Transcription is shown relative to *ACT1* gene transcription.

4.3 Discussion:

The overall the aim of this project is to identify those genes co-regulated by the Swi-Snf and Tup1-Cyc8 chromatin remodelling complexes. To achieve this, the aim was to identify the transcriptome of *cyc8* mutant cells, where genes under Tup1-Cyc8 repression should be de-repressed. To then identify which of these genes require Swi-Snf for transcription, the aim was to identify which of those genes de-repressed in a *cyc8* mutant additionally mutated for Swi-Snf activity, are shut down again. These genes would be designated as the co-regulated genes.

The experiments described here, therefore characterised double deletion mutants comprising a *cyc8* gene deletion in combination with various Swi-Snf sub unit gene mutations to determine which double mutant would be best to use in the transcriptomics analysis to identify the genes co-regulated by Tup1-Cyc8 and Swi-Snf. Specifically, following the analysis of Swi-Snf mutant phenotypes in chapter 3, the *snf2*, *snf2K798A*, *swi3* and *snf5* mutations were individually combined with a *cyc8* mutant and these mutants were characterised to see which double mutant would be the best to use in the transcriptomics analysis. The *CYC8* gene was chosen for deletion, and not *TUP1*, since an *cyc8* mutant should be representative of a strain totally deficient in Tup1-Cyc8 activity as Tup1 occupancy should be abolished at Tup1-Cyc8 target genes in an *cyc8* mutant, whereas Cyc8 might persist in a *tup1* mutant (Fleming *et al*. 2014).

The *FLO1* and *SUC2* genes are two examples of known Swi-Snf and Tup1-Cyc8 co-regulated genes (Fleming and Pennings 2007; Fleming and Pennings 2001). I therefore examined transcription of these genes in the *snf2*, *snf2K798A, swi3* and *snf5* mutants in the presence and absence of *CYC8* (Fig. 4.2). The aim was to determine the contribution to *FLO1* and *SUC2* de-repression in the absence of *CYC8* by Snf2, Swi3 and Snf5. In a *cyc8* mutant, where the Tup1-Cyc8 co-repressor is absent, these genes were de-repressed, consistent with the observed flocculation phenotype in this strain (Fig. 4.2). In the *cyc8* mutant additionally deleted for *snf2, swi3* or *snf5*, we would expect the de-repression to be abolished. Indeed, the results showed that in a *cyc8* mutant additionally deleted for *snf2*, *swi3* or containing Snf2 deficient in its activity (the *snf2K798A* mutant), the *FLO1* de-repression was abolished compared to that seen in the *cyc8* single mutant (Fig. 4.2A). However, the additional deletion of *snf5* in the *cyc8* background only reduced

FLO1 transcription 2-fold compared to that seen in the *cyc8* single mutant. A similar result was also seen at *SUC2*, although the mRNA levels in the *snf2 cyc8* and *snf2K798A cyc8* double mutants were slightly different (Fig. 4.2B). Therefore, the Snf2 and Swi3 sub units contributed most to transcription of these genes in the absence of Tup1-Cyc8 dependent repression, whilst Snf5 was only partially required for transcription. *PMA1* transcription in all of the strain backgrounds was not significantly altered (Fig. 4.2C), suggesting that the changes in transcription at *FLO1* and *SUC2* were gene-specific effects and not a consequence of a general impact on transcription in these mutants.

I also examined whether the complexes regulated expression of their own, or each other's sub units (Fig. 4.3). The *CYC8* transcription analysis showed a high transcription in *swi3* mutant and there is no difference in other mutants. In *SWI3* transcription was significantly low in *cyc8*, *snf2 cyc8* and *snf2K798A cyc8*, other mutants shown no different. In *SNF2* transcription the level of mRNA was high in *swi3* and there was no difference in other mutants. In *SNF5* the transcription of *swi3 cyc8* was high and no difference in other mutants.

Overall, the transcription revealed no difference in *cyc8*, *swi3*, *snf2* or *snf5* mRNA levels in either of the deletion mutant strains compared to wt regarding to the level of the mRNA was very low relative to actin. Thus, Swi-Snf does not appear to regulate transcription of its own sub units or of Cyc8, and Cyc8 does not appear to regulate transcription of Swi-Snf sub units.

Matching with the mRNA results, there were reductions in the protein levels of all the Swi-Snf proteins detected in an *CYC8* gene deletion mutant. This was similar to the decrease in transcription seen for the genes of the Swi-Snf complex tested in the *cyc8* mutant. It was observed that a reduction of the Swi3 protein in the *snf2* mutant and Snf6 in the *swi3* mutant reflected the Swi-Snf module structure which was suggested by Dutta *et al*. 2017, whereby the loss of Snf6 decreased the association of Swi3. In addition, the Swi3 module needs to interact with the Snf5 module to ensure association with the Snf2 module.

Surprisingly though, whereas RT-qPCR suggested *CYC8* mRNA levels were significantly high in a *swi3* mutant, Cyc8 protein levels were almost undetectable in the absence of

Swi3. This data suggests that the absence of Swi3 from the Swi-Snf complex impacts the stability of the Cyc8 protein. It would be interesting to test whether this is evidence of a direct interaction between the Swi-Snf and Tup1-Cyc8 complexes (Fig. 4.5).

The net result of these experiments was that *snf5* and *swi3* were not taken forward as genes to be mutated in the *cyc8* background for the transcriptome analysis. Instead, it was decided to pursue the complete *snf2* gene deletion for use in combination with a *cyc8* gene deletion. Therefore, experiments were performed to test the phenotypes of *snf2*, *cyc8* and *snf2 cyc8* mutants prior to the global transcriptome analysis. The results of these experiments confirmed a role for Cyc8 and Snf2 in regulating general and fermentative growth, flocculation, cell wall metabolism and response to DNA damage. The results identifying the cohort of Swi-Snf and Tup1-Cyc8 co-regulated genes should shed light on how these complexes influence such diverse cellular functions.

The Snf2 sub unit provides the ATPase activity which is essential for the chromatin remodelling activity of the Swi-Snf complex (Dutta *et al*. 2017). Thus, we had expected the *snf2* gene deletion and the catalytically dead *snf2K798A* mutant to show the same phenotypes. However, this was often not the case. It was the full gene deletion (*snf2*) that had the greatest impact on cell function. Recent research has suggested that the Snf2 sub unit is integral to complex stability (Dutta *et al*. 2017). In *snf2* mutants, the authors had shown there was the greatest loss of Swi-Snf sub unit associations, suggesting the complex had largely dissociated in the absence of *snf2*. Conversely, it would be expected that the *snf2K798A* mutant, although catalytically dead, still resides within a structurally intact Swi-Snf complex (Martens & Winston, 2002). The difference in phenotypes between the *snf2* deletion and the *snf2K798A* mutant therefore suggests that the other proposed sub modules within the complex do perform cellular functions independent of the Snf2-dependent ATPase activity. With this in mind, it was decided to use the *snf2* and *snf2K798A* single and *snf2 cyc8* and *snf2K98A cyc8* double mutants for the global transcription analysis to uncover the Swi-Snf and Tup1-Cyc8 co-regulated genes.

Chapter 5

RNA-Seq analysis to identify Swi-Snf and Tup1-Cyc8 co-regulated genes

5.1 Introduction:

Swi-Snf is an ATP-dependent complex required for the regulation of transcription of 2 - 10% of yeast genes (Dutta *et al*. 2014; Shivaswamy & Iyer, 2008; Yen *et al*. 2012). Conversely, the Tup1-Cyc8 complex represses 3-5% of genes in *Saccharomyces cerevisiae* including genes involved in glucose repression, and various stress responses (Fleming *et al*. 2014; Smith and Johnson 2000).

The most-well characterised genes under the control of Swi-Snf and Tup1-Cyc8 are the *FLO1* and *SUC2* genes (Fleming and Pennings 2007; Fleming and Pennings 2001; Gavin and Simpson 1997). However, the total number of genes regulated by Swi-Snf and Tup1-Cyc8 are unknown.

The main aim of this project is to determine all of the genes co-regulated by Swi-Snf and Tup1-Cyc8, acting as an activator and repressor of transcription, respectively. I aimed to identify these genes by comparing the global transcription profile from a *cyc8* single mutant to that of a *snf2 cyc8* double mutant (Fig. 5.1). The methodology involved identifying genes whose expression are de-repressed compared to wt in the *cyc8* mutant strain, and which are then reduced to near wt levels in the *snf2 cyc8* double mutant. The *snf2* gene mutation was chosen for use in this analysis over other Swi-Snf mutations as from experiments that were performed in the previous chapter (Chapter 4), this sub-unit had the greatest impact on transcription pattern and cellular phenotypes.

To identify the co-regulated genes, this study determined global gene expression under regulation of Tup1-Cyc8 and Swi-Snf by using RNA-Seq technology to measure mRNA levels in wt, *snf2*, *cyc8*, *snf2 cyc8* double mutants (Fig. 5.1). This study also included an analysis using a *snf2* mutant strain which contains a single amino acid substitution mutation comprising a lysine to alanine change at position 798. This mutation resides in the active site of the Snf2 protein and renders the Swi-Snf complex catalytically dead for ATPase activity (Martens & Winston, 2002). A Swi-Snf complex containing the *snf2K798A* mutation, although inactive for chromatin remodelling, is expected to remain intact (Dutta *et al*. 2017; Martens & Winston, 2002), as opposed to the *snf2* gene deletion strain which is expected to cause the dissociation of the bulk of the Swi-Snf complex (Dutta *et al*. 2017). Thus, by comparing the results from an intact but inactive Swi-Snf

complex to a largely disrupted Swi-Snf complex we might gain insight into the possible different contributions to gene regulation by the Snf2 ATPase-dependent activity and the structure of the rest of the complex.

Using RNA-Seq technology (Fig. 5.2), the transcriptomes of these strains were identified and compared to reveal those genes co-regulated by Swi-Snf functioning as an activator of transcription and Tup1-Cyc8 acting as a repressor of transcription. Other categories of genes under control of Swi-Snf and Tup1-Cyc8 were also identified and analysed. For example, this study identified those genes at which Swi-Snf was acting as a repressor and Tup1-Cyc8 was functioning in gene activation. Together, a diverse set of genes were identified and analysed which are subject to positive and negative regulation of transcription by both the Swi-Snf and Tup1-Cyc8 complexes.

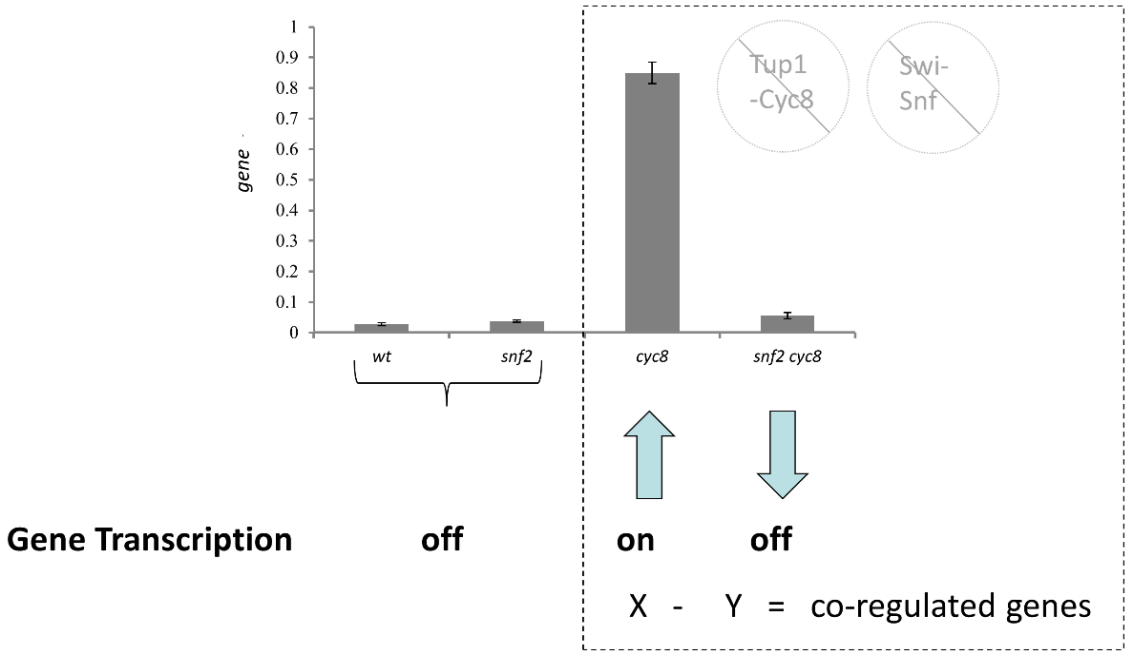

Figure 5.1 The strategy of identification of the genes co-regulated by Swi-Snf and Tup1-Cyc8. The schematic illustrates genes whose the transcription level is repressed in wt and *snf2* single mutants due to Tup1-Cyc8 functioning as a repressor. In the absence of the Tup1-Cyc8 repressor (*cyc8* mutant) these genes are de-repressed. The genes co-regulated by Tup1-Cyc8 functioning as an activator and Swi-Snf working as an activator can be identified by comparing the genes de-repressed in *cyc8* to those genes which show a reduction of transcription in the *snf2 cyc8* double mutant. The aim is to designate this cohort of genes as the co-regulated genes.

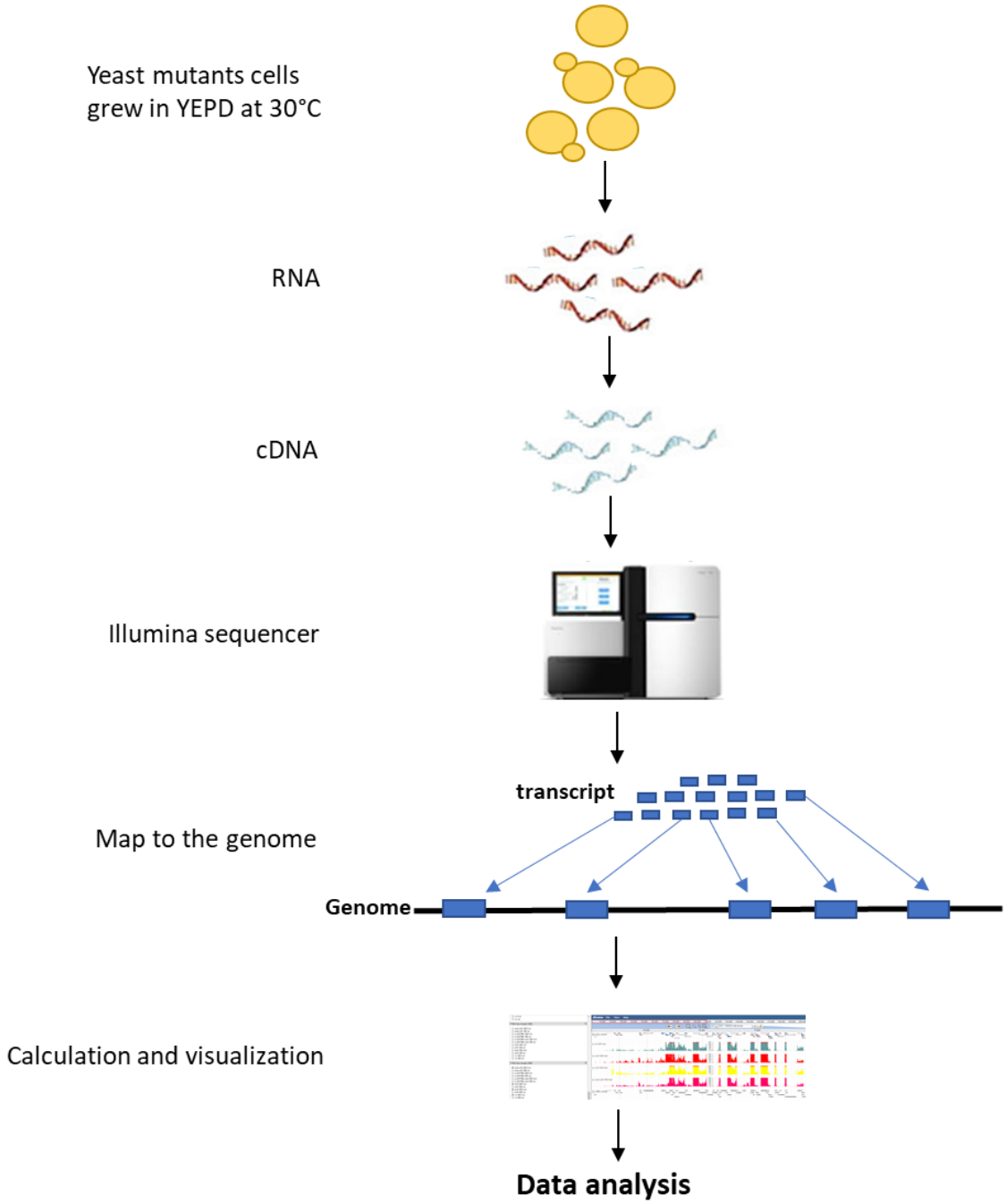

Figure 5.2 Transcription analysis using RNA-Seq. A schematic to show the principle steps involved using RNA -Seq technology to identify global gene transcription levels. Steps include isolation of total RNA, preparation of cDNA, cDNA sequencing, mapping of sequencing reads back to the genome, visualisation of reads on a genome browser and data analyses to reveal differential gene transcription profiles (Wolf, 2013).

5.2 Results:

5.2.1 Identification of uniquely regulated genes in the *snf2*, *snf2K798A* and *cyc8* single mutant strains, and in the *snf2 cyc8* double mutant:

In order to identify the genes co-regulated by Tup1-Cyc8 acting as a repressor and Swi-Snf acting as an activator, genes which were up- and down-regulated more than two-fold were listed in the *snf2*, *snf2K798A* and *cyc8* single mutants compared to wt, and in the *snf2 cyc8* and *snf2K798A cyc8* double mutant strains compared to the *cyc8* single mutant. A heat map was then generated of these 965 genes by Dr Karsten Hokamp to show the differential levels of transcription in each mutant (Fig. 5.3) (appendix I, Table S1). Each row represents a gene and each column represents a mutant. The heatmap also groups genes together by their similarity in gene expression patterns (Galili *et al*. 2018; Wickham, 2009). The red colour indicates the upregulated genes while the blue colour indicates the downregulated genes.

In the *cyc8* strain compared to wt, the majority of the genes are highly upregulated, as indicated by the red colour, which is consistent with the well characterised role of the Tup1-Cyc8 complex as a repressor (Parnell & Stillman, 2011)(Fig. 5.3). Interestingly, there are also three to four small groups of genes which are downregulated in *cyc8* mutant.

In the *snf2* mutant strain in which the catalytic subunit of Swi-Snf was fully deleted, most of the genes were downregulated compared to wt, as indicated by the blue colour. This is consistent with the Swi-Snf complex having been previously classified as a co-activator (Clapier *et al*. 2017; Dutta *et al*. 2017) (Fig. 5.3). A similar result was observed in the Snf2 mutant in which a single amino acid substitution has crippled the ATPase activity. However, there were also some groups of genes that were upregulated in both *snf2* mutants, suggesting a negative impact upon transcription by Swi-Snf. There were also some distinct differences in the transcription patterns between *snf2* and *snf2K798A* with each mutant showing some specific genes up- and down-regulated compared to wt.

When the *cyc8* mutant was compared to the *snf2 cyc8* and *snf2K798A cyc8* double mutants, the majority of the previously upregulated genes were downregulated, as indicated by the blue colour. However, there were also a few groups of genes that were

upregulated. This is consistent with Tup1 acting mainly as a repressor of transcription whilst Snf2 predominantly acts as an activator at the de-repressed Tup1-dependent genes. Interestingly, there were distinct differences in the impact upon Tup1-dependent transcription depending on whether the *SNF2* gene was fully removed or whether the Snf2 protein's catalytic activity was impaired by a single amino acid mutation.

Overall, the data revealed that Tup1 acts predominantly as a repressor of gene transcription whilst Snf2 plays a predominantly positive role at those genes de-repressed in the absence of Tup1. Furthermore, there is a difference on the impact of Snf2 upon gene transcription depending on whether the Snf2 protein is absent or is present, but catalytically crippled for its ATPase activity.

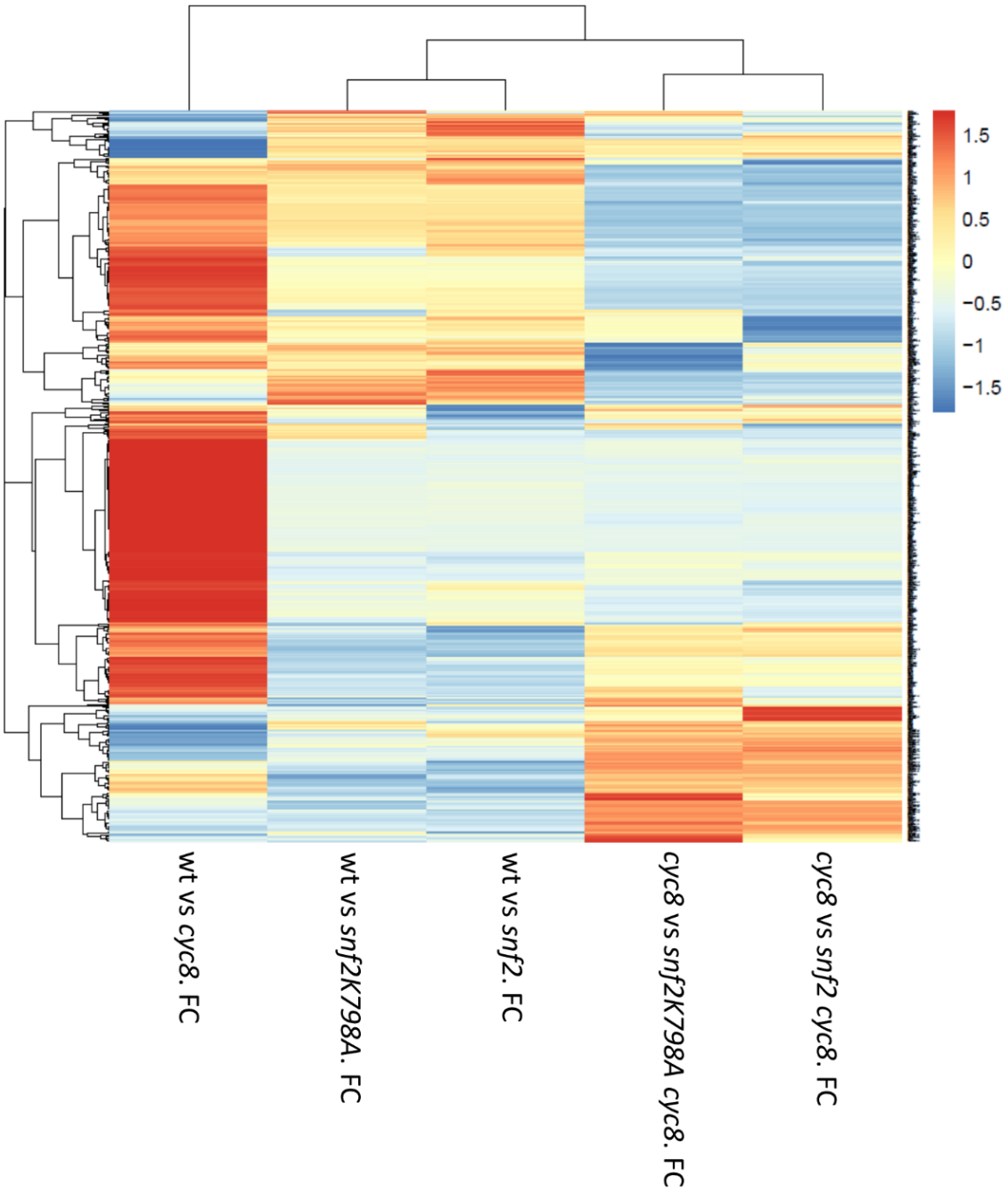

Figure 5.3 Visualisation of differential gene expression in strains deficient for Snf2 and Cyc8. A cluster heat map in which the rows represent genes, and the columns represent mutants. Each cell is colorized based on the comparative level of expression (>2-fold change up (red)/down (blue) and FDR of <0.05) in the strains indicated. The calculation of the fold-change (FC) is based on Z-scores for each gene and the expression values from the samples were averaged, the mean set to 0, and the standard deviations calculated. Heatmap2 R packaging was used to generate this figure (Metsalu & Vilo, 2015). The heat map was generated by Dr. Karsten Hokamp.

5.2.2 Gene transcription profile in the *cyc8* mutant:

The previous heatmap identified that unique groups of genes were at least 2-fold up- and down-regulated in *cyc8* single mutants compared to wt. In total, 575 genes (8.6% of the total number of genes) were up-regulated at least 2-fold in the *cyc8* mutant compared to wt, indicating that these genes were repressed by Tup1-Cyc8 (Fig. 5.4A) (Appendix I, Table S2). Conversely, 158 genes were down-regulated in the *cyc8* mutant (2.3% of the total gene number) suggesting that these genes require Cyc8 as an activator (Fig. 5.4B) (Appendix I, Table S3). An example of a gene that was upregulated in *cyc8* was *RNR3* (*YIL066c*) and a downregulated gene was *BAR1* (*YIL015w*) (Fig 5.4B).

Many of the most highly regulated genes as indicated by their fold-changes in *cyc8*, are cell wall gene families including *PAU*, *FLO* and *TIR* families (Table 5.1). Genes also include glucose-repressed carbohydrate transport and utilisation genes such as the *HXT* and *MAL* genes.

Conversely, the most highly down-regulated genes as indicated by their fold-changes in *cyc8*, include numerous genes involved in retrotransposition and genes involved in phosphate metabolism (Table 5.1).

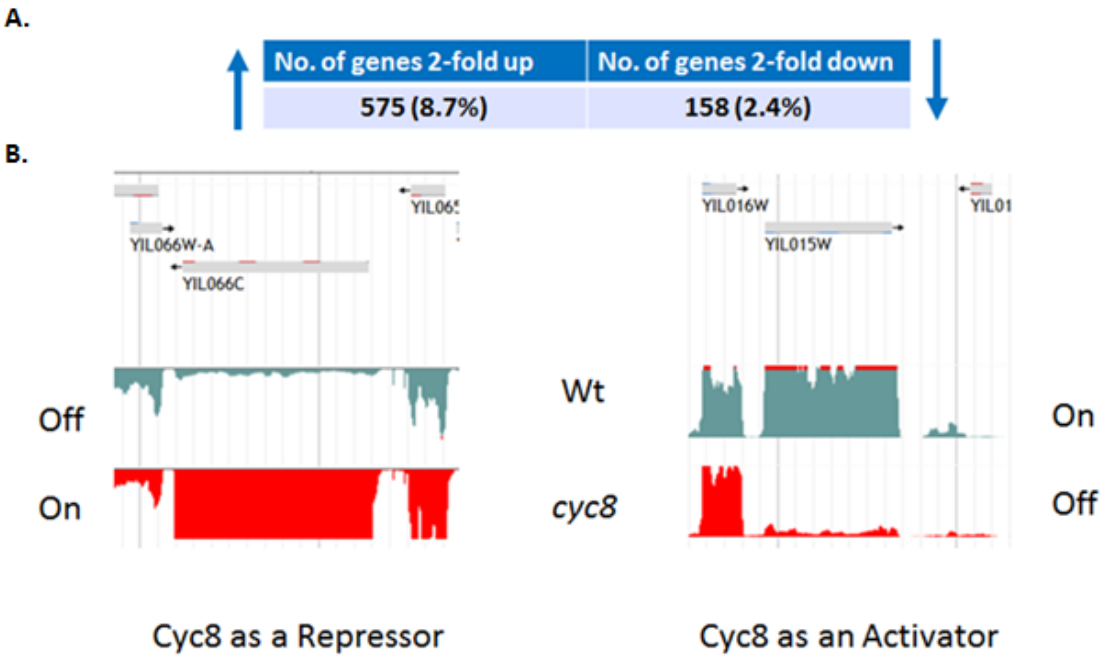

Figure 5.4 Genes regulated more than 2-fold in a *cyc8* mutant. A: The number of genes that were 2-fold up (575) and down regulated (158) in the *cyc8* mutant compared to wild type (wt). **B**: J-browse image shows the transcription levels of *YIL066C* (*RNR3)* and *YIL015W* (*BAR1*) in wt (green) and *cyc8* (red).

Gene	Description of protein product	wt vs *cyc8* FC up
PAU13	Seripauperin-13, cell wall protein	6987.89
PAU24	Seripauperin-24, cell wall protein	4368.65
PAU12	Seripauperin-12, cell wall protein	1523.16
HXT17	Hexose transporter	1134.83
PAU5	Seripauperin-5, cell wall protein	907.31
HXT13	Hexose transporter	720.47
DAN1	Cell wall protein	627.71
PAU20	Seripauperin-20, cell wall protein	504.64
YNR071C	Uncharacterized isomerase	400.9
VBA5	Vacuolar basic amino acid transporter 5	303.86
RCK1	Serine/threonine-protein kinase	244.15
TIR2	Cell wall Protein	202
DSF1	Mannitol dehydrogenase	197.17
YMR279C	Uncharacterized transporter	188.37
IMA2	Oligo-1,6-glucosidase, amylase	178.7
HXT15	Hexose transporter	164.88
PAU19	Seripauperin-19, cell wall protein	156.43
FLO1	Flocculation protein	149.92
MAL12	Alpha-glucosidase	147.54
PUT4	Proline-specific permease, amino acid transporter	117.67
PAU15	Seripauperin-15, cell wall protein	115.71
IMA1	Importin subunit alpha	102.93
TIR4	Cell wall protein	100.95
YML083C	Putative uncharacterized protein	100.56
TIR1	Cell wall Protein	92.45
STL1	Sugar transporter	91.52
FLO9	Flocculation protein	90.37
YFL051C	Uncharacterized membrane protein	83.37
IMA1	Oligo-1,6-glucosidase, amino acid transporter	77.94
PAU7	Seripauperin-7, cell wall protein	77.47
YLR012C	Uncharacterized protein	74.85
SGA1	Glucoamylase, intracellular sporulation-specific	72.83
HBN1	Putative nitroreductase	68.52
AQY1	Aquaporin-1	66.54

Gene	Description of protein product	wt vs *cyc8* FC up
HSP12	Heat shock protein	65.39
GAT4	spore wall assembly protein	61.12
RNR3	Ribonucleoside-diphosphate reductase	60.09
YHR022C	Uncharacterized protein	59.03
SET4	SET domain-containing protein	57.76
YMR317W	Uncharacterized protein	54.09
PRR2	Serine/threonine-protein kinase	50.89
SUC2	Invertase	47.7
MAL32	Alpha-glucosidase	44.17
HUG1	MEC1-mediated checkpoint protein	43.08
YML131W	Uncharacterized membrane protein	42.68
YBR201C-A	Putative uncharacterized protein	41.46
FLO11	Flocculation protein	40.03
DAK2	Dihydroxyacetone kinase	38.76
TDA8	Topoisomerase I damage affected protein	38.72
SHC1	Sporulation-specific activator	38.24

Table 5.1 The top 50 up-regulated genes in a *cyc8* mutant. The top 50 upregulated genes (red) are listed with their gene product descriptions. The values show transcription fold change (FC) in *cyc8* compared to wt. The genes description according to panther gene ontology (Mi *et al*. 2017).

Gene	Description of protein product	wt vs *cyc8* FC down
PHM6	Phosphate metabolism protein	-52.09
SPL2	Putative cyclin-dependent kinase inhibitor	-34.66
YMR045C	Transposon Ty1-MR1 Gag-Pol polyprotein	-33.8
YBL005W-B	Transposon Ty1-BL Gag-Pol polyprotein	-31.69
PHO12	Acid phosphatase	-30.97
ARO10	Transaminated amino acid decarboxylase	-28.32
DIP5	Dicarboxylic amino acid permease	-27.98
YBL005W-A	Transposon Ty1-BL Gag-Pol polyprotein	-25.66
YDR365W-B	Transposon Ty1-DR6 Gag-Pol polyprotein	-23.26
YMR045C	Transposon Ty1-MR1 Gag-Pol polyprotein	-22.64
YJR029W	Transposon Ty1-JR2 Gag-Pol polyprotein	-21.11
PHO5	Repressible acid phosphatase	-17.41
YJR027W	Transposon Ty1-JR1 Gag-Pol polyprotein	-16.18
MFA1	Mating hormone A-factor	-15.77
YDR261C-D	Transposon Ty1-DR4 Gag-Pol polyprotein	-15.47
YHR214C-B	Transposon Ty1-H Gag-Pol polyprotein	-15.35
BAR1	Barrierpepsin, aspartic protease	-14.65
YGR027W-B	Transposon Ty1-GR1 Gag-Pol polyprotein	-14.02
YOL103W-B	Transposon Ty1-OL Gag-Pol polyprotein	-13.6
YPR158C-D	Transposon Ty1-PR3 Gag-Pol polyprotein	-11.86
PHO84	Inorganic phosphate transporter PHO84	-11.67
YLR227W-B	Transposon Ty1-LR3 Gag-Pol polyprotein	-11.06
YLR256W-A	Transposon Ty1-MR1 Gag-Pol polyprotein	-10.97
OPT2	Oligopeptide transporter	-10.76
YOR192C-C	Uncharacterized protein	-10.52
YOR142W-B	Transposon Ty1-OR Gag-Pol polyprotein	-9.47
IMD2	Inosine-5'-monophosphate dehydrogenase	-9.27
YER138W-A	Putative uncharacterized protein	-9.07
YNL054W-B	Transposon Ty1-MR1 Gag-Pol polyprotein	-9.01
FUS1	Nuclear fusion protein	-8.46
ARO9	Aromatic amino acid aminotransferase	-8.4
YGR038C-B	Transposon Ty1-GR2 Gag-Pol polyprotein	-8.23
VTC3	Vacuolar transporter chaperone	-7.65
SRD1	Pre-rRNA-processing protein	-7.47

Gene	Description of protein product	wt vs *cyc8* FC down
CIT2	Citrate synthase, peroxisomal	-7.46
YNL054W-A	Transposon Ty2-OR1 Gag-Pol polyprotein	-7.33
YOR192C-B	Transposon Ty2-OR1 Gag-Pol polyprotein	-7.2
SST2	GTPase-activating protein for Gpa1,	-6.57
NDJ1	Non-disjunction protein 1	-6.56
YER138C	Transposon Ty1-ER1 Gag-Pol polyprotein	-6.46
YPR137C-B	Transposon Ty1-PR1 Gag-Pol polyprotein	-6.44
GPX2	Glutathione peroxidase-like peroxiredoxin 2	-6.43
YNL284C-B	Transposon Ty1-NL1 Gag-Pol polyprotein	-6.32
YAR009C	Truncated transposon Ty1-A Gag-Pol polyprotein	-6.2
PHO11	Acid phosphatase	-5.74
FIG1	Factor-induced gene 1 protein	-5.69
YPR158W-B	Transposon Ty1-PR2 Gag-Pol polyprotein	-5.65
HO	Homothallic switching endonuclease	-5.13
AGA1	A-agglutinin anchorage subunit	-5.09
EEB1	Medium-chain fatty acid ethyl ester synthase/esterase 1	-5.05

Table 5.2 The top 50 downregulated genes in a *cyc8* mutant. Table lists the top 50 genes which are most downregulated, the blue colour indicates the lowest transcription fold change (FC) most of the genes were playing role as retrotransposon. The genes description according to panther gene ontology (Mi *et al*. 2017).

5.2.2.1 Gene specific validation of *cyc8* RNA-Seq data:

575 genes were shown to be de-repressed more than 2-fold compared to wt in the *cyc8* mutant suggesting that these genes are repressed by Cyc8, presumably in the context of the Tup1-Cyc8 repressor complex. To validate this set of genes, RNA was extracted from wt and *cyc8* strains in triplicate, and transcription from *IMA1*, *FLO1* and *SUC2* were measured (Fig. 5.5B). The transcription level of the genes were completely repressed in wt, while it was highly transcribed in *cyc8* (Fig. 5.5B).

Overall, there was a good correlation between the fold change difference in transcription detected between *cyc8* (up-regulation) and wt from both the gene specific analysis and the RNA-Seq data. Indeed, a difference in fold-change between wt and *cyc8* of 77- and 35.8-fold change were detected for the RNA-Seq and the gene specific analysis, respectively, at *IMA1* (Fig. 5.5C).

Although Tup1-Cyc8 is most commonly characterised as a repressor of gene transcription, transcription from 158 genes was downregulated in the *cyc8* mutant compared to wt, suggesting an activator role for Cyc8 at these genes. RNA-Seq data showed that *DIP5* was transcribed in wt, while it was repressed in *cyc8* (Fig. 5.5A). This data was confirmed by RT-qPCR (Fig. 5.5B). Together, for the genes selected, the RNA-Seq data was validated by gene -specific RT-qPCR analysis suggesting the RNA-Seq data is of high quality.

A.

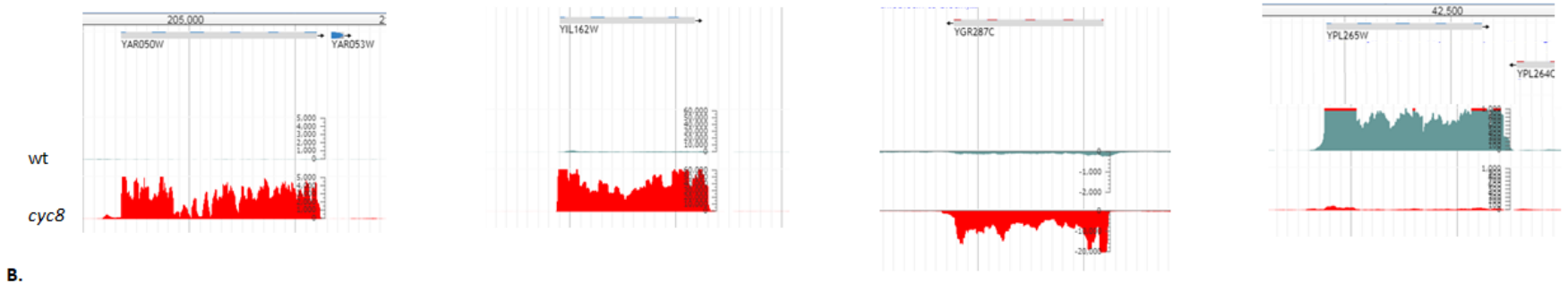

B.

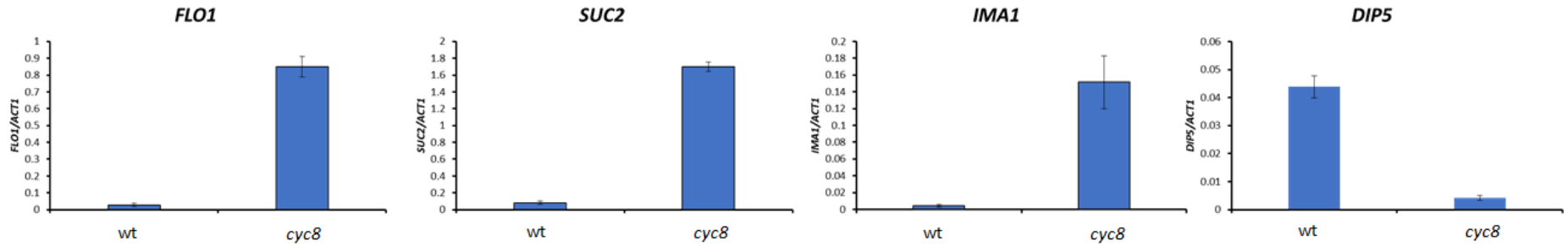

C.

Gene	wt vs *cyc8* (RNA-Seq) fold change	wt vs *cyc8* (RT- qPCR) fold change
FLO1	149.92	30.1
SUC2	47.7	2.7
IMA1	77.94	35.8
DIP5	-27.9	-10.5

Figure 5.5 Validation of *cyc8* RNA-Seq data by RT-qPCR at specific gene targets. A: J-browse screen-shot to show read counts across the *IMA1, FLO1, SUC2* upregulation genes and *DIP5* downregulation gene in the wt and *cyc8* mutants. **B:** RNA-Seq data confirmed by gene-specific RT-qPCR. **C:** The fold change in wt vs *cyc8* in RNA-Seq and RT-qPCR. Error bars represent standard deviation of three independent biological replicates.

5.2.2.2 *cyc8* mutant transcriptome gene ontology analysis:

5.2.4.2.1 Cyc8 acting as a gene repressor:

Next, the gene ontology of the 575 genes 2-fold upregulated in the *cyc8* mutant compared to wt were analysed. Importantly, these genes were expected to have Tup1-Cyc8 act as a repressor. Using the *Saccharomyces cerevisiae* database system (SGD) (Cherry *et al*. 1998) the genes were classified into three annotation sets; Biological process, Molecular function and Cellular component. In the Biological process category, 70 genes were identified as involved in drug metabolic processes (GO ID:0017144), including the *BIO* genes included *BIO3*, *BIO2* and *BIO5* which are involved in biotin pathway (vitamin H). Interestingly, these genes were acquired by horizontally gene transfer (HGT) from bacteria (Hall *et al*. 2005; Hall and Dietrich 2007). 60 genes were also identified in the cell wall organization or biogenesis category (GO ID: 0071554), including the *FLO* gene family which is involved in cell to cell adhesion. 57 genes were classified within the carbohydrate metabolic process category (GO ID:0005975), including the *SUC2* gene which encodes an invertase and the *MAL* gene family involved in maltose transport. Most of these genes were located at subtelomeric region.

In the Molecular function category, the greatest number of genes (84 genes) were classified as having transmembrane transporter activity (GO ID: 0022857). This cohort of genes included the *HXT* sugar transporters. A further 80 genes were classified as having oxidoreductase activity (GO ID: 0016491) and included the *CTT1* gene which encodes a protein which protects the cell from oxidative damage due to high hydrogen peroxide levels. In the cellular component category, the largest cohort of 100 genes were involved in the plasma membrane (GO ID: 0005886) and included the *HSP12* gene which encodes a protein involved in organisation of the plasma membrane in response to stress (Fig. 5.6) (Appendix I, Table S4).

Overall, these data confirm a role for Tup1-Cyc8 in repressing the expression of genes involved in a diverse array of cellular functions, including repression of a large number of sugar metabolism and stress response genes.

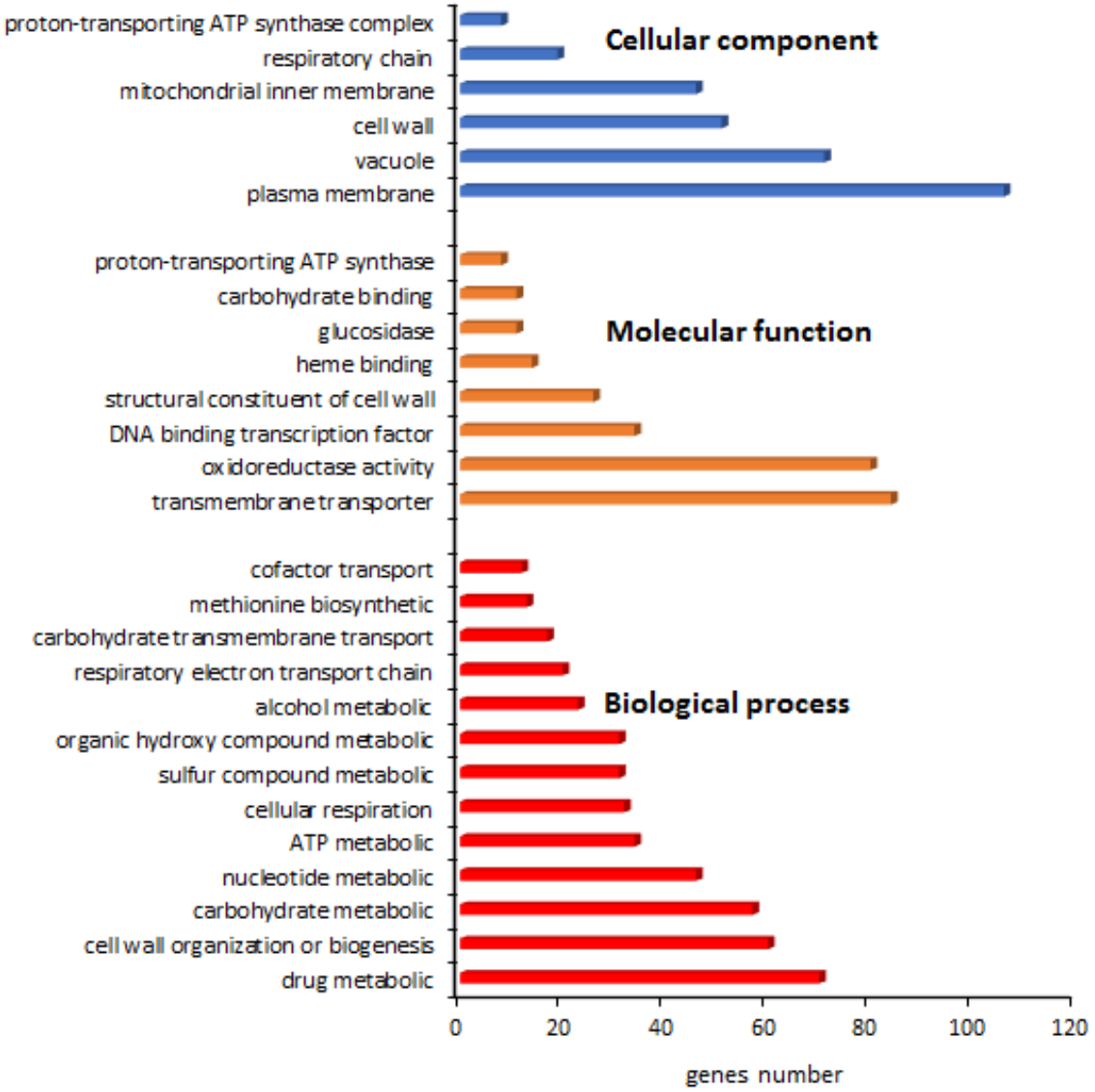

Figure 5.6 Gene ontology analysis of genes upregulated in a *cyc8* mutant. Column chart for the ontology analysis of genes upregulated more than 2-fold in a *cyc8* mutant compared to wt, which are consistent with genes whose expression are repressed by the Tup1-Cyc8 complex. Red represents the biological process category, orange indicates the molecular function category, and blue indicates the cellular component category according to the *Saccharomyces* genome database (SGD). Results are shown for genes with P value < 0.001.

5.2.2.2.2 Gene ontology analysis of genes where Cyc8 functions as an activator:

Although Tup1-Cyc8 is best known as a repressor, 158 genes were identified to have 2-fold down regulation in the *cyc8* mutant suggesting that Tup1-Cyc8 acts as an activator at these genes. These genes were therefore classified into the three annotation sets; Biological process, Molecular function and Cellular component, using the *Saccharomyces cerevisiae* database system (SGD)(Cherry *et al*. 1998).

In the biological process category, 32 genes were classified as being involved in DNA integration (GO ID:0015074), and a further 32 in organic acid metabolic processes (GO ID:0006082). This included the *ENO2* gene which encodes a phospopyruvate hydrolase, which is involved in glycolysis and gluconeogenesis, and whose transcription is induced by the presence of glucose.

In the molecular function category 49 genes encode metal ion binding proteins (GO ID: 0046872), and proteins with hydrolyse activity (GO ID:0016787), including the *PEX10* and *CAR1* genes, respectively. In the Cellular component category, the majority of the genes (39 genes) are retrotransposon nucleocapsid encoding genes (GO ID: 0000943), such as *YNL284C-A* (Fig. 5.7) (Appendix I, Table S5).

Together, there are a surprisingly large number of genes encoding proteins with diverse functions that are down regulated in the absence of Cyc8. However, it was interesting to see that a large number of genes involved on phosphate metabolism and retrotransposition seemed to require Cyc8 for activation.

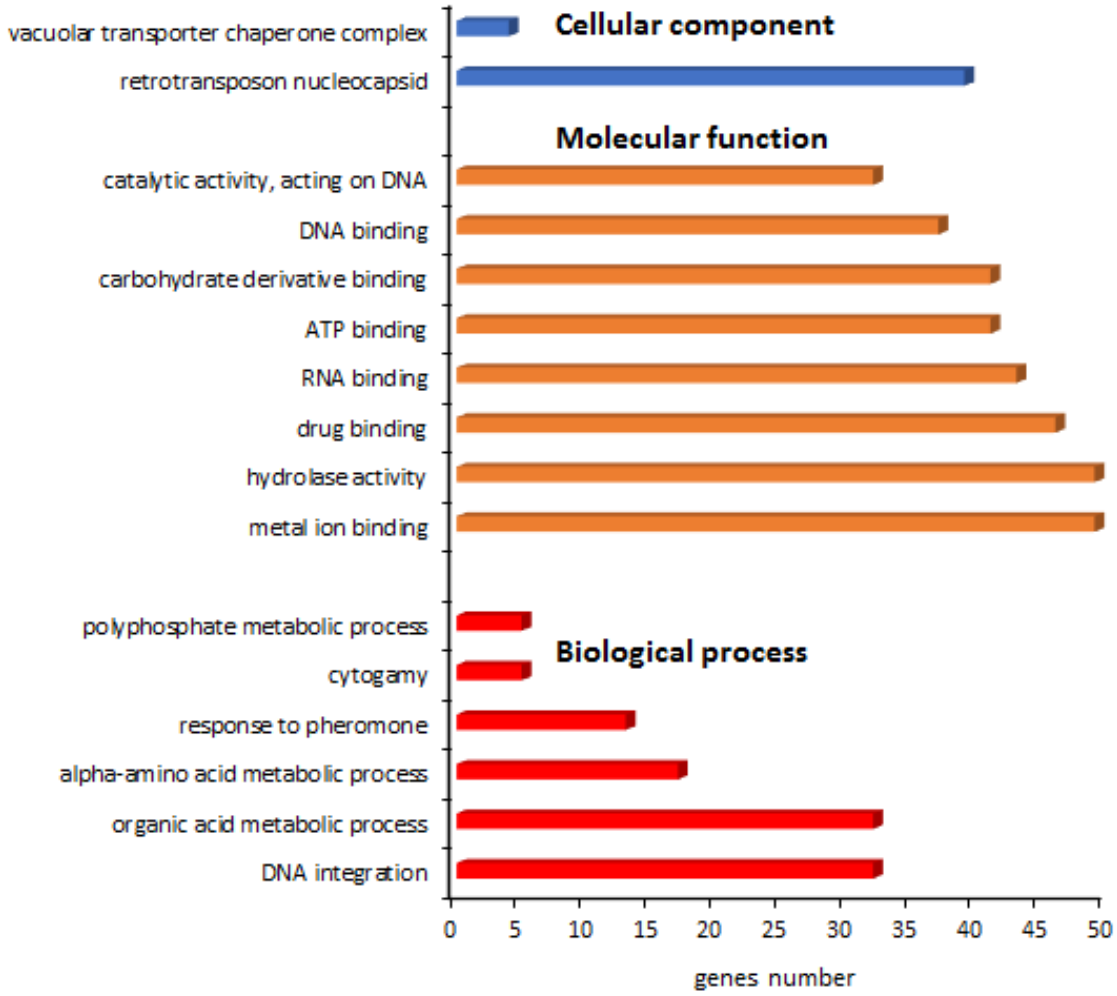

Figure 5.7 Gene ontology analysis of downregulated genes in a *cyc8* mutant. Column charts for the *cyc8* mutant genes using the *Saccharomyces* genome analyses database. Red represents the biological process category, orange indicates the molecular function category, and blue indicates the cellular component category. Results are shown for genes with P value < 0.001.

5.2.2.3 Analysing Cyc8-repressed stress response genes:

The gene ontology analysis revealed that 57 genes that were subject to Cyc8-dependent repression of transcription were involved in cellular response to stress. Therefore, these genes further classified into specific stress response groups to examine which genes were subject to Cyc8 repression, and to what extent they were de-repressed in the absence of Cyc8 (Fig. 5.8).

Using the SGD gene ontology, the 57 up-regulated genes in *cyc8* were classified into five groups according to cellular response; (i) heat (GO:0009408), (ii) oxidative stress (GO:0006979), (iii) osmotic stress (GO:0006970), (iv) starvation (GO:0042594) and (v) DNA damage (GO:0006281) (Fig. 5.8).

Of the heat and oxidative stress response genes that were repressed by Cyc8, the *FLO1* and *HSP12* genes were the most de-repressed in its absence. The *HBN1* oxidative response gene, encoding a possible nitroreductase, was also greatly de-repressed in the absence of Cyc8. *Xbp1*, an important transcription factor with a role in yeast stationary phase, was also de-repressed in the absence of Cyc8. Of the genes that respond to osmotic stress response and starvation, *ENA1,* which encodes a Na^+ pump, was highly upregulated in the *cyc8* mutant. When de-repressed genes were grouped according to the DNA damage response, *Rad54*, *RAD16* and *RAD28* were all de-repressed alongside the *HUG1* gene, which encodes a ribonucleotide reductase inhibitor, and *HUG1*was the most highly up-regulated of these genes (Fig. 5.8).

Overall, the data suggest that Cyc8 is responsible for repressing a variety of structural stress response related genes in addition to various stress-response specific transcription factors including the Msn4 activator and, interestingly, an array of transcription repressors (Xbp1, Rox1, Nrg1/2 and Mig2).

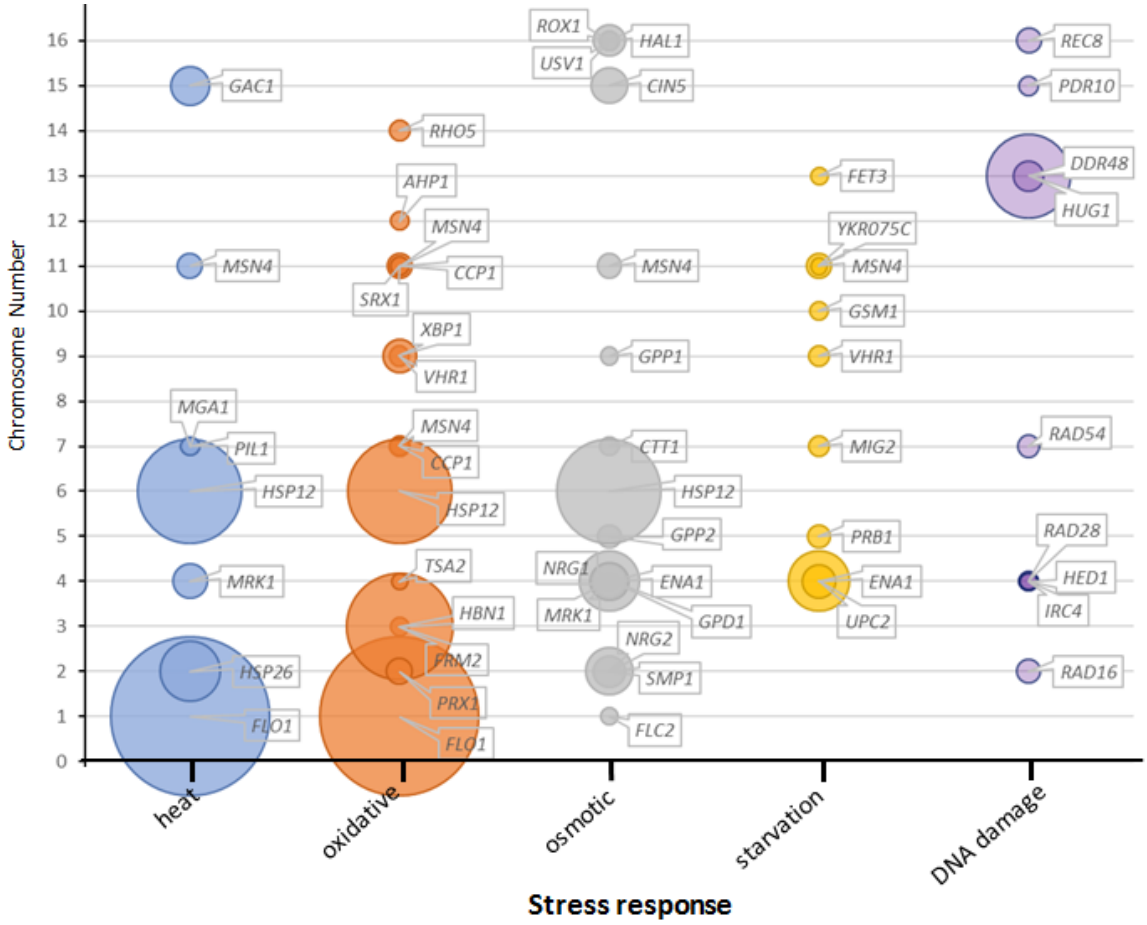

Figure 5.8 Stress response genes up-regulated in *cyc8*. Bubble plot for five families of stress response genes according to SGD database where the x value represents each family and the Y value reflects the chromosome number on which the gene is located. The bubble size represents the Log2 fold-change in the *cyc8* mutant compared to wt. Each family was further identified with a colour code.

5.2.2.4 Analysing Cyc8 repressed cell wall genes:

Chapter 4 examined how Tup1-Cyc8 had an effect on the cell wall organisation when *cyc8* was deleted. The transcription data also suggested that cell wall protein encoding genes were upregulated in a *cyc8* mutant. Therefore, specific cell wall gene families were further examined to elucidate whether they were up-regulated in the *cyc8* mutant. Interestingly, five families of genes were found to play a role in the cell wall. Of the Flocculation (*FLO*) gene family, which encode lectin-like cell wall proteins which are responsible for the flocculation phenotype, the *FLO1*, *FLO5*, *FLO9*, *FLO10* and *FLO11* genes were all de-repressed to a great extent in the absence of *cyc8*. Members of the similar delayed anaerobic (DAN) and TIp1-Related families of cell wall mannoproteins, including the *DNA1* and *TIR1* genes, were also highly de-repressed in the *cyc8* mutant. Other cell wall genes under Cyc8 control included the *UTR2*, *UTR4* and *UTR5* gene members of the Unidentified Transcript family which encode chitin transglucosylases and a large family of genes called the seripauperin or *PAU* gene family. The *PAU* genes were the largest cell wall mannoprotein gene family repressed by Cyc8 and included 15 genes which were among the most de-repressed in the absence of Cyc8 (Fig. 5.9).

Overall, the data reveals that numerous cell wall protein gene families are subject to some of the strongest repression by Cyc8.

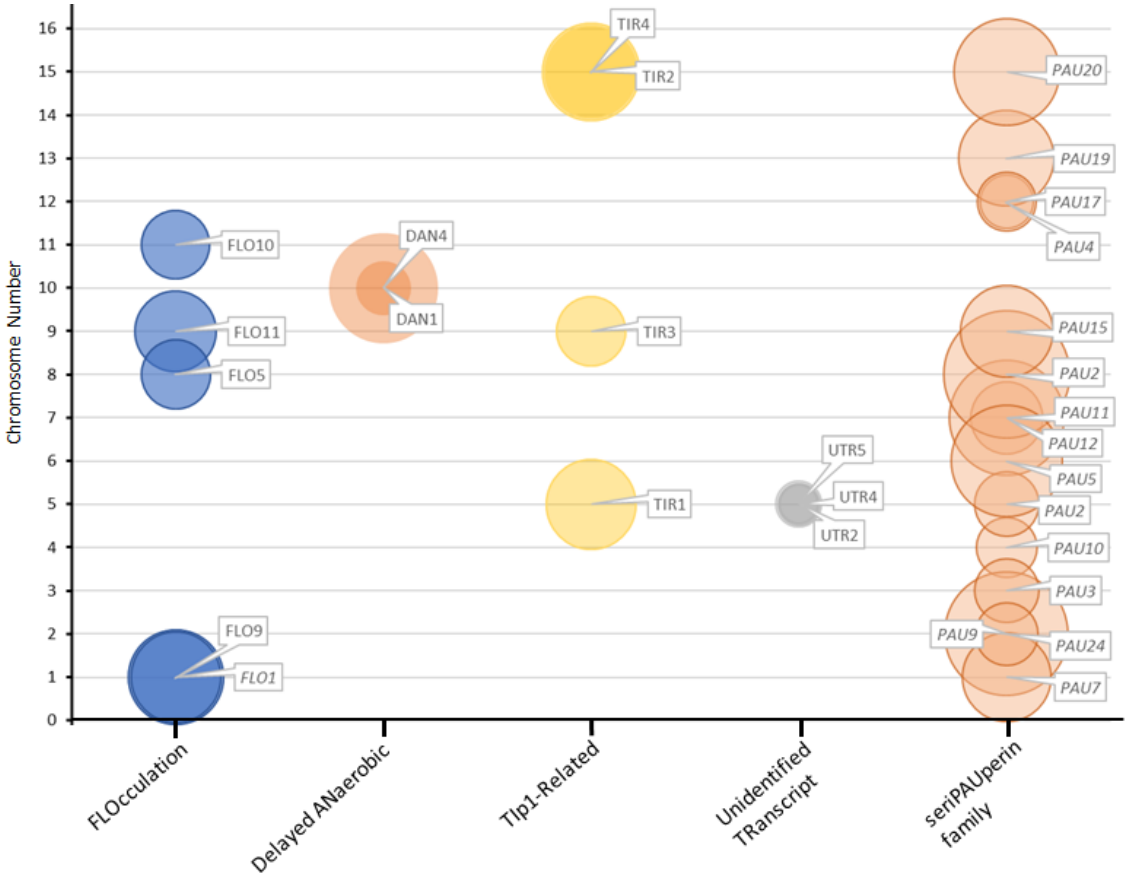

Figure 5.9 Cell wall gene families up-regulated in *cyc8*. Bubble plot for four families of cell wall, the X value represents each family, the Y value reflects the chromosome number in which the gene is located. The bubble size represents the Log2 fold-change in transcription level in the *cyc8* mutant compared to wt. Each family was identified with a specific colour code.

5.2.2.5 Chromosomal location of genes up-regulated in the *cyc8* mutant:

I next analysed the chromosomal location and level of transcription of the 575 genes up-regulated in the *cyc8* mutant to determine if genes in distinct chromosomal regions were specifically subject to Cyc8 repression or not. The data of each gene location along the chromosomes was taken from the *Saccharomyces* genome database (SGD) (Cherry *et al*. 1998). The 16 chromosome centromeres were set as zero and the chromosome sizes and gene positions were normalized according to that. Each chromosome number and size are shown in (Fig. 5.10). The location of the genes is indicated by a circle, and the size of the circle reflects the level of gene expression in the *cyc8* mutant relative to wt (Fig. 5.10).

When plotted, the results suggested that the genes de-repressed in the absence of Cyc8 were evenly dispersed across all 16 chromosomes. However, further analysis revealed that of the 575 genes upregulated in the absence of Cyc8, 17.5% of these genes (100 genes) were located in subtelomeric regions (indicated in red) which were defined as being within 30 kb near a chromosome end (Fig. 5.10). This is statistically significant as the sub telomer regions only comprise 7% of the entire yeast genome yet are enriched for *cyc8*-repressed genes. Furthermore, the *cyc8* repressed genes located in these subtelomeric regions showed a significantly higher level of de-repression in the absence of *cyc8* compared to the Cyc8 repressed genes located elsewhere on the chromosome (Fig. 5.11, compare red bubbles with yellow bubbles, respectively). The majority of these subtelomeric genes were cell wall gene families including the *PAU* and *FLO* genes, although other genes involved in carbohydrate metabolism like the *MAL* and *HXT* gene families were also present.

Four *cyc8* repressed genes, *ATP6*, *COX1*, *COB* and *BI4* were also found located on the mitochondrial chromosome (data not shown).

Together, the data shows that the genes most robustly repressed by Cyc8 reside in the sub-telomeric regions and include many genes encoding cell wall proteins.

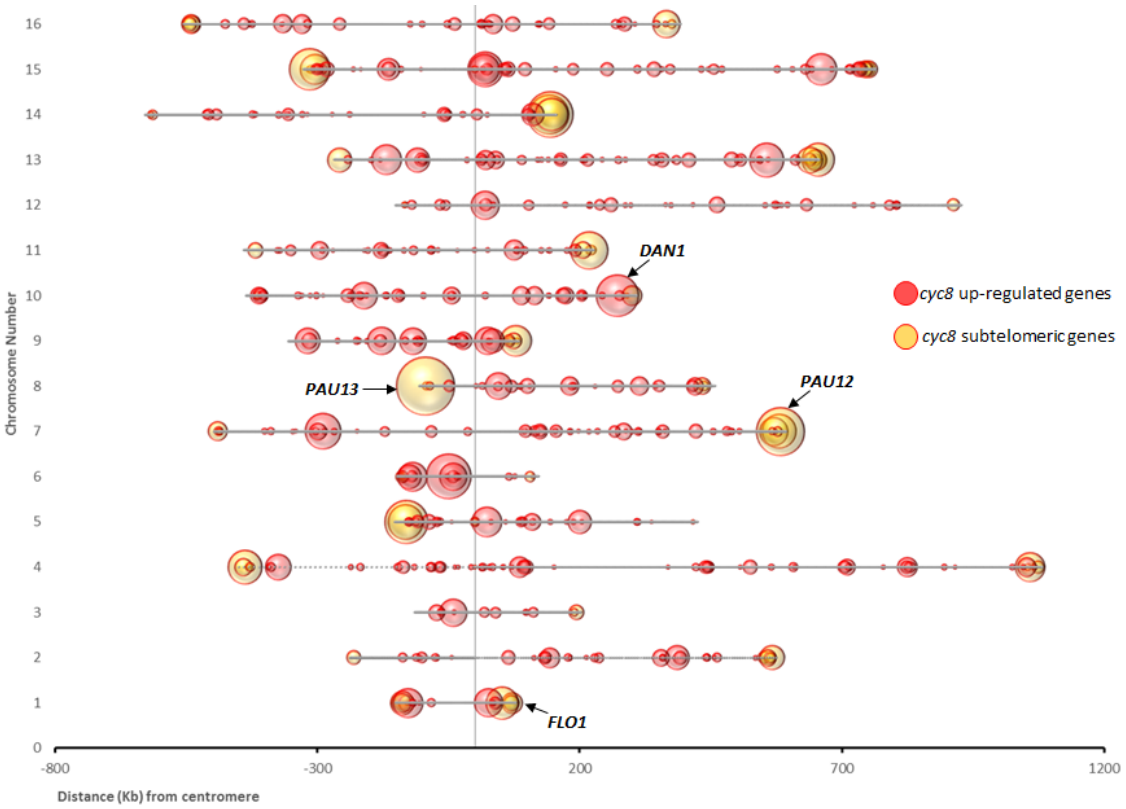

Figure 5.10 Chromosomal location of genes up-regulated in a *cyc8* mutant. 'Bubble' plot showing the location and the fold change in transcription of the 571 genes up regulated more than 2-fold in a *cyc8* mutant compared to wt. Chromosome centromeres were set as zero and the chromosome sizes and gene positions were normalized accordingly. Each chromosome's number and size are shown. The location of the de-repressed genes are indicated by a circle, and the circle area represents the fold increase in transcription of genes in a *cyc8* mutant. The yellow bubbles with a red outline represent subtelomeric genes, while red bubbles represent genes located elsewhere on the chromosome.

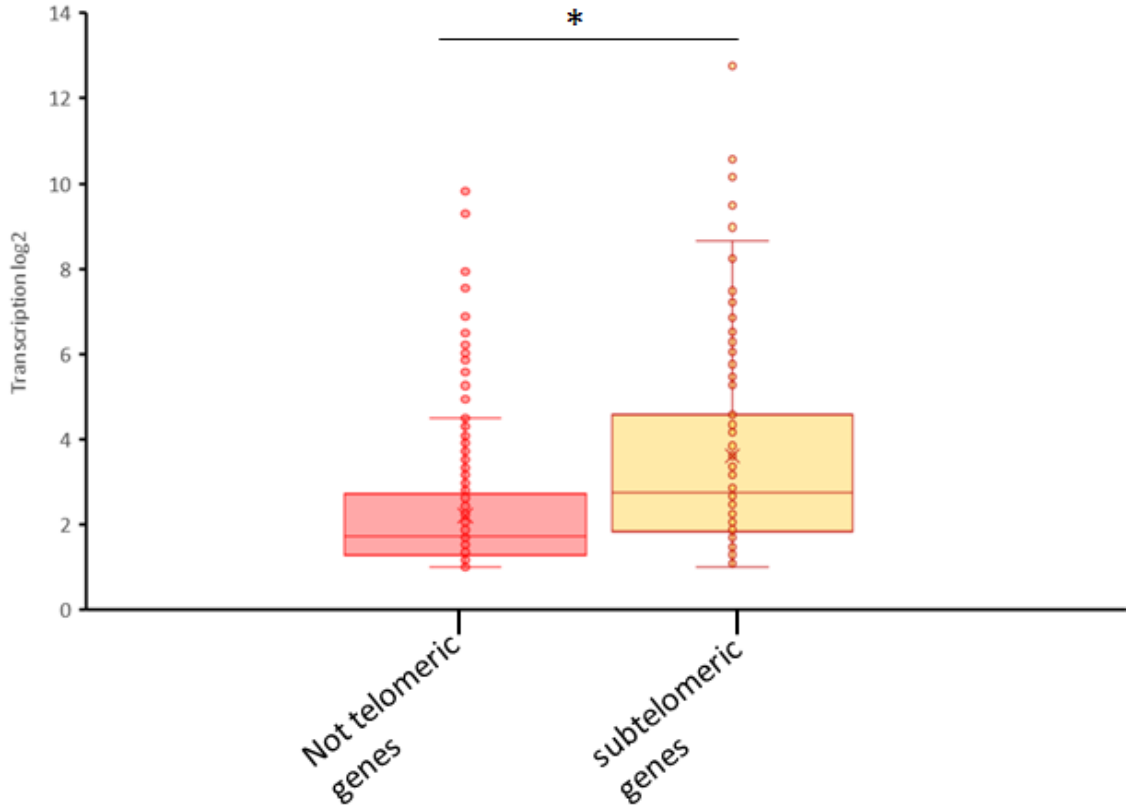

Figure 5.11 The transcription level of subtelomeric and non subtelomeric genes de-repressed more than 2-fold in a *cyc8* mutant. Box-whisker chart represents the level of transcription above 2-fold change of genes in subtelomeric (red box) and non subtelomeric (yellow box) gene regions. The asterisks indicate of P value < 0.001 obtained from a student's t-test.

5.2.2.6 Investigating clustering of genes regulated (repressed) by Cyc8:

Next, it was elucidated whether the genes repressed by Cyc8 were located individually or were found within groups, and if so, in what orientation.

196 of the genes de-repressed more than 2-fold in the *cyc8* mutant (34% of the total Cyc8-repressed genes) were organised into 82 gene groups of 2 or more genes (Fig. 5.12). Within these groups, there were 57 groups (71.4% of the groups) of 2 genes, 18 groups containing 3 genes and 7 groups of 4 genes (Fig. 5.12A).

Analysis of the 57 groups containing pairs of Cyc8 repressed genes revealed there was not a bias for genes being in any particular orientation. Indeed, there was no significant difference in whether genes were orientated convergently, divergently or facing in the same sense or antisense direction (Fig. 5.12B).

The gene groups were further organised by clustering analysis to generate a clustering dendrogram. The cluster measured the distance between the genes identifying 199 genes which were in 82 groups of genes, then it measured the distance between the farthest points of two clusters and all the possible points between two clusters (Fig. 5.13).

The bubble plot in (Fig. 5.14) shows the relative transcription de-repression levels of the genes in these groups in the absence of *cyc8*. The results suggested that there was not a specific location of where these groups would be found across the chromosomes with groups being dispersed in subtelomeric and non subtelomeric regions and varying in their level of de-repression (Fig. 5. 14).

Furthermore, gene ontology analysis showed that these groups of genes were not enriched for any particular functions. In summary, these analyses showed that the genes most robustly repressed by Cyc8 reside within the subtelomeric regions and include many genes encoding cell wall proteins. Although there was evidence for Cyc8 repressed genes being found within groups of two or more genes, the genes within these groups showed no particular orientation bias and did not have any obvious shared functions.

A.

Number of the genes in each group	Number of the group
4 genes	7
3 genes	18
2 genes	57
Total	**82**

B.

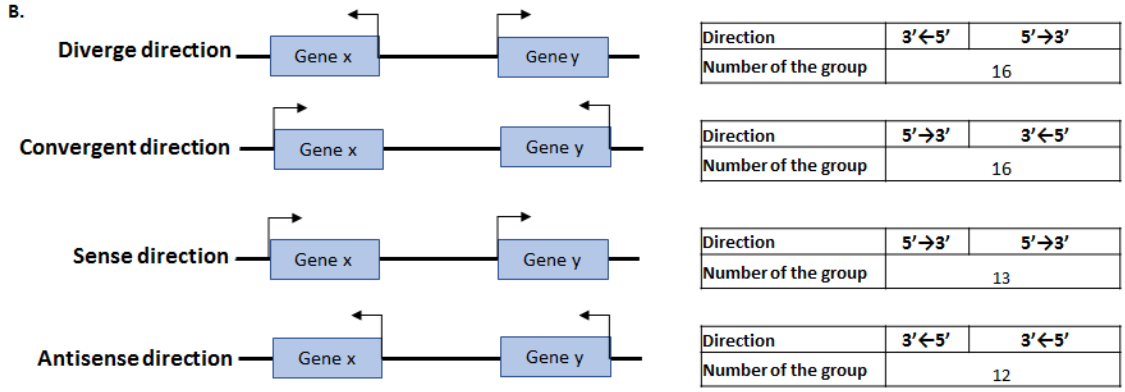

Direction	3'←5'	5'→3'
Number of the group	16	

Direction	5'→3'	3'←5'
Number of the group	16	

Direction	5'→3'	5'→3'
Number of the group	13	

Direction	3'←5'	3'←5'
Number of the group	12	

Figure 5.12 Grouping and orientation of genes de-repressed in a *cyc8* mutant. A: the genes number in each group and the number of groups. **B:** the grouped genes number and orientation.

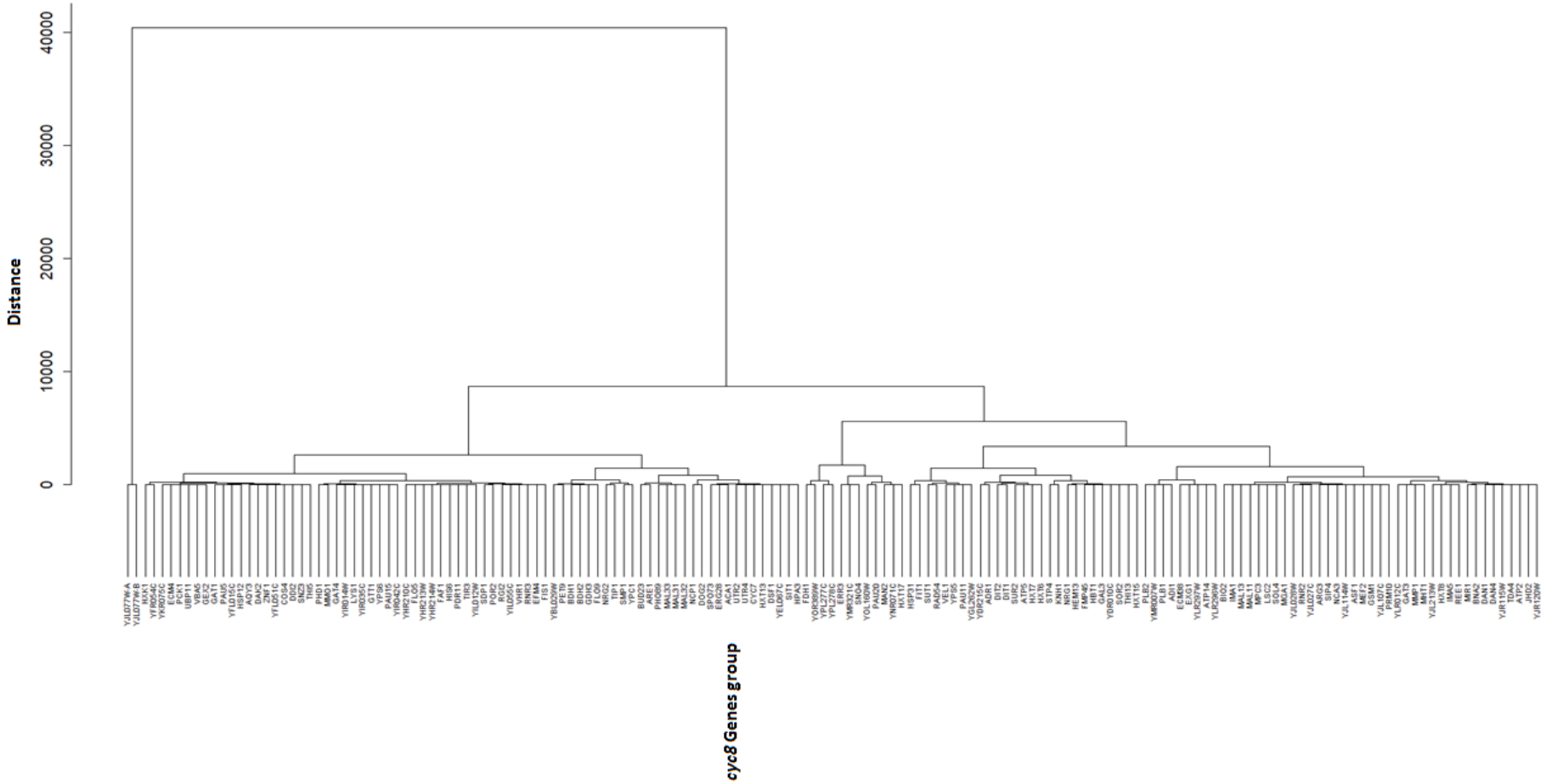

Figure 5.13 Cluster dendrogram of the grouped genes location within the Tup1-Cyc8 regulon. The cluster identified 82 grouped genes in *cyc8* mutants. The horizontal axis of the dendrogram represents the distance or dissimilarity between clusters, the vertical axis represents the objects and clusters. The horizontal position of the split, shown by the short vertical bar, gives the distance between the two clusters.

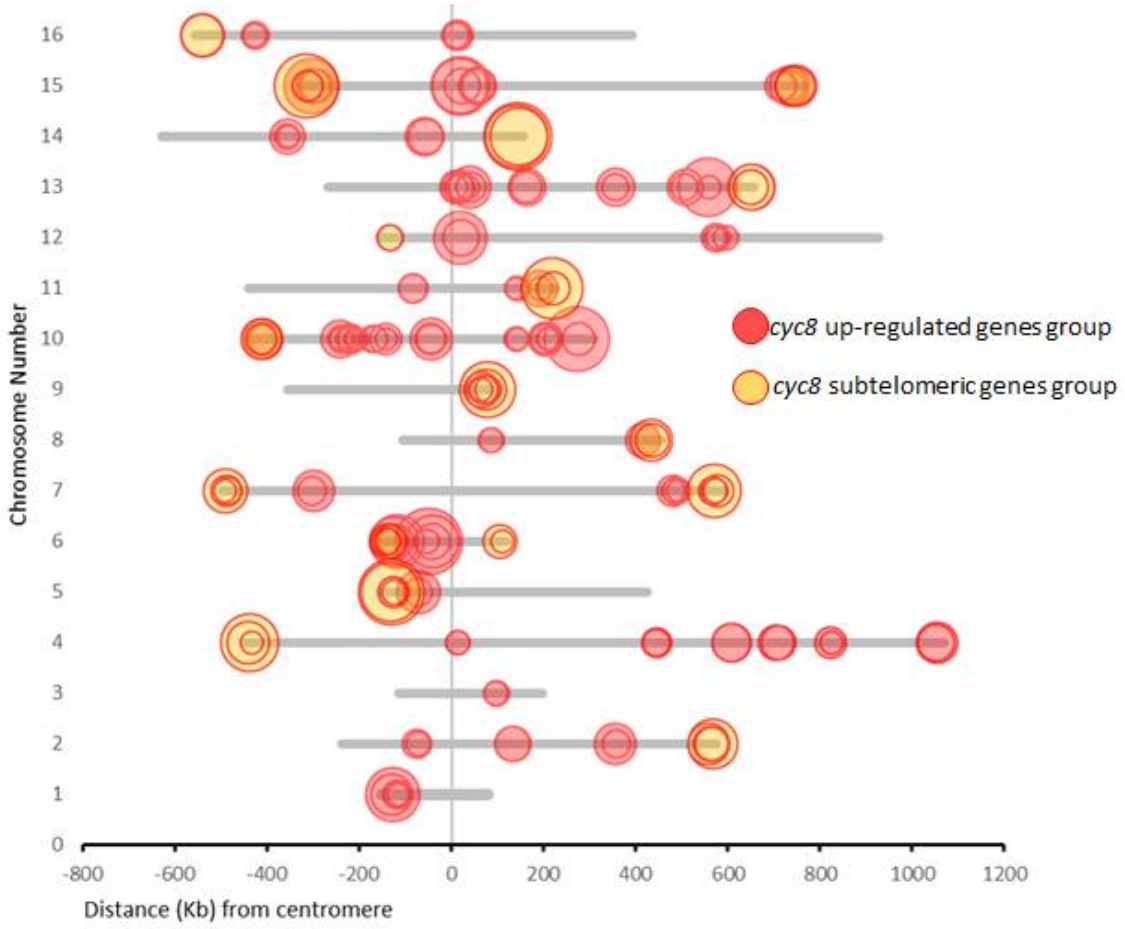

Figure 5.14 Location and level of de-repression of Cyc8-repressed gene clusters. 'Bubble' plot showing the location and the change in transcription of the 82 groups of *cyc8*-repressed genes. Circle area represents the fold increase in transcription of genes in a *cyc8* mutant. Each line represents the chromosome number and shows the gene location.

5.2.3 Gene transcription profiles in a *snf2* deletion mutant:

In the *snf2* gene deletion mutant, in which the *KAN* gene has replaced the *SNF2* open reading frame, 278 (4.2%) genes were downregulated at least 2-fold compared to wt, indicating these genes required Swi-Snf for activation (Fig. 5.15A) (Appendix I, Table S6). There were also 208 genes that were up-regulated in the *snf2* mutant, suggesting Snf2 acted negatively on transcription at these genes (Fig. 5.15A) (Appendix I, Table S7). An example of a gene which was downregulated *QDR2* (*YIL121W*) and upregulated *DLD3* (*YEL071W*) in the absence of Snf2, as depicted in J-browse, is shown in (Fig. 5.15B).

The down-regulated genes in the *snf2* mutant varied widely in function but the most highly down-regulated genes comprised numerous genes involved in transposition *(YJR029W)*, sugar transport (*HXT7*) and phosphate metabolism (*PHO84*) (Table 5.3). The highly up-regulated genes in *snf2* the genes had different roles like carbohydrate and amino acid transport (Table. 5.4).

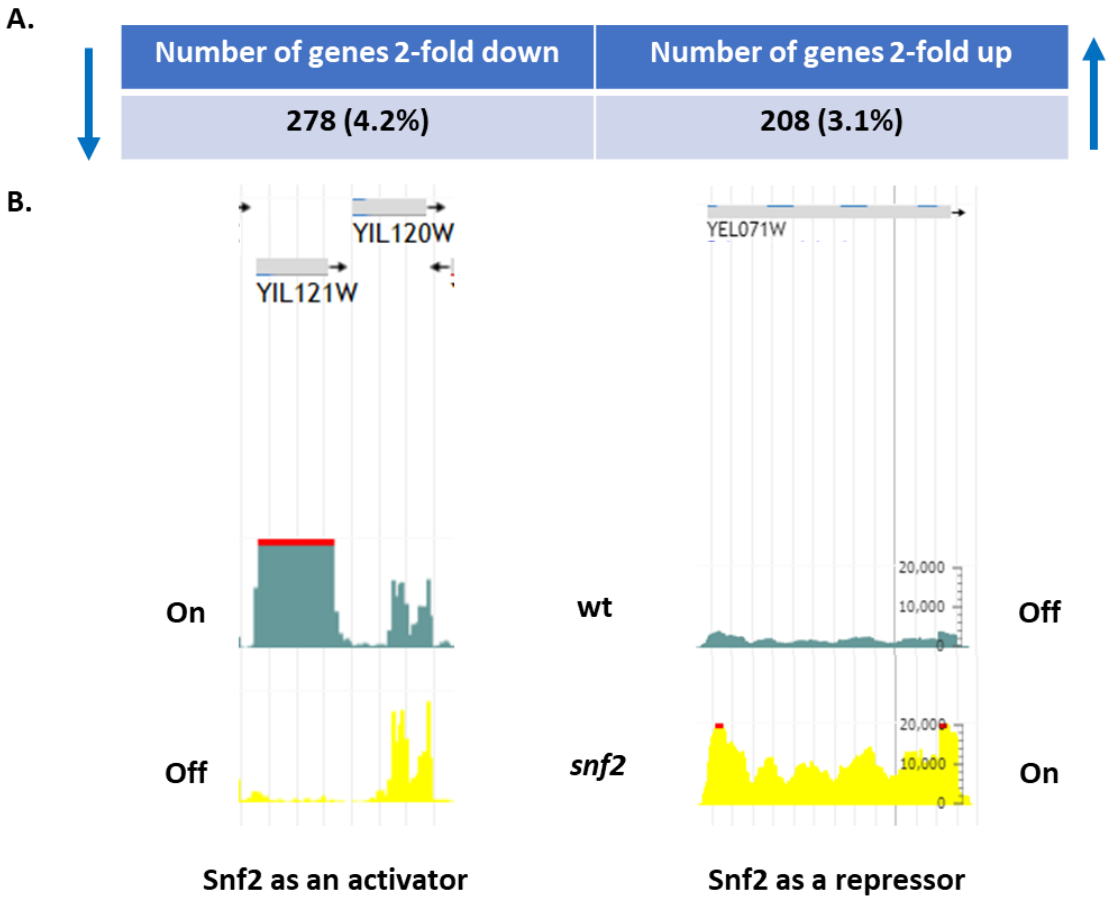

Figure 5.15 Genes regulated more than 2-fold in a *snf2* gene deletion mutant. A. The number of genes that were 2- fold up- and down- regulated in a *snf2* gene deletion mutant with 4.2% upregulated and 3.1% 2- fold downregulated genes. **B**: J-browse image to show the transcription level of *YIL121W* (*QDR1*) which was upregulated in wt while it is downregulated in *snf2;* also shown is *YEL071W* (*DLD3*) which is upregulated in wt and downregulated in *snf2*. Green colour reflects wt transcription yellow colour reflect *snf2* transcription.

Gene	Description of protein product	wt vs *snf2* FC down
PHO84	Inorganic phosphate transporter	-184.63
SPL2	Putative cyclin-dependent kinase inhibitor	-139.26
PTR2	Peptide transporter	-96.27
QDR2	Quinidine resistance protein	-62.27
PHO12	Acid phosphatase	-44.35
RSB1	Sphingoid long-chain base transporter	-42.39
YDR365W-B	Transposon Ty1-DR6 Gag-Pol polyprotein	-40.96
YLR256W-A	Transposon Ty1-LR3 Gag-Pol polyprotein	-31.43
YGP1	Yeast glycol protein, cell wall	-30.17
PHO5	Repressible acid phosphatase	-27.49
YRO2	heat shock and acid stress protein	-26.92
HXT7	High-affinity hexose transporter	-24.21
TIR1	Cold shock-induced protein TIR1, cell wall protein	-23.07
YPR158W-B	Transposon Ty1-PR2 Gag-Pol polyprotein	-22.68
PHO11	Acid phosphatase	-22.62
YHB1	Flavohemoprotein	-22.07
YMR046C	Transposon Ty1-LR3 Gag-Pol polyprotein	-21.3
YMR045C	Transposon Ty1-LR3 Gag-Pol polyprotein	-21.09
HO	Homothallic switching endonuclease	-20.77
MRH1	Membrane protein, heat shock	-19.73
YGR027W-B	Transposon Ty1-GR1 Gag-Pol polyprotein	-19.27
YBL005W-B	Transposon Ty1-BL Gag-Pol polyprotein	-18.63
YDR261C-D	Transposon Ty1-DR4 Gag-Pol polyprotein	-18.6
YBL005W-A	Transposon Ty1-BL Gag-Pol polyprotein	-18.35
YLR227W-B	Transposon Ty1-LR3 Gag-Pol polyprotein	-18.15
YOL103W-B	Transposon Ty1-OL Gag-Pol polyprotein	-16.13
TIP1	Temperature shock, cell wall protein	-15.42
YJR029W	Transposon Ty1-JR2 Gag-Pol polyprotein	-15.34
PHM6	Phosphate metabolism protein	-14.79
YPR158C-D	Transposon Ty1-PR3 Gag-Pol polyprotein	-14.69
ARO10	Transaminated amino acid decarboxylase	-14.55
OPT2	Oligopeptide transporter	-14.35
YJR027W	Transposon Ty1-JR1 Gag-Pol polyprotein	-13.43
NDJ1	Non-disjunction protein	-13.19
GSY1	Glycogen [starch] synthase isoform	-13.05

Gene	Description of protein product	wt vs *snf2* FC down
YHR214C-B	Transposon Ty1-H Gag-Pol polyprotein	-12.81
YGR035C	Uncharacterized protein	-12.55
HSP12	12 kDa heat shock protein	-12.44
YER053C-A	Uncharacterized protein	-12.12
YPR137C-B	Transposon Ty1-PR1 Gag-Pol polyprotein	-12.06
PHO3	Constitutive acid phosphatase	-11.75
GPH1	Glycogen phosphorylase	-11.19
RPI1	Negative RAS protein regulator protein	-11.13
YER138C	Transposon Ty1-ER1 Gag-Pol polyprotein	-10.96
TIR3	Cell wall protein	-10.46
RGI1	Respiratory growth induced protein 1	-10.25
TPO4	Polyamine transporter 4	-10.1
HMS1	Probable transcription factor	-9.97
HSP30	Heat shock protein	-9.75
VTC3	Vacuolar transporter chaperone	-9.5

Table 5.3 The top 50 genes down-regulated in a *snf2::KAN* mutant. The top 50 downregulated genes in the *snf2*::*KAN* mutant strain (more than 2-fold down-regulated compared to wt) were listed along with their product descriptions and fold-changes (FC); the blue colour indicates a negative transcription fold change compared to wt. The genes description according to panther gene ontology (Mi *et al*. 2017).

Gene	Description of protein product	wt vs *snf2* FC
SER3	D-3-phosphoglycerate dehydrogenase	17.21
THI5	4-amino-5-hydroxymethyl-2-methylpyrimidine phosphate synthase	13.08
THI12	4-amino-5-hydroxymethyl-2-methylpyrimidine phosphate synthase	12.72
SFC1	Succinate/fumarate mitochondrial transporter	12.67
SUL2	Sulfate permease 2	11.81
MET2	Homoserine O-acetyltransferase	10.19
MET3	Sulfate adenylyltransferase	9.98
STR3	Cystathionine beta-lyase	8.41
BNA2	Indoleamine 2,3-dioxygenase	8.09
MMP1	S-methylmethionine permease 1	7.52
SEO1	Probable transporter	7.24
PAU2	Seripauperin-2, cell wall protein	7.23
YGL007C-A	Uncharacterized protein	7.11
AAD15	Putative aryl-alcohol dehydrogenase	6.74
SUL1	Sulfate permease 1	6.62
ARG3	Ornithine carbamoyltransferase	6.61
YPR064W	Uncharacterized protein	6.61
MET6	5-methyltetrahydropteroyltriglutamate-homocysteine methyltransferase	6.5
FIT3	Facilitator of iron transport 3	6.31
FIT1	Facilitator of iron transport 1	6.2
PDC6	Pyruvate decarboxylase isozyme 3	5.88
MET10	Sulfite reductase [NADPH] flavoprotein component	5.86
YPL062W	Uncharacterized protein	5.84
MET5	Sulfite reductase [NADPH] subunit beta	5.73
AAC1	ADP,ATP carrier protein 1	5.69
BRP1	Uncharacterized protein	5.41
YIR042C	Uncharacterized protein	4.85
HXT11	Hexose transporter	4.72
YMR244W	Uncharacterized protein	4.7
YMR122C	Uncharacterized protein	4.7
YAR068W	Uncharacterized protein	4.49
YPR078C	Uncharacterized protein	4.49
GAP1	General amino-acid permease	4.42
YPR015C	Zinc finger protein	4.41

Gene	Description of protein product	wt vs *snf2* FC
YHL037C	Uncharacterized protein	4.41
ARG5,6	Arginine requiring	4.29
HBN1	Putative nitroreductase	4.23
CAR1	Arginase	4.23
CPA2	Carbamoyl-phosphate synthase arginine-specific large chain	4.22
DLD3	D-2-hydroxyglutarate--pyruvate transhydrogenase	4.17
MET14	Adenylyl-sulfate kinase	4.13
SPS22	Sporulation-specific protein	4.02
YJL077W-A	Uncharacterized protein	3.95
LDS2	Outer spore wall protein	3.94
MXR1	Peptide methionine sulfoxide reductase	3.87
MET13	Transcriptional regulator	3.86
YKL071W	Uncharacterized oxidoreductase	3.85
CLD1	Cardiolipin-specific deacylase 1, mitochondrial	3.84
REC8	Meiotic recombination protein	3.81
YKL107W	Uncharacterized oxidoreductase	3.77

Table 5.4 The top 50 genes up-regulated in a *snf2::KAN* mutant. The top 50 upregulated genes in *snf2* were listed along with their descriptions and fold-changes, the red colour indicates the highest transcription fold-change (FC) of the genes whose products had varied functions. The genes description according to panther gene ontology (Mi *et al*. 2017).

5.2.3.1 Gene validation *snf2* RNA-Seq data:

The results from the RNA-Seq analysis showed that in a *snf2* gene deletion mutant (*snf2*::*KAN*) 278 genes were downregulated more than 2-fold compared to wt, whilst 208 genes were upregulated. To validate this set of genes, the expression of the *ZRT1* gene was analysed by RT-qPCR (Fig. 5.16B). The results showed a ~2.5-fold down-regulation of this gene occurred in the *snf2* mutant versus wt, which was consistent with the~5-fold decrease detected using RNA-Seq (Fig. 5.16C).

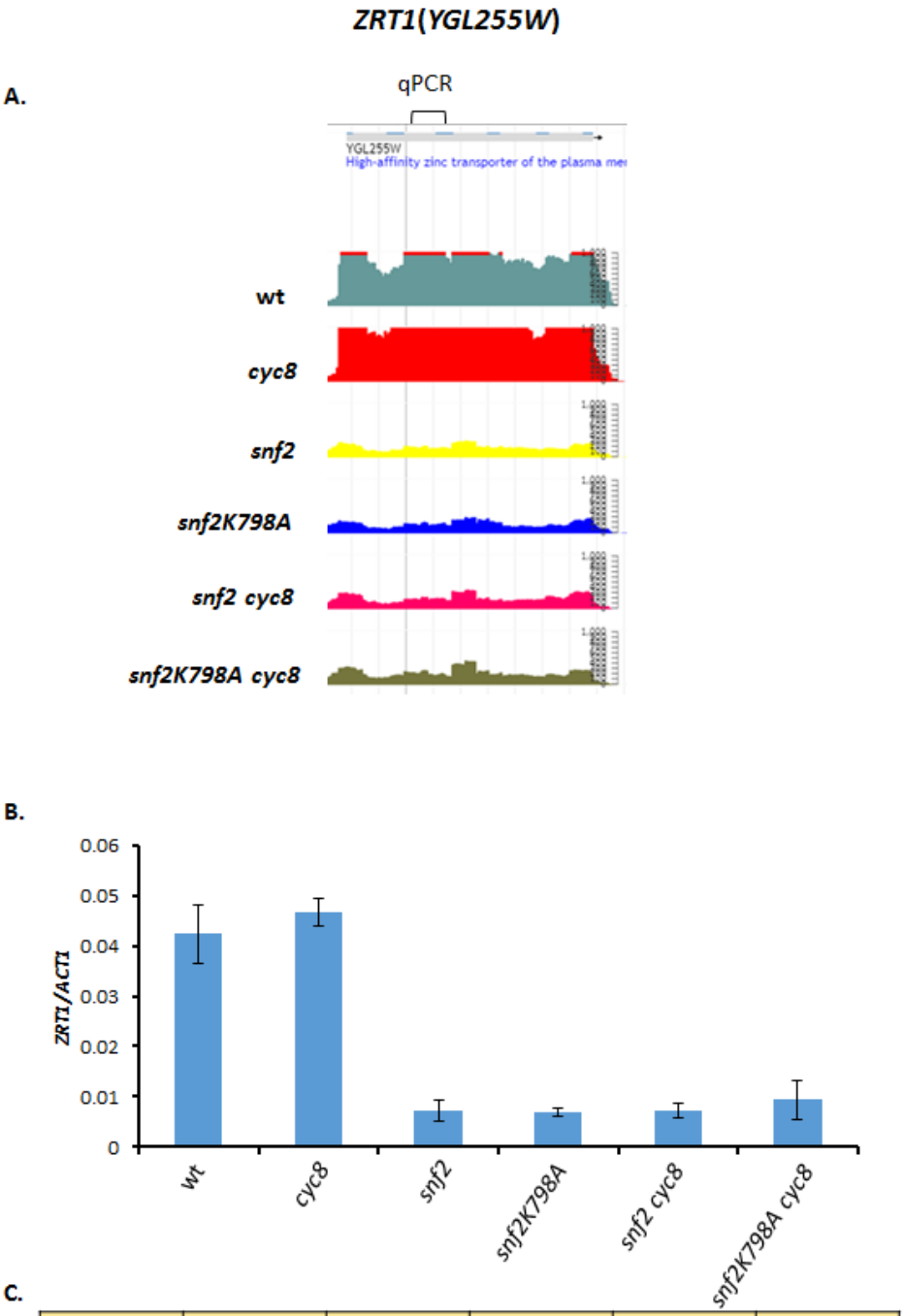

C.

snf2 FC down	WT vs cyc8 FC	WT vs *snf2* FC	WT vs *snf2K798A* FC	*cyc8* vs *snf2 cyc8* FC	*cyc8* vs *snf2 cyc8* FC
ZRT1	1.68	-5.5	-5.57	-6.8	-6.81

Figure 5.16 *ZRT1* transcription. A: J-browse screen-shot to show read counts across the *ZRT1 genes* in the strains indicated. **B:** Data was confirmed by gene-specific RT-qPCR analysis. **C:** Quantification of the fold-change in transcription level (RNA-Seq) shown in A; the red colour indicates a high transcription level, and the blue colour indicates the low level of transcription.

5.2.3.2 Gene ontology analysis of genes whose transcription is altered in a *snf2* mutant:

5.2.3.2.1 Snf2 acting as an activator of gene expression:

In order to define the 278 genes with a 2-fold upregulation in the *snf2* gene deletion mutant, gene ontology analysis using the *Saccharomyces* genome database (SGD) was used. Genes were characterised into three annotation sets; (i) biological process, (ii) molecular function and (iii) cellular component (Fig. 5.17) (Appendix I, Table S8).

In the biological process category, 39 genes played a role in transmembrane transport, (GO ID: 0055085), another 39 genes were involved in oxidation-reduction processes, and (GO ID:0055114), 36 genes were classified as having a role in transposition (GO ID: 0032196). A further 29 genes were each classed as involved with DNA integration (GO:0015074) and cell wall organisation (GO:0071555).

When genes were classified according to molecular function, most of the genes (130 genes) were defined as having 'catalytic activity' (GO:0003824) and included the *ENO1* gene which encodes an Enolase I, involved in glycolysis.

In the Cellular component category, 52 of the genes were involved with the plasma membrane (GO ID: 0005886), 38 genes were vacuole associated (GO ID 0005773), and 31 genes were cell wall related (GO ID: 0005618). In summary, a wide variety of genes require the *SNF2* gene for transcription, suggesting Snf2 acts as an activator of transcription at these genes. However, it is interesting to note that prevalent among those genes most dependent upon Snf2 for transcription were genes involved in transposition and phosphate metabolism.

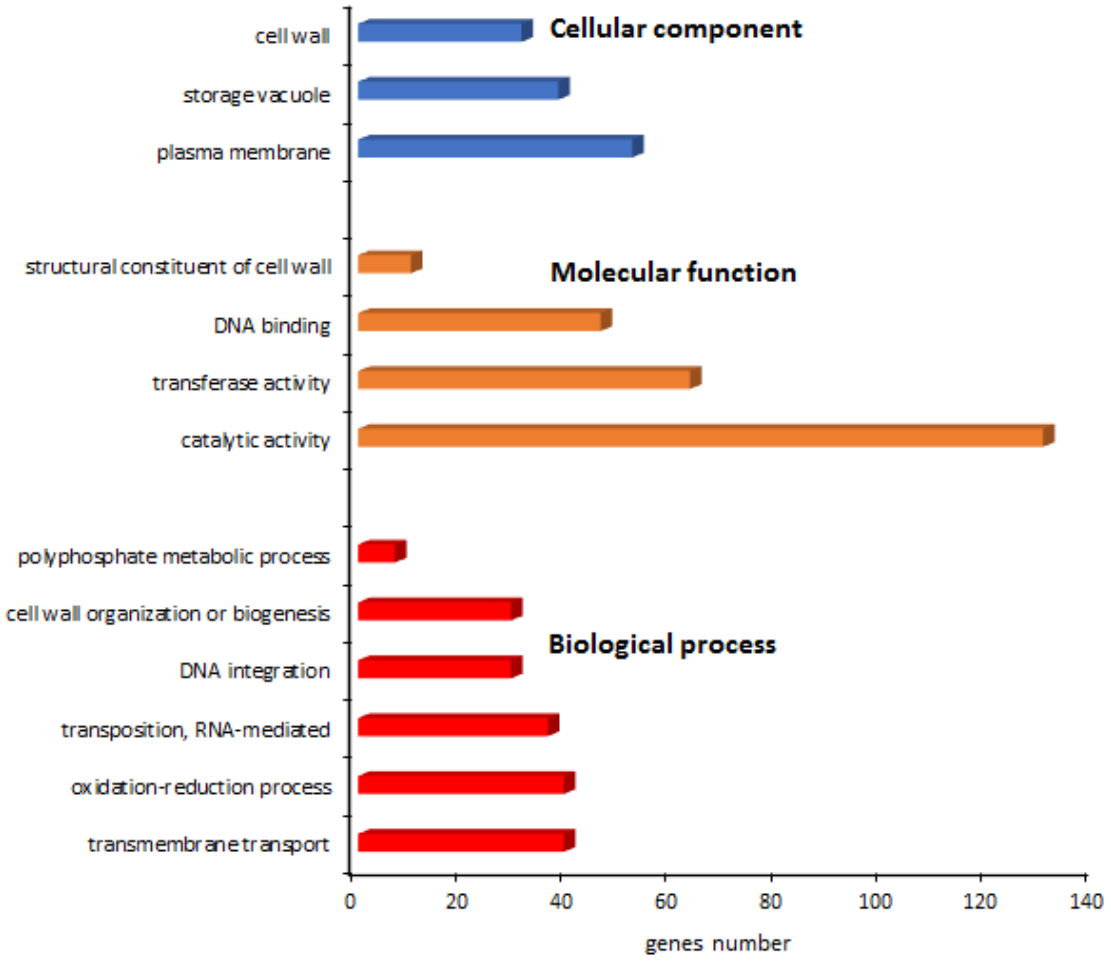

Figure 5.17 Gene ontology analysis of genes at least 2-fold down-regulated in a *snf2* gene deletion mutant. Column charts for the *snf2* mutant gene ontology using the *Saccharomyces* genome analyses database (SGD). Red represents the biological process category, orange indicates the molecular function category, and the blue lines indicate the cellular component category. Results are shown after filtering for genes with P value < 0.001.

5.2.3.2.2 Snf2 acting as a repressor:

Intriguingly, the expression of 208 genes were at least 2-fold upregulated in the *snf2* gene deletion mutant compared to wt suggesting that Swi-Snf plays a role as a repressor at these genes. Gene ontology analysis was applied to define this set of genes using three annotation sets; (i) biological process, (ii) molecular function and (iii) Cellular component (Fig. 5.18) (Apendix I, Table S9).

In the biological process category, 36 of the genes functioned within cellular amino acid metabolic processes (GO ID: 0006519) and 38 genes were involved in oxidation-reduction processes (GO ID: 0055114), for example *DLD3* gene which encode 2-hydroxyglutarate transhydrogenase.

In the molecular function category, 26 genes had oxidoreductase activity (GO ID: 0016491), and 19 and 15 genes were involved with cofactor (GO ID: 0048037) and coenzyme binding, respectively (GO ID:0050662).

In the cellular component category, the majority of the genes (62 genes) were membrane related (GO ID: 0031224), whilst 15 genes played a role in the cell wall (GO ID: 0005618).

Thus, despite Snf2 and the Swi-Snf complex generally being considered an activator of transcription, our analysis showed that in the absence of Snf2, a high number of genes of varying function were de-repressed suggesting Snf2 has a repressive role at these genes.

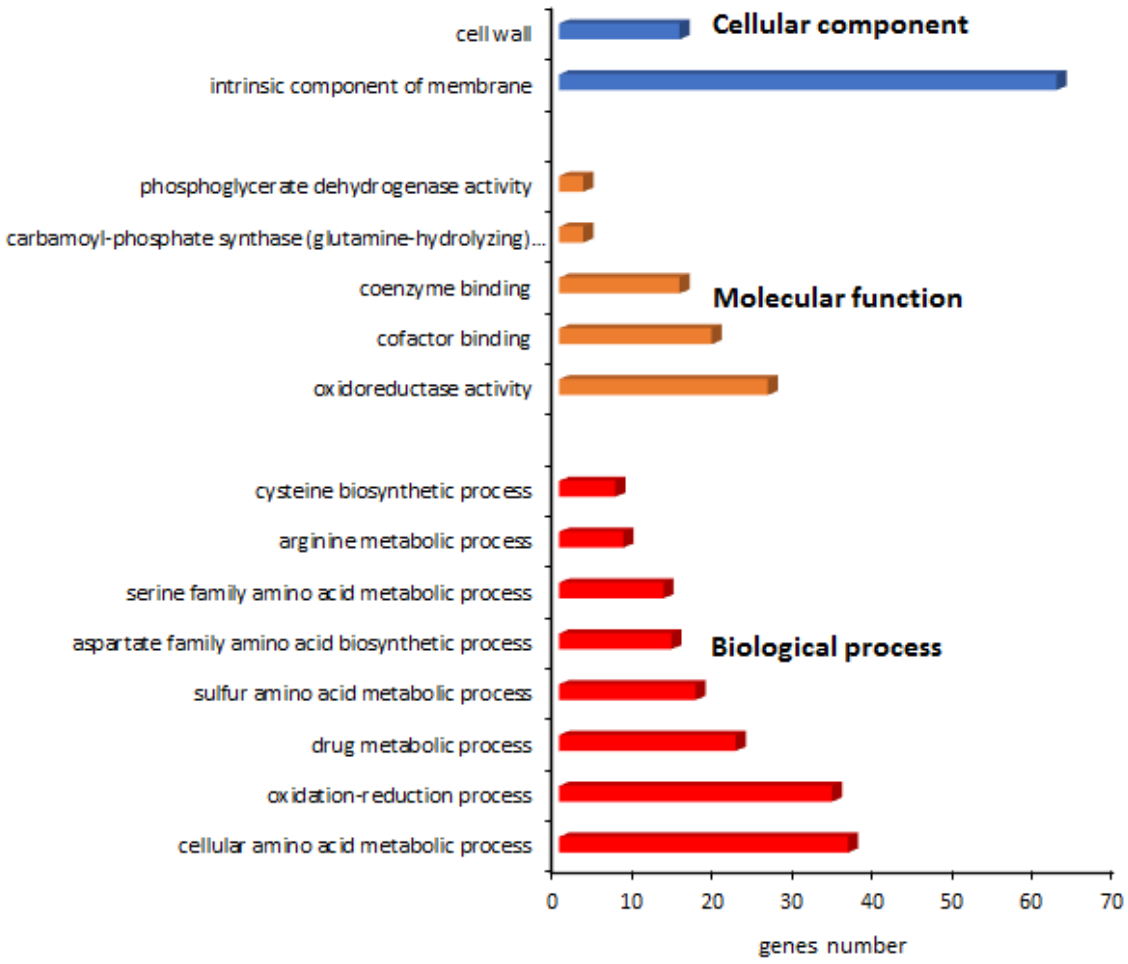

Figure 5.18 Gene ontology analysis of genes with a 2-fold increase in expression in a *snf2* mutant. Column charts for the *snf2* mutant genes ontology using the *Saccharomyces* genome analyses database (SGD). Red represents the biological process category, orange indicates the molecular function category, and blue represents the cellular component category. Results are shown for genes with P value < 0.01.

5.2.3.3 Investigating stress response genes down regulated in a *snf2* deletion mutant:

In the previous results chapters 3 and 4, stress response assessment assays using spot tests found that various Swi-Snf mutants had a variety of phenotypes. Therefore, the 278 downregulated genes in the *snf2* mutant were analysed for genes involved in various stress responses including, response to heat (GO:0009408), response to oxidative stress (GO:0006979), response to osmotic stress (GO:0006970), response to starvation (GO:0042594) and response to DNA damage (GO:0006281).

The results revealed that 30 out of the 278 genes (~10%) were stress response genes, with 10 genes involved in response to heat stress, including the heat response genes *HSP12*, *HSP26* and *HSP30,* which were downregulated the most. 13 genes were identified to be involved in response to oxidative stress including *GPX2*, which is encode a glutathione peroxidase. Nine genes involved in the osmatic stress response were downregulated in the *snf2* mutant including the heat shock genes *HSP12* and *HSP30*. There were six genes involved in the starvation response that were downregulated with transcription of *PHO5,* encoding an acid phosphatase, and *PHM6,* involved in phosphate metabolism being most reduced. Finally, DNA damage response related genes were downregulated, and of these, the most downregulated was *DDR48*, which encodes a DNA damage responsive protein (Fig. 5.19).

Together the results show that Snf2 is positively required for varying levels of transcription of genes involved in the cells response to numerous stresses.

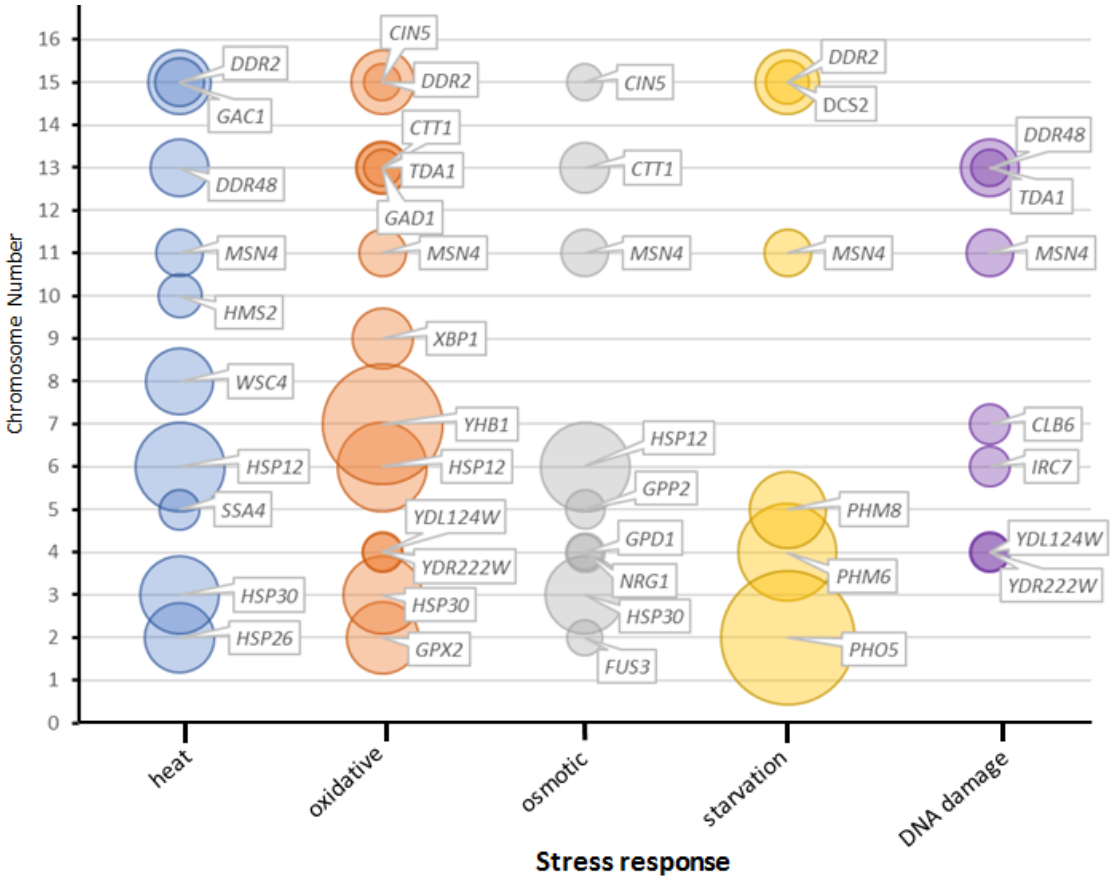

Figure 5.19 Stress response genes downregulated in a *snf2* deletion mutant. Bubble plot showing transcription level and chromosomal location for five families of stress response genes; heat response (blue), oxidative stress (orange), osmatic stress (gray), starvation stress (yellow) and DNA damage (purple). The X value represents each family, the Y value reflects the chromosome number in which each gene is located, while the bubble size represents the transcription-fold decrease in the *snf2* mutant compared to wt.

5.2.3.4 Chromosomal location of genes down- regulated in a *snf2* mutant:

I next analysed the chromosomal location and the level of transcription fold decrease of the 278 downregulated genes in the *snf2* mutant compared to wt.

The results showed that the genes downregulated in the absence of Snf2 were spread evenly over the chromosomes with only 22 genes (7.9%) of the 277 downregulated genes being located in the subtelomeric regions (indicated in yellow) (Fig. 5.20). Only one gene was located on the mitochondrial chromosome (Mito chromosome) called *VAR2* (data not shown).

The transcription level of the subtelomeric vs non subtelomeric genes was next analysed in order to determine if there was any differences in transcriptional fold-changes of Snf2-dependent genes located in these two distinct chromosomal regions. However, the results showed no statistically significant difference in the level of downregulation of genes in a *snf2* mutant, regardless of whether the genes were found in subtelomeric or non subtelomeric regions (Fig. 5.21). In summary, the genes which were downregulated in a *snf2* mutant showed no bias for any particular chromosomal location and were subject to similar levels of positive control by Snf2 regardless of gene location.

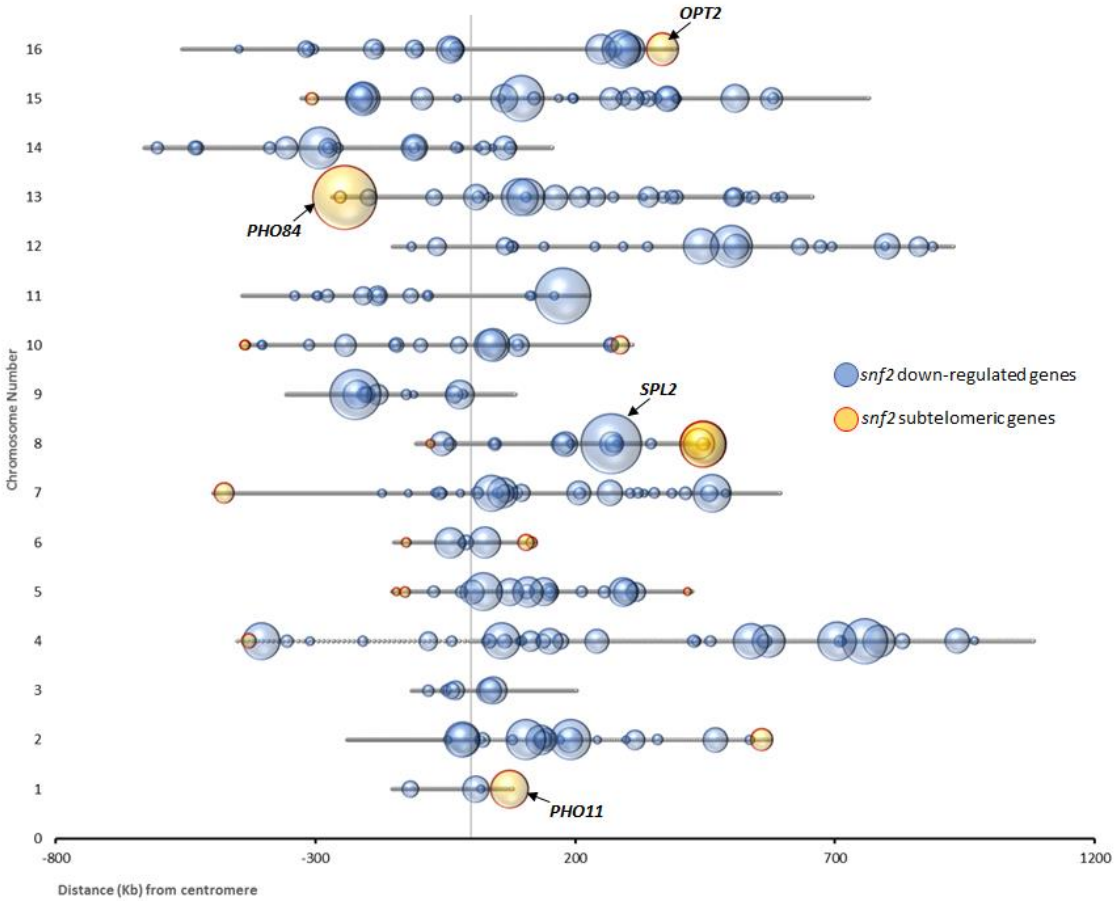

Figure 5.20 Location of genes down-regulated in a *snf2* mutant. 'Bubble' plot showing the location and the change in transcription of the 277 genes which had at least 2-fold downregulation in a *snf2* deletion mutant. Circle position reflects gene location, circle area represents the fold decrease in transcription of genes in a *snf2* mutant relative to wt. Each line represents the chromosome number. Red and yellow represents the subtelomeric genes while blue indicates the non-subtelomeric genes on the chromosome. The data of each chromosome and gene were provided from *Saccharomyces* genome database (SGD) (Cherry *et al*. 1998). All 16 chromosomes centromeres were set in zero and the chromosomes size and genes position were normalized according to that.

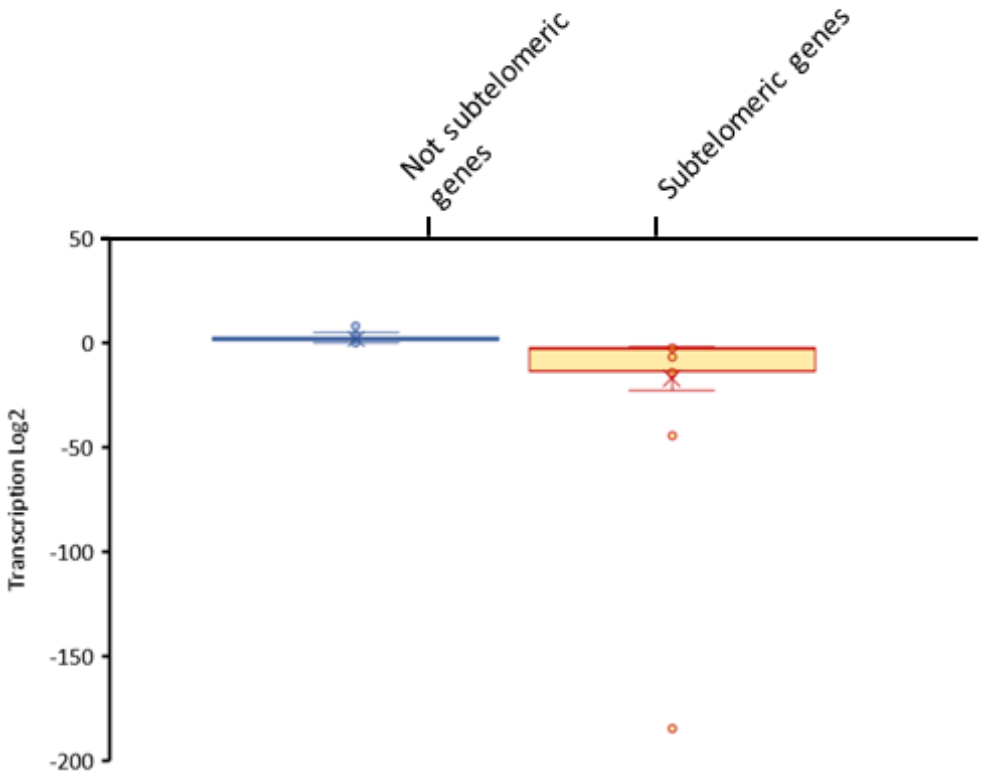

Figure 5.21 The transcription level of subtelomeric and non subtelomeric genes which were down-regulated in a *snf2* mutant. Box chart represents the level of the transcription in $\log_2$ (at least 2-Fold change down)**.** The subtelomeric genes are indicated by the yellow box and the blue box indicates non telomeric genes.

5.2.3.5 Investigating clustering of genes subject to Snf2 regulation of transcription:

Genes that were down-regulated in the *snf2* mutant were next analysed to determine whether these genes were found in groups of genes or were located individually.

The results showed that only 12 groups of genes were downregulated in the absence of *snf2* compared to wt, with 11 groups of two genes and just one group containing three genes (Fig. 5.22A).

The orientation of the genes found within these groups were examined, and it was observed that two groups of genes were divergently arranged, two groups were convergent, and genes arranged in a tandem sense or antisense manner were each found in four other groups (Fig. 5.22B).

The gene groups were further organised by clustering analysis to generate a clustering dendrogram. The cluster measured the distance between the genes identifying 25 genes which were in 12 groups of genes, then it measured the distance between the farthest points of two clusters and all the possible points between two clusters (Fig. 5.23). I found that only two groups contained pairs of functionally related genes. One group contained the *PHO3* and *PHO5* genes whose products play a role in phosphate metabolism, and the other group contained the *CLB1* and *CLB6* genes whose products are involved in cell cycle progression.

Finally, the chromosomal position of these groups of Snf2-dependent genes were analysed and visualised along with their fold-change in transcription in the *snf2* mutant compared to wt. The data showed that the groups were found located on ten of the 16 chromosomes in various chromosomal locations. The levels of downregulation of the genes varied with half of the groups showing a similar level of downregulation, whilst the genes in the other six groups were downregulated to different extents. Thus, the level of downregulation of gene transcription of genes found in different groups and genes within the same groups varied (Fig. 5.24).

Together, this analysis revealed that the genes that were at least 2-fold downregulated in the *snf2* mutant, and which might be subject to Snf2 acting as an activator for their transcription, did not appear to be located at any particular chromosomal regions.

Further, they were not found in a significant number of groups and were downregulated to various levels regardless of being grouped or independently located. In addition, the majority of genes found within the 12 groups of genes were not functionally related.

A.

Number of the genes in each group	Number of the group
3 genes	1
2 genes	11
Total	**12**

B.

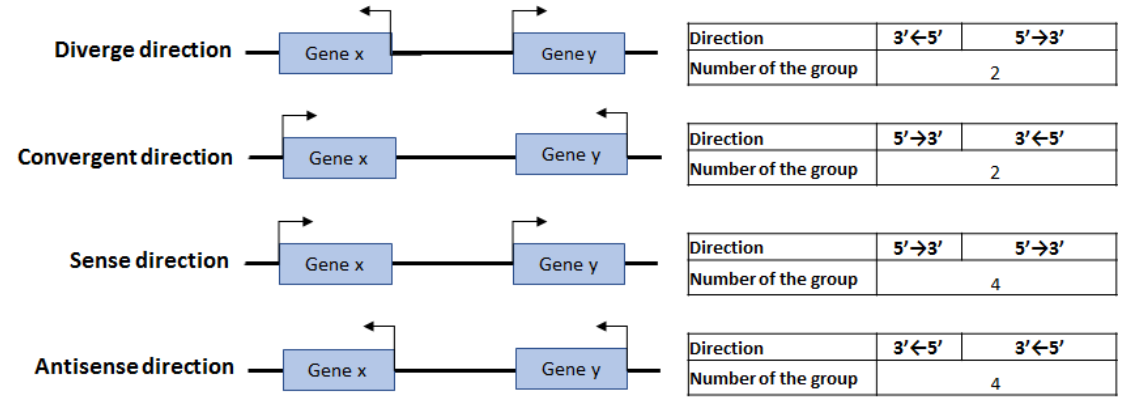

Direction	3'←5'	5'→3'
Number of the group	2	

Direction	5'→3'	3'←5'
Number of the group	2	

Direction	5'→3'	5'→3'
Number of the group	4	

Direction	3'←5'	3'←5'
Number of the group	4	

Figure 5.22 The transcription direction of the grouped genes down-regulated in *snf2* mutant. A: The number of genes in each group. **B:** The direction of the transcription of each group.

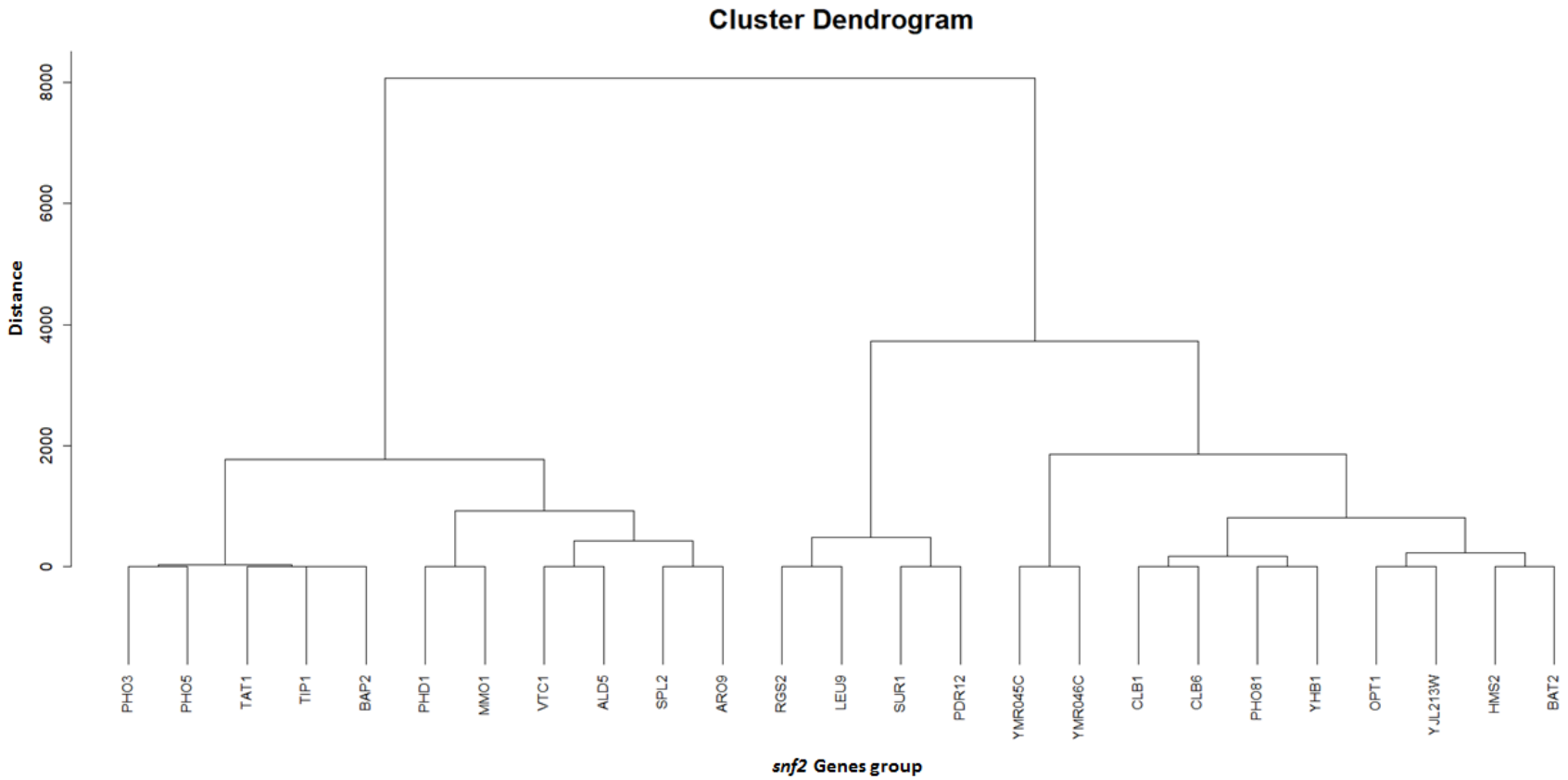

Figure 5.23 Cluster dendrogram of the *snf2* grouped genes location. The cluster identified 12 groups of genes in *snf2* mutants. The horizontal axis of the dendrogram represents the distance or dissimilarity between clusters, the vertical axis represents the objects and clusters. The horizontal position of the split, shown by the short vertical bar, gives the distance between the two clusters.

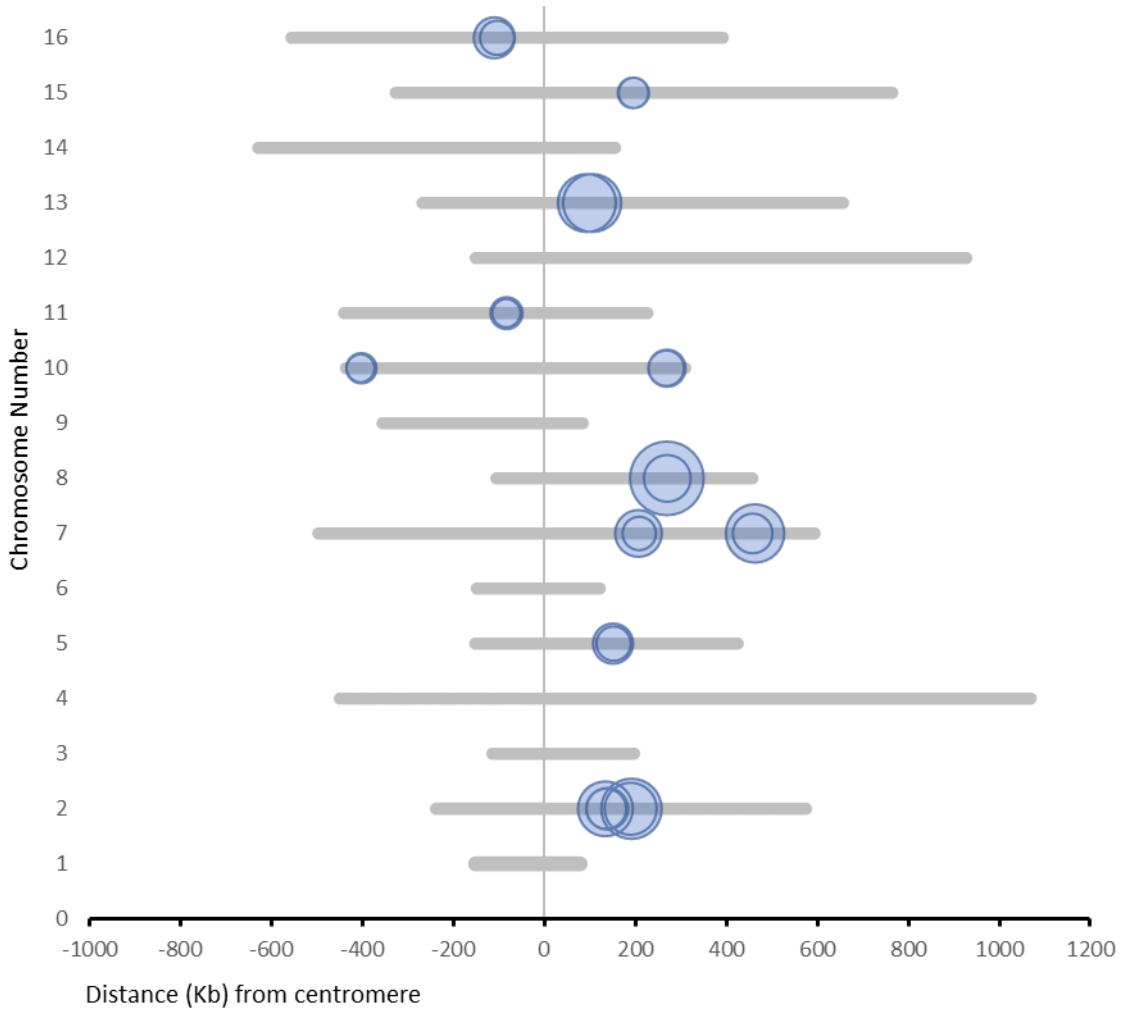

Figure 5.24 Clustering of genes down-regulated in a *snf2* mutant. 'Bubble' plot showing the clustering of genes and the change in transcription of the 12 groups of Swi-Snf downregulated genes. Circle area represents the fold-decrease in transcription of genes in a *snf2* mutant. Each line represents the chromosome number.

5.2.4 Gene transcription profiles in a *snf2K798A* mutant:

In the previous sections, gene transcription in a Snf2 full gene deletion mutant was analysed, and it was proposed that in the absence of the *snf2* subunit, the structural integrity of the Swi-Snf complex is severely compromised (Dutta *et al*. 2017). Therefore, in this section, global transcription in a *snf2* mutant which contains a lysine to arginine amino acid substitution (*snf2K798A*) which nullifies the catalytic activity of the Snf2 protein was analysed. It is expected that this mutant, although catalytically dead for Snf2 activity, will contain an intact Swi-Snf complex. Thus, the aim was to compare the results from a strain containing an inactive and dissociated Swi-Snf complex (*snf2*) with a strain containing an intact but inactive Swi-Snf complex (*snf2K798A*). This way it was hoped to determine whether Swi-Snf has any ATPase independent roles.

Following RNA-Seq analysis in the *snf2K798A* catalytically dead mutant strain, 248 genes were down regulated more than 2-fold relative to wt, indicating these genes required Swi-Snf as an activator (Fig. 5.25A) (Appendix I, Table S10). Conversely, there were 145 genes upregulated at least 2-fold compared with wt indicating that Swi-Snf plays a role as a repressor at these genes (Fig. 5.25A) (Appendix I, Table S11). An example for a gene which was downregulated (*YDR119W-A*) and an upregulated gene (*YJL008W*) in the *snf2K798A* mutant as presented in J-browse, is shown in (Fig. 5.25B).

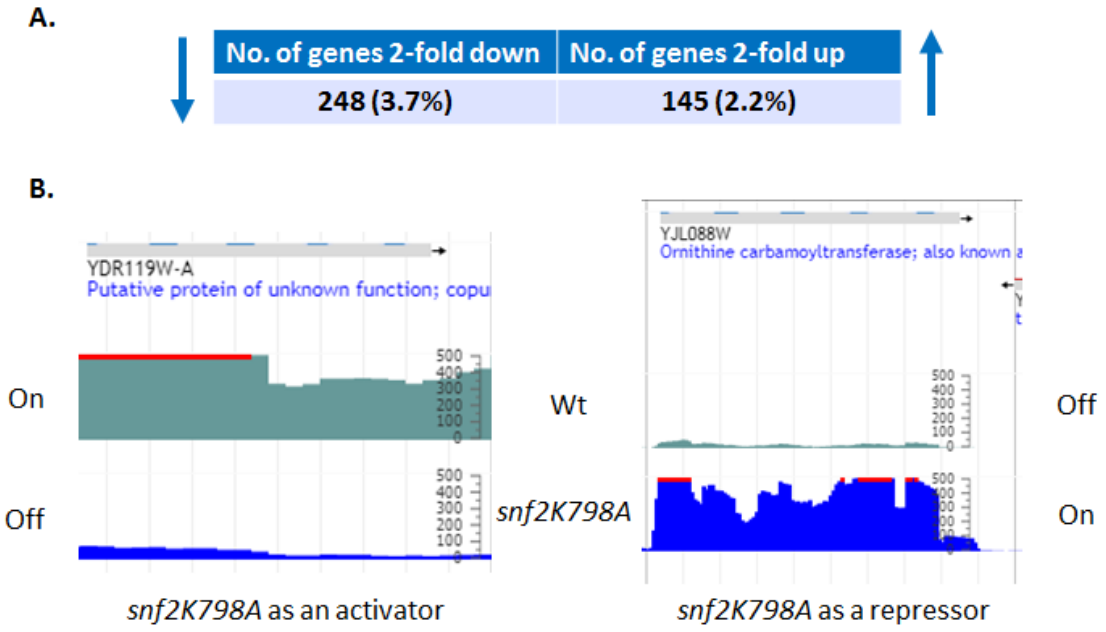

Figure 5.25 Genes with more than 2-fold change in expression in a *snf2K798A* mutant. **A**: The number of genes that were 2- fold up- and down- regulated in *snf2K798A* mutant with 4.2% upregulated and 3.1% 2- fold downregulated. **B**: J-browse snapshot depicting the transcription level of *QDR1* (*YIL121W*) which is upregulated in wt and downregulated in *snf2K798A*. *BAR1* (*YEL071W*) was upregulated in wt and downregulated in *snf2*. Green colour reflects wt transcription blue colour reflect *snf2K798A* transcription.

Using RT-qPCR analysis, the *SER3* gene was chosen to validate this sets of genes (Fig. 5.30A). The results showed that in wt *SER3* gene transcription was highly repressed while it was de-repressed in the *snf2K798A* and *snf2 mutants.* Interestingly, the level of de-repression of *SER3* was almost two-fold higher compared to wt than that seen in the *snf2* mutant (Fig. 5.30C).

A.

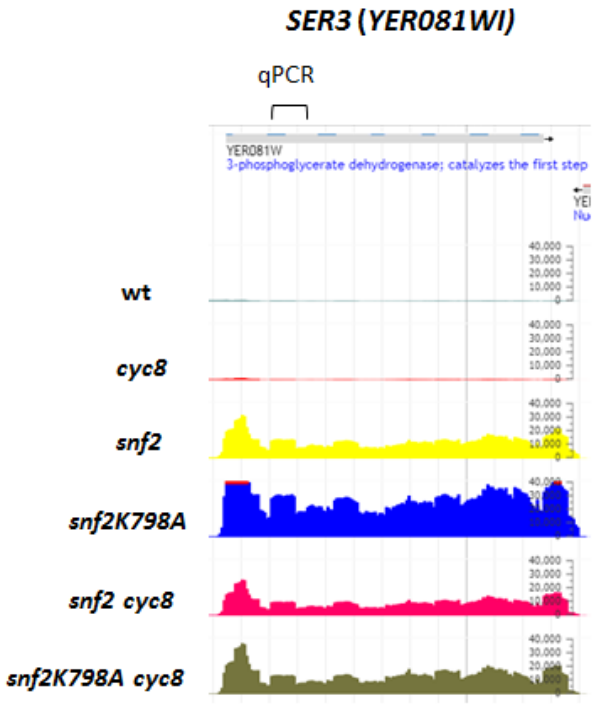

B.

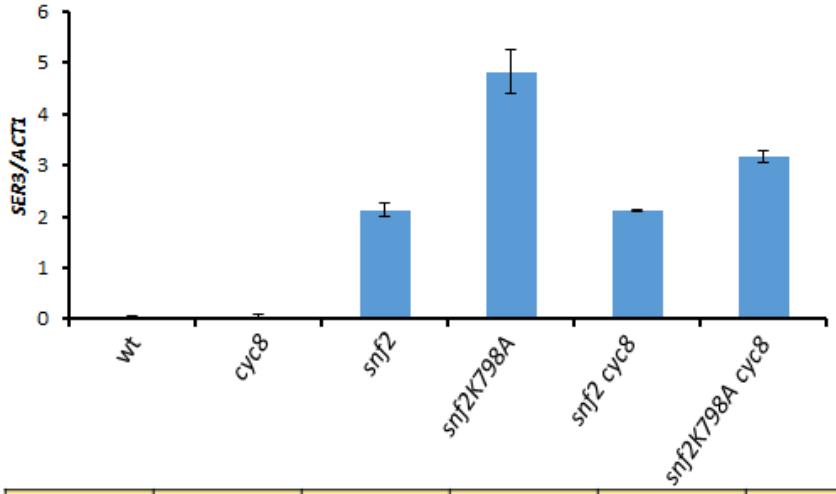

C.

snf2K798R FC up	WT vs *cyc8* FC	WT vs *snf2* FC	WT vs *snf2K798R* FC	*cyc8* vs *snf2* *cyc8* FC	*cyc8* vs *snf2* *cyc8* FC
SER3	1.11	17.21	40.76	16.32	20.55

Figure 5.26 *SER3* transcription. A: J-browse screen-shot to show read counts across the *SER3* genes in the strains indicated. **B:** Data was confirmed by gene-specific RT-qPCR analysis. **C:** The fold change in transcription level profile (RNA-Seq) shown in A; the red colour indicates high transcription levels, the blue colour indicates the low level of transcription. Error bars represent standard deviation of three independent biological replicates.

5.2.4.1 Comparing the down-regulated genes in the *snf2* and *snf2K798A* mutants:

Since Swi-Snf has been best characterised as a co-activator of transcription, the genes which had at least 2-fold down-regulated in the *snf2* full deletion mutant and in the *snf2K798A* catalytically dead mutant were compared.

The Venn diagram shows that a cohort of 223 genes were shared between the two *snf2* mutants, whilst 55 genes were uniquely down-regulated in *snf2* and just 25 genes were uniquely down-regulated in *snf2K798A* (Fig. 5.27). Thus, almost 75% of the total number of genes down-regulated in both the *snf2* and *snf2K798A* mutants are shared.

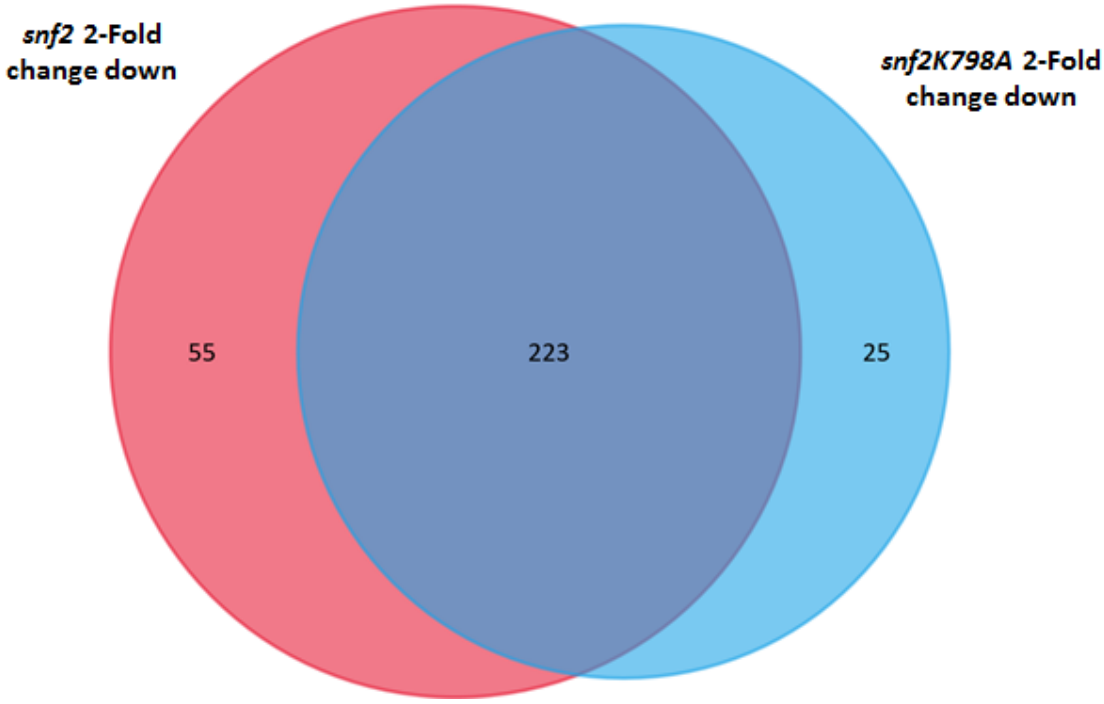

Figure 5.27 Swi-Snf down-regulated genes, *snf2* vs *snf2K798A*. Venn diagram to identify the genes shared and uniquely down-regulated (at least 2-fold change down) in *snf2* and *snf2K798A* mutants. .

5.2.4.2 Comparing the transcription levels of *snf2* and *snf2K798A* down-regulated genes:

I next looked to see if the downregulated genes in the *snf2* and *snf2K798A* mutants were downregulated to different extents or not. By comparing the average level of transcription of the 226 overlapping downregulated genes in the *snf2* and *snf2K798A* mutants, the results showed there was no difference in the transcription level of the overlapping subset of downregulated genes (Fig. 5.28).

Similarly, I compared the overall transcription level of the 55 genes uniquely downregulated in the *snf2* mutant with the overall level of transcription of the 25 genes uniquely downregulated in the *snf2K798A* mutant. The results showed there was no significant difference.

Together, the results show that although a large cohort of genes are similarly downregulated whether Snf2 is absent or present, but in a catalytically dead form. There are 55 genes which require the full Snf2 protein product for activation, and another set of genes which are uniquely dependent upon the Snf2 catalytic activity.

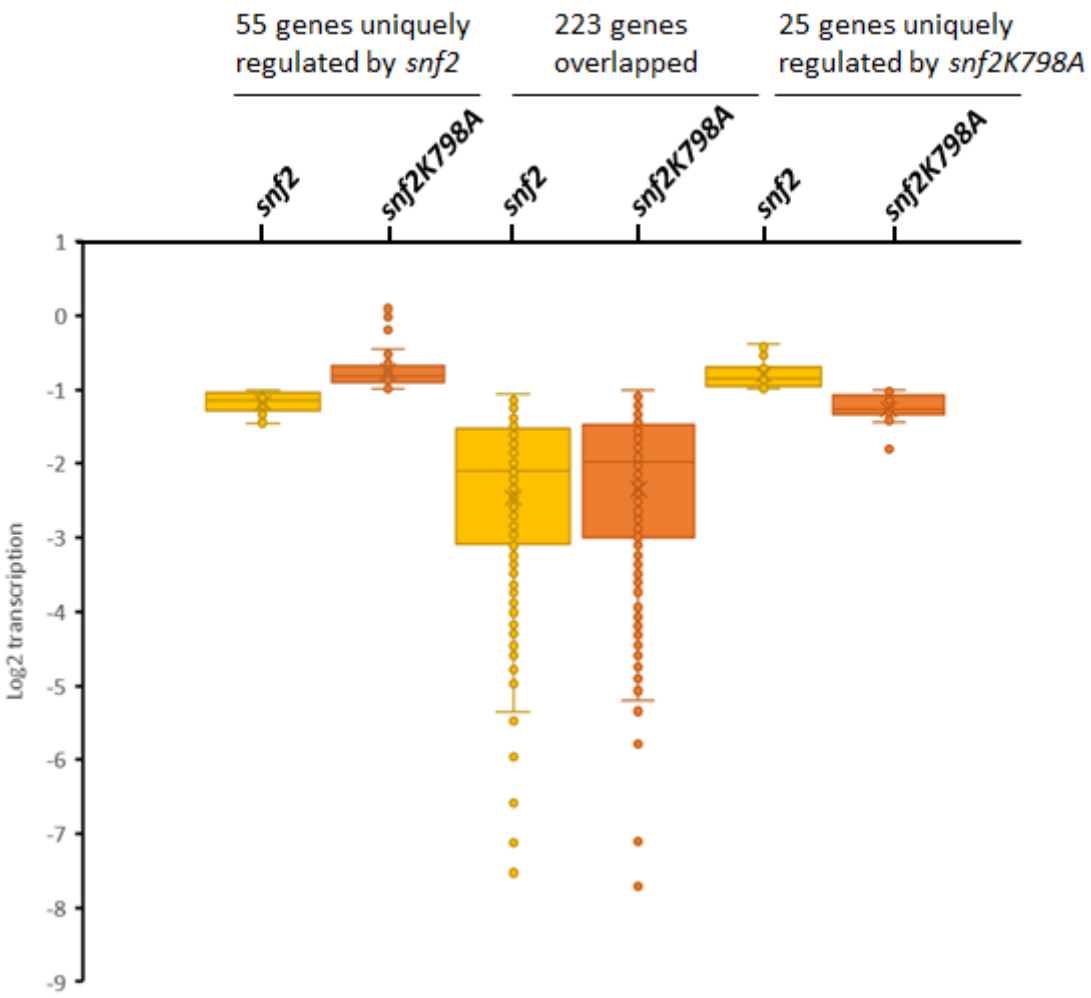

Figure 5.28 Comparing the transcription level of down-regulated genes in *snf2* and *snf2K798A* mutants. Box plot of transcription of the shared and unique sub sets of genes which are downregulated in a *snf2* and *snf2K798A* mutant. The medium line in each box show the average of the transcription.

5.2.4.3 The gene ontology difference between *snf2* and *snf2K798A* down-regulated genes:

In order to find if the genes uniquely downregulated in the *snf2* and *snf2K798A* mutants had specific functions, panther gene ontology analysis was used to identify the function of these genes (Mi *et al*. 2017). The results showed that there was a wide variety of functions attributed to the genes uniquely downregulated in the *snf2* and *snf2K798A* mutants. No obvious specific functions for the genes uniquely downregulated in either the *snf2* full deletion or *snf2K798A* mutant were apparent (Fig. 5.29A & B).

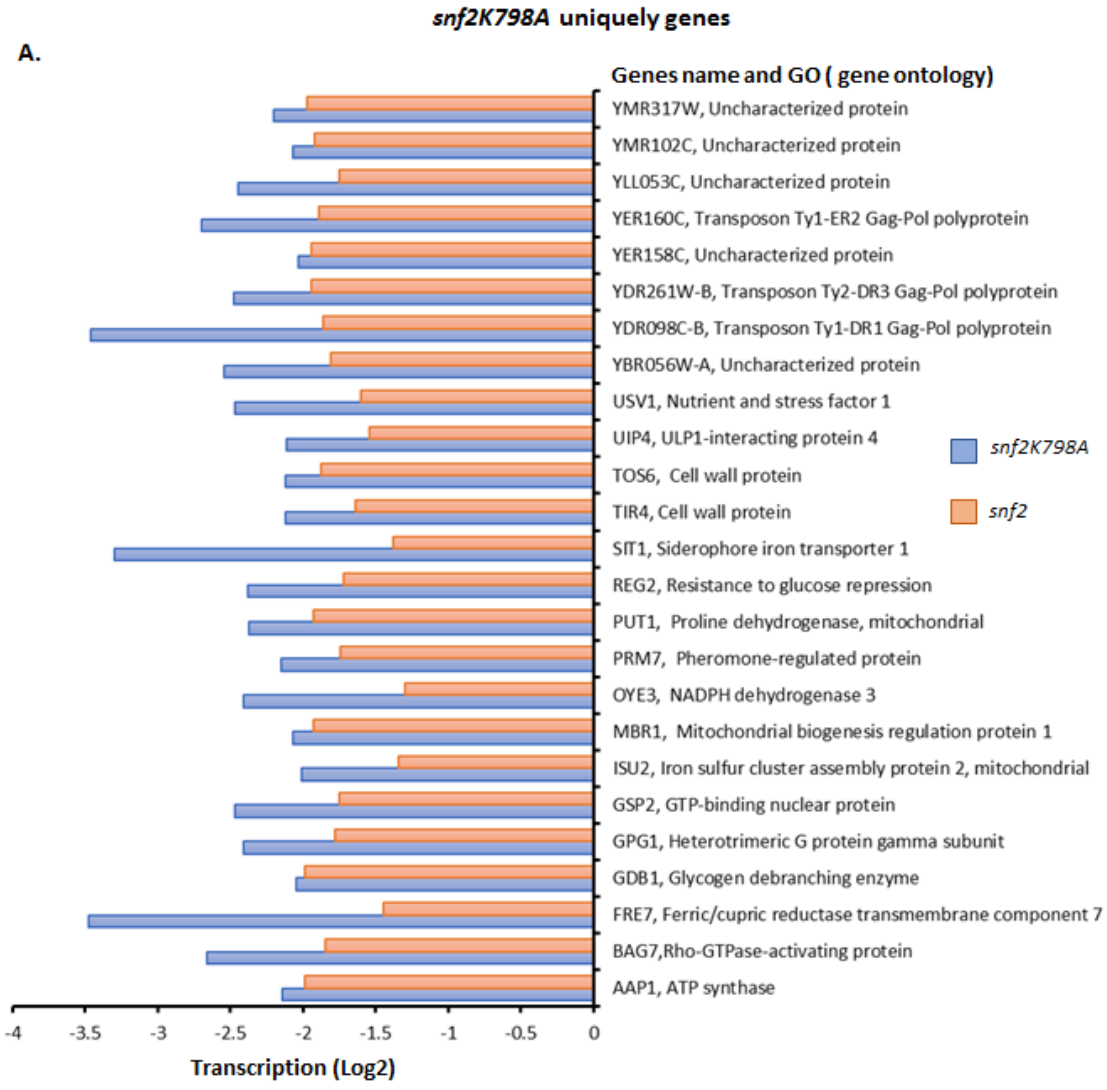
snf2K798A uniquely genes
A.
Genes name and GO (gene ontology)
YMR317W, Uncharacterized protein
YMR102C, Uncharacterized protein
YLL053C, Uncharacterized protein
YER160C, Transposon Ty1-ER2 Gag-Pol polyprotein
YER158C, Uncharacterized protein
YDR261W-B, Transposon Ty2-DR3 Gag-Pol polyprotein
YDR098C-B, Transposon Ty1-DR1 Gag-Pol polyprotein
YBR056W-A, Uncharacterized protein
USV1, Nutrient and stress factor 1
UIP4, ULP1-interacting protein 4
TOS6, Cell wall protein
TIR4, Cell wall protein
SIT1, Siderophore iron transporter 1
REG2, Resistance to glucose repression
PUT1, Proline dehydrogenase, mitochondrial
PRM7, Pheromone-regulated protein
OYE3, NADPH dehydrogenase 3
MBR1, Mitochondrial biogenesis regulation protein 1
ISU2, Iron sulfur cluster assembly protein 2, mitochondrial
GSP2, GTP-binding nuclear protein
GPG1, Heterotrimeric G protein gamma subunit
GDB1, Glycogen debranching enzyme
FRE7, Ferric/cupric reductase transmembrane component 7
BAG7,Rho-GTPase-activating protein
AAP1, ATP synthase
snf2K798A
snf2
-4
-3.5
-3
-2.5
-2
-1.5
-1
-0.5
0
Transcription (Log2)

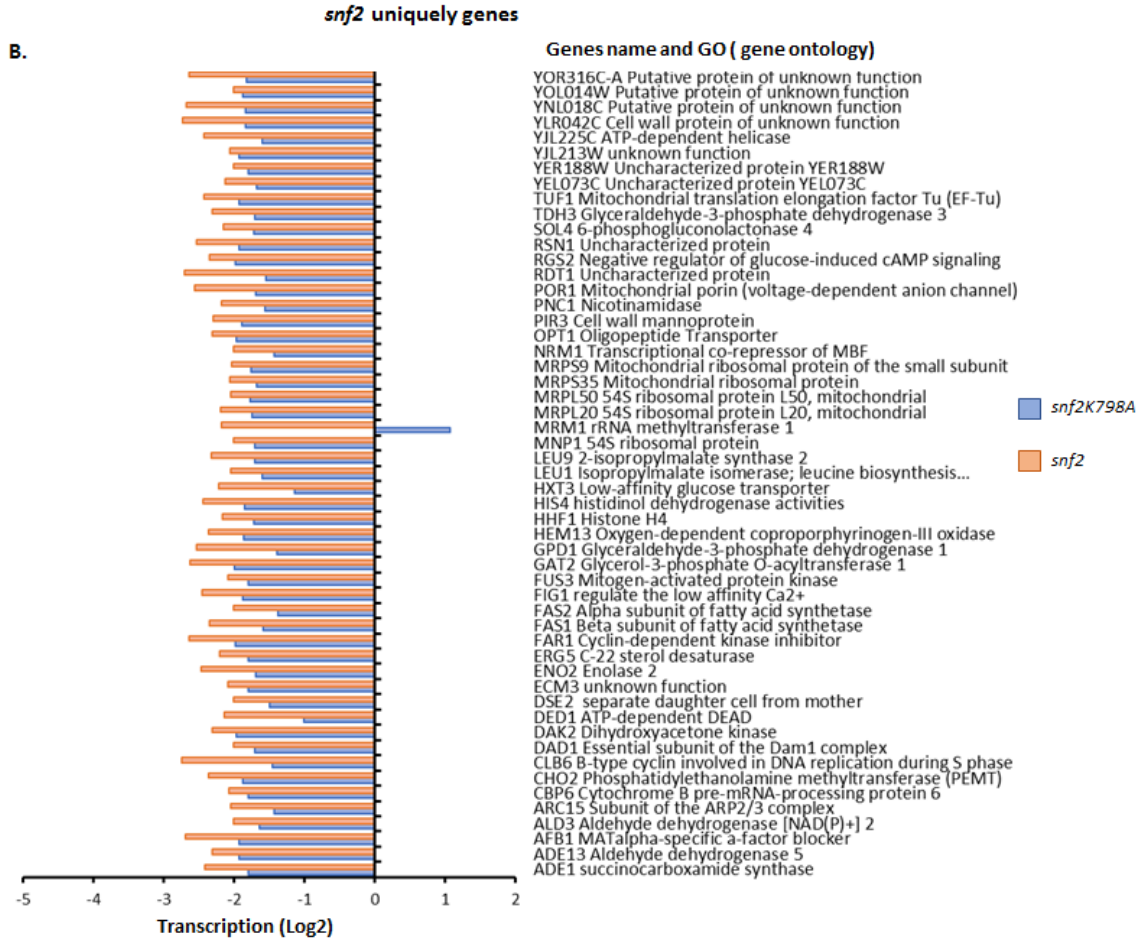

Figure 5.29 Gene ontology analysis of uniquely down-regulated genes in *snf2K798A* and *snf2* single mutants. Column graphs show the different in the transcription in each **A:** *snf2* and **B:** *snf2K798A* and the gene function.

5.2.4.4 Comparison of the genes up-regulated in *snf2* and *snf2K798A* mutants:

The genes with at least two-fold increase in expression in the *snf2* and *snf2K798A* mutants were next compared. The Venn diagram revealed that a cohort of 132 genes were similarly upregulated in the *snf2* and *snf2K798A* mutants, whilst, 76 genes were uniquely upregulated in *snf2* while just 13 genes were uniquely upregulated in *snf2K798A* (Fig. 5.30).

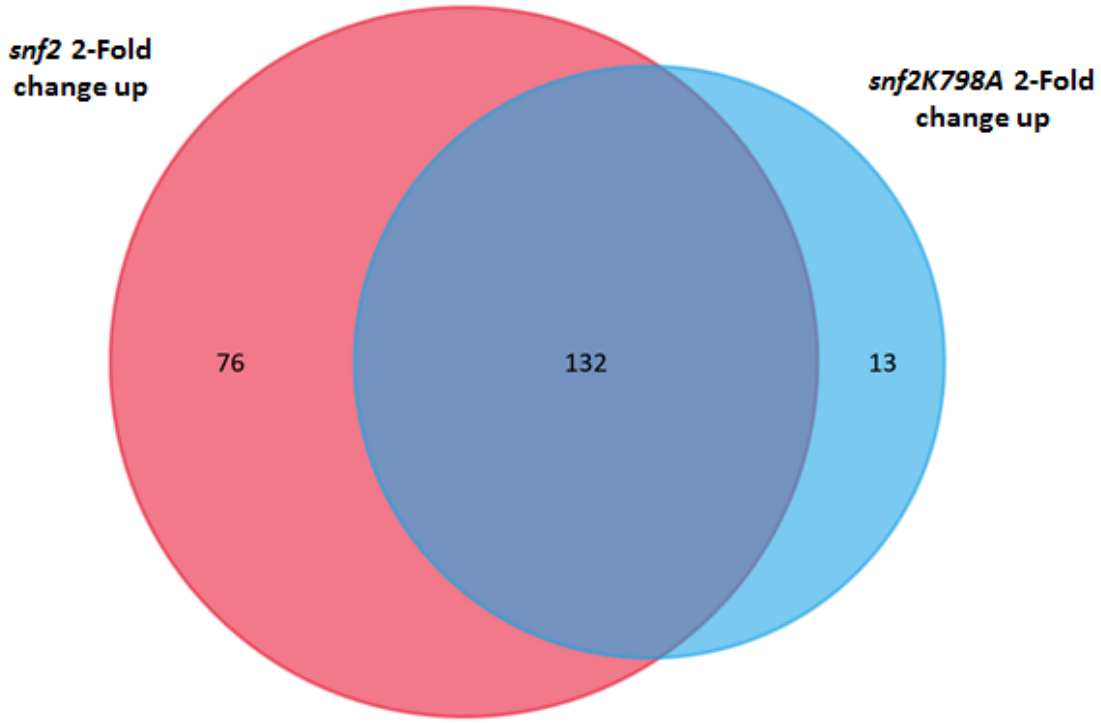

Figure 5.30 Swi-Snf up-regulated genes; *snf2* vs *snf2K798A*. Venn diagram to identify the genes uniquely upregulated in *snf2* and the uniquely upregulated in *snf2K798A* genes which had at least 2-fold change up. 133 genes were overlapping. 76 genes were unique in *snf2* while 13 genes were unique in *snf2K798A*.

5.2.4.5 Gene ontology analysis of genes uniquely up-regulated in *snf2* and *snf2K798A* mutants:

In order to find out if there were specific functionally related genes uniquely upregulated in the *snf2* and the catalytically dead *snf2K798A* mutant, panther gene ontology analysis was used to classify these genes. The results showed that there was a wide variety of functions associated with the genes uniquely upregulated in the two *snf2* mutant strains. No obvious group of genes were apparent as being uniquely upregulated in the *snf2* or *snf2K798A* mutant (Fig. 5.31A & B).

In summary, these analyses compared the impact upon transcription due to the loss of the Snf2 sub-unit in which the Swi-Snf complex has been proposed to fall apart, with the impact upon transcription due to the loss of Swi-Snf ATPase activity only, in which the Swi-Snf complex has been proposed to remain intact. The results showed that there was a similar impact upon transcription of a large shared cohort of genes regardless of if Swi-Snf integrity or activity was disrupted. However, some genes were uniquely sensitive to having Swi-Snf either effectively absent or inhibited in activity only.

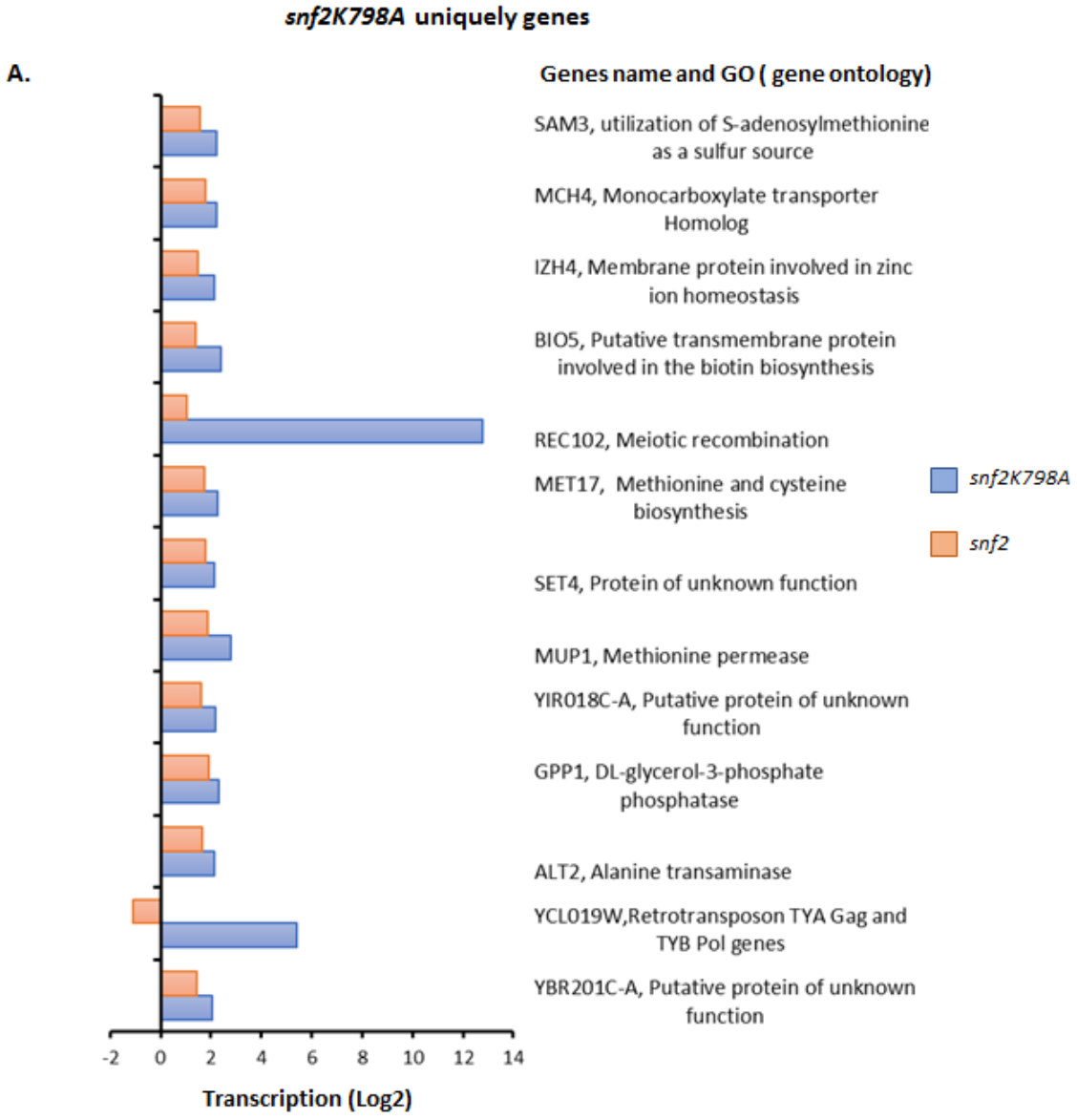
snf2K798A uniquely genes
A.
Genes name and GO (gene ontology)
SAM3, utilization of S-adenosylmethionine as a sulfur source
MCH4, Monocarboxylate transporter Homolog
IZH4, Membrane protein involved in zinc ion homeostasis
BIO5, Putative transmembrane protein involved in the biotin biosynthesis
REC102, Meiotic recombination
MET17, Methionine and cysteine biosynthesis
SET4, Protein of unknown function
MUP1, Methionine permease
YIR018C-A, Putative protein of unknown function
GPP1, DL-glycerol-3-phosphate phosphatase
ALT2, Alanine transaminase
YCL019W,Retrotransposon TYA Gag and TYB Pol genes
YBR201C-A, Putative protein of unknown function
snf2K798A
snf2
-2
0
2
4
6
8
10
12
14
Transcription (Log2)

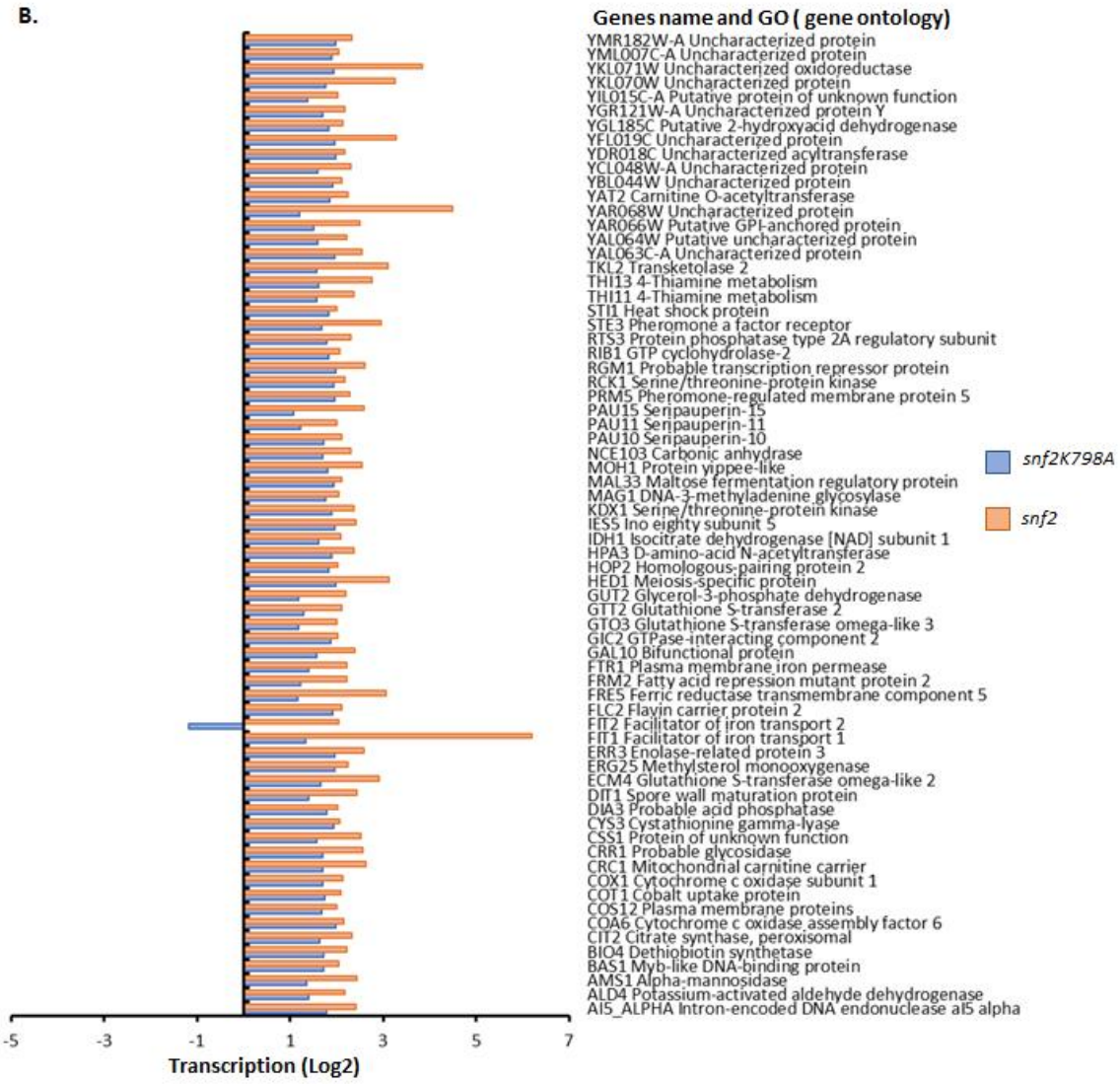

Figure 5.31 Gene ontology analysis of genes uniquely up-regulated in *snf2K798A* and *snf2* single mutants. Column graphs show the different in the transcription in each **A:** *snf2* and **B:** *snf2K798A* and the gene function.

5.2.5 Identification of the genes co-regulated by Swi- Snf and Tup1- Cyc8:

The main aim of this project was to identify the genes co-regulated by Swi-Snf acting as an activator, and Tup1-Cyc8 acting as a repressor. In order to identify this cohort of co-regulated genes a Venn diagram was made from the subset of the genes more than two-fold upregulated in the *cyc8* mutant and the genes downregulated by more than 2-fold in the *snf2 cyc8* double mutant. The overlap in the Venn diagram revealed a cohort of 115 genes which should indicate those genes de-repressed in the Cyc8 mutant which are then repressed again when *snf2* is additionally deleted (Fig. 5.32).

However, since some of these genes (115) could also be present due to their being solely de-repressed in the *snf2* mutant, a three-way Venn diagram was prepared in which the 755 genes down-regulated less than 2-fold in *snf2* (Swi-Snf act as an activator) were also added. (Fig. 5.33). The results revealed 102 genes overlapped which should indicate those genes repressed by Tup1-Cyc8 and which require Swi-Snf for activation.

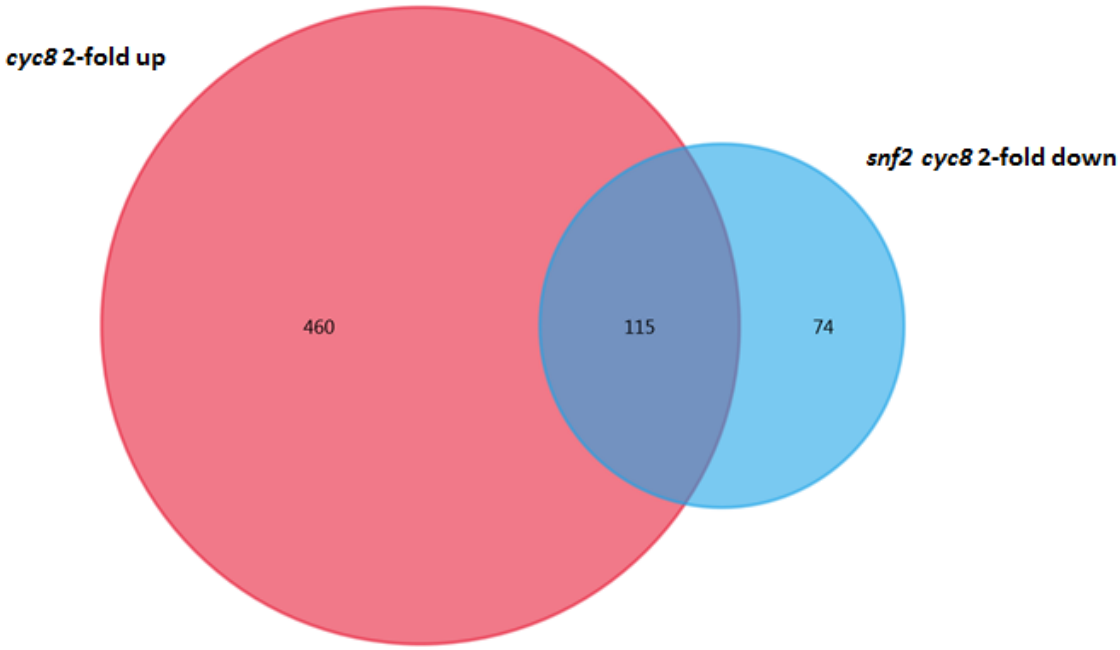

Figure 5.32 Snf2 and Cyc8 co-regulated genes. Venn diagram to show 115 co-regulated genes (Swi-Snf as an activator and Tup1-Cyc8 as repressor) genes overlapping in *cyc8* genes which were upregulated at least 2-fold vs *snf2 cyc8* genes which were at least 2-fold downregulated. Fun rich program was used to perform the Venn diagram (M. Pathan *et al*. 2015).

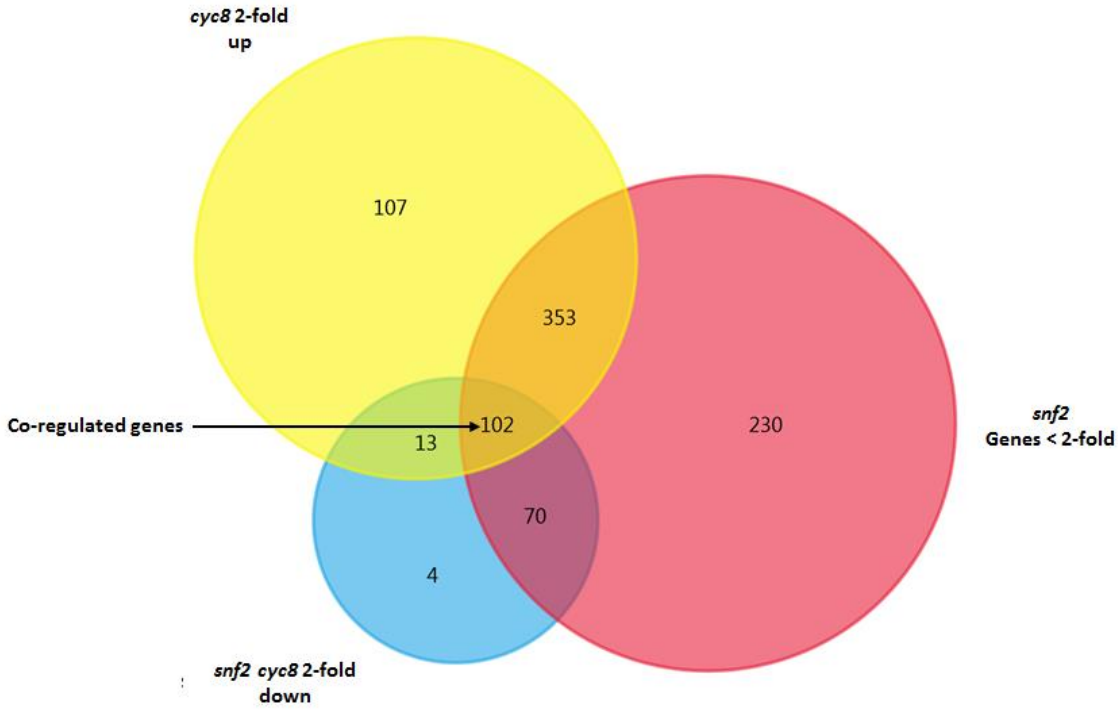

Figure 5.33 Snf2 and Cyc8 co-regulated genes. Venn diagram to show 102 co-regulated genes (Swi-Snf as an activator and Tup1-Cyc8 as repressor) genes overlapping in *cyc8* genes which were upregulated at least 2-fold vs *snf2 cyc8* genes at least 2-fold downregulated, and then additionally compared with *snf2* the genes downregulated < 2-fold vs *snf2 cyc8* genes at least 2-fold downregulated. Fun rich software was used to perform the Venn diagram (M. Pathan *et al*. 2015).

Gene	Description of protein product	wt vs *snf2 cyc8* FC down	wt vs *snf2* FC down	wt vs *cyc8* FC up
HXT17	Hexose transporter	-74.07	-1.13	1134.83
PAU13	Seripauperin-13, cell wall protein	-72.23	1.3	6987.89
HXT13	Hexose transporter	-57.88	-1.3	720.47
PAU20	Seripauperin-20, cell wall protein	-35.44	1.32	504.64
PAU5	Seripauperin-5, cell wall protein	-34.67	1.32	907.31
FLO1	Flocculation protein	-31.71	1.56	149.92
TIP1	Temperature shock-inducible protein	-30.88	-15.42	6.9
HSP26	Heat shock protein	-22.56	-7.63	22.24
FLO11	Flocculation protein	-19.19	1.01	40.03
DAK2	Dihydroxyacetone kinase	-17.82	-2.3	38.76
YNR071C	Uncharacterized isomerase	-16.1	1.31	400.9
SUC2	Invertase	-14.81	1.04	47.7
TIR3	Cell wall protein	-12.35	-10.46	15.47
YMR317W	Uncharacterized protein	-11.86	-1.97	54.09
YER053C-A	Uncharacterized protein	-11.66	-12.12	14.55
PAU19	Seripauperin-19, cell wall protein	-11.05	1.32	156.43
FMP48	Probable serine/threonine-protein kinase	-11.04	-4.31	7.38
PAU24	Seripauperin-24, cell wall protein	-10.51	1.46	4368.65
BDH2	Probable diacetyl reductase [(R)-acetoin forming]	-10.36	-4.08	3.46
YHR022C	Uncharacterized protein	-10.34	-3.08	59.03
PAU12	Seripauperin-12, cell wall protein	-9.29	1.24	1523.16
PIR3	Cell wall mannoprotein	-8.14	-2.29	16.35
FLO5	Flocculation protein	-7.54	1.32	14.74
DSF1	Mannitol dehydrogenase	-7.35	1.26	197.17
NCA3	Beta-glucosidase-like protein, mitochondrial	-5.66	-6.2	9
ARN1	Siderophore iron transporter	-5.54	-1.22	3.7
PDC5	Pyruvate decarboxylase isozyme	-5.49	-1.17	9.21
PAU7	Seripauperin-7, cell wall protein	-5.01	1.37	77.47
DIT2	Cytochrome	-4.98	1.14	6.69
TIR4	Cell wall protein	-4.95	-1.64	100.95
PHO89	Phosphate permease, transporter	-4.87	-6.47	13.26
IME1	Meiosis-inducing protein 1	-4.79	1.48	11.02
PRY1	Protein PRY1, Sterol binding protein	-4.78	-2.78	7.92
CTT1	Catalase T	-4.7	-4.01	2.63

Gene	Description of protein product	wt vs *snf2 cyc8* FC down	wt vs *snf2* FC down	wt vs *cyc8* FC up
YJR115W	Uncharacterized protein	-4.58	-1.35	5.85
TDH1	Glyceraldehyde-3-phosphate dehydrogenase	-4.55	-3.31	2.72
YNL194C	Uncharacterized plasma membrane protein	-4.55	-6.48	6.68
SPS100	spore wall maturation	-4.32	-1.2	6.94
HSP12	12 kDa heat shock protein	-4.31	-12.44	65.39
VBA5	Vacuolar basic amino acid transporter	-4.26	1.62	303.86
HXT1	Low-affinity glucose transporter	-4.03	-1.03	3.55
BIO5	7-keto 8-aminopelargonic acid transporter	-3.99	1.4	7.04
PAU17	Seripauperin-17, cell wall protein	-3.92	1.71	5.19
MAN2	Mannitol dehydrogenase	-3.86	-1.18	147.54
YER188W	Uncharacterized protein	-3.84	-2	2.19
SIT1	Siderophore iron transporter	-3.81	-1.38	2.52
STL1	Sugar transporter	-3.62	1.44	91.52
AQY1	Aquaporin, spore-specific water channel	-3.57	-1.06	66.54
YSR3	Dihydrosphingosine 1-phosphate phosphatase	-3.5	-1.3	3.51
FLO9	Flocculation protein	-3.25	1.49	90.37

Table 5.5: The top 50 Snf2 and Cyc8 co-regulated genes. The top 50 co-regulated genes in *snf2* and *cyc8* were listed along with their descriptions and fold-changes, the red colour indicates the highest transcription fold-change (FC) and the blue colour indicates a negative transcription fold change of the genes whose products had varied functions. The genes description according to panther gene ontology (Mi *et al*. 2017).

5.2.5.1 Validation of RNA-Seq co-regulated gene data by RT-qPCR:

In order to confirm the 102 co-regulated genes, *FLO1* and *SPS100* were chosen as example genes in which to validate this sub-set of genes. The RNA-Seq analysis showed that *FLO1* was repressed in wt, *snf2K798A* and *snf2* strains, while it was highly de-repressed in *cyc8* mutants, and subsequently repressed again in the *snf2 cyc8* and *snf2K798A cyc8* double mutants (Fig. 5.34A, C). This result was validated when analysed by RT-qPCR (Fig. 5.34B).

The *SPS100* gene was also repressed in wt, *snf2* and *snf2K798A* mutants, while de-repressed almost 7-fold in the *cyc8* single mutant. However, *SPS100* transcription was decreased in the *snf2 cyc8* and *snf2K798A* double mutants (Fig. 5.35A, C). RT-qPCR analysis showed the same trends (Fig. 5.35B).

Thus, the RNA-Seq data and gene-specific RT-qPCR analysis is in good agreement and show clear co-regulation of these genes by Swi-Snf (activator) and Tup1-Cyc8 (repressor).

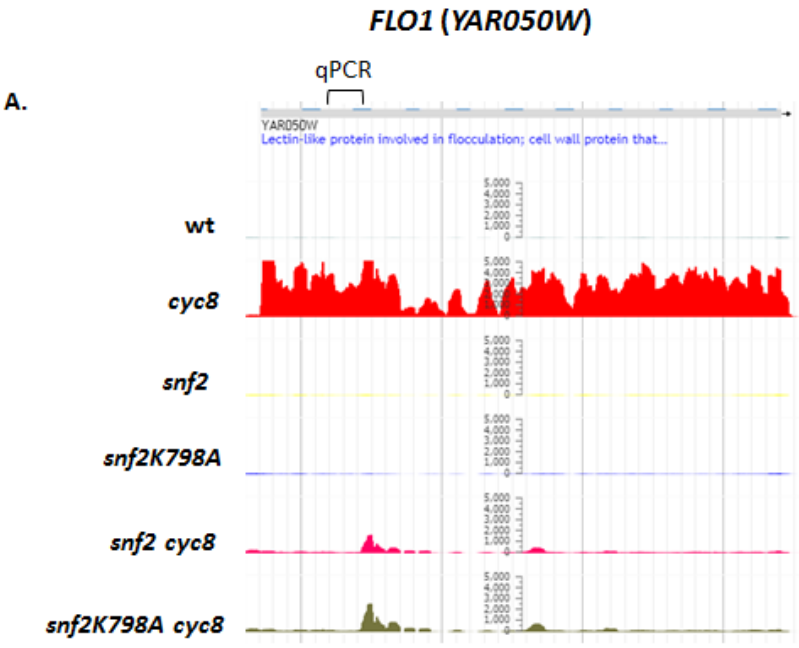

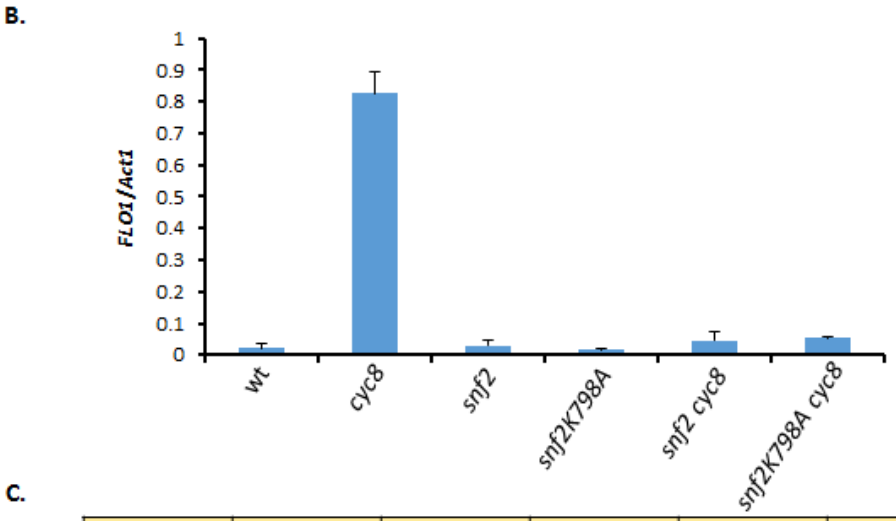

C.

snf2 cyc8 co-regulated	WT vs *ssn6* FC	WT vs *snf2* FC	WT vs *snf2K798R* FC	Ssn6 vs *snf2* *ssn6* FC	ssn6 vs snf2 ssn6 FC
FLO1	149.92	1.56	1.37	-31.71	-26.01

Figure 5.34 *FLO1* transcription. A: J-browse screen-shot to show read counts across the *FLO1 genes* in the strains indicated. **B:** Data was confirmed by gene-specific RT-qPCR analysis. **C:** The fold change in transcription level profile as determined by RNA-Seq shown in A. Red indicates a high transcription level, blue indicates the low level of transcription. Error bars represent standard deviation of three independent biological replicates.

A.

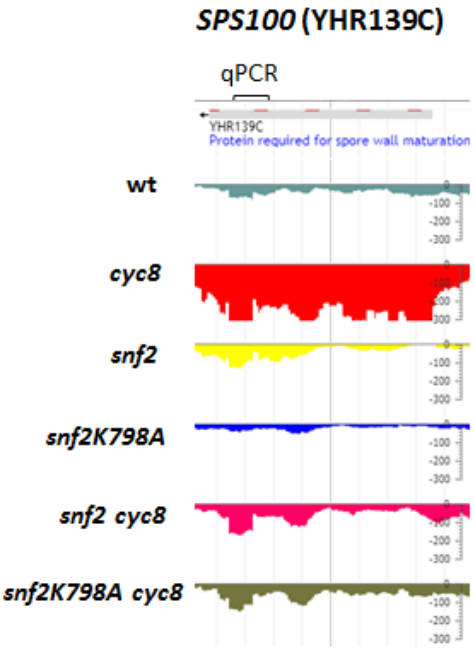

B.

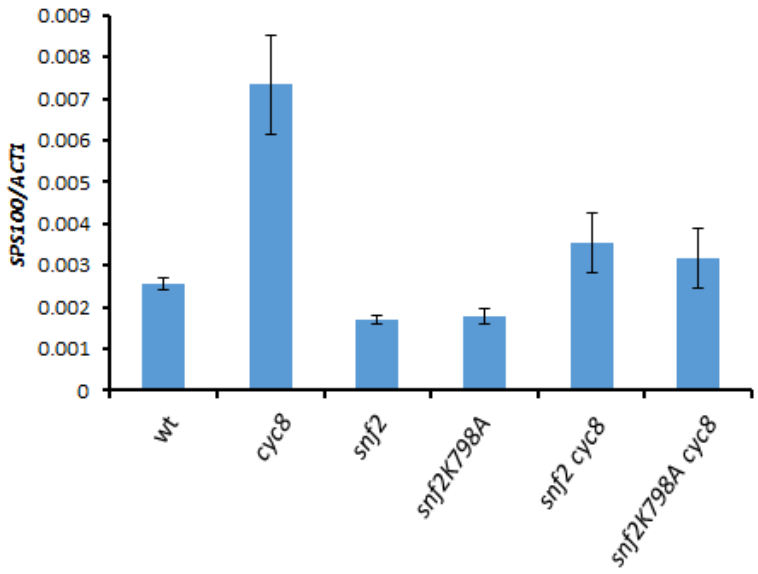

C.

snf2 cyc8 co-regulated	WT vs *cyc8* FC	WT vs *snf2* FC	WT vs *snf2K798R* FC	*cyc8* vs *snf2 cyc8* FC	*cyc8* vs *snf2 cyc8* FC
sps100	6.94	-1.2	-1.92	-4.32	-4.82

Figure 5.35 *SPS100* transcription. A: J-browse screen-shot to show read counts across the *SPS100 genes* in the strains indicated. **B:** Data was confirmed by gene-specific RT-qPCR analysis. **C:** The fold change in transcription level profile as determined by RNA-Seq shown in A. Red indicates a high transcription level, blue indicates a low level of transcription. Error bars represent standard deviation of three independent biological replicates.

5.2.5.2 Gene ontology analysis of Snf2 and Cyc8 co-regulated genes:

Next, the 102 Snf2 and Cyc8 co-regulated genes were analysed by gene ontology. When the genes were categorised according to biological process, molecular function and cellular component groups, the majority of genes in each case were found to be involved with the cell wall and sugar transport across the plasma membrane (Fig. 5.36) (Appendix I, Table S13).

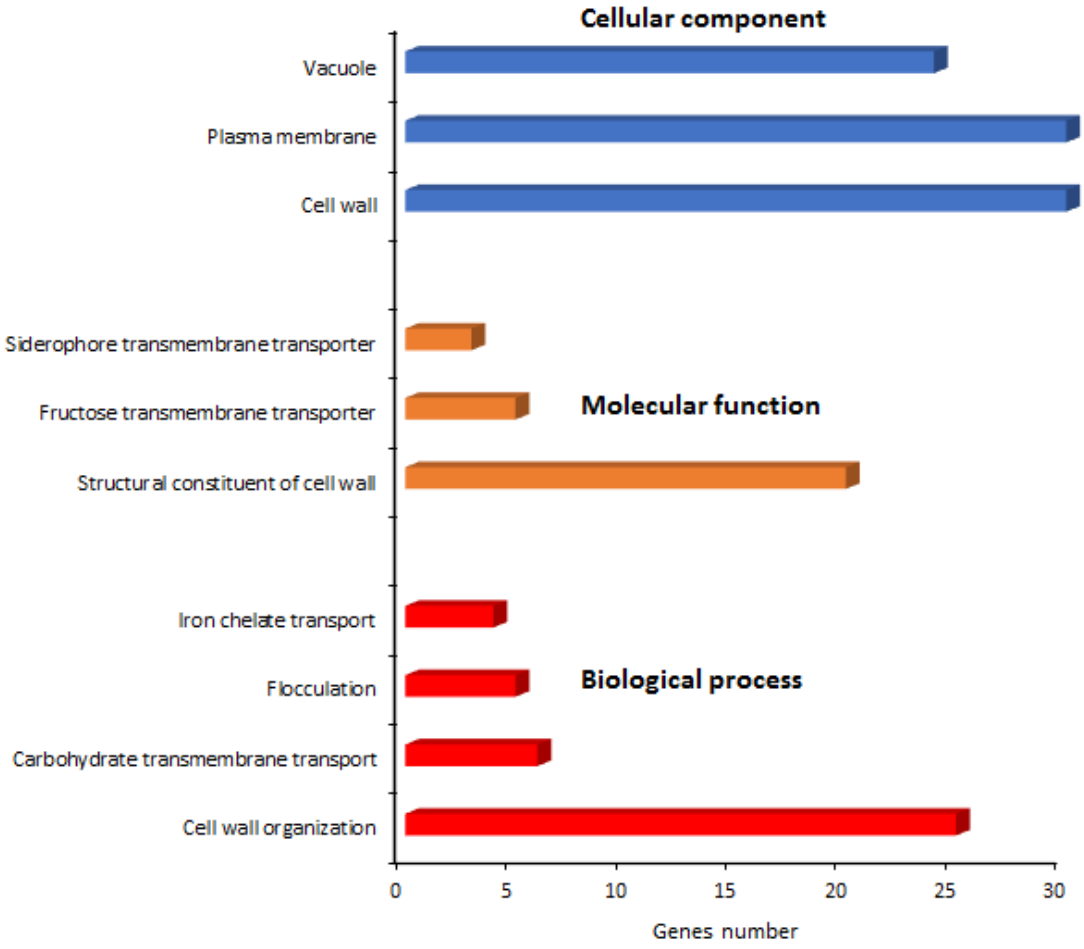

Figure 5.36 Gene ontology analysis of 102 Swi-Snf and Tup1-Cyc8 co-regulated genes. Column charts for the 102 co-regulated genes identified from the *cyc8* vs *snf2 cyc8* vs *snf2* analysis using the *Saccharomyces* genome data base (SGD). Red represent the biological process category, orange indicates the molecular function category and blue indicates the cellular component category. Results are shown for genes with P value < 0.001.

5.2.5.3 Chromosomal location of Snf2 and Cyc8 co-regulated genes:

The location of the 102 Snf2 and Cyc8 co-regulated genes on each chromosome was next identified, along with the fold change decrease in transcription of each gene in the *snf2 cyc8* double mutant compared to the *cyc8* single mutant (Fig. 5.37). Thus, the gene location of the genes was reflected by the circle position, and the size of the circle reflects the level of gene repression.

Strikingly, the results showed that 31 genes (30.3%) of the 102 co-regulated genes were located in subtelomeric regions (Fig. 5.37) yellow circles with red edges. This is a statistically significant enrichment in the subtelomeric regions for the co-regulated genes since the subtelomeric regions only represent 7% of the yeast genome yet harbour 30% of the co-regulated genes. Furthermore, the co-regulated genes located in the subtelomeric regions showed a significantly greater fold decrease in transcription in the double mutant compared to transcription levels in the Cyc8 mutant compared to those genes which were not subtelomeric (Fig 5.38). This suggests that the subtelomeric genes were subject to the greatest level of Tup1-Cyc8 mediated gene repression.

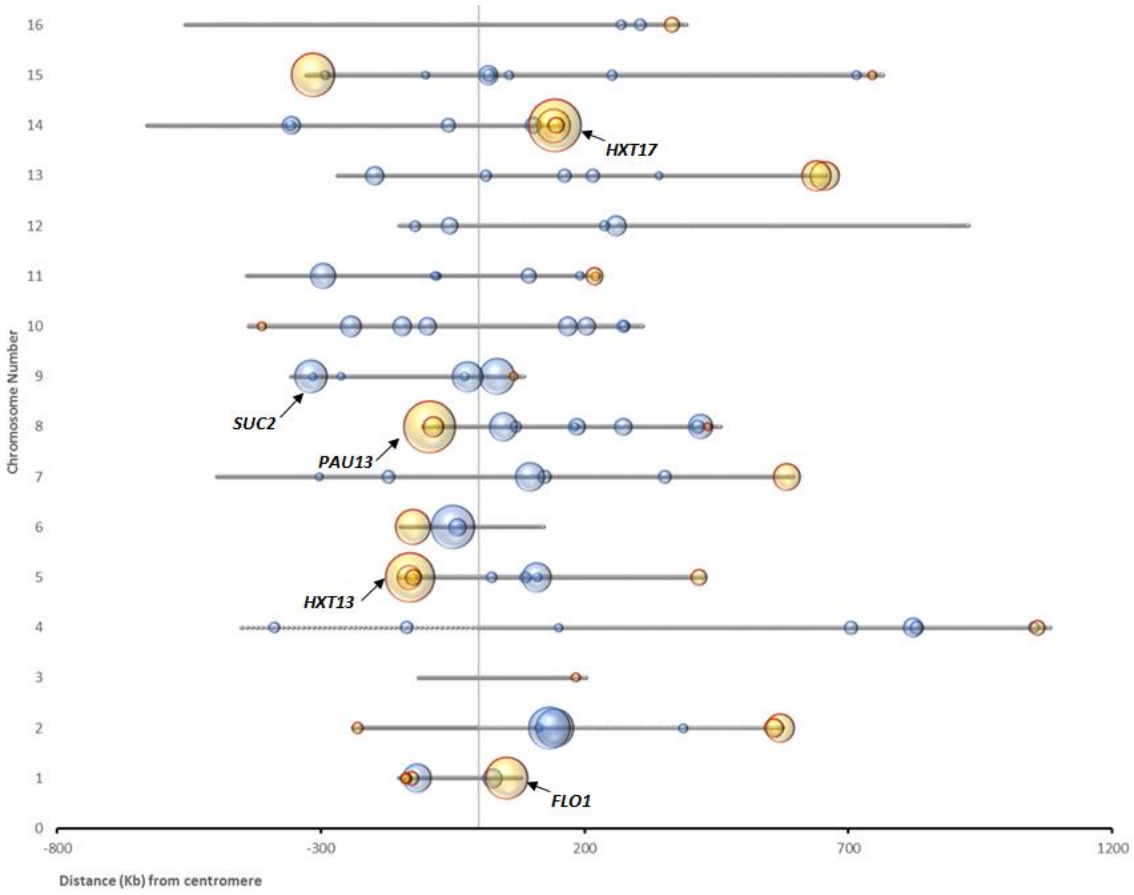

Figure 5.37 Chromosomal location and transcription fold change of Snf2 and Cyc8 co-regulated genes. 'Bubble' plot showing the location and the change in transcription of the 102 Swi-Snf and Tup1-Cyc8 co-regulated genes when transcription in the *cyc8* mutant was compared to levels in the *snf2 cyc8* double mutant. Circle area represents the fold decrease in transcription of genes in a *cyc8* mutant (up) vs *snf2 cyc8* (down) mutant. Each line represents the chromosome number.

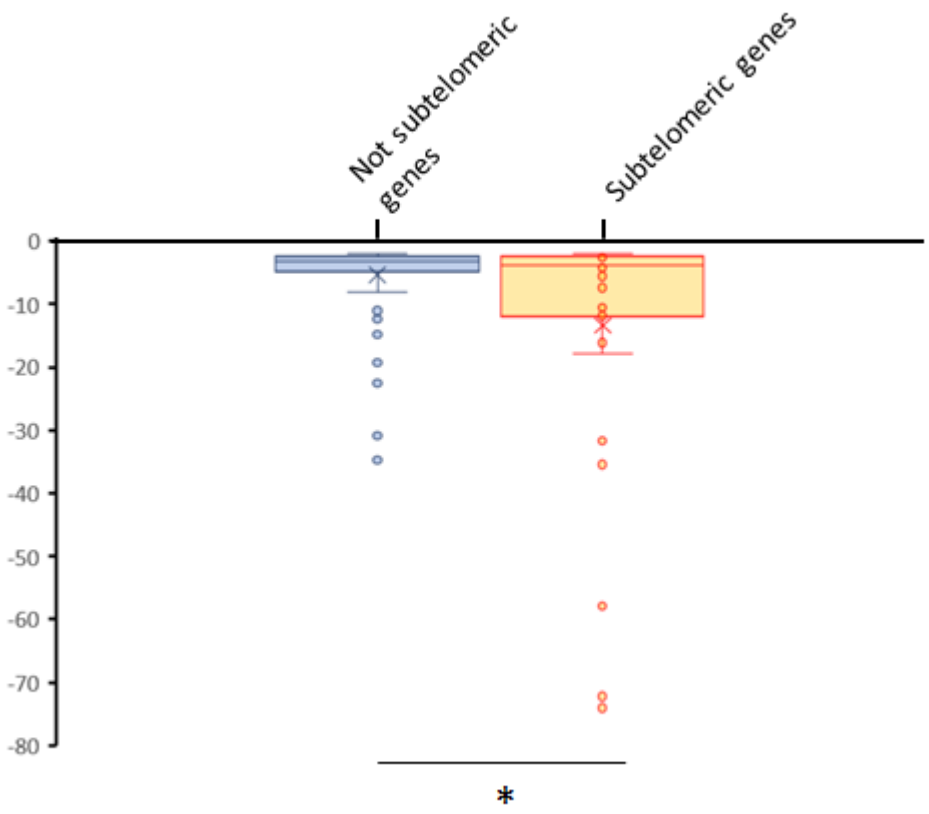

Figure 5.38 The transcription fold change of Snf2 and Cyc8 co-regulated genes located in non subtelomeric and subtelomeric regions. Box plot represents the overall change in transcription in *cyc8* mutants compared to *snf2 cyc8* mutants. The subtelomeric Tup1-Cyc8 and Swi-Snf co-regulated genes are indicated in yellow and the non subtelomeric genes were indicated in blue. The asterisks indicates of P value < 0.001 obtained from a student's t-test.

5.2.5.4 Chromosomal location and orientation of Swi-Snf and Tup1-Cyc8 co-regulated genes:

It was next investigated whether any of the co-regulated genes were located in groups. The results showed that of the co-regulated genes only 6 groups of genes were identified comprising 5 groups containing 2 genes and just one group containing 3 genes (Fig. 5.39A). The orientation of genes in these groups showed no bias for being in one particular orientation over another (Fig. 5.39B), and only two of the groups containing two genes harboured genes of a similar function (Fig.5.40). These two groups of genes contained the cell proteins *DAN1* and *DAN4* in one group and the *TIR2* and *TIR4* genes which encode cell wall mannoprotein and they were expressed under anaerobic condition (Table 5.5).

Thus, most of the 102 co-regulated genes appear to be under Swi-Snf and Tup1-Cyc8 control in isolation from the other co-regulated genes.

A.

Number of the genes in each group	Number of the group
3 genes	1
2 genes	5
Total	**6**

B.

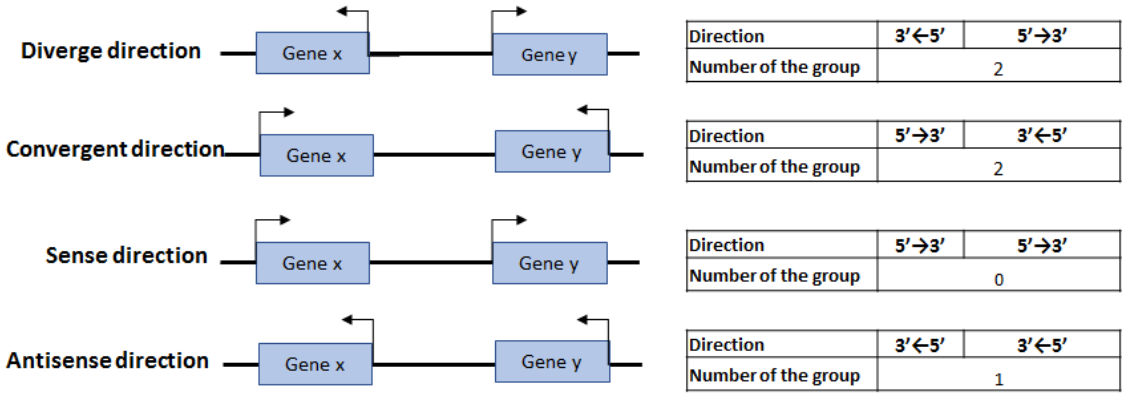

Direction	3′←5′	5′→3′
Number of the group	2	

Direction	5′→3′	3′←5′
Number of the group	2	

Direction	5′→3′	5′→3′
Number of the group	0	

Direction	3′←5′	3′←5′
Number of the group	1	

Figure 5.39 The transcription direction of the co-regulated genes group. A: Table of the number of genes in each group. **B:** Number of the gene groups with transcriptional direction.

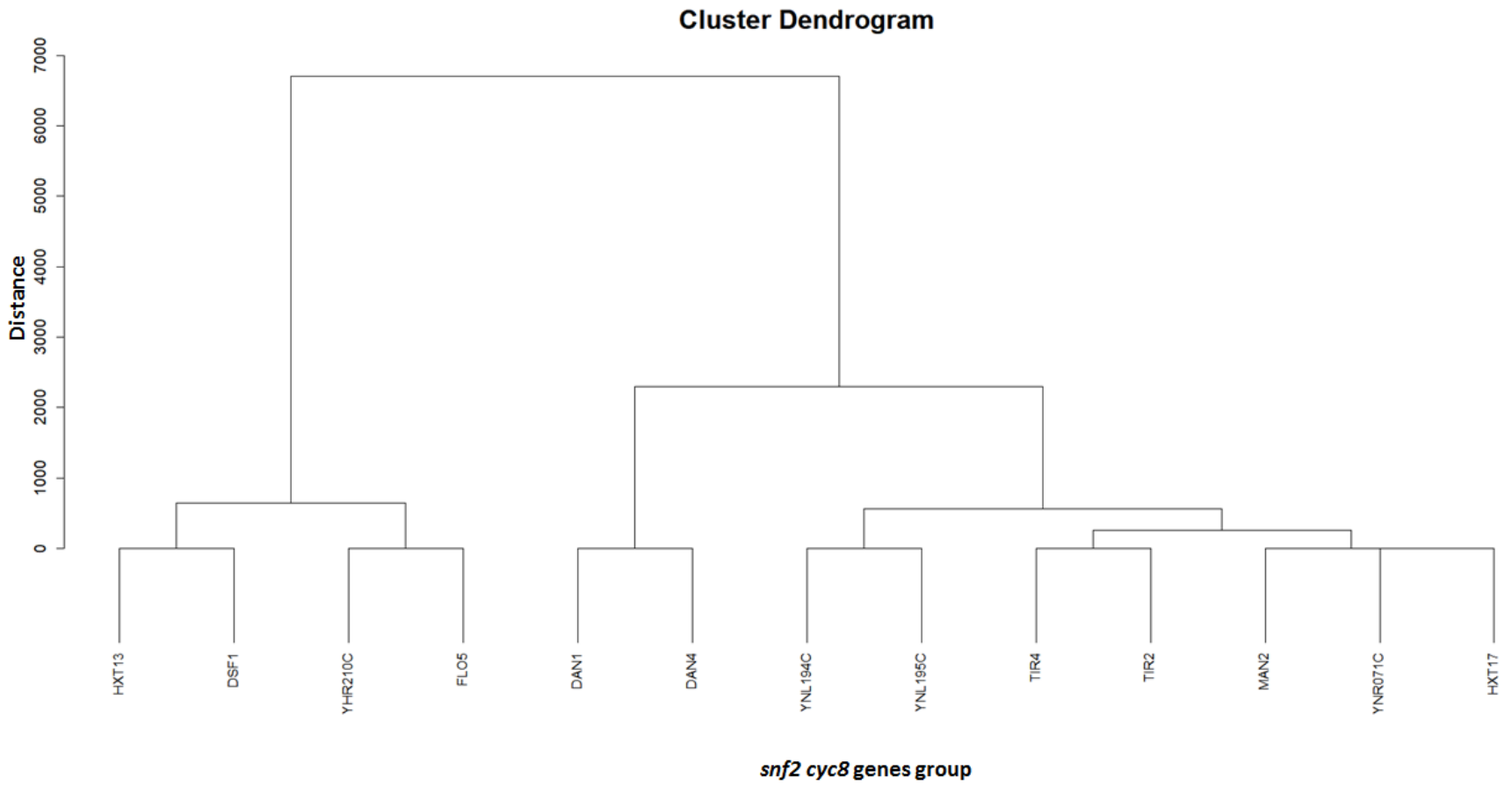

Figure 5.40 Cluster dendrogram of the co-regulated genes group location. The chart identified 6 groups of genes co-regulated by Tup1-Cyc8 and Swi-Snf**.** The vertical axis of the dendrogram represents the distance or dissimilarity between clusters, the horizontal axis represents the objects and clusters. The horizontal position of the split, shown by the short vertical bar, gives the distance between the two clusters.

gene	Description
HXT13	Hexose transporter
DSF1	Mannitol dehydrogenase
YHR210C	Uncharacterized isomerase
FLO5	Flocculation protein
DAN1	Cell wall protein
DAN4	Cell wall protein
YNL194C	Uncharacterized plasma membrane protein
YNL195C	Uncharacterized protein
YNR071C	Uncharacterized isomerase
HXT17	Hexose transporter
MAN2	Mannitol dehydrogenase
TIR4	Cell wall protein
TIR2	Cold shock-induced protein

Table 5.6 The groups of co-regulated genes: Table showing the six co-regulated groups of genes, of which some of them were related function.

5.2.5.5 Investigating the relationship between upstream intergenic region size and levels of gene transcription of the 102 co-regulated genes:

Whether there was a relationship between upstream intergenic region size and the levels of gene transcription in the various mutants for the 102 co-regulated genes was next analysed. This was because it previously hypothesised that those genes with large upstream intergenic region (or upstream gene free regions) would show the greatest changes in transcription in the presence and absence of Cyc8 and Snf2. Specifically, the fold decrease in transcription of the 102 genes in the *snf2 cyc8* double mutant versus the *cyc8* single mutant against the length of gene free upstream region for each gene was plotted.

The results showed that most of the genes with upstream intergenic region size less than 5000 bp and the transcription with about -20-fold-change in expression. However, *FLO1* whose product is involved in flocculation, and *DAN4* which encodes a cell wall protein have the biggest upstream intergenic region size with 9141 bp with a -31.71-fold change in expression in *snf2 cyc8,* and 7411 bp with a -2.39-fold change, respectively. The smallest upstream intergenic region in *snf2 cyc8* was the carbohydrate transporter encoding gene, *HXT17,* with -74.07 and upstream intergenic region size 1949 bp.

Overall, the results observed no relation between upstream intergenic region size and transcription level in *snf2 cyc8* (Fig. 5.41).

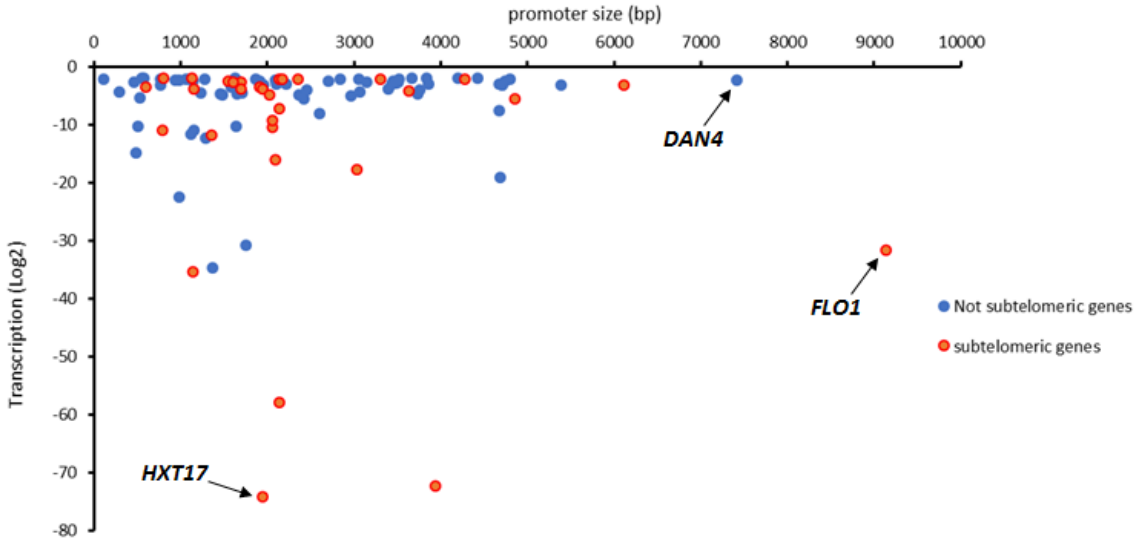

Figure 5.41 The relationship between the co-regulated genes transcription levels and the upstream intergenic region size. The *snf2 cyc8* downregulated genes were plotted against the upstream intergenic region size in a scatter plot.

5.2.5.6 Identification of Swi-Snf and Tup1- Cyc8 co-regulated genes using the *snf2K789A* mutant instead of the *snf2::KAN* mutant:

The analysis was next repeated to find Swi-Snf and Tup1-Cyc8 co-regulated genes using the 'catalytically dead' *snf2K798A* mutant instead of the *snf2::KAN* full gene deletion. The rationale for this analyses was to investigate whether there would be a difference in the co-hort of co-regulated genes depending on whether the Swi-Snf complex was intact but inactive (*snf2K798A*) or was both inactive and structurally disrupted (*snf2::KAN*).

In order to identify the Swi-Snf (as an activator) and Tup1-Cyc8 (as a repressor) co-regulated genes a three-way Venn diagram was prepared from the two-fold de-repressed genes in the *cyc8* mutant compared to wt, the two-fold downregulated genes from the *cyc8* mutant compared to *snf2K798A cyc8* double mutant analysis, and the two fold down-regulated genes in the *snf2K798A* mutant compared to wt (fig. 5.42) (Appendix I, Table S14). This latter data set was included to remove those genes which are subject to *snf2* activation independent of *cyc8*.

The results revealed 77 overlapping genes which should be representative of those genes co-regulated by Swi-Snf acting as an activator and Tup1-Cyc8 acting as a repressor.

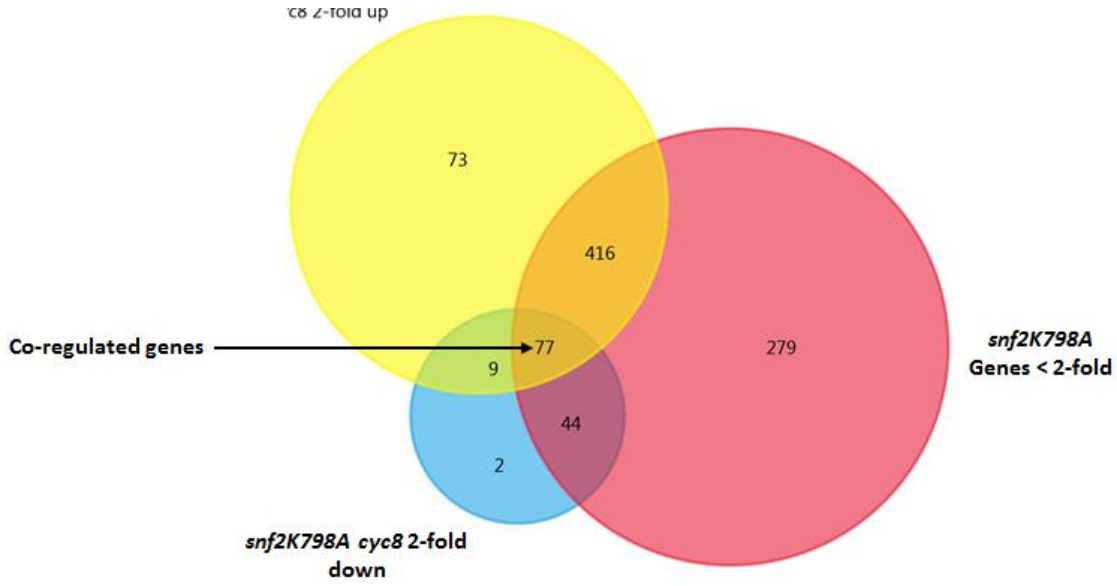

Figure 5.42 Swi-Snf and Tup1-Cyc8 co-regulated genes using a *snf2K798A* mutant. Venn diagram to show 77 co-regulated genes (Swi-Snf as an activator and Tup1-Cyc8 as repressor) overlapping in *cyc8* where genes were upregulated at least 2-fold vs *snf2 cyc8* where genes were at least 2-fold downregulated, and also additionally compared with *snf2K798A* where the genes were downregulated < 2-fold vs *snf2K798A cyc8.* Fun rich program was used to perform the Venn diagram (M. Pathan *et al*. 2015).

5.2.5.7 Comparison between the co- regulated *snf2 cyc8* vs *snf2K798A cyc8* genes:

In order to see the difference between our identification of the co-regulated genes depending on whether the full *snf2* deletion mutant or the *snf2K798A* catalytic dead mutant was used, a Venn diagram was made of the 102 genes identified in (Fig. 5.33), and the 77 co-regulated genes as described in the previous section (Fig. 5.43).

The data showed that of the 102 and 77 genes identified above, 68 genes were overlapping, 34 genes were unique for when the *snf2* full deletion was used in the analysis, whereas 9 genes were uniquely identified from when the *snf2K798A* mutant was used.

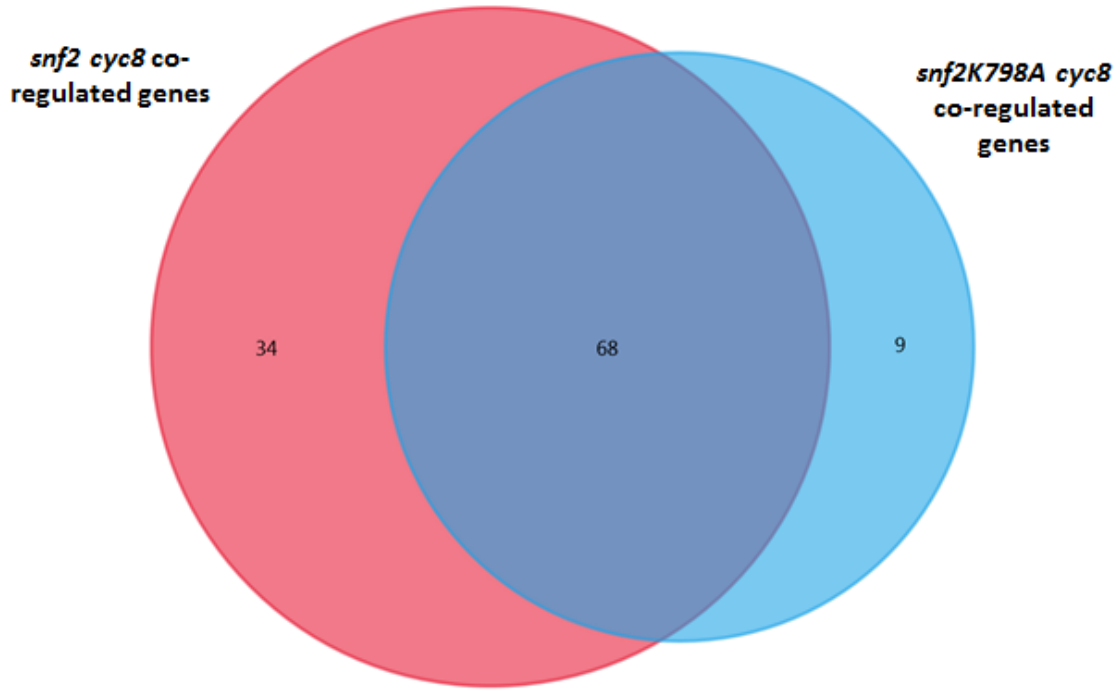

Figure 5. 43 Comparison between co-regulated genes in *snf2 cyc8* vs *snf2K798A cyc8* genes. Venn diagram showing a comparison between 102 co-regulated genes in *snf2 cyc8* full deletion and *snf2K798A cyc8* catalytic dead mutants, identifying the different of co-regulated genes. The Venn showed 68 co-regulated genes overlapping in *snf2 cyc8* vs *snf2K798A cyc8.* Fun rich program been was used to perform the Venn diagram (M. Pathan *et al*. 2015).

5.2.5.8 Comparing co-regulated gene transcription levels depending on whether the *snf2* or *snf2K798A* mutants were used:

Next it was examined whether there was a difference in the transcription level between the co-regulated genes identified using the *snf2 cyc8* and *snf2K798A cyc8* mutants. The difference in the transcription levels for the shared genes was calculated, and the uniquely identified co-reg genes identified when the *snf2* full gene deletion and the *snf2* amino acid substitution mutants were used (Fig. 5. 44).

The results showed that there was no significant difference in the overall drop in transcription of the shared co-regulated genes identified in the double mutants compared to the *cyc8* mutant whether the *snf2* full gene deletion or the catalytically dead *snf2K798R* mutant was used. Similarly, there was no significant difference in the overall fold change in transcription of the 34 genes unique to the *snf2 cyc8* mutant and the 9 genes unique to the *snf2K798A cyc8* mutant (Fig. 5.44).

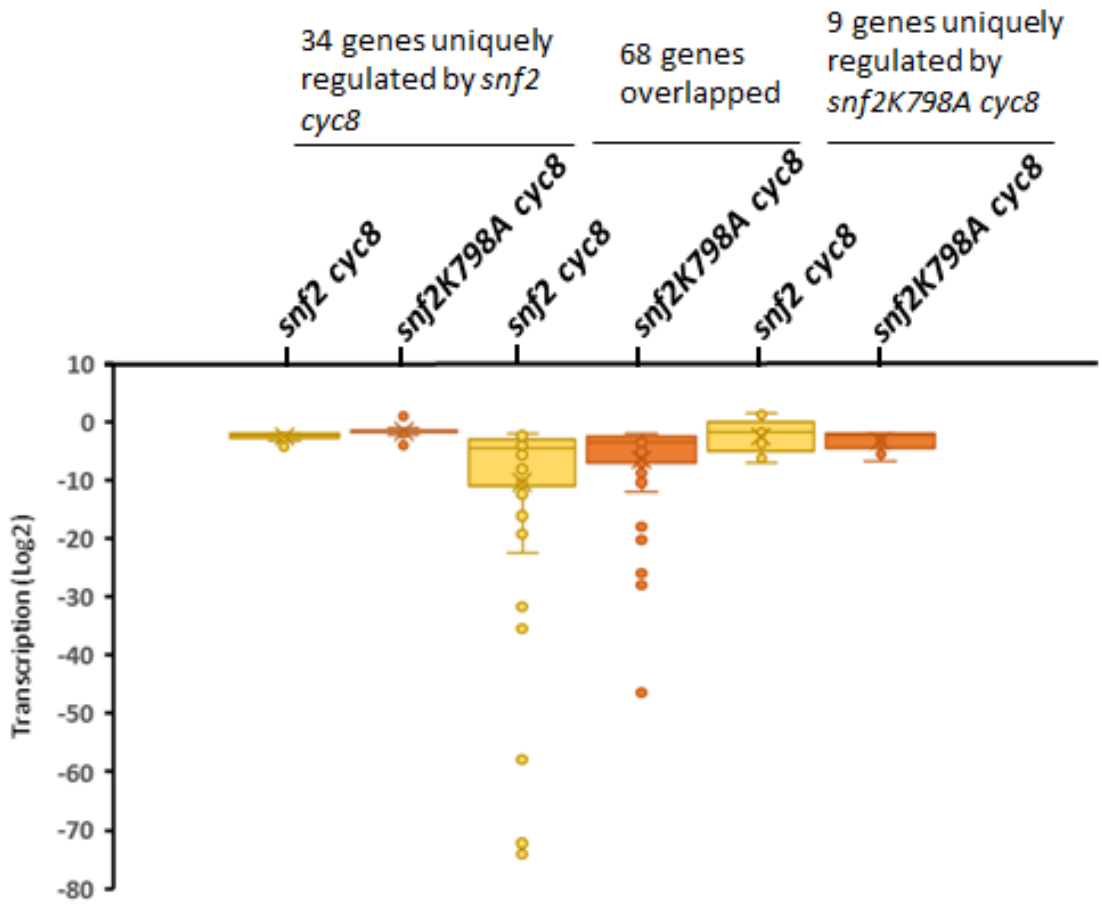

Figure 5.44 The transcription level in *snf2 cyc8* and *snf2K798A cyc8*. Box plot of transcription in *snf2 cyc8* and *snf2K798A cyc8*, the medium line shows the main of the transcription value, there was no significant difference between *snf2 cyc8* and *snf2K798A cyc8*.

5.2.5.9 Gene ontology analysis of the co-regulated genes unique to the *snf2 cyc8* and *snf2K798A cyc8* mutants:

Next, gene ontology analysis was applied to the unique co-regulated genes using the *snf2 cyc8* and *snf2K798A cyc8* mutants (Fig. 5.45A & B). The results showed that there was no specifically unique function in the 36 genes unique to the either *snf2 cyc8* full deletion mutant analysis or the 9 unique genes identified using the *snf2K798A cyc8* mutant.

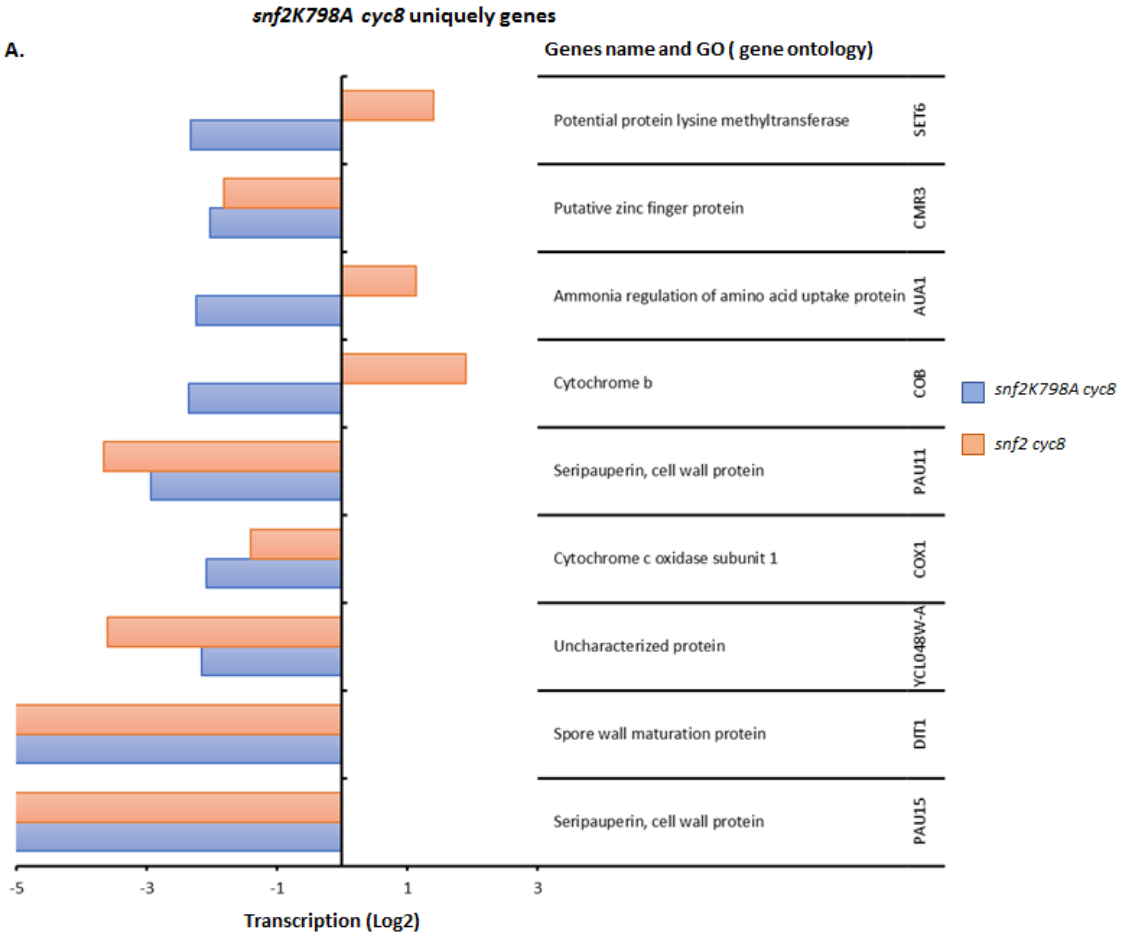
snf2K798A cyc8 uniquely genes
A.
Genes name and GO (gene ontology)
Potential protein lysine methyltransferase
SET6
Putative zinc finger protein
CMR3
Ammonia regulation of amino acid uptake protein
AUA1
Cytochrome b
COB
Seripauperin, cell wall protein
PAU11
Cytochrome c oxidase subunit 1
COX1
Uncharacterized protein
YCL048W-A
Spore wall maturation protein
DIT1
Seripauperin, cell wall protein
PAU15
snf2K798A cyc8
snf2 cyc8
-5
-3
-1
1
3
Transcription (Log2)

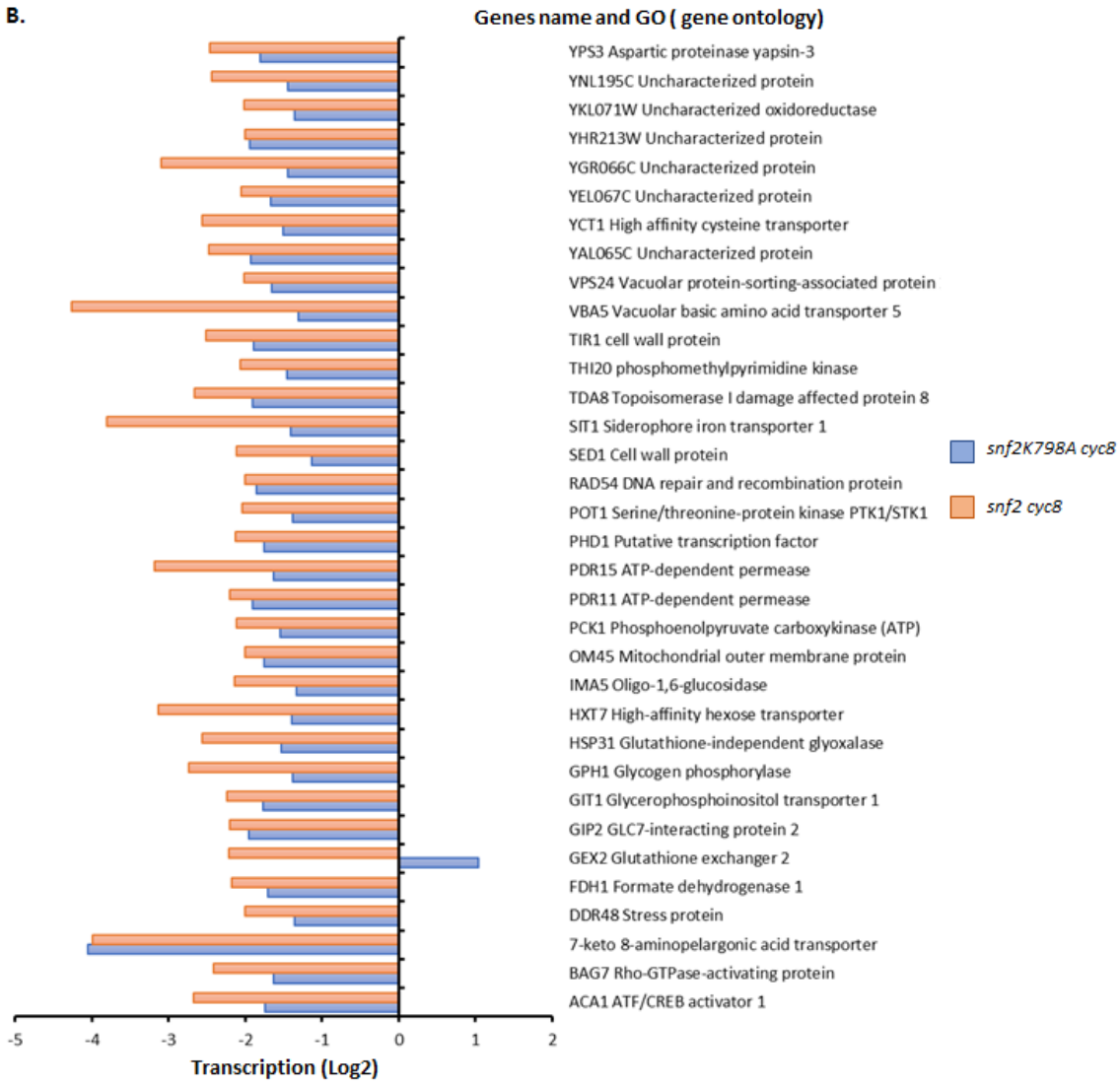

Figure 5.45 Gene ontology analysis of uniquely co-regulated genes in *snf2K798A cyc8* and *snf2 cyc8* double mutants' genes. Column graphs show the difference in the transcription in each **A:** *snf2* and **B:** *snf2K798A* and the gene function.

In summary, this study identified and characterised the co-hort of yeast genes subject to co-regulation by Swi-Snf as an activator and Tup1-Cyc8 as a repressor. This analysis was performed using both a *snf2* full gene deletion, in addition to a site-specific catalytically dead *snf2* mutant. The results showed that similar sets of genes were co-regulated regardless of whether the Snf2 protein was absent or if the Snf2 protein was present but inactive. Strikingly, the cohort of co-reg genes were found to be enriched in sub telomeric regions, and these genes were subject to the most robust regulation of transcription by Tup1-Cyc8 and Swi-Snf. Furthermore, the co-regulated genes were enriched for gene families encoding cell wall proteins and carbohydrate uptake and utilisation genes such as the *FLO* and *HXT* gene families. Another family of genes subject to robust co-regulation were the *PAU* genes which encode cell wall mannoprotein and were also localised near the ends of chromosomes.

5.2.6 Tup1-Cyc8 and Swi-Snf genes clustering:

This study next examined the frequency of when the genes up-regulated in *cyc8* single mutants (Cyc8 as a repressor) and the genes down-regulated in *snf2* single mutants (Snf2 as an activator) were located beside each other, the identified genes were combined.

The results showed that there were 40 groups of gene clusters at which Swi-Snf acted as an activator, and Tup1-Cyc8 acted as a repressor. Of these groups, 22 contained 2 genes, 8 groups contained 3 genes, 7 groups contained 4 genes, and there were 3 groups that contained 5 genes (Fig. 5.46 A).

Analysis of the orientation of the pairs of adjacent genes in these groups showed no particular bias for one orientation over another, where 6 groups were in both divergent and convergent in direction, and 2 groups were in a sense and antisense direction (Fig. 5.46 B).

The results showed that the location of the groups were found located in different regions of the chromosome including 6 groups located at subtelomeric region (Fig. 5.47*)*.

The gene ontology of the genes in these groups was next examined. However, there was no obvious specific related function for genes contained in any of the groups.

An example for one of the groups containing five genes subject to regulation by Swi-Snf and Tup1-Cyc8 is shown in addition to a table showing the functions of the genes within this group (Fig. 5.48 A and B).

In summary, although there are instances in the genome of groups of adjacent genes being subject to Swi-Snf and Tup1-Cyc8 control, the bulk of genes under co-regulation by these complexes are individually dispersed and enriched in sub telomeric regions.

A.

Number of the genes in each group	Number of the group
5 genes	3
4 genes	7
3 genes	8
2 genes	22
Total	**40**

B.

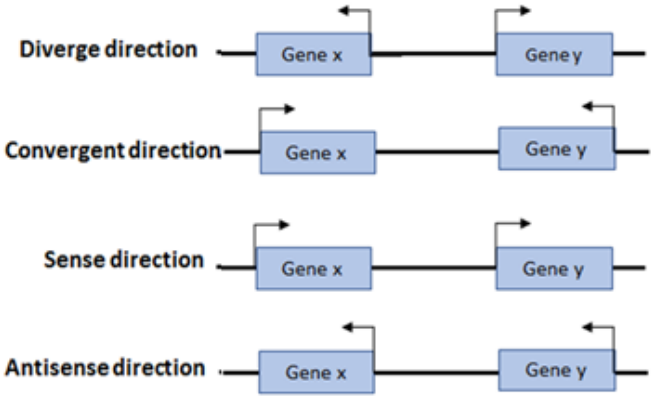

Direction	3'←5'	5'→3'
Number of the group	6	

Direction	5'→3'	3'←5'
Number of the group	6	

Direction	5'→3'	5'→3'
Number of the group	5	

Direction	3'←5'	3'←5'
Number of the group	5	

Figure 5.46 The transcription direction of the genes group in *snf2* and *cyc8* single mutants. A: The divergent direction and bidirectional direction of one gene group (gene x and y) for example. **B:** Table of the number grouped genes in each direction.

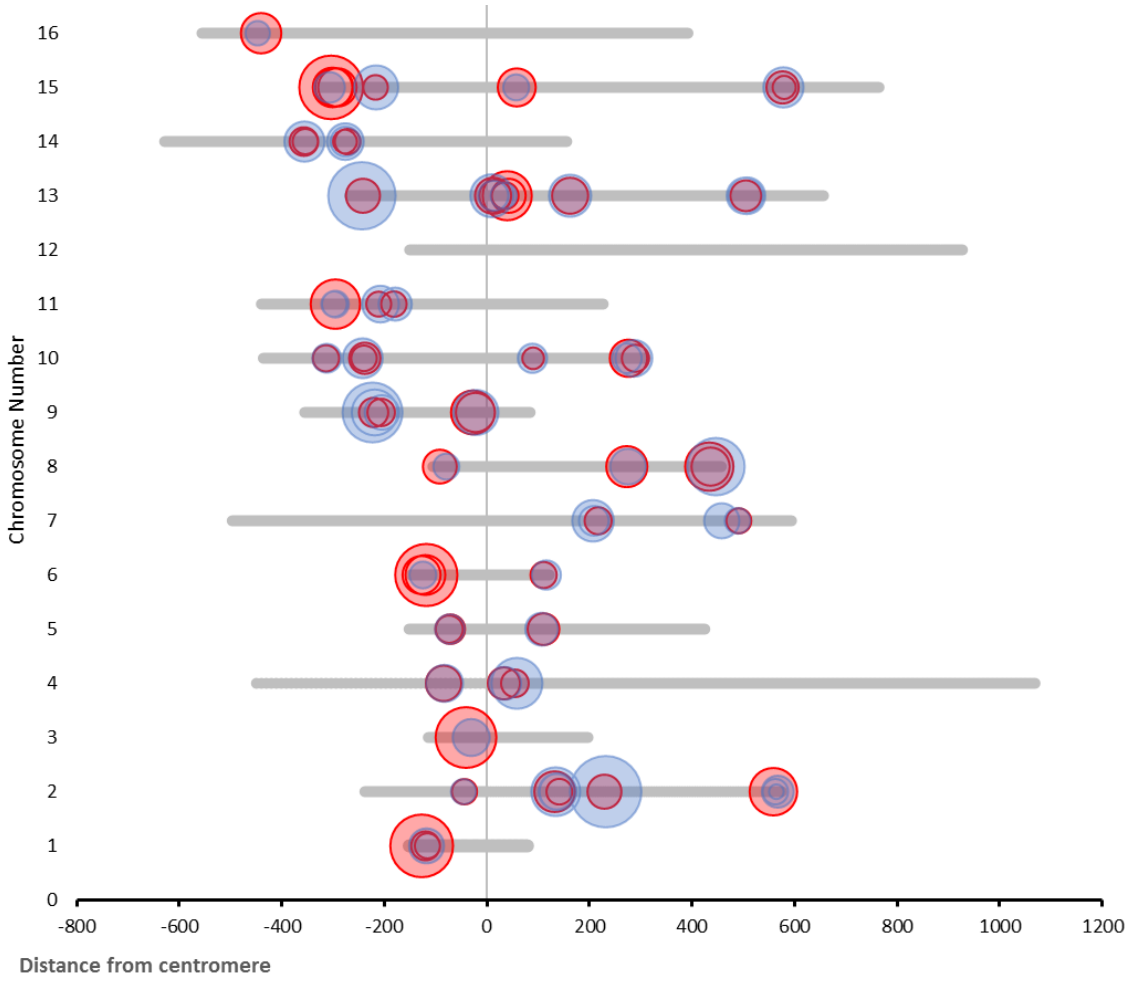

Figure 5.47 Genes clustering of the genes group in *snf2* and *cyc8* single mutants. 'Bubble' plot showing the genes clustering and the change in transcription of the 12 group of Swi-Snf and Tup1-Cyc8 co-regulated genes. Circle area represents the fold decrease in transcription of genes in a *snf2 cyc8* mutant. Each line represents the chromosome number.

A.

Gene	Systematic Name	Gene ontology	chromosome	Start	End	wt vs snf2 FC	wt vs cyc8 FC
NRG2	*YBR066C*	Probable transcriptional regulator NRG2	II	370037	370699	1.01	6.64
TIP1	*YBR067C*	Temperature shock, cell wall protien	II	372103	372735	-15.42	6.9
BAP2	*YBR068C*	permease, amino acid transcporter	II	373861	375690	-4.29	-1.02
TAT1	*YBR069C*	permease 1, amino acid transporeter	II	376574	378433	-4.79	-1.82
ALG14	*YBR070C*	UDP-N-acetylglucosamine transferase subunit ALG14	II	379221	379934	2.5	2.13

B.

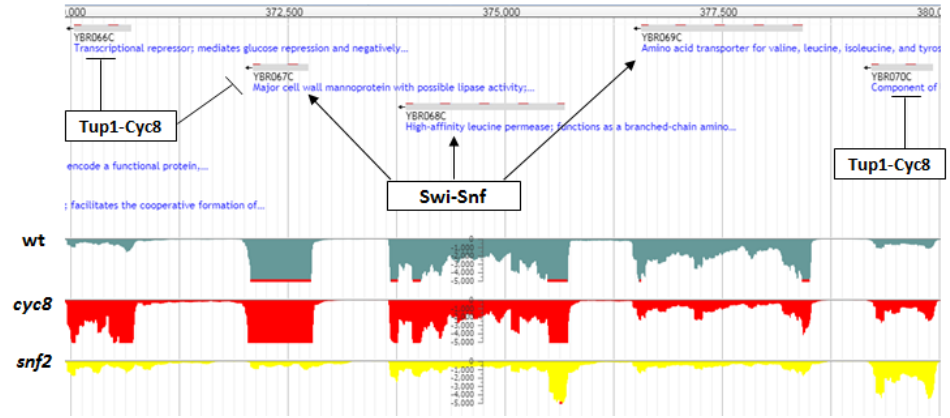

Figure 5.48 Example for one of the *snf2* and *cyc8* genes group. Five genes were located in one group under regulation either by Swi-Snf or Tup1-Cyc8 or both together. **A:** Table of the genes, the genes ontology and the fold change up or down at least 2-Fold in *snf2* and *cyc8*. **B:** screen shot of J-browse showed the location of the genes and the organisation of Swi-Snf and Tup1-Cyc8 of this group.

5.7 Discussion:

The aim of this project was to identify those genes under repression by Tup1-Cyc8 and which require Swi-Snf for activation. The well-known example of this set of genes were the *FLO1* and *SUC2* genes (Fleming and Pennings 2007; Fleming and Pennings 2001) while the rest of these genes were unknown.

The data presented in chapter 3 and 4 demonstrated that *SNF2* was the best Swi-Snf subunit to be used for this analysis since Snf2 is the catalytic heart of the protein complex (Dutta *et al*. 2017). This study therefore chose to perform the transcriptome analysis using a mutant deleted for the entire Snf2 subunit, where the complex is reportedly unstable (Dutta *et al*. 2017), as well as a *snf2K798A* mutant, where the complex is intact, but lacking its ATPase dependent chromatin remodelling activity (Martens & Winston, 2002). Comparison of the results from these different mutants may offer insight into the currently unknown ATPase-independent roles of this important complex. The work also used a *cyc8* mutant to cripple the Tup1-Cyc8 complex, in which Tup1 will not be able to interact with its target sites in the absence of Cyc8 (Fleming *et al*. 2014). Ultimately *snf2 cyc8* and *snf2K798A cyc8* double mutants were used for the transcriptome analysis to discover the co-regulated genes transcription by comparing global transcription in these mutants to transcription in the *cyc8* single mutant.

With regards the transcriptome analysis, 575 (8.7%) genes were up-regulated more than 2-fold in the absence of Cyc8 were identified, suggesting that these genes are normally repressed by the Tup1-Cyc8 complex (Table 5.1).

This result was consistent with the results from previously published studies (Chen *et al*. 2013), and those generated by (Brenda Lee, Fleming lab, Trinity college Dublin (Unpublished data)) the result observed that the majority of the genes were match with about 317 genes (Appendix I, Table S4).

Interestingly, my data also identified 158 (2.4%) genes that were down-regulated at least 2-fold in the *cyc8* deletion mutant (Table 5.2), which confirms data that suggests that Tup1-Cyc8 could also play role as an activator (Alexandraki *et al*. 2004; Zhang and Reese 2005). Indeed, a recent study showed that deletion of *CYC8* and *TUP1* reduced the transcription level of *TAT1* and *TAT2*. The study revealed that Cyc8 and Tup1 were

indeed acting as co-activator via the action of Stp1 a transcription factor (Tanaka & Mukai, 2015). Importantly our data also contained these two genes which were at least 2-fold change down-regulated in the *cyc8* mutant.

Tup1-Cyc8 acting as a repressor has been shown to play a large variety of roles in cell function highlighting the importance of this complex for the regulation of many different transcription pathways and cell health (Fig.5.6). One type of gene family that was identified as being under the negative regulation of the Tup1-Cyc8 complex was the *PAU* gene family. This is a very large family that contains 24 genes, 19 of which are located in subtelomeric regions, which are important for cell wall organisation (Z. Luo & van Vuuren, 2009). The data also showed that the *FLO* gene family, which encode proteins that play a role in cell-cell adhesion in response to environmental stress and include the *FLO1* gene, which were also located in subtelomeric regions (Fleming and Pennings 2001; Soares 2011).

This transcriptome analysis revealed 575 genes that were upregulated more than 2-fold in the *cyc8* mutant were located in various different chromosomal areas across all the 16 chromosomes in *Saccharomyces cerevisiae*. However, 100 of the 575 genes were located in the subtelomeric regions of the chromosomes which I defined as being within 30 Kb of each end of a chromosome, considering that such subtelomeric sequences comprise only 7% of the genome (Barton *et al*. 2003) (Fig. 5.10), and yet almost 20% of the upregulated genes reside in this region, showing a significant enrichment of Cyc8 upregulated genes within the subtelomeric regions (Fig. 5.11).

Interestingly, 196 genes were found to be clustered in the *cyc8* mutant with 82 groups containing between 2 and 4 genes. Analysis of the orientation of the genes within these groups showed that 16 group were divergent and convergent, 13 group were in the sense direction and 12 group were in the antisense direction (Fig 5.12 A and B). However, these gene clusters showed no specific chromosome location as they were located evenly in across all areas of the genome (Fig. 5.14).

On the other hand, for our transcription analysis in the *snf2* mutant, our data suggested that Swi-Snf regulates up to 278 genes as an activator. This is consistent with previously published data sets (Dutta *et al*. 2017; Dutta *et al*. 2014; Sudarsanam *et al*. 2000)

(Appendix I, Table S8). Many of the top 50 most downregulated genes in the *snf2* mutant encoded retrotransposons (Table 5.3). It was proposed that there was five known transposable element families in yeast (Ty1-Ty5), the majority with about 75% of retrotransposon in *S. cerevisiae* were Ty1 and Ty2 element which they were a member of vast set of transposable genetic elements (Hani & Feldmann, 1998). The majority of our results showed Ty1 element which was proposed that was modulated by Swi-Snf (Anon 1991; Curcio *et al*. 2015). The retrotransposon-related Ty1 were also found in the list of Cyc8 downregulated genes (Fig. 5.2).

Interestingly, 208 genes were also found that were upregulated more than two-fold in the *snf2* mutant (Table 5.4), suggesting that Swi-Snf could also play a role as a repressor. *SER3* was the best-known example of these genes at which Swi-Snf has been shown to directly repress its transcription (Martens & Winston, 2002).

The data presented was consistent with other studies, and highlights the cellular importance of the Swi-Snf complex (Dutta *et al*. 2017; Sudarsanam *et al*. 2000). Indeed, these data confirmed that Snf2 regulated the transcription of a diverse set of genes including genes involved in cell wall organisation, catalytic activity and many stress response genes (Fig. 5.17).

The genes under regulation by Swi-Snf functioning as an activator were located in various places across the chromosomes with 22 (7.9%) of the genes were located at the subtelomeric region (Fig. 5.20). The genes were located at subtelomeric did not show a statistically significant difference in transcription than whose located in other regions of the chromosomes (Fig. 5.21).

There were only 12 groups of genes that were upregulated /downregulated in the *snf2* mutant, and these were located in various places across the chromosomes (Fig. 5.22).

We also analysed the Swi-Snf transcriptome in the *snf2K798A* catalytic dead mutant where the complex has been proposed to remain intact but inactive for Snf2 ATPase activity (Dutta *et al*. 2017). In this mutant, 248 genes were down-regulated in *snf2K798A* mutants, suggesting that Swi-Snf plays a role as an activator at these genes. Also, 146 genes were upregulated reflecting that Swi-Snf may play a role as a repressor at these genes (Fig. 5.25).

One of the aims of this study was to identify whether Swi-Snf requires the ATP-utilization for its action or whether the shape of the complex could play also a role. A comparison of the genes that were downregulated in both the *snf2* full deletion and *snf2K798A* catalytic dead mutants was made. The data showed that they shared a large cohort of 223 genes whilst there were only 55 and 25 uniquely downregulated in the *snf2* and *snf2K798A* mutants, respectively (Fig. 5.27). This study also investigated the transcription level of the sets of genes that were downregulated in both mutants and found that and there was no statistically significant difference in the levels of upregulation of genes depending on whether Snf2 was absent or present, yet catalytically dead (Fig. 5.28). This research also analysed whether there was a specific function of the genes uniquely downregulated in the *snf2* mutant and the genes uniquely downregulated in the *snf2K798A* mutant. The results suggested that there was not any obvious functionally related or specific roles of these genes (Fig. 5.29). A similar situation was also found for the upregulated genes in the *snf2* and *snf2K798A* mutants (Fig. 5.30). Thus, for the large part there was no statistically significant difference in the impact upon the numbers of genes whose transcription was altered whether *snf2* was absent or present, yet inactive. In addition, the fold difference in transcription of these genes compared to wt was similar whether either *snf2* was absent or present, yet inactive.

The main aim of the project was to identify the genes co-regulated by Swi-Snf acting as an activator, and Tup1-Cyc8 acting as a repressor. This was achieved by comparing the transcription fold increase in the *cyc8* single mutant, with the transcription fold decrease in the *cyc8* mutant additionally deleted for *snf2* (*snf2 cyc8* double mutant). Our data suggested that 102 genes were repressed by Tup1-Cyc8 and activated by Swi-Snf (Fig. 5.32 and 5.33) (Table 5.5).

Gene ontology analysis revealed that most of the co-regulated genes were either involved with cell wall organisation or played a role in carbohydrate transport and utilisation (Fig. 5.36).

It was proposed that *FLO1* was under the antagonistic mechanism of Tup1-Cyc8 and Swi-Snf activity (Fleming and Pennings 2001), which is involved in cell wall flocculation. This

study expands on previous findings, and includes *FLO5*, *FLO9* and *FLO11* which are members of the *FLO* family.

The invertase encode gene *SUC2* were previously well characterised as being under the antagonistic mechanism of the Tup1-Cyc8 and Swi-Snf (Fleming & Pennings, 2007), which is also was identified in this study. The results identified a carbohydrate gene families, like *HXT*, which includes *HXT1*, *HXT4*, *HXT7*, *HXT13* and *HXT17*, which are involved in glucose transport (Ozcan & Johnston, 1995). *IMA5* encoding alpha-glucosidase was also identified.

S. cerevisiae adapts to the lack of the oxygen (hypoxia) by expression many of genes. This research recognized *DAN1* and *DAN4*, which encode cell wall mannoproteins induced under anaerobic conditions, similar to *TIR* genes were this research identified *TIR1*, *TIR2*, *TIR3* and *TIR4*. *S*. *cerevisiae* has previously been shown to have *DAN/TIR* genes encoding nine cell wall mannoproteins (Abramova *et al*. 2001). It has also been shown that the Swi-Snf is required to robustly activate these genes with Rpd3, and Tup1-Cyc8 is required to repress these genes under aerobic conditions with co-operation with heme-repressor factor Rox1 (O. Sertil *et al*. 2003; Sertil *et al*. 2007).

Strikingly, a high percentage of the co-regulated genes (30.3%) were located in subtelomeric chromosomal regions, which was defined as being within 30 kb of each chromosome end (Fig. 5.37). Furthermore, the genes located in these subtelomeric regions showed the greatest fold drop in transcription in the *snf2 cyc8* double mutant compared to the *cyc8* single mutant. It was reported that the subtelomeres contain specific gene families which reflects the organism's lifestyle such as *MAL* genes families involved in maltose fermentation (Brown *et al*. 2010). In this project the results show additional co-regulated genes families located at subtelomeric regions, including the subtelomeric *PAU* gene family which is involved in the oxidative stress response, as well as *HXT* family of genes involved in carbohydrate metabolism and the *FLO* gene family which is involved in flocculation.

Together, these data suggest that the co-regulated genes were enriched in subtelomeric regions and that genes located in subtelomeres were the most robustly regulated by Tup1-Cyc8 acting as a repressor, and Swi-Snf acting as an activator (Fig.

5.38). This result expands the vision of the *FLO1* genes which is located in subtelomeric region in the chromosome 1 that was robustly regulated by the action of Tup1-Cyc8 and Swi-Snf (Fleming & Pennings, 2001; Fleming *et al*. 2014).

The results indicated that 6 groups of genes that were located beside each other in the genome (Fig. 5.39), two of these groups were functionally related, where the first one was included *DAN1* and *DAN4,* and the second one included *TIR2* and *TIR4*. Interestingly, all of these genes are expressed under anaerobic condition and they encode cell wall mannoproteins (Abramova *et al*. 2001) (Fig. 5.40) (Table 5.6).

This research hypothesised that the robust changes in transcription would be in those genes with large promoters, especially the genes which were located in the subtelomeric regions, which is defined in this project as being 30 Kb at the end of each chromosome. The exact definition of this region varies in eukaryotes from 20 Kb to several hundred Kb in mammals (Cohn *et al*. 2006; Mefford & Trask, 2002). These areas have low gene density and comprise only 7% of the whole genome (Barton *et al*. 2003). These areas are subjected to robust chromatin remodelling; an obvious example was the well-characterised *FLO1* gene (Fleming & Pennings, 2001). In this project, the regulation of globally identified co-regulated genes were investigated; the upstream intergenic region size of each gene was estimated and plotted against the decrease of the transcription in *snf2 cyc8* vs *cyc8*. The results observed no relation between upstream intergenic region size and transcription level in *snf2 cyc8* (Fig. 5.41). However, the observation of Fleming and Penning was true for just *FLO1* gene which showed the longest upstream intergenic region size with 9141 bp and a -31.71-fold change in expression in *snf2 cyc8*.

When the analysis examined the Swi-Snf and Tup1-Cyc8 co-regulated genes using the *snf2K798A*, mutant instead of the *snf2* mutant, only 77 genes were downregulated more than 2-fold in the *snf2K798A cyc8* double mutant compared to the *cyc8* single mutant suggesting these genes were co-regulated by Tup1-Cyc8 as a repressor, and Swi-Snf an activator (Fig. 5.42). Comparing this data with that found using the *snf2 cyc8* double mutant, there was no significant difference between the transcription fold changes in the *snf2 cyc8* double mutant and the *snf2K798A cyc8* double mutant compared to *cyc8*. Only 34 genes were uniquely 2-fold down regulated in the *snf2 cyc8* mutant compared

to 9 genes that were uniquely 2-fold down regulated in the *snf2K798A cyc8* double mutant (Fig. 5.43).

In the final analysis in this chapter, this author investigated the frequency of co-localization of the genes upregulated in *cyc8* single mutants, and the genes downregulated in *snf2* single mutants, which could indicate a special organisation of these complexes or a novel mechanism of action. 40 groups (Fig. 5.46) of genes were identified. However, these groups had no related function or specific organisation of Tup1-Cyc8 and Swi-Snf. The biggest groups were depicted in the updated J-browse image (Fig. 5.48).

In summary, the Tup1-Cyc8 which was represented by deletion of *CYC8,* was shown to be responsible for de-repression of 575 (8.7%) genes of the whole genome and shown to have the ability also to activate 158 (2.3%). In contrast the activator Swi-Snf, which was represented in this research as the *snf2* full deletion mutant and *snf2K798A,* the catalytic dead mutant, was shown to have activation activity at 280 (4.2%) genes and repression activity at 208 (3.1%) genes in *snf2* mutants. ATP-hydrolysing is the main source of Swi-Snf activity and data analysis showed no obvious difference in this activity between *snf2K798A* with the *snf2* full deletion. The main finding in this chapter is the identification of the 102 co-regulated genes under the antagonistic mechanism of Tup1-Cyc8 and Swi-Snf. It is not clear if the 102 genes are under the direct control of the two complexes due evidence from the global change in RNA levels.

However, the global change in RNA levels raised a question are the 102 genes under the direct function of the Tup1-Cyc8 and Swi-Snf.

Chapter 6

Investigating genome-wide Cyc8 and Snf2 occupancy

6.1 Introduction:

The co-repressor Tup1-Cyc8 and the co-activator Swi-Snf play a critical role for the regulation of gene transcription (Becker & Hörz, 2002). Our RNA-Seq data identified the total number of genes that were down- and up- regulated in Tup1-Cyc8 and Swi-Snf chromatin remodelling complex deficient mutants. The data suggested that the Tup1-Cyc8 complex repressed 575 genes, while Swi-Snf, acting as an activator, regulated 278 genes. Our transcriptome data analysis also suggested that 102 genes were under the antagonistic control of Tup1-Cyc8 as a repressor and Swi-Snf as an activator. However, the transcription analysis provides the sets of genes that could be either under the direct or indirect control of these two complexes.

To classify the genes directly regulated by these two complexes, I analysed previously published global chromatin immunoprecipitation (ChIP-Seq) data sets which had mapped the location of Snf2 and Tup1 across the *Saccharomyces cerevisiae* genome. The aim was to correlate the occupancy of Tup1 and Snf2 with the genes I had identified as being co-regulated by Swi-Snf and Tup1-Cyc8.

6.2 Result:

6.2.1 Mapping Snf2 across the genome:

The published global chromatin immunoprecipitation (ChIP-Seq) analysis was performed using an antibody against the catalytic Snf2 subunit (Wong & Struhl, 2011). The raw data was accessed from the public data base in NCBI (accession number SRA044839.1) and Dr.Karsten Hokamp performed peak calling analysis to provide the Snf2 occupancy profiles.

The data showed 142 sites of Snf2 occupancy with most sites present in gene promoters (121), and a minority in open reading frames (15) or intergenic regions (4) (Table 6.1). The 50 most highly occupied sites are shown in (Table 6.2) and demonstrate that Snf2 occupancy was associated with genes of varying function (Appendix II, Table S1).

Snf2 occupancy (number of sites)			
Snf2 in wt	**Promoter**	**Open reding frame**	**Intergenic region**
142	**121**	**15**	**4**

Table 6.1: Snf2 occupancy sites: The number of the Snf2 peaks position within promoters, open reading frames (ORF) or downstream intergenic regions is indicated.

Genes	Description	Position	Peak score
YLR154C-G	Uncharacterized protein	Intergenic	34280.2
UTR5	Uncharacterized protein	ORF	3101.2
SPO20	Sporulation-specific protein	promoter	2758.1
YLR112W	Uncharacterized protein	promoter	2509.8
YKL097C	Uncharacterized protein	ORF	2388
BRP1	Uncharacterized protein	ORF	2342.8
ZRT2	Zinc-regulated transporter	promoter	2202.9
ENV9	Probable oxidoreductase	promoter	2193.9
SSA1	Heat shock protein	promoter	2026.8
PUT4	Proline permease	promoter	1927.5
YIR018C-A	Uncharacterized protein	promoter	1850.8
VHR1	Transcription factor	promoter	1832.7
YDR010C	Uncharacterized protein	ORF	1814.7
HAP4	Transcriptional activator	promoter	1688.3
YPR064W	Uncharacterized protein	ORF	1665.7
BTN2	Modulates arginine uptake, Batten disease	promoter	1661.2
MOT3	Transcriptional activator/repressor	promoter	1638.6
AGP1	General amino acid permease	promoter	1598
UTR2	Probable glycosidase	promoter	1579.9
PCL1	Nuclear distribution protein nudE homolog	promoter	1561.9
FAS1	Fatty acid synthase subunit beta	promoter	1548.3
SDS23	Protein involved in cell separation	promoter	1548.3
SPO24	Sporulation protein 24	promoter	1548.3
SED1	Cell wall protein	promoter	1543.8
DIP5	Dicarboxylic amino acid permease	promoter	1512.2
TYE7	Serine-rich protein	promoter	1512.2
FAA1	Long-chain-fatty-acid--CoA ligase	promoter	1503.2
ZEO1	Zeocin resistance	promoter	1494.2
ZPR1	Zinc finger protein	promoter	1394.9
SER3	D-3-phosphoglycerate dehydrogenase	promoter	1390.3
TEC1	Ty transcription activator	promoter	1340.7
AAC1	ADP,ATP carrier protein	promoter	1300.1
HCM1	Transcription factor	promoter	1277.5
MEP3	Ammonium transporter	promoter	1268.5
YHR007C-A	Uncharacterized protein	Intergenic	1259.4
ZRT1	Zinc-regulated transporter	promoter	1223.3
GID8	Glucose-induced degradation protein	promoter	1209.8

Genes	Description	Position	Peak score
RNH203	Proline-specific permease	promoter	1191.7
MAM3	Protein required for mitochondrial morphology	promoter	1173.7
FKS1	1,3-beta-glucan synthase component	promoter	1169.2
HXT3	Low-affinity glucose transporter	promoter	1160.1
LCL1	Long chronological lifespan protein	ORF	1155.6
CLN2	G1/S-specific cyclin	promoter	1151.1
GIC2	GTPase-interacting component	promoter	1137.6
TAL1	Transaldolase	promoter	1137.6
LST8	Target of rapamycin complex subunit	promoter	1106
NDE1	External NADH-ubiquinone oxidoreductase	promoter	1096.9
HOR7	Uncharacterized protein	promoter	1083.4
RNH203	Ribonuclease H2 subunit C	promoter	1078.9
CMR3	Putative zinc protein	promoter	1074.4

Table 6.2 The top 50 Snf2 occupancy sites: The top 50 sites of Snf2 occupancy were listed in the table according to the peak score. Associated gene names and gene functions are listed. The gradient of red colour indicates the peak score increase, with the reddest being the highest peak score (highest occupancy). The peak score was calculated by converting the P value to log 10 so the lower P value the higher the peak score. The peaks were mapped relative to the nearest transcription start site (TSS) or nearest transcription termination site (TTS). The position of the peaks within promoters, open reading frames (ORF) or downstream intergenic regions is indicated.

6.2.1.1 Comparing Snf2 occupancy with gene transcription profiles in a *snf2* deletion mutant:

Our RNA-Seq data observed 278 genes that were down-regulated at least 2-fold compared to wt in a *snf2* deletion mutant, suggesting the Swi-Snf complex acts as an activator at these genes (Table 5.3). There were also 208 genes that were up-regulated in the *snf2* mutant suggesting Swi-Snf can act as a repressor at these genes (Table 5.4). The previously published chromatin immunoprecipitation (ChIP-Seq) analysis data revealed that there were 146 sites of Snf2 occupancy across the entire yeast genome (Wong & Struhl, 2011).

I therefore first compared the 278 genes that were down-regulated at least 2-fold in the *snf2* gene deletion mutant with the 146 Snf2 occupancy sites. The results showed that only 27 of the down-regulated genes and the Snf2 occupancy sites overlapped (Fig. 6.1).

The 27 genes are shown in (Table 6.3) and include genes involved in the stress response such as *DDR2* which is involved in DNA damage response. Other genes were involved in metabolism, such as the *HXT3*, which is a glucose transporter and *FAS1*, which encodes the beta subunit of fatty acid synthetase. Similarly, the *ARO10* gene encodes phenylpyruvate decarboxylase which is involved in the Ehrlich pathway (Hazelwood *et al*. 2008) and is shown in (Fig.6.2).

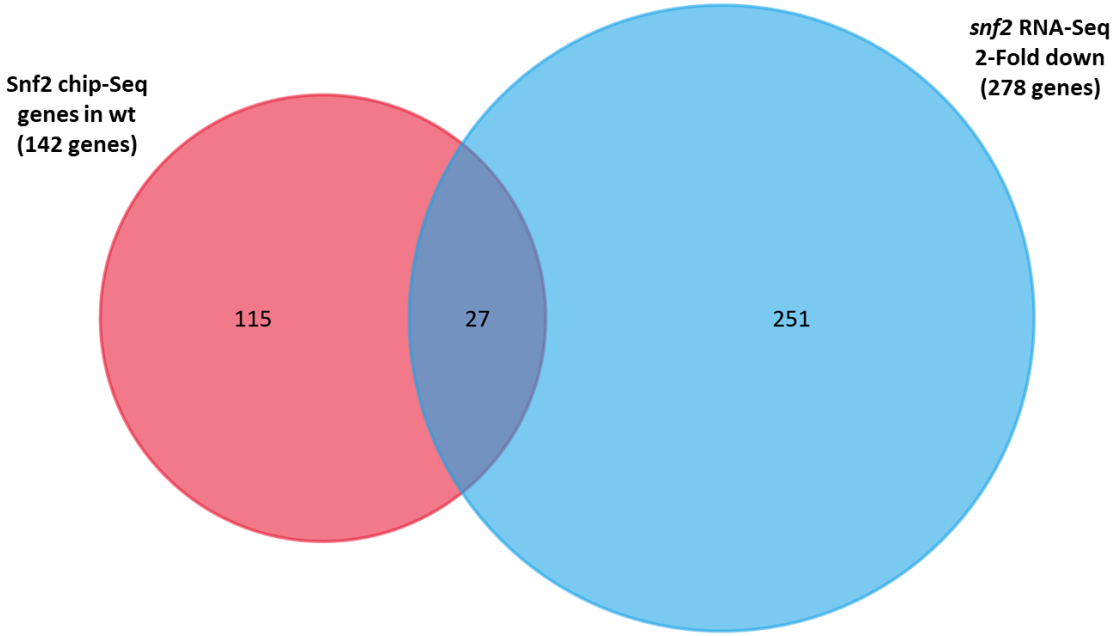

Figure 6.1 Comparison between Snf2 occupancy and genes whose transcription is down-regulated in a *snf2* deletion mutant. Venn diagram to show 27 genes down-regulated at least 2-fold in a *snf2* mutant compared to genes showing Snf2 occupancy in their vicinity. Fun rich software was used to perform the Venn (M. Pathan *et al*. 2015).

Gene	Description	wt vs *snf2* Fold change	Peak score	Distance from TSS	Position
YHB1	Flavohemoprotein	-22.07	776.4	-436	Promoter
RPI1	Negative RAS protein regulator protein	-11.13	911.9	-932	Promoter
ARO10	Transaminated amino acid decarboxylase	-11.13	934.4	-344	Promoter
ZEO1	Zeocin resistance	-9.34	1494.2	-471	Promoter
PHM8	Phosphate metabolism protein	-9.24	744.8	-319	Promoter
SED1	Cell wall protein	-8.64	1543.8	-874	Promoter
ARO9	Aromatic amino acid aminotransferase	-7.27	609.4	-178	Promoter
MNN1	Alpha-1,3-mannosyltransferase	-7.2	1015.7	-753	Promoter
WSC4	Cell wall integrity and stress response	-7.14	681.6	-364	Promoter
YOR142W-B	Transposon Ty1-OR Gag-Pol polyprotein	-6.39	469.5	-724	Promoter
DDR2	DNA damage Responsive	-6.38	826.1	-452	Promoter
CYC1	Cytochrome c	-6.21	957	-339	Promoter
ZRT1	Zinc-regulated transporter	-5.5	1223.3	-305	Promoter
HOR7	Uncharacterized protein	-4.77	1083.4	-339	Promoter
HAP4	Transcriptional activator	-4.77	1688.3	-734	Promoter
STP4	Zinc finger protein	-4.7	690.7	-723	Promoter
AGP1	General amino acid permease	-3.98	1598	-587	Promoter
GAC1	Serine/threonine-protein phosphatase	-3.86	564.3	-970	Promoter
PDR15	ATP-dependent permease	-3.57	650	-388	Promoter
PDR5	Pleiotropic ABC efflux transporter	-3.43	753.9	-472	Promoter
CLN1	G1/S-specific cyclin	-3.18	821.6	-524	Promoter
POR1	Mitochondrial outer membrane protein	-2.55	320.5	-26	Promoter
CHO2	Involved in methylation pathway	-2.36	817.1	-340	Promoter
FAS1	Fatty acid synthase subunit beta	-2.35	1548.3	-664	Promoter
HXT3	Low-affinity glucose transporter	-2.22	1160.1	-373	Promoter
TEC1	Ty transcription activator	-2.11	1340.7	-452	Promoter
MMO1	Unknown function	-2.07	830.6	-648	Promoter

Table 6.3: The 27 genes down regulated in a *snf2* mutant at which Snf2 was detected: The table represents the set of genes which were down regulated in a *snf2* mutant at which Snf2 was detected by ChIP-Seq. The blue colour gradient indicates the level of fold decrease in transcription in the *snf2* mutant compared to wt; the red colour gradient indicates the peak score of each gene, with the most red indicating the greatest peak score which indicates the greatest Snf2 occupancy. The distance of the Snf2 ChIP signal relative to the nearest gene transcription start site (TSS, +1) was also represented (in base-pairs (bp)). The position of the peaks within promoters, open reading frames (ORF) or downstream intergenic regions is indicated.

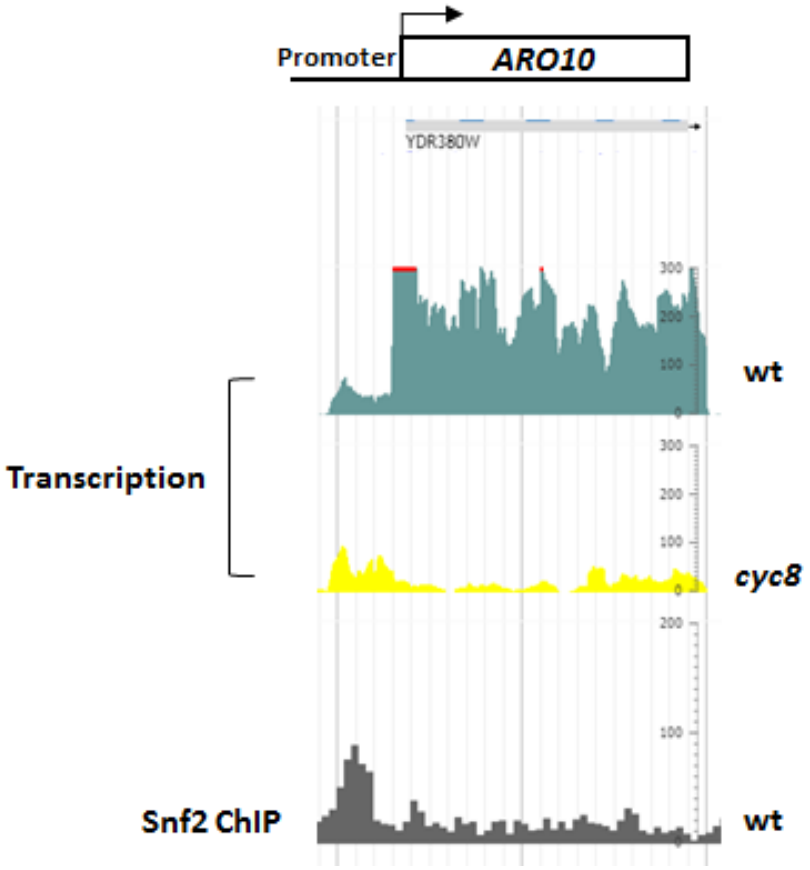

Figure 6.2 Snf2 occupancy and transcription in genes down-regulated in *snf2* mutants. *ARO10* (*YDR380W*) gene as an example for down-regulated genes in *snf2*. Transcription was high in wt, in *snf2* mutants the level of transcription was abolished. The Snf2 localization peak is shown.

6.2.1.2 Chromosomal location of Snf2 occupancy sites at genes down regulated in a *snf2* mutant:

I next analysed the genomic location of the 27 genes which are down regulated in the *snf2* mutant and to which Snf2 was directly mapped. These genes represent the genes most likely to be directly dependent upon Snf2 for transcription.

The results showed that these genes were found on most of the chromosomes and, with the exception of *ZRT1*, were all found out with chromosomal sub telomeric regions. The fold drop in transcription of these genes in the *snf2* mutant also varied with the greatest fold down regulation being for *YHP1* and *ARO10* transcription (Fig.6.3).

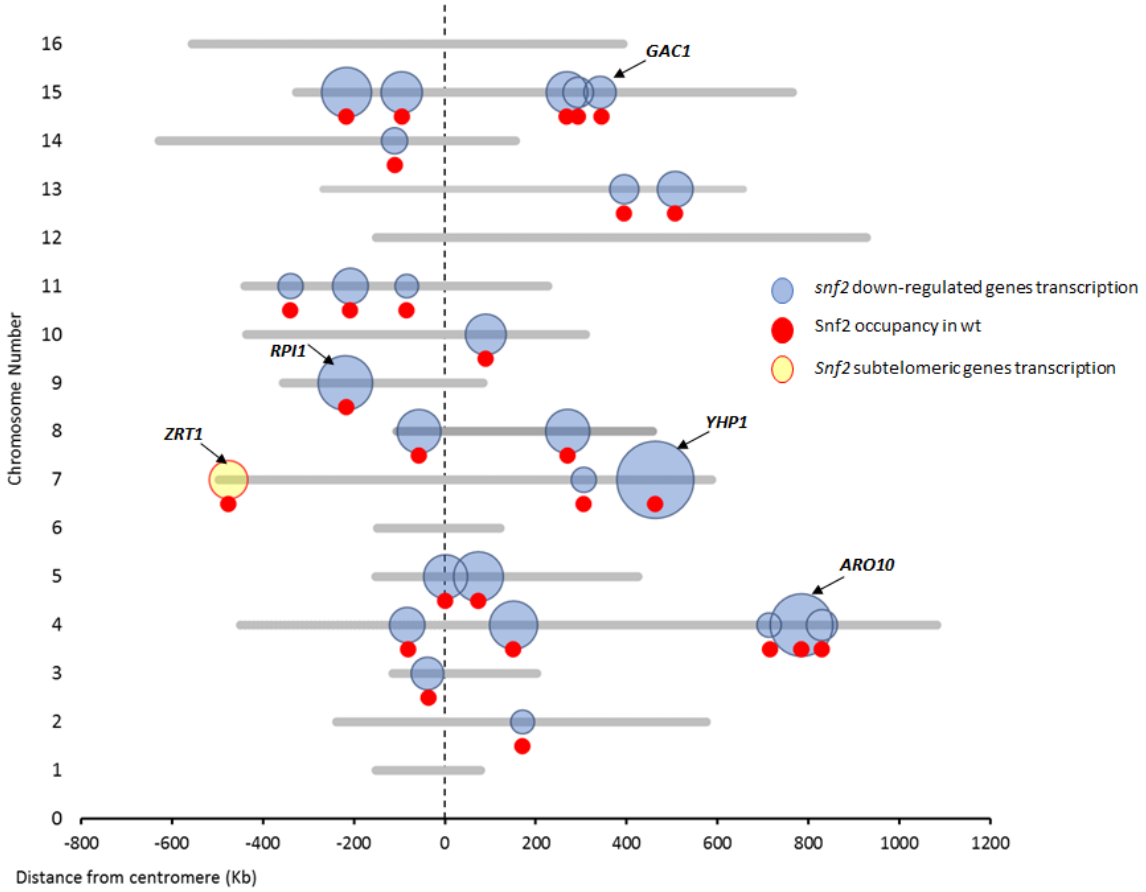

Figure 6.3 Chromosomal location of *snf2* down-regulated genes at which Snf2 occupancy was detected in wt. 'Bubble' plot showing the location and the fold decrease in transcription of the 27 genes down regulated in a *snf2* mutant and at which Snf2 was detected by ChIP-Seq. The data of each chromosome and gene were provided from *Saccharomyces* genome database (SGD) (Cherry *et al*. 1998). All 16 chromosome centromeres were set as zero and the chromosomes sizes and gene positions were normalized relative to that. Each lane reflects the chromosome number and size, the position of the genes was reflected by the blue circle position and the size of the circle reflects the level of gene transcription decrease in the *snf2* mutant relative to wt. The dark red circle under the chromosome indicates the location of each Snf2 peak on the chromosome.

6.2.1.3 The relationship between Snf2 occupancy relative to the gene transcription start site and Snf2-dependent positive regulation of transcription:

I next examined whether there was a relationship between the site of Snf2 occupancy relative to the associated gene transcription start site and the transcription fold decrease in a *snf2* deletion mutant. The results showed that Snf2 at these genes was always found in the gene promoter at positions varying from 26 to 970 bp upstream of the transcription start site (TSS). However, there was no relation between the transcription fold change in the *snf2* mutant and the distance of the site of Snf2 occupancy from the transcription start site (TSS).

Indeed, the *YHP1* gene, which showed the greatest fold difference in transcription in the *snf2* mutant, had Snf2 located -436 bp from the TSS, whilst the genes with Snf2 located the nearest (*POR1*) and the farthest (*GAC1*) from the TSS showed similar levels of transcription fold drops in the *snf2* mutant at -2.5 and -3.4-fold respectively (Fig. 6.4 and Table 6.3).

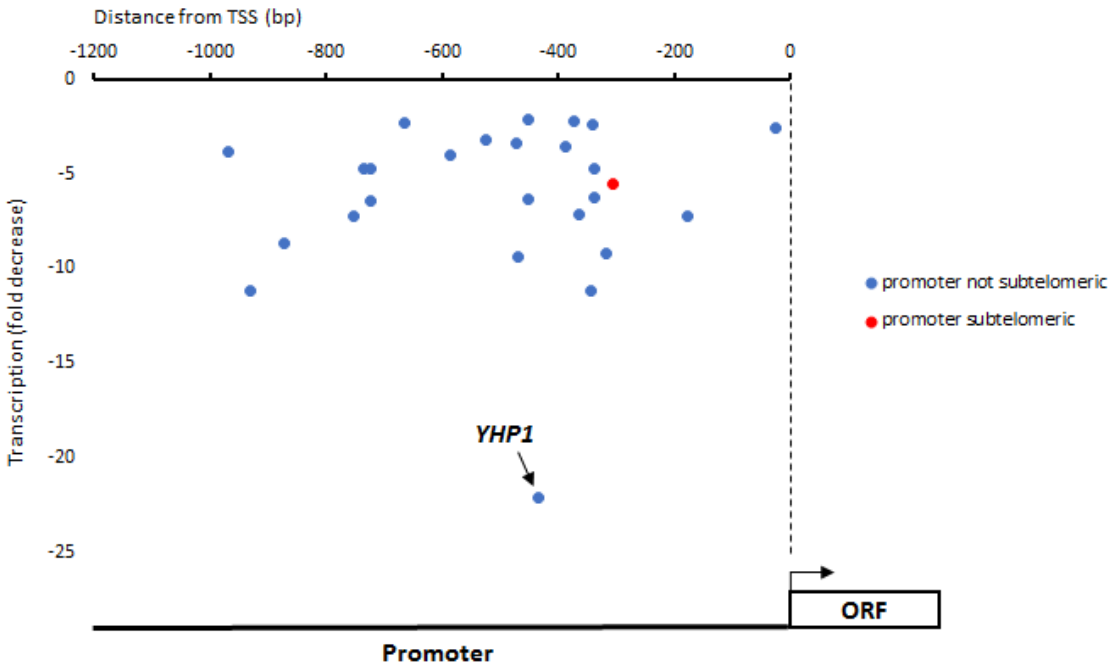

Figure 6.4 The relation between the transcription fold decrease in a *snf2* mutant and the distance of Snf2 occupancy relative to the TSS. the fold down-regulation of gene transcription in a *snf2* mutant were plotted against the distance of Snf2 occupancy relative to each genes transcription start site (TSS). Genes found within (red) and out with (blue) the sub telomeric regions are indicated.

6.2.1.4 Snf2 occupancy at genes up-regulated in a *snf2* mutant:

Our RNA-Seq data also observed 208 genes that were up-regulated at least 2-fold in the *snf2* mutant, suggesting the Swi-Snf complex acts as a repressor at these genes (Table 5.4). I therefore repeated the previous analyses at these genes to determine if Snf2 could be found at these genes, and if so, where it was located relative to the transcription start site. I first compared the 208 genes that were up-regulated in *snf2* at least 2-fold with the 142 Snf2 occupancy sites detected by ChIP-Seq. The result showed that only 19 up-regulated genes showed Snf2 being present (Fig. 6.5).

Importantly, the *SER3* gene was present in this cohort of genes, which was a previously identified gene known to be repressed by Swi-Snf (Martens & Winston, 2002) (Table 6.4).

When the cut off for consideration of a gene under *snf2* control was dropped to a 1.5-fold up-regulation, 23 genes overlapped (Fig. 6.6).

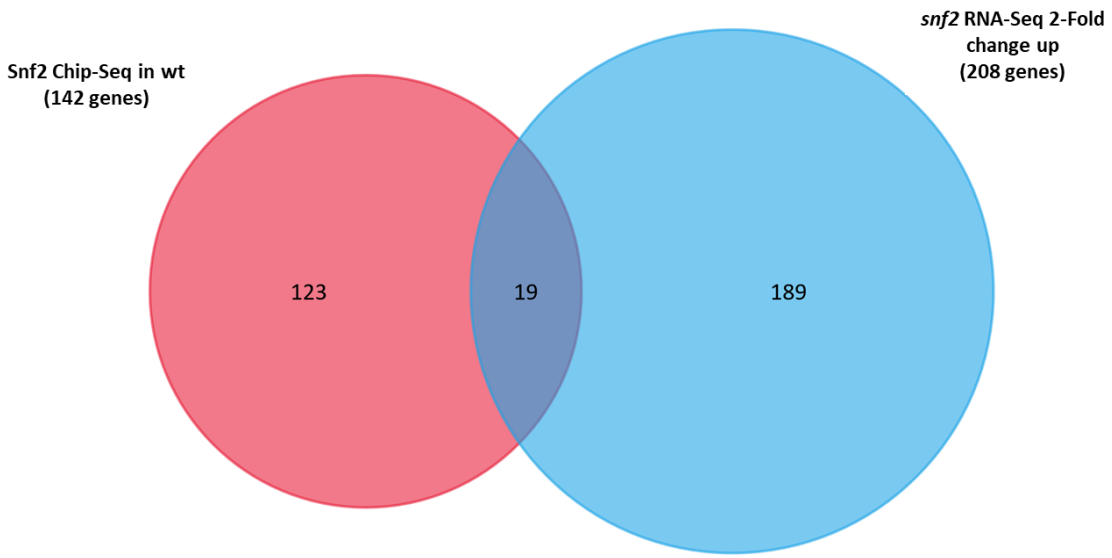

Figure 6.5 Comparison between Snf2 occupancy and genes 2-fold up-regulated in *snf2* mutant. Venn diagram to show 19 up-regulated genes at least 2-fold change up overlapping in Snf2 ChIP-Seq in wt vs *snf2* genes up-regulated 2-fold. Fun rich software was used to perform the Venn diagram (M. Pathan *et al*. 2015).

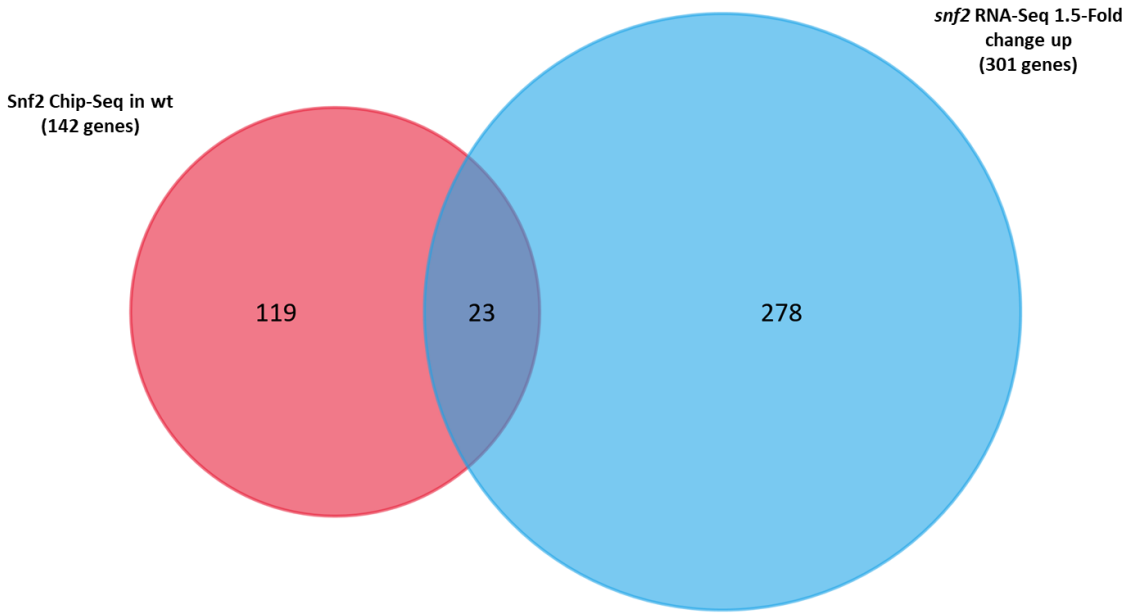

Figure 6.6 Comparison between Snf2 occupancy and genes 1.5-fold up-regulated in *snf2* mutant. Venn diagram to show 23 up-regulated genes at least 1.5-fold change up overlapping in Snf2 ChIP-Seq in wt vs *snf2* genes up-regulated 1.5-fold. Fun rich software was used to perform the Venn diagram (M. Pathan *et al*. 2015).

Gene	Description	wt vs *snf2* fold change	Peak score	Distance from TSS (bp)	Position
SER3	D-3-phosphoglycerate dehydrogenase	17.21	1390.3	-619	promoter
YPR064W	Uncharacterized protein	6.61	1665.7	223	ORF
AAC1	ADP,ATP carrier protein	5.69	1300.1	-208	promoter
BRP1	Uncharacterized protein	5.41	2342.8	278	promoter
YMR122C	Uncharacterized protein	4.7	821.6	28	ORF
PUT4	Proline-specific permease	3.68	1927.5	-436	promoter
FRE4	Ferric reductase	3.58	379.2	-446	promoter
YFL051C	Uncharacterized membrane protein	3.38	546.2	-654	promoter
YDR010C	Uncharacterized protein	3.27	1814.7	63	ORF
YKL097C	Uncharacterized protein	3.26	2388	136	ORF
YAP6	AP-1-like transcription factor	3.11	1548.3	-528	promoter
SPO20	Sporulation-specific protein	2.91	2758.1	-821	promoter
ATG41	Autophagy-related protein	2.72	884.8	-431	promoter
SPO24	Sporulation protein	2.72	1548.3	-387	promoter
YLR112W	Uncharacterized protein	2.42	2509.8	-142	promoter
UTR5	Uncharacterized protein	2.34	3101.2	248	ORF
ERG25	Methylsterol monooxygenase	2.24	1047.3	-547	promoter
YML007C-A	Uncharacterized protein	2.05	803.5	-189	promoter
GIC2	GTPase-interacting component	2.02	1137.6	-403	promoter
YDR215C	Uncharacterized protein	1.94	993.1	392	ORF
GPP1	glycerol-1-phosphatase	1.93	699.7	451	ORF
RNH203	Ribonuclease H2 subunit C	1.73	1191.7	-1273	promoter
YIR018C-A	Uncharacterized protein	1.62	1850.8	-1084	promoter

Table 6.4: The 23 genes occupied by Snf2 which are up-regulated in *snf2* mutant: Table represents the set of genes which were up regulated in a *snf2* mutant at which Snf2 was detected by ChIP-Seq. The red colour gradient indicates the level of fold increase in transcription in the *snf2* mutant compared to wt; the second column red colour gradient indicates the peak score of each gene, with the most red indicating the greatest peak score which indicates the greatest Snf2 occupancy. The distance of the Snf2 ChIP signal relative to the nearest gene transcription start site (TSS, +1) was also represented (in base-pairs (bp)). The position of the peaks within promoters, open reading frames (ORF) or downstream intergenic regions is indicated.

6.2.1.5 Chromosomal location of genes up regulated in a *snf2* mutant which are occupied by Snf2:

I next analysed the location of the 23 up-regulated genes at which Snf2 occupancy was detected. The results showed that the up-regulated genes in the *snf2* mutant at which Snf2 could be detected were found on 11 of the 16 chromosomes at regions other than the subtelomeric or telomeric regions (Fig. 6.7).

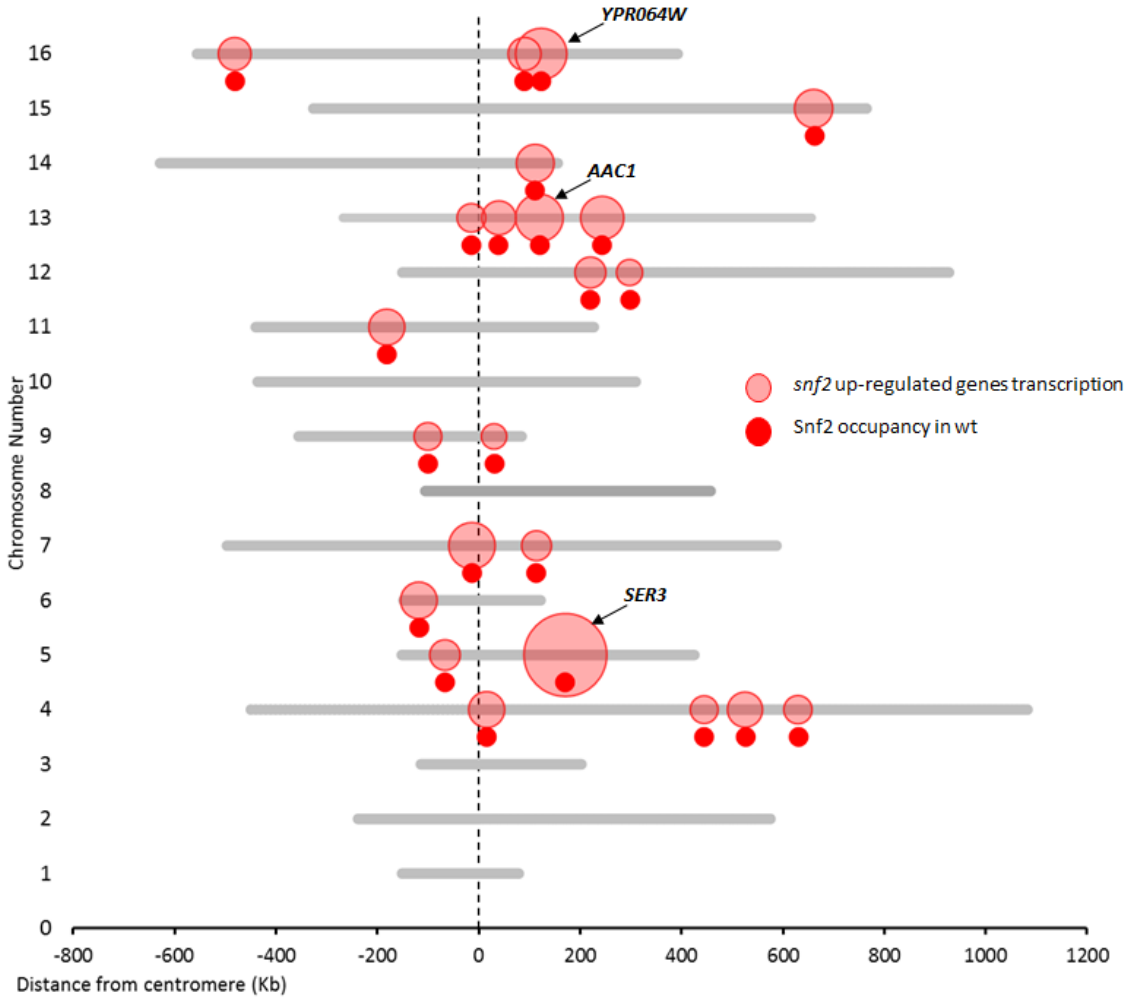

Figure 6.7 Chromosomal location of Swi-Snf in wt up-regulated genes. 'Bubble' plot showing the location and the fold change in transcription of the 23 Swi-Snf up-regulated genes. The data of each chromosome and gene were provided from *Saccharomyces* genome database (SGD) (Cherry *et al*. 1998). All 16 chromosomes centromere were set at zero and the chromosomes size and genes position were normalized according to that. Each lane reflects the chromosome number and size, the position of the genes was reflected by the red circle position and the size of the circle reflects the level of gene transcription. The dark red cycle under the chromosome indicated the location of the Swi-Snf in the chromosome for each gene.

6.2.1.6 The relationship between Snf2 occupancy relative to the gene transcription start site and up-regulation of gene transcription in a *snf2* mutant:

The data showed that Snf2 occupancy could be detected at only 23 genes which were up-regulated in the absence of *snf2* which suggests that Snf2 acts as a repressor of transcription at these genes. I investigated the relationship between the distance of Snf2 occupancy from the associated gene transcription start site (TSS) and the level of transcription de-repression in the absence of *snf2*.

The results showed that 15 of the Snf2 occupancy sites at these negatively regulated genes were located in the gene promoter, whilst 8 of the genes showed Snf2 occupancy in their open reading frames. For those genes occupied by Snf2 in the promoter the distance from the TSS varied from -1273 to –189 bp upstream of the TSS, whilst Snf2 occupancy in the ORF ranged from 28 to 451 bp away from the TSS (Fig. 6.8).

Interestingly, with the exception of *SER3*, for the genes at which Snf2 was located in the promoter, the fold change in transcription of the genes in the *snf2* mutant was less, the further away Snf2 was located from the transcription start site. A similar result was also visible for the genes at which Snf2 was located in the open reading frame. This might suggest that Snf2 might exert a greater negative effect upon transcription the closer it is located to the TSS. However, the exception was at *SER3* which showed a 17.2-fold de-repression in the *snf2* mutant and had Snf2 occupancy at -619bp from the TSS (Fig. 6.8).

In summary, Snf2 occupancy was only detected at 50 of the genes whose transcription was altered more than two-fold in a *snf2* mutant. In these cases, Snf2 was found across many of the chromosomes and was largely present in internal chromosomal regions as opposed to chromosome ends. With regards Snf2 occupancy at those genes whose transcription is reduced in a *snf2* mutant, which represent genes at which Swi-Snf acts as an activator, Snf2 was found solely in gene promoters. At these genes, where Snf2 acts as an activator, there was no correlation between the site of Snf2 occupancy relative to the TSS and the level of gene transcription down regulation in the absence of Snf2.

Conversely, for genes up-regulated in the *snf2* mutant, and which represent genes at which Swi-Snf acts as a repressor, Snf2 was found located in either the promoter or the gene coding region. Interestingly at these genes, there was evidence to suggest that the closer the site of Snf2 to the TSS, the greater the level of repression by Snf2 at that gene.

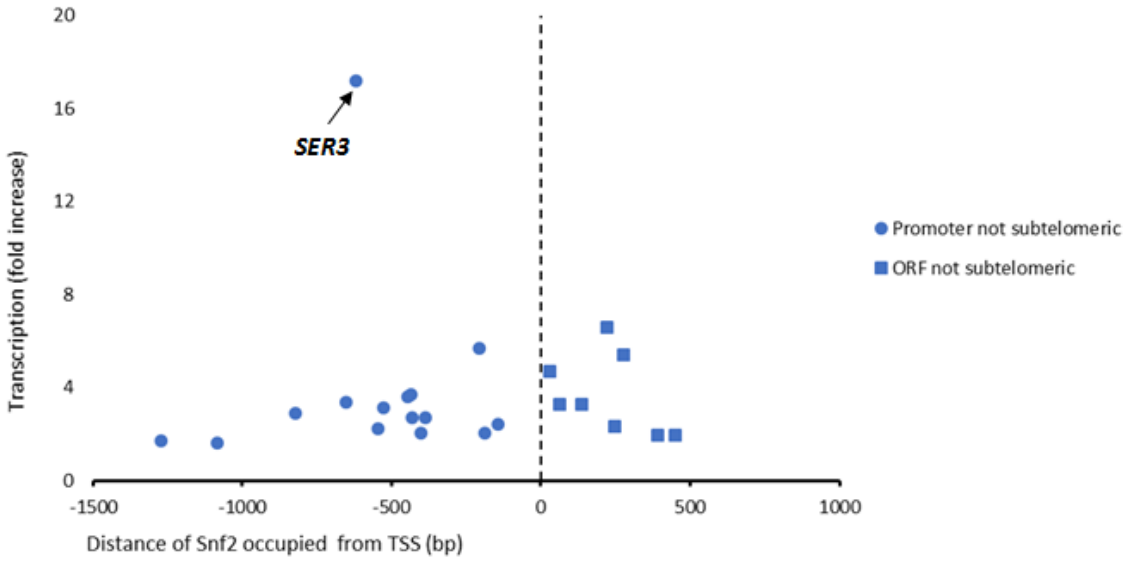

Figure 6.8 The relationship between Snf2 occupancy and the *snf2* transcription fold increase in a *snf2* mutants. The *snf2* transcription up-regulated genes were plotted against the distance from the transcription TSS in scatter plot. The plot showed increase in transcription nearest the distance from the TSS region except for *SER3* genes.

6.2.2 Mapping Tup1 occupancy across the yeast genome:

The data for the global chromatin immunoprecipitation (ChIP-Seq) of Tup1 was taken from a published data set that used antibodies against the Tup1 subunit (Wong & Struhl, 2011).

The data showed 601 sites were occupied by Tup1 which were located predominantly in gene promoters (421 genes) (Table 6.5) (Appendix II, Table S2). However, 137 sites resided within open reading frames (ORFs), and 43 sites were located in intergenic regions, which were defined as the peak being closer to a gene transcription termination site (TTS) than a transcription start site (TSS). In each site of Tup1 occupancy were revealed as being discrete binding sites as opposed to a diffuse pattern of Tup1 occupancy. Thus, the data suggests that Tup1 occupies particular sites as opposed to spreading across large genomic regions.

The top 50 genes showing the greatest peaks of Tup1 occupancy are shown in (Table 6.6) and include genes of varying functions such as the *IME1* transcription factor encoding gene and the *FLO9*, flocculin-encoding gene. Interestingly the genes with the highest Tup1 occupancy (highest peak score) were the *YHL041W* and *YLR154C-G* genes which are of unknown function and had Tup1 located in the promoter and intergenic region, respectively. Two genes in the table are also listed as having Tup1 associated with the ORF. Although the peak of Tup1 is clearly centred in the middle of the *YLR112W* open reading frame, the peak of Tup1 associated with the *TIP1* gene actually seems more promoter specific. Thus, Tup1 occupies sites on most chromosomes, binds at specific sites as opposed to spreading over large domains and can be found in promoters, ORFs and non-coding intergenic regions.

Tup1 occupancy (number of sites)			
Tup1 in wt	**Promoter**	**Open reading frame**	**Intergenic region**
601	**421**	**137**	**43**

Table 6.5: Tup1 in wt occupancy sites: The number of the Tup1 peaks position within promoters, open reading frames (ORF) or downstream intergenic regions is indicated

Genes	Description	Position	Peak score
YHL041W	Uncharacterized protein	promoter	25495.8
YLR154C-G	Uncharacterized protein	intergenic	22640
IME1	Meiosis-inducing protein	promoter	22410
FLO9	Flocculation protein	promoter	20077.8
YBL029C-A	Uncharacterized protein	promoter	19006.8
GAC1	Serine/threonine-protein phosphatase	promoter	18911.6
SPO20	Sporulation-specific protein	promoter	17507.6
GID8	Glucose-induced degradation protein	promoter	17404.4
CMR3	Putative zinc finger protein	promoter	17396.5
YGR050C	Uncharacterized protein	promoter	17285.4
FRE4	Ferric reductase transmembrane component	promoter	17126.8
CIN5	Transcription factor	intergenic	17007.8
RPI1	Negative RAS protein regulator protein	promoter	15706.8
YBL044W	Uncharacterized protein	promoter	14580.4
ZRT2	Zinc-regulated transporter	promoter	14397.9
ACA1	ATF/CREB activator	promoter	13977.5
YOR029W	Uncharacterized protein	promoter	13866.4
MMO1	Uncharacterized protein	promoter	13834.7
IMA2	Oligo-1,6-glucosidase	promoter	13596.7
YJR146W	Uncharacterized protein	promoter	13557
YPR064W	Uncharacterized protein	promoter	13120.7
HXT6	High-affinity hexose transporter	promoter	13017.6
PUT4	Proline-specific permease	promoter	12597.2
YAP6	AP-1-like transcription factor	promoter	12264
GTT1	Glutathione S-transferase	promoter	11700.8
SED1	Cell wall protein	promoter	11597.7
YOR032W-A	Uncharacterized protein	promoter	11240.7
HAP4	Transcriptional activator	promoter	10852
SUT2	Sterol uptake protein	promoter	10669.5
YFL051C	Uncharacterized membrane protein	promoter	10614
RPS3	40S ribosomal protein S3	Promoter	10050.8
ENA1	Sodium transport ATPase	promoter	9535.1
YLR412C-A	Uncharacterized protein	intergenic	9535.1

Genes	Description	Position	Peak score
YIR018C-A	Uncharacterized protein	promoter	9519.3
TIP1	Temperature shock-inducible, cell wall protein	ORF	9313
RRN5	Transcription initiation factor	promoter	8741.9
MNN1	Alpha-1,3-mannosyltransferase	promoter	8646.7
UTR2	Probable glycosidase	promoter	7964.5
NRG1	Transcriptional regulator	promoter	7853.4
YLR112W	Uncharacterized protein	ORF	7726.5
YHR177W	Uncharacterized protein	promoter	7702.7
VHR1	Transcription factor	promoter	7671
GIC2	GTPase-interacting component	promoter	7663
MGA1	Heat shock protein	intergenic	7544
CUP9	Homeobox protein	promoter	7496.4
AQY1	Aquaporin-1	promoter	7409.2
BRP1	Uncharacterized protein	promoter	7242.6
ICS2	Increased copper sensitivity protein	promoter	7242.6
WSC4	Cell wall integrity and stress response	promoter	7131.5
BSC1	Uncharacterized protein	Promoter	6996.7

Table 6.6: The 50 sites showing the highest Tup1 occupancy: The top 50 genes associated with the greatest level of Tup1 occupancy were listed in the table according to the occupancy peak score. The gradient of red colour indicates the peak score increase, with the most red being the highest peak score (highest occupancy). The peak score was calculated by converting the P value to log 10 so the lower P value the higher peak score. The peaks are mapped relative to the nearest transcription start sit (TSS) or nearest transcription termination site (TTE). The position of the peaks within promoters, open reading frames (ORF) or downstream intergenic regions is indicated and added to the table.

6.2.2.1 Comparing Tup1 occupancy with gene transcription profiles in a *cyc8* deletion mutant:

Our RNA-Seq data identified that a total of 733 genes were up or down regulated more than two-fold in the absence of Cyc8. Specifically, 575 were up-regulated in the *cyc8* mutant suggesting Tup1-Cyc8 acts as a repressor at these genes, whilst 158 genes were down regulated, implicating Tup1-Cyc8 as having an activating role at these genes. We therefore wanted to analyse if there was evidence for the Tup1-Cyc8 complex as being present at these 733 genes which would indicate a direct role for this complex in regulating their transcription.

We therefore first compared the 575 up-regulated genes in a *cyc8* mutant, and which should represent the genes at which Tup1-Cyc8 acts as a repressor, with the 601 sites of Tup1 occupancy. Importantly, a *cyc8* mutant should be similarly indicative of the loss of Tup1, since the model for Tup1-Cyc8 proposes that Cyc8 is the adaptor protein for complex binding such that without Cyc8, Tup1 occupancy is lost (Fleming *et al*. 2014).

The results showed that 175 of the 575 genes up-regulated in the *cyc8* mutant were occupied by Tup1 (Fig. 6.9). These genes included the *HXT13* gene which is involved in hexose transport and the *FLO9* and *FLO10* genes which are involved in cell-cell aggregation (Fig. 6.10) (Table 6.7) (Appendix II, Table S3). Interestingly, the *FLO1* and *SUC2* gene which is known to be repressed by Tup-Cyc8 is not in the list even though occupancy of Tup1 at the promoter has been reported (Fleming and Pennings 2001; Fleming and Pennings 2007).

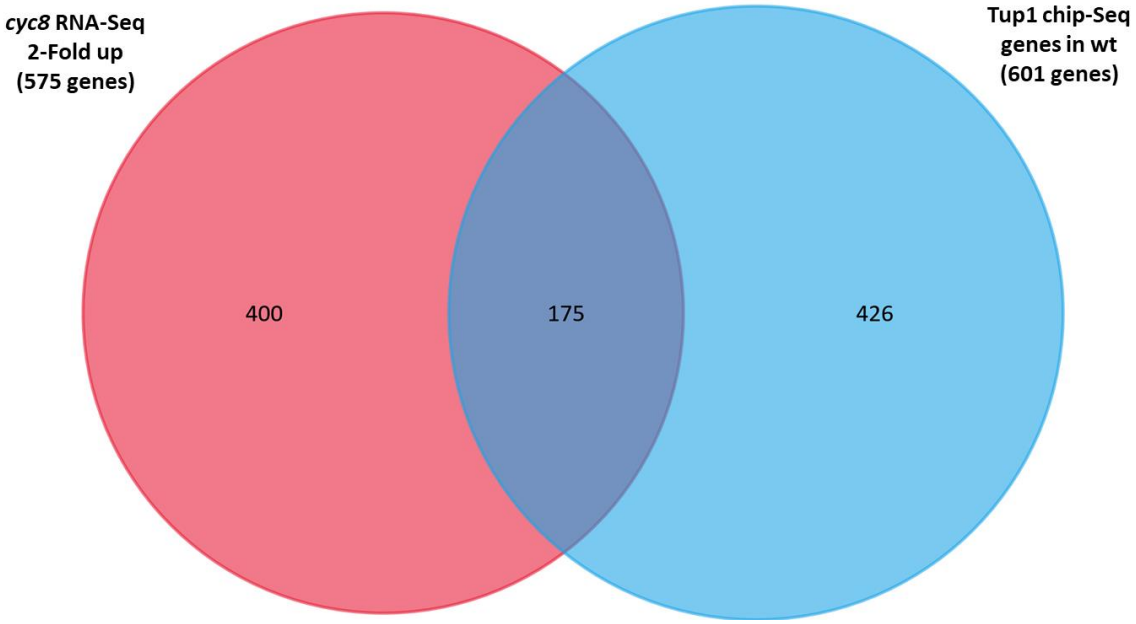

Figure 6.9 Comparison between Tup1 occupancy and genes up-regulated in a *cyc8* mutant. Venn diagram to show 175 genes up-regulated at least 2-fold in a *cyc8* mutant were associated with a site of Tup1 occupancy. Fun rich software was used to perform the Venn diagram (M. Pathan *et al*. 2015).

Tup1 occupancy at repressed genes (number of sites)			
Tup1 in wt	**Promoter**	**Open reading frame**	**Intergenic region**
175	146	20	9

Table 6.7: Tup1 occupancy sites at repressed genes: The number of the Tup1 peaks position within promoters, open reading frames (ORF) or downstream intergenic regions is indicated.

Gene	Description	wt vs *cyc8* fold change up	Tup1 occupancy (Peak score)	Distance from TSS (bp)	Position
PAU5	Seripauperin-5	907.31	3419	612	intergenic
HXT13	Hexose transporter	720.47	5838.5	-458	promoter
RCK1	Serine/threonine-protein kinase	244.15	6909.4	-611	promoter
TIR2	Cold shock-induced protein	202	2427.4	-648	promoter
DSF1	Mannitol dehydrogenase	197.17	5600.5	-684	promoter
YMR279C	Uncharacterized protein	188.37	1507.2	-339	promoter
PUT4	Proline-specific permease	117.67	12597.2	-491	promoter
IMA2	Oligo-1,6-glucosidase	102.93	13596.7	-407	promoter
TIR1	Cold shock-induced protein	92.45	4267.8	-402	promoter
FLO9	Flocculation protein	90.37	20077.8	-753	promoter
YFL051C	Uncharacterized membrane protein	83.37	10614	-738	promoter
IMA1	Oligo-1,6-glucosidase	77.94	4037.8	-401	promoter
HBN1	Putative nitroreductase	68.52	1126.4	-180	promoter
AQY1	Aquaporin-1	66.54	7409.2	-662	promoter
GAT4	Protein involved in spore wall assembly	61.12	1729.3	-216	promoter
YHR022C	Uncharacterized protein	59.03	4664.4	-468	promoter
SET4	SET domain-containing protein	57.76	1554.8	-923	promoter
PRR2	Serine/threonine-protein kinase	50.89	3125.5	-414	promoter
YML131W	Uncharacterized membrane protein	42.68	539.4	-183	promoter
YBR201C-A	Putative uncharacterized protein	41.46	2744.7	-323	promoter
TDA8	Topoisomerase I damage affected	38.72	1245.4	-1092	promoter
FRE4	Ferric reductase	32.29	17126.8	-486	promoter
GAP1	General amino-acid permease	22.59	2689.2	-766	promoter
ENA1	Sodium transport ATPase	22.55	9535.1	-634	promoter
HSP26	Heat shock protein	22.24	2054.6	-527	promoter
HXT2	High-affinity glucose transporter	19.07	6885.6	-459	promoter
YPL277C	Uncharacterized protein	17.95	1055.1	-176	promoter
HSP31	Glutathione-independent glyoxalase	17.84	896.4	-407	promoter
SPO20	Sporulation-specific protein	15.69	17507.6	-815	promoter
FLO5	Flocculation protein	14.74	2951	-462	promoter
YER053C-A	Uncharacterized protein	14.55	1475.5	-570	promoter
SMP1	Transcription factor	14.12	1626.2	-340	promoter
YOR389W	Uncharacterized protein	13.76	539.4	-156	promoter

Gene	Description	wt vs *cyc8* fold change up	Tup1 occupancy (Peak score)	Distance from TSS (bp)	Position
FLO10	Flocculation protein	13.73	5989.2	-874	promoter
SUT1	Sterol uptake protein	13.73	2705.1	-727	promoter
PHO89	Phosphate permease	13.26	2760.6	-517	promoter
HXT6	High-affinity hexose transporter	13.18	13017.6	-476	promoter
YAL064W	Putative uncharacterized protein	12.58	1911.8	-506	promoter
CWP1	Cell wall protein	11.68	4378.9	-429	promoter
JEN1	Carboxylic acid transporter	11.05	610.8	-639	promoter
IME1	Meiosis-inducing protein	11.02	22410	-874	promoter
PAU3	Seripauperin-3	10.22	483.9	608	intergenic
FSH1	Family of serine hydrolases	10.06	3506.3	-255	promoter
TDA6	Putative vacuolar protein	9.65	3442.8	-325	promoter
GAC1	Serine/threonine-protein phosphatase	9.5	18911.6	-987	promoter
YMR206W	Uncharacterized protein	9.43	880.5	-559	promoter
YOL085C	Uncharacterized protein	9.42	4045.7	143	ORF
YAP6	AP-1-like transcription factor	9.3	12264	-522	promoter
NRG1	Transcriptional regulator	9.22	7853.4	-438	promoter
NCA3	Beta-glucosidase-like protein	9	2062.5	-668	promoter

Table 6.8: The top 50 genes showing Tup1 occupancy which are up-regulated in *cyc8* mutant: Table represents the top 50 set of genes which were up regulated in a *cyc8* mutant at which Tup1 was detected by ChIP-Seq. The red colour gradient indicates the level of fold increase in transcription in the *cyc8* mutant compared to wt; the second column red colour gradient indicates the peak score of each gene, with the most red indicating the greatest peak score which indicates the greatest Tup1 occupancy. The distance of the Tup1 ChIP signal relative to the nearest gene transcription start site (TSS, +1) was also represented (in base-pairs (bp)). The position of the peaks within promoters, open reading frames (ORF) or downstream intergenic regions is indicated and added to the table.

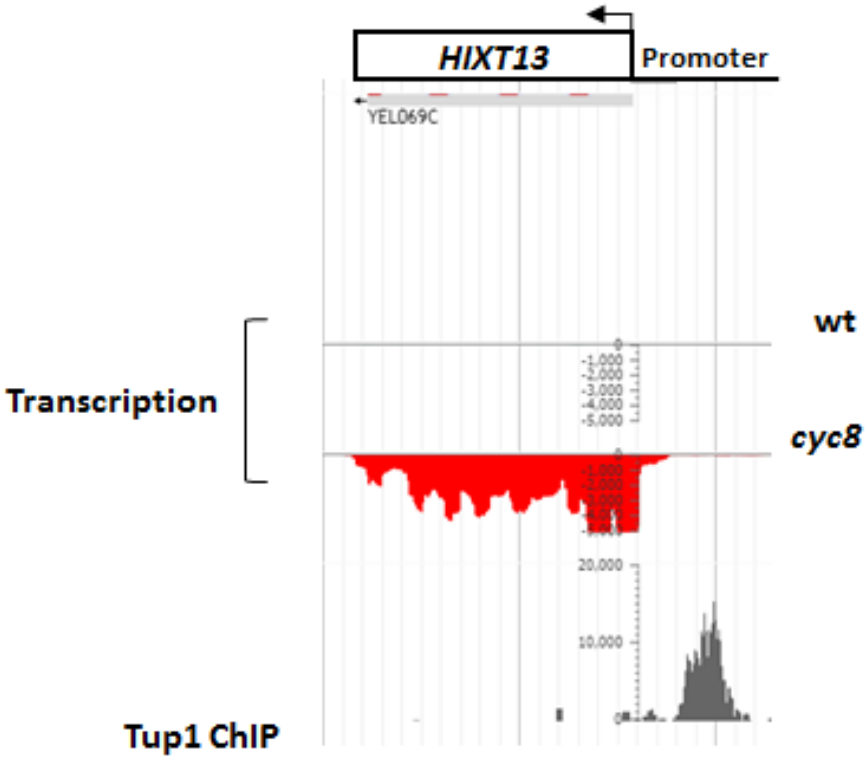

Figure 6.10 Tup1 occupancy and transcription at a gene up-regulated in *cyc8* mutant. *HIXT13* (*YEL069C*) gene as an example for up-regulated genes in *cyc8.* The transcription level was off in wt while was highly derepressed when *cyc8* was deleted. The Tup1 localization peak is shown.

6.2.2.2 Chromosomal location of Tup1 occupancy sites at genes up regulated in a *cyc8* mutant:

I next analysed the genomic location of the 175 Tup1 occupancy sites found at genes which are de-repressed in the *cyc8* mutant and which should represent those genes repressed by Tup1-Cyc8.

The results showed that these sites of occupancy were spread over all of the yeast chromosomes, with 30 sites (17% of Tup1 sites) residing within sub-telomeric regions whilst the remaining sites were located in various regions along chromosomes out with the sub telomeric regions. The majority of the subtelomeric genes associated with Tup1 were involved in carbohydrate transport like the *HXT13* and *MAL32* genes which encode a hexose transporter and maltase enzyme respectively. Other subtelomeric genes included the *FLO9* and *FLO10* flocculin encoding genes. Other stress response genes notable as having Tup1 associated with them were located at non sub telomeric regions such as the *RCK1* gene which is involved in oxidative stress response (Fig. 6.11).

Thus, although Tup1 can be found associated with many types of genes across all the chromosomes, there is an enrichment of Tup1 in the sub telomeric regions at genes involved in sugar uptake and utilisation and stress responses such as flocculation. Indeed, 30% of the genes de-repressed in a *cyc8* mutant and which contain Tup1 in their locale were found within subtelomeric regions which comprise only 7% of the total yeast genome. Furthermore, many of these subtelomeric genes which had Tup1 sites were highly de-repressed in the absence of Cyc8.

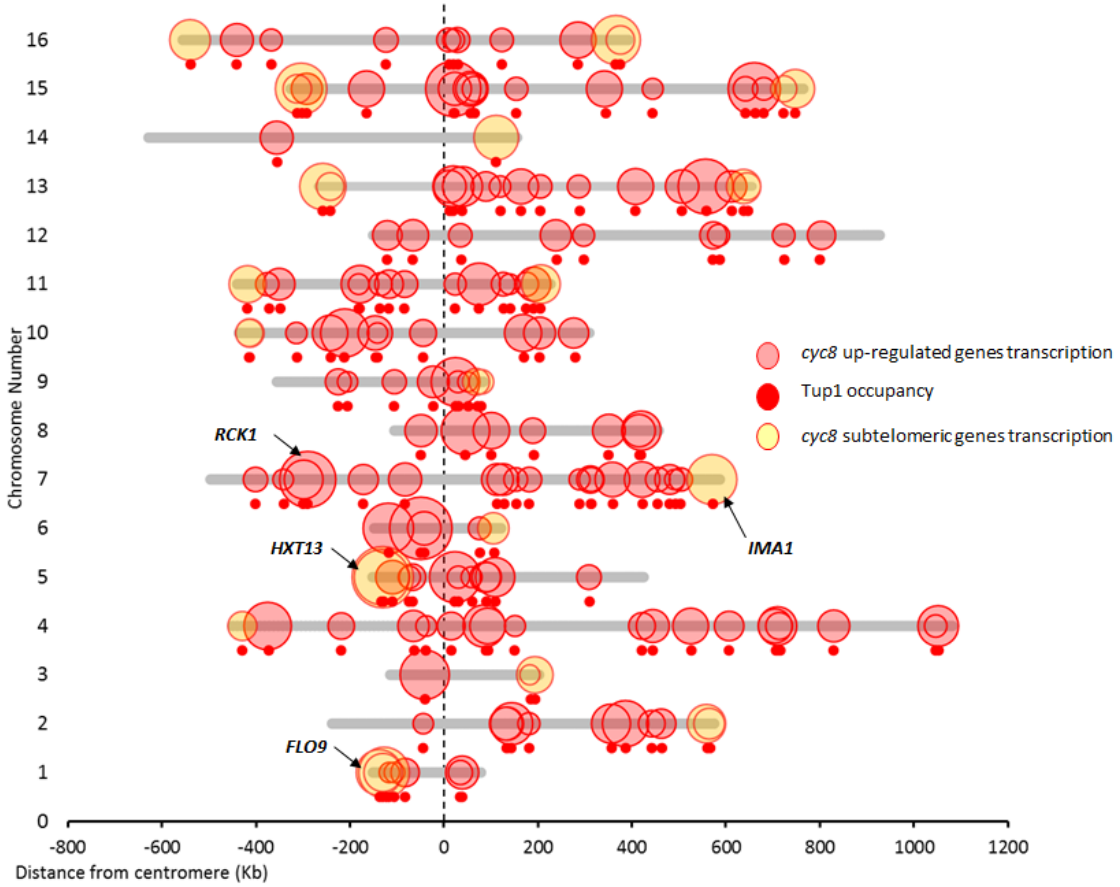

Figure 6.11 Tup1 occupancy at genes de-repressed in a *cyc8* mutant. 'Bubble' plot showing the location and the de-repression of transcription of the 175 genes at least 2-fold change up regulated in a *cyc8* deletion mutant. The data of each chromosome and gene were provided from *Saccharomyces* genome database (SGD) (Cherry *et al*. 1998). All 16 chromosome centromeres were set at zero and the chromosome size and gene positions were normalized according to that. Each lane reflects the chromosome number and size. The positions of the genes were reflected by the red circle position and the size of the circle reflects the level of gene transcription. The dark red circle under the chromosome indicates the location of Tup1.

6.2.2.3 The relation between the distance of Tup1 occupancy from the transcription start site and gene de-repression in a *cyc8* mutant:

I next investigated whether there was any relationship between the level of de-repression in the *cyc8* mutant and the position of the Tup1 occupancy site relative to the TSS. Specifically, I wanted to know whether there was evidence for the distance of Tup1 occupancy relative to the TSS having an impact upon the level of gene repression exerted by Tup1(-Cyc8). To analyse this the transcription data (fold up) in the *cyc8* mutant was plotted against the distance of Tup1 occupancy from the associated gene transcription start site (TSS) (Fig. 6.12). The results showed that the majority of the Tup1 occupancy sites were located around -500 from the TSS and that these genes showed the highest de-repression in a *cyc8* mutant. The two genes at which the distance of Tup1 from TSS region was greatest were the *CTT1* gene, whereby Tup1 was located -2902bp upstream from the TSS and *MGA1* which had Tup1 located 1869 bp downstream from the TSS. De-repression at these genes in the absence of *cyc8* was similarly low; 2.63 -fold for *CTT1* and 2.4-fold for *MGA1*. Indeed, the data suggests that the optimum site for Tup1 repression is when Tup1 is located around -500 bp upstream of the TSS, and that the repressive effect of Tup1 tapers off the further up or downstream Tup1 is from this site. An aberration from this observation is seen at the *PAU5* gene whereby Tup1 is located 612 bp downstream from the TSS, and 244 bp downstream of the gene itself, and is de-repressed in the absence of Cyc8 to a similarly high extent as the *HXT13* gene which shows the highest de-repression of all genes (Fig. 6.12). Finally, there seemed no difference upon this relationship whether the genes in question were located in or out with subtelomeric regions.

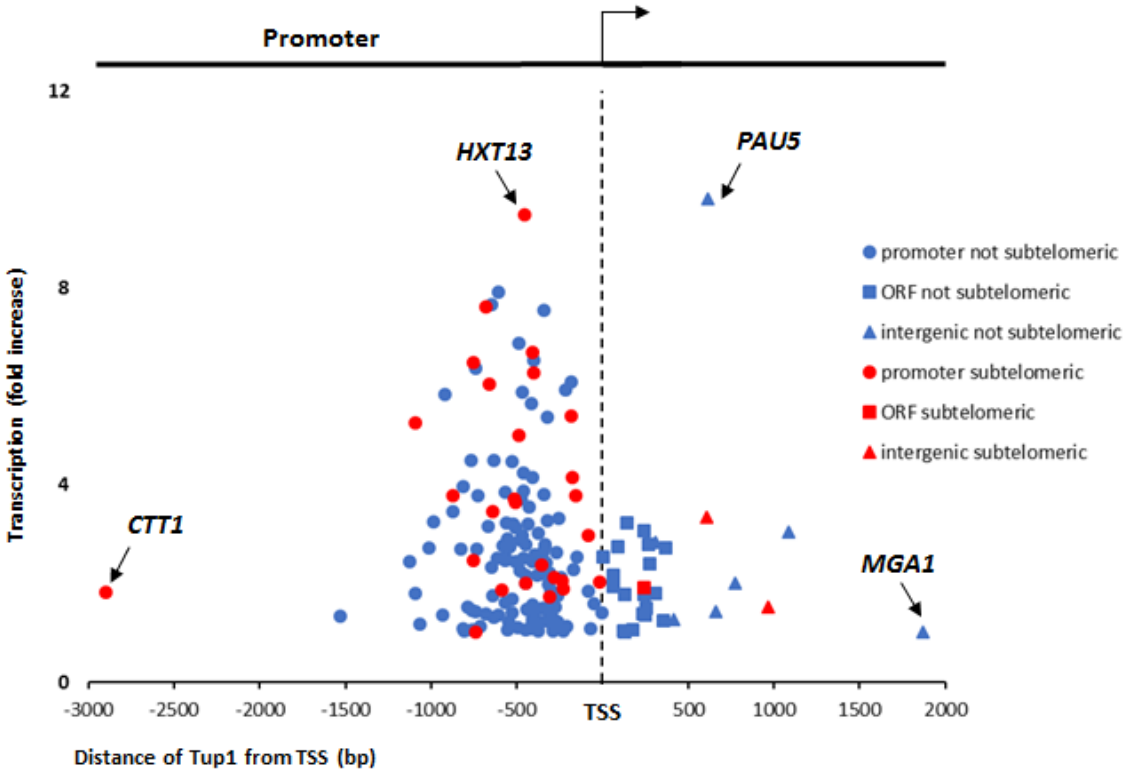

Figure 6.12 The relationship between gene de-repression in a *cyc8* mutant and the distance of Tup1 from the TSS. The transcription fold up-regulation of genes in a *cyc8* mutant were plotted against the distance of Tup1 occupancy from the transcription start site (TSS). Two chromosomal regions were identified, non subtelomeric genes in blue and subtelomeric genes in red. Three occupancy categories were defined under the two regions in Tup1 occupancy were located in promoters, open reding frames (ORF) and intergenic.

6.2.2.4 Comparing Tup1 occupancy with genes down-regulated in a *cyc8* deletion mutant:

We identified that 158 genes were down-regulated at least 2-fold in a *cyc8* mutant, suggesting that Tup1-Cyc8 acts as an activator at these genes.

I therefore repeated the previous analyses at these genes to determine if Tup1 could be found at these genes, and if so, where was it located relative to the transcription start site. I first compared the 158 genes that were down-regulated in *cyc8* at least 2-fold with the 601 Tup1 occupancy sites detected by ChIP-Seq. The result showed that only 20 down-regulated genes showed Tup1 being present (Fig. 6.13). Here, Tup1 was found at 17 promoters, no open reading frame or intergenic region and 2 genes in exon.

Most of the 20 genes encoded proteins displaying catalytic or transport activity including the *DIP5* gene, which had the greatest fold increase in transcription in the *cyc8* mutant and which is an amino acid transporter. Similarly, *AGP3* and *CAR2* genes encode amino acid permeases whilst *GAL2* encodes a galactose permease involved in galactose uptake. The *PHO5* acid phosphatase gene, which is another classically studied gene subject to chromatin mediated regulation of transcription, was also in this cohort of genes (Korber & Hörz, 2004; Lohr, 1997; Rando & Winston, 2012) (Table 6.8). Interestingly, although the *CYC8* gene was aberrantly included in this analysis due to the fact that the gene has been deleted, the data does clearly show a peak of Tup1 upstream of the *CYC8* ORF. Thus, there is evidence for Tup1 possibly directly promoting the transcription of a handful of metabolically important genes. Furthermore, Tup1 binds upstream of the *CYC8* gene raising the possibility of regulation of *CYC8* transcription by Tup1. The *DIP5* J-browse screen shot was included as an example of genes in this category (Fig. 6.14).

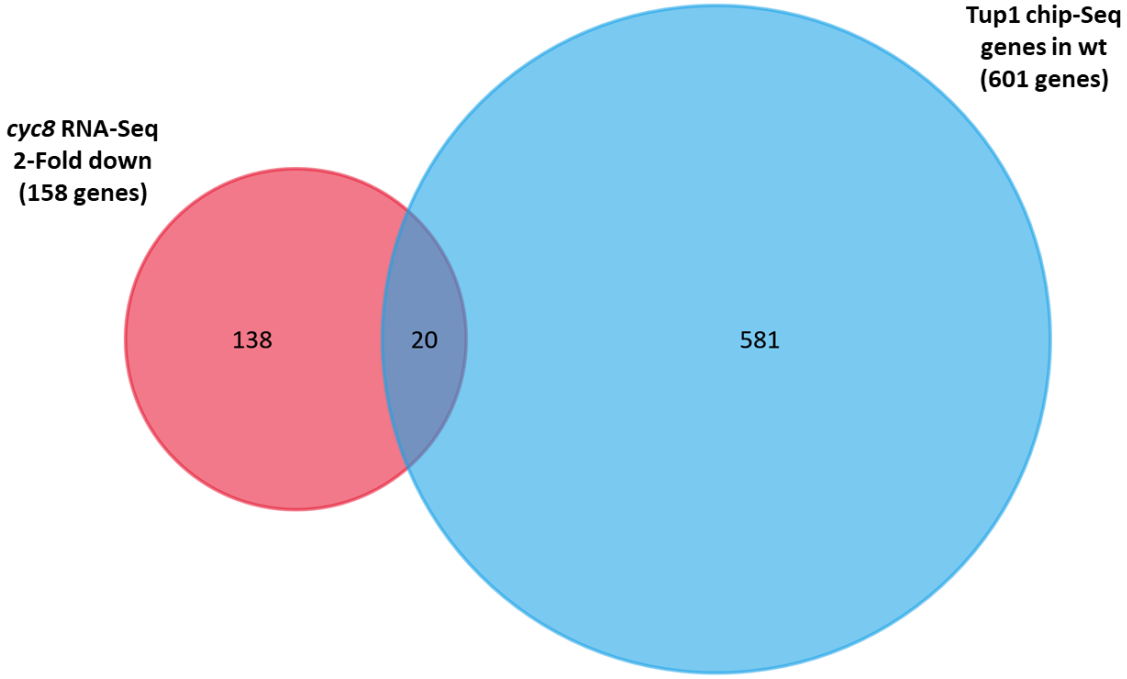

Figure 6.13 Comparison between Tup1 occupancy in genes down-regulated in a *cyc8* mutant. Venn diagram to show 20 genes down-regulated at least 2-fold change in a cyc8 mutant were associated with a site of Tup1 occupancy. Fun rich software was used to perform the Venn diagram.

Gene	Description	wt vs *cyc8* fold change	Peak score	Distance from TSS (bp)	Position
DIP5	Dicarboxylic amino acid permease	-27.98	4394.7	-620	promoter
PHO5	Repressible acid phosphatase	-17.41	777.4	-219	promoter
NDJ1	Putative cystathionine beta-lyase	-6.56	531.5	565	exon
HO	Homothallic switching endonuclease	-5.13	1499.3	-1959	promoter
BAT2	aminotransferase	-3.37	2348.1	-338	promoter
ALD5	Aldehyde dehydrogenase	-3.33	944	-300	promoter
CAR2	Ornithine aminotransferase	-2.92	912.3	-230	promoter
HIS4	Histidine biosynthesis	-2.76	721.9	1038	exon
IRC15	Microtubule associated protein	-2.67	713.9	-189	promoter
VHR2	Alpha-factor-transporting ATPase	-2.6	1015.4	-582	promoter
IRC7	Beta-lyase	-2.59	745.7	-594	promoter
PDR5	ATP-transporter protein	-2.56	3664.9	-509	promoter
ATG41	Autophagy-related protein	-2.35	793.3	-382	promoter
CYC8	General transcriptional corepressor	-2.35*	2157.7	-659	promoter
AGP3	General amino acid permease	-2.26	4593.1	2647	intergenic
BNA1	3-hydroxyanthranilate 3,4-dioxygenase	-2.15	372.8	-119	promoter
STE6	ATP-transporter protein	-2.14	856.7	-153	promoter
GAL2	Galactose transporter	-2.11	1420	-302	promoter
YCR022C	Uncharacterized protein	-2.01	4220.2	145	promoter
VTC5	Vacuoler transport chaperone complex	-2	6076.5	-662	promoter

Table 6.9: The 20 genes showing Tup1 occupancy which are down-regulated in a *cyc8* mutant: The table represents the set of genes which were down regulated in a *cyc8* mutant at which Tup1 was detected by ChIP-Seq. The blue colour gradient indicates the level of fold decrease in transcription in the *cyc8* mutant compared to wt; the red colour gradient indicates the peak score of each gene, with the most red indicating the greatest peak score which indicates the greatest Tup1 occupancy. The distance of the Tup1 ChIP signal relative to the nearest gene transcription start site (TSS, +1) was also represented (in base-pairs (bp)). The position of the peaks within promoters, open reading frames (ORF) or downstream intergenic regions is indicated.

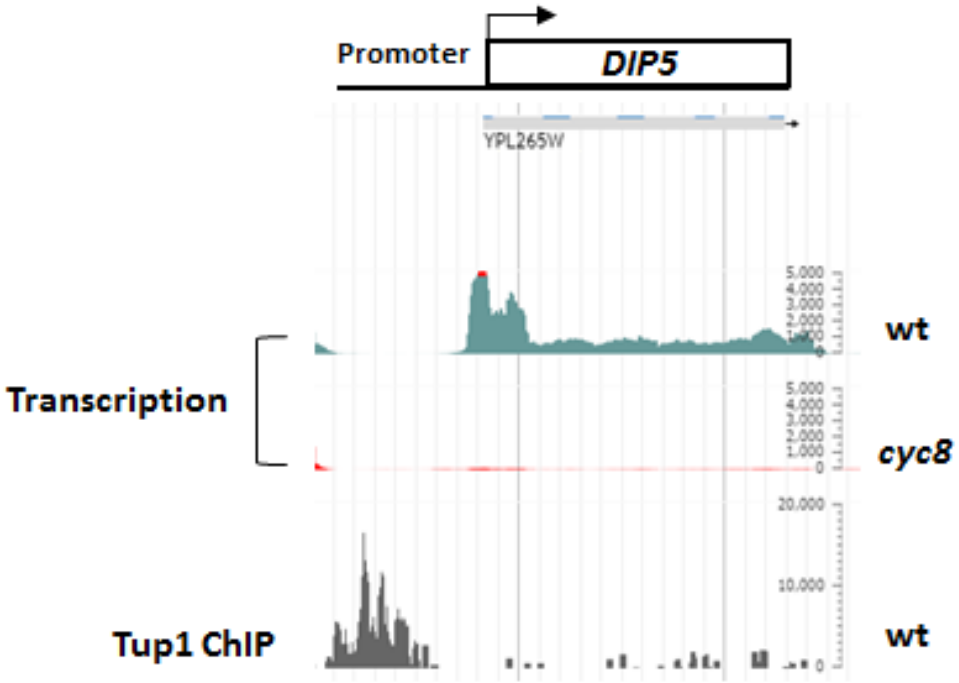

Figure 6.14 J-browse screen shot for a gene at which Cyc8 may act as an activator. Screen shot of the *DIP5* gene (YPL265w) as an example of a down-regulated gene in the *cyc8* mutant. The Tup1 localization peak was also shown.

6.2.2.5 Comparing Tup1 occupancy with gene transcription profiles of genes up regulated in a *cyc8* deletion mutant:

I next compared the genome wide occupancy of Tup1 with the fold change in transcription of the 20 genes down-regulated (> 2-fold) in the *cyc8* mutant. These genes represent the genes at which Tup1 might be directly acting as an activator of transcription.

The results showed that there was no obvious pattern of localisation of these genes on the yeast genome that correlated with gene transcription in the *cyc8* mutant. Indeed, the genes were found on 10 of the 16 chromosomes at various regions along the chromosomes, and the two genes showing the greatest decrease in transcription, *DIP5* and *PHO5*, were found flanking a sub-telomeric region and nearer the centromere, respectively. Only two of the genes (*AGP3* and *IRC7*) were located in the sub-telomere. Interestingly, both of these genes were located on chromosome 6 (Fig. 6.15), and neither showed a large drop in transcription in the *cyc8* mutant.

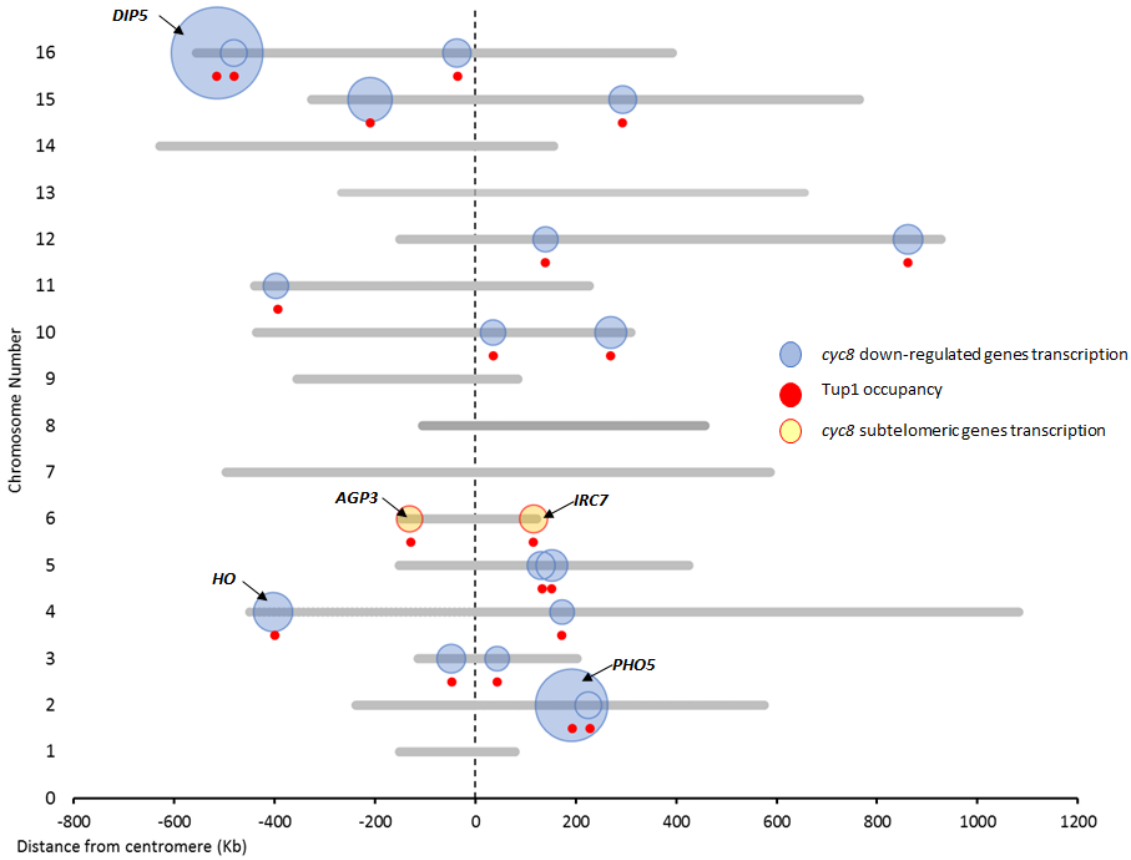

Figure 6.15 Location and level of genes down-regulated in a *cyc8* mutant which show Tup1 occupancy. 'Bubble' plot showing the location and the change in transcription of the 20 genes at least 2-fold change down-regulated in a *cyc8* deletion mutant. The data of each chromosome and gene were provided from *Saccharomyces* genome database (SGD) (Cherry *et al*. 1998). All the 16 chromosomes centromere were set in zero and the chromosomes size and genes position were normalized according to that. Each lane reflects the chromosome number and size, the position of the genes was reflected by the circle position and the size of the circle reflects the level of gene transcription. The dark red circle indicates the location of Tup1 in the chromosome for each gene.

6.2.2.6 The relationship between the distance of Tup1 occupancy from the transcription start site and gene activation in a *cyc8* mutant:

I next investigated whether there was any relationship between the decrease in transcription in the *cyc8* mutant and the position of the Tup1 occupancy site relative to the TSS.

To address this, the transcription data (fold down) in *cyc8* were plotted against the distance of Tup1 occupancy from the transcription start site (TSS) (Fig. 6.16). The results showed that most sites of Tup1 occupancy at the genes whose transcription was reduced in the absence of *cyc8* were located at the promoter, within 500 bp of the TSS, although 3 sites were located in the ORF and one site was positioned in the intergenic region downstream of the ORF. The greatest transcription decrease in the *cyc8* mutant was for the *DIP5* gene, which encodes an amino acid transporter, and where Tup1 was located 620 bp upstream of the TSS. Tup1 was located furthest away from the TSS at the *HO* gene which showed a 5-fold decrease in transcription in the *cyc8* mutant. Thus, for those genes at which Tup1 plays a positive role in transcription, Tup1 was generally located around 500 bp upstream of the TSS, and there was no correlation with distance of Tup1 relative to the TSS and the fold decrease in transcription in the absence of Cyc8 (Fig. 6.16).

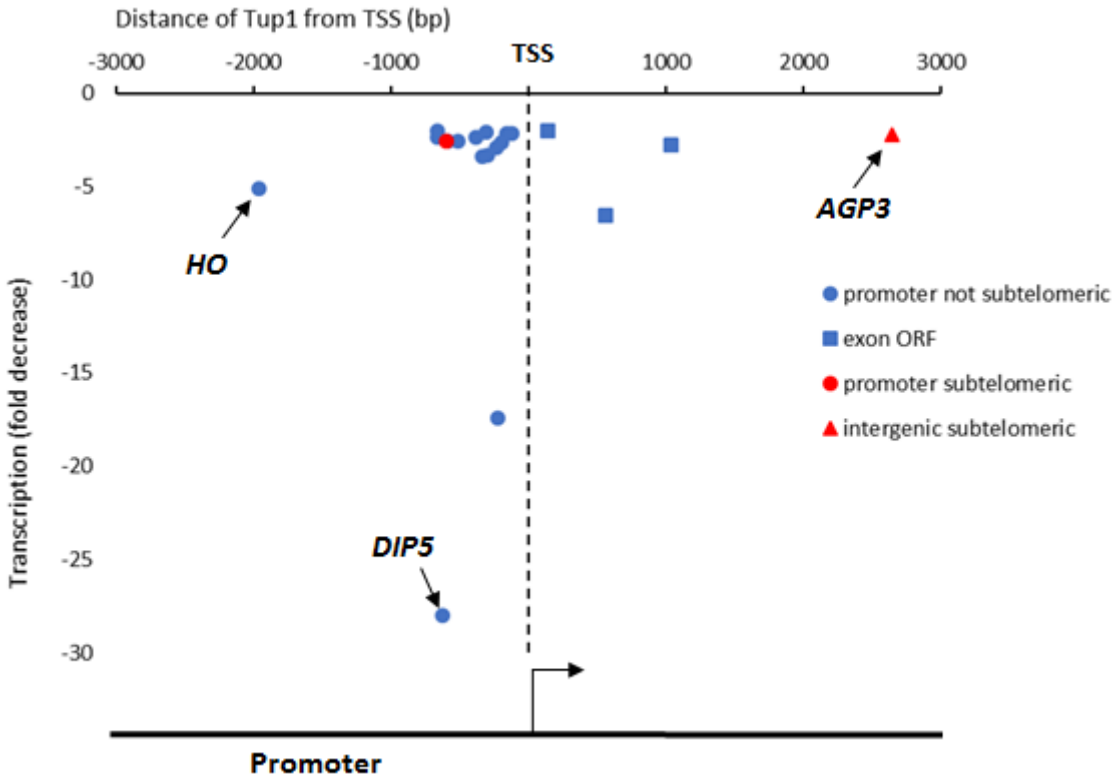

Figure 6.16 The relationship between the *cyc8* down-regulated transcription vs the Tup1-Cyc8 distance from TSS. the *cyc8* transcription down-regulated genes were plotted against the distance from the transcription start site (TSS) in scatter plot. Two chromosomal regions were identified, non subtelomeric genes in blue and subtelomeric genes in red. Three occupancy categories were defined under the two regions in Tup1 occupancy were located in promoters, open reding frames (ORF) and intergenic.

6.2.3 Analysis of Tup1 and Snf2 occupancy at Tup1-Cyc8 and Swi-Snf co-regulated genes:

I next wanted to analyse the sites of occupancy of the Snf2 protein in the presence and absence of Tup1 to identify any interplay between the two complexes. I therefore utilised the data generated by Wong and Struhl in which they analysed Snf2 occupancy by ChIP-Seq in a Tup1 anchor away strain (Wong & Struhl, 2011). Thus, I could assess the global Snf2 occupancy both before and after Tup1 was conditionally removed from the nucleus via the anchor away technique.

Specifically, I wanted to test two models for how the genes we had identified from the RNA-Seq analysis as being co-regulated by Tup1-Cyc8 as a repressor and Swi-Snf as an activator could be regulated. In model one, Snf2 could be recruited to the co-regulated gene promoters when Tup1 was absent. A prediction of this model would be that Snf2 would only occupy a gene region following the removal of Tup1 by anchor away.

An alternative model (Model 2) would be that Snf2 could already be present at Swi-Snf and Tup1-Cyc8 co-regulated genes whereby its activity is enhanced, or Snf2 would be further enriched, in the absence of Tup1. A prediction of this model would be that these co-regulated genes would have both Tup1 and Snf2 already present at the gene promoters prior to activation.

The raw data for this analysis was taken from NCBI accession number SRA044839.1 (Wong & Struhl, 2011). Dr. Karsten Hokamp retrieved and analysed the data to provide a list of Tup1 occupancy sites and Snf2 occupancy sites according to when Tup1 was present or absent. All subsequent analysis was performed by myself.

6.2.3.1 Identification of genes at which both Snf2 and Tup1 are present:

I first wanted to compare the occupancy sites of Tup1 and Snf2 in a wild type strain grown on YPD to determine if they occupied distinct sites or both proteins could be found at the same region. I therefore constructed a Venn diagram of the total Snf2 (142 genes) and Tup1 (601 genes) occupancy sites previously analysed (Fig. 6.17).

The data revealed that Snf2 occupied 37 sites distinct from Tup1 whilst Tup1 occupied 496 sites distinct from Snf2. Importantly Snf2 and Tup1 occupancy were both detected

at sites associated with a cohort of 105 genes suggesting a possible co-occupancy of these proteins at these genes.

The cohort of genes at which both Snf2 and Tup1 could be detected included genes of varying functions, the top 50 most occupied of which are shown in (Table 6.9). Genes of interest in this table include the cell wall protein encoding genes *FLO9* and *SED1*. Also included in this list of potentially co-occupied gene associated sites was the *CYC8* gene itself, suggesting a possible regulatory role upon *CYC8* transcription by the Swi-Snf and Tup-Cyc8 complexes (Fig. 6.18).

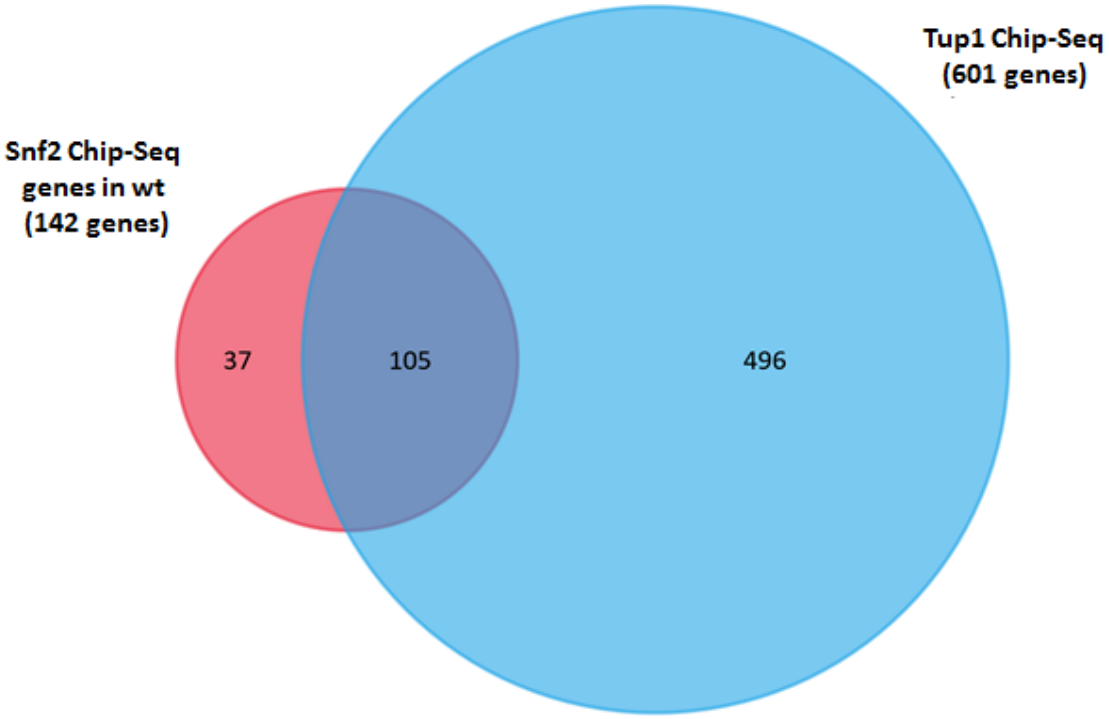

Figure 6.17 The binding profile of Tup1 and Snf2. Venn diagram to show genes where both Snf2 and Tup1 could be detected by ChIP-Seq. Snf2 ChIP-Seq data in wt and Tup1 ChIP-Seq data were obtained from Wong and Struhl, 2011. Fun rich software was used to prepare the Venn diagram (M. Pathan *et al*. 2015).

		Tup1 in wt		Snf2 in wt	
Gene	**Description**	**peak score**	**Distance from TSS (bp)**	**Peak score**	**Distance from TSS (bp)**
YHL041W	Uncharacterized protein	25495.8	-296	514.6	-297
YLR154C-G	Uncharacterized protein	22640	2435	34280.2	2713
FLO9	Flocculation protein	20077.8	-753	514.6	-663
YBL029C-A	Uncharacterized protein	19006.8	-565	1033.7	-575
GAC1	Serine/threonine-protein phosphatase	18911.6	-987	564.3	-970
SPO20	Sporulation-specific protein	17507.6	-815	2758.1	-821
GID8	Glucose-induced degradation protein	17404.4	-547	1209.8	-532
CMR3	Putative zinc finger protein	17396.5	-407	1074.4	-604
FRE4	Ferric reductase	17126.8	-486	379.2	-446
RPI1	Negative RAS protein regulator protein	15706.8	-905	911.9	-932
ZRT2	Zinc-regulated transporter	14397.9	-77	2202.9	-266
YOR029W	Uncharacterized protein	13866.4	279	880.3	252
MMO1	Uncharacterized protein	13834.7	-640	830.6	-648
YPR064W	Uncharacterized protein	13120.7	251	1665.7	223
PUT4	Proline-specific permease	12597.2	-491	1927.5	-436
YAP6	AP-1-like transcription factor	12264	-522	1024.7	-528
GTT1	Glutathione S-transferase	11700.8	-2902	577.8	-2848
SED1	Cell wall protein	11597.7	-812	1543.8	-874
HAP4	Transcriptional activator	10852	-1087	1688.3	-734
SUT2	Sterol uptake protein	10669.5	-297	952.5	-301
YFL051C	Uncharacterized membrane protein	10614	-738	546.2	-654
YIR018C-A	Uncharacterized protein	9519.3	-1067	1850.8	-1084
RRN5	transcription initiation factor	8741.9	548	938.9	613
MNN1	Alpha-1,3-mannosyltransferase	8646.7	-844	1015.7	-753
UTR2	Probable glycosidase	7964.5	-313	1579.9	-338
YLR112W	Uncharacterized protein	7726.5	57	2509.8	-142
VHR1	Transcription factor	7671	-759	1832.7	-744
GIC2	GTPase-interacting component	7663	-531	1137.6	-403
CUP9	Homeobox protein	7496.4	-1039	866.7	-1006
BRP1	Uncharacterized protein	7242.6	323	2342.8	278

		Tup1 in wt		Snf2 in wt	
Gene	**Description**	**peak score**	**Distance from TSS (bp)**	**Peak score**	**Distance from TSS (bp)**
WSC4	Cell wall integrity and stress response	7131.5	-367	681.6	-364
MOT3	Transcriptional activator/repressor	6385.9	-490	1638.6	-500
YKL097C	Uncharacterized protein	5965.4	176	2388	136
HXT3	Low-affinity glucose transporter	5838.5	-458	1160.1	-373
AAC1	ADP,ATP carrier protein	5711.6	-206	1300.1	-208
YDR010C	Uncharacterized protein	5640.2	63	1814.7	63
ZRT1	Zinc-regulated transporter	5537.1	-477	1223.3	-305
FKS1	1,3-beta-glucan synthase component	5140.4	-591	1169.2	-601
ENV9	Probable oxidoreductase	4775.5	-377	2193.9	-363
AMN1	Antagonist of mitotic exit network	4458.2	-553	898.3	-531
HOR7	Uncharacterized protein	4458.2	-338	1083.4	-339
RNH203	Ribonuclease H2 subunit C	4426.5	-295	1191.7	-1273
DIP5	Dicarboxylic amino acid permease	4394.7	-620	1512.2	-551
TYE7	Serine-rich protein	4267.8	-1278	1512.2	-874
TEC1	Ty transcription activator	3926.7	-416	1494.2	-471
COA2	Cytochrome c oxidase assembly factor	3918.8	-263	979.6	-256

Table 6.10: The top 50 genes at which both Snf2 and Tup1 were detected by ChIP-Seq: The table represents the top 50 genes where both Tup1 and Snf2 were detected by ChIP-Seq and ranked according to Tup1 peak scores. The red colour gradient indicates the relative increase of peak score for Tup1 and Snf2, with the most red correlating with the highest peak score (highest occupancy). The distance of each site of occupancy up- (negative values) or down- stream (positive values) from the nearest gene transcription start site (TSS) is indicated (in bp).

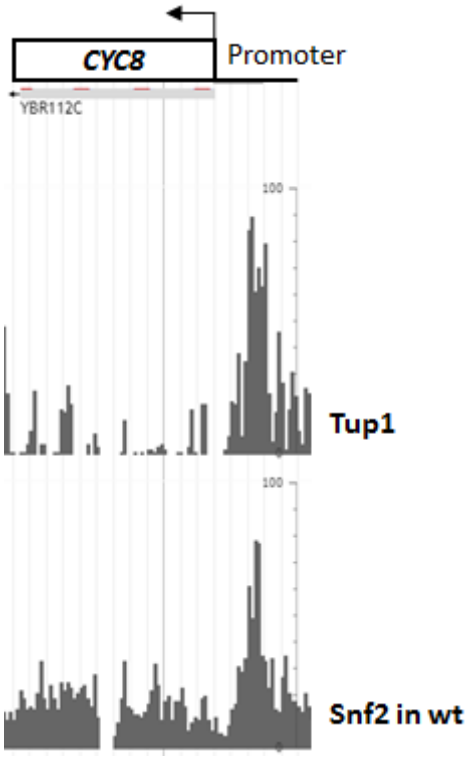

Figure 6.18 J-browse screen shot to show occupancy of both Tup1 and Snf2 at the *CYC8* gene promoter. Screen shot from J-browse to show the *CYC8* gene as an example of a gene where both Snf2 and Tup1 could be detected by ChIP-Seq in wt (no rapamycin; Tup1 present).

6.2.3.2 Analysis of the genes at which both Snf2 and Tup1 can be detected:

The Snf2 and Tup1 chip data revealed that Snf2 and Tup1 could both be detected at regions associated with a cohort of 105 genes. I therefore wanted to investigate the positioning of the proteins at these genes to determine how close together or far apart Snf2 and Tup1 were bound.

I first did a scatter plot to show the Tup1 and Snf2 occupancy sites at all of the 105 genes (Fig. 6.19 A). As can be seen, the sites for Tup1 and Snf2 at these gene regions showed a significant overlap in their average binding sites, which were predominantly located in the promoter at a site ~500 bp upstream of the ATG (scatter Fig 6.19 B). The two notable exceptions to this were where Tup1 and Snf2 bound almost 3 kb upstream of the *GTT1* transcription start site and bound ~ 2.2 Kb downstream of the transcription stop site of the *YLR154C-G* gene. Overall, there were 85 sites for Snf2 and Tup1 found at gene promoters, whilst 18 and 3 sites (*YLR154C*-G, *ILV5* and *CHA1*) were found in ORFs and downstream intergenic regions respectively (Fig. 6.19 C). Interestingly, at the *CHA1* gene Snf2 was found at the promoter -201 bp upstream from TSS, whilst Tup1 was found in the ORF/IG region at 1307 bp from TSS region or 224 bp downstream of the TTS. At *ILV5* gene Snf2 was found at the ORF at 591 bp from TSS, and Tup1 was found in the promoter at -354 bp also another peak was found in the ORF at 360 bp from TSS region (Fig. 6.19 B).

I next examined how close or how far apart the Snf2 and Tup1 proteins were bound at target genes (Fig. 6.20). The results showed that 10 genes had Tup1 and Snf2 located within 5 bp of each other's binding sites. However, the majority of Tup1 and Snf2 binding 44 occurred within 11 to 50 bp of each other (Fig. 20 A and B). Two genes, *CHA1* and *RNH203* were associated with Tup1 and Snf2 located over 500 bp apart. As described previously, at *CHA1*, Tup1 and Snf2 were located 1106 bp apart with Snf2 being located in the gene promoter and Tup1 being located after the transcription stop site. At the *RNH203* gene, Snf2 and Tup1 were located 278 bp apart. Tup1 was found located at two location -295 and -1253 bp upstream of the TSS, whilst Snf2 was located -241 bp upstream of the TSS (Fig. 6.20 C).

In summary, the putative co-occupancy of Tup1 and Snf2 at genes predominantly occurred in the promoter of target genes at a region -500 bp upstream of TSS and consisted of Tup1 and Snf2 being within 11-50 bp of each other at these genes.

A.

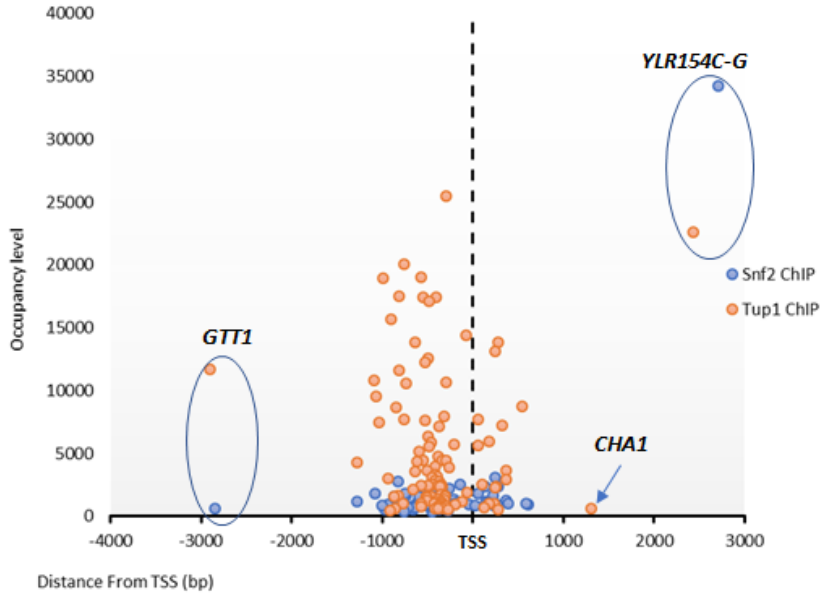

B.

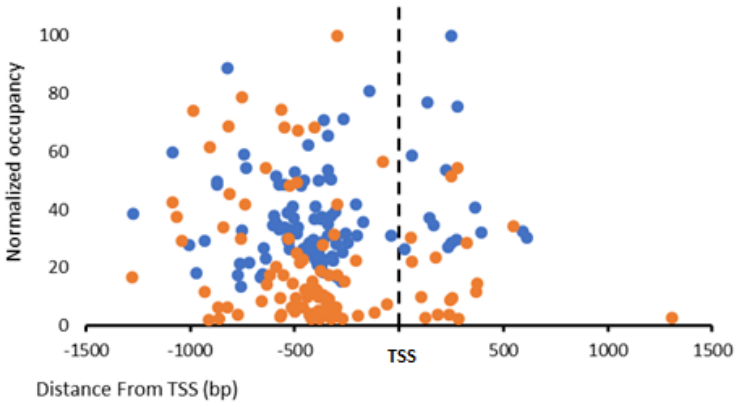

C.

Number of Tup1 and Snf2 co-occupaied sites				
Promoter	**ORF**	**Downstream IG region**	**Promoter plus ORF**	**Promoter plus IG**
84	18	*YLR152C-G*	*ILV5*	*CHA1*

Figure 6.19 The location of Tup1 and Snf2 occupancy at genes where both proteins could be detected. (A) the Tup1 and Snf2 distance from TSS region in (bp) were plotted against Tup1 and Snf2 peak score. (B) scatter plot shown in (A) except with *GTT1* and *YLR154C-G* data point removed and Tup1 and Snf2 ChIP data normalise to the value showing the highest occupancy (set in 100). (C) the number of Tup1 and Snf2 occupancy sites were listed in a table.

A.

Distance between Tup1 and Snf binding at gene regions (In base pairs)	Number of genes
0 - 5	10
5-10	11
11-50	44
51-100	18
101-250	15
251-500	5
Greater than 500	2

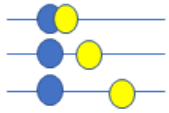

B.

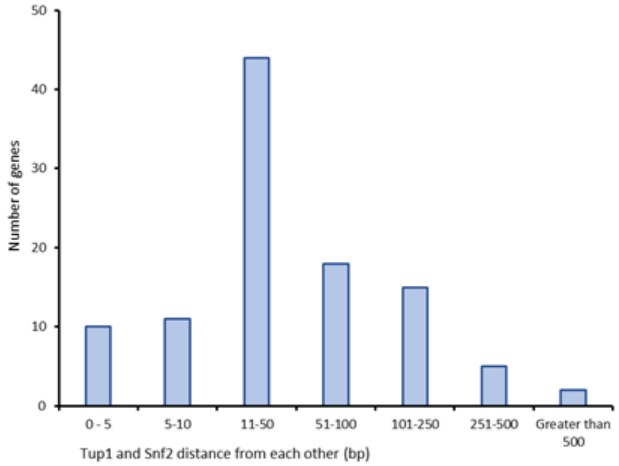

C.

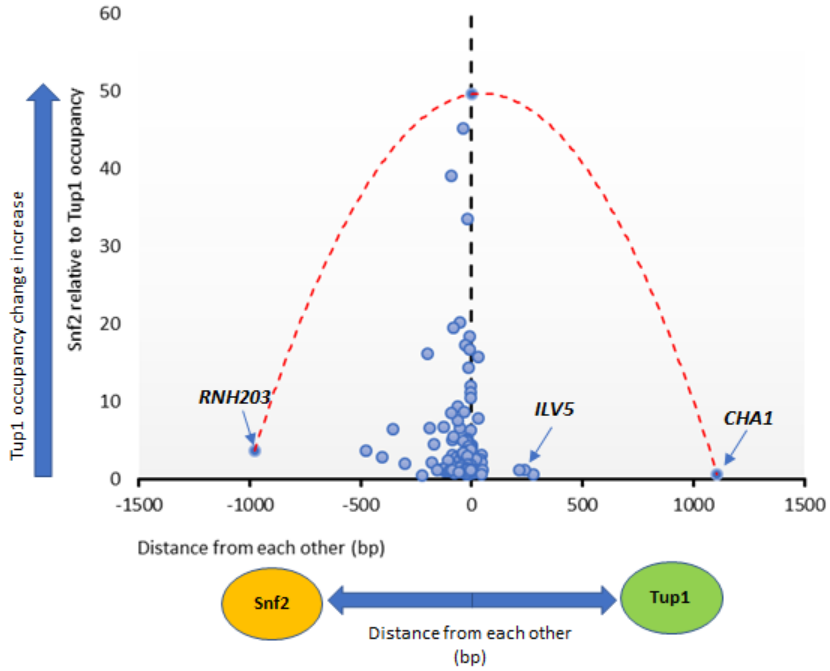

Figure 6.20 Distance of Tup1 and Snf2 from each other. The distance of Tup1 and Snf2 from each other in (bp) were listed in table (A) in 7 categories. These categories were plotted in column chart (B). (C) scatter plot showed the distance far of Snf2 and Tup1 from each other in (bp) (X) were plotted against the Snf2 relative occupancy to Tup1, the highest in (Y) showed the higher peak different between them.

6.2.4 Mapping global Snf2 occupancy in the absence of Tup1:

Having established the binding profiles of Tup1 and Snf2 in wt cells, I next wanted to analyse the sites of occupancy of the Snf2 protein in the absence of Tup1. I wanted to test the hypothesis that those genes we had identified from the RNA-Seq analysis as being co-regulated by Tup1-Cyc8 as a repressor and Swi-Snf as an activator would either (i) have Snf2 recruited to their promoters when Tup1 was absent (Model 1) or (ii) be further enriched for Snf2 occupancy at genes where Snf2 and Tup1 were already present (Model 2).

I therefore utilised the data generated by Wong and Struhl in which they analysed Snf2 occupancy by ChIP-Seq in a Tup1 anchor away strain. Thus, I could assess the global Snf2 occupancy both before and after Tup1 was conditionally removed from the nucleus via the anchor away technique (Wong & Struhl, 2011).

The raw data was taken from NCBI accession number SRA044839.1 (Wong & Struhl, 2011). Dr. Karsten Hokamp retrieved and analysed the data to provide a list of Snf2 occupancy sites according to when Tup1 was present or absent. All subsequent analysis was performed by myself.

The data showed that when Tup1 was removed from the nucleus, 250 sites were occupied by Snf2 which were located predominantly in gene promoters (216 genes) (Appendix II, Table S4), although 20 sites resided within open reading frames (ORFs), whilst 13 sites were located in intergenic regions downstream of ORFs.

6.2.4.1 Analysis of Swi-Snf occupancy sites in the absence of Tup1:

To investigate whether these 250 Snf2 occupancy sites represented recruitment of Snf2 to unique sites within the genome after Tup1 removal I compared the Snf2 ChIP-Seq data from before anchor away of Tup1 with the Snf2 occupancy profile after Tup1 was anchored away. The results showed loss of Snf2 occurred from 38 previously occupied sites, while 146 new sites became occupied by Snf2. Interestingly, 104 genes remained associated with Snf2 regardless of whether Tup1 was present or absent. Analysis of the occupancy levels at these sites revealed that Snf2 was slightly further enriched in the absence of Tup1 (Fig. 6.22).

Thus, Snf2 is bound to 142 sites in wt yeast when Tup1 is present. However, following the depletion of Tup1 by anchor away, only 38 of these Snf2 occupancy sites are lost, whilst Snf2 persists at 104 of these previously occupied sites at slightly higher levels. Importantly Snf2 is recruited to 146 new sites.

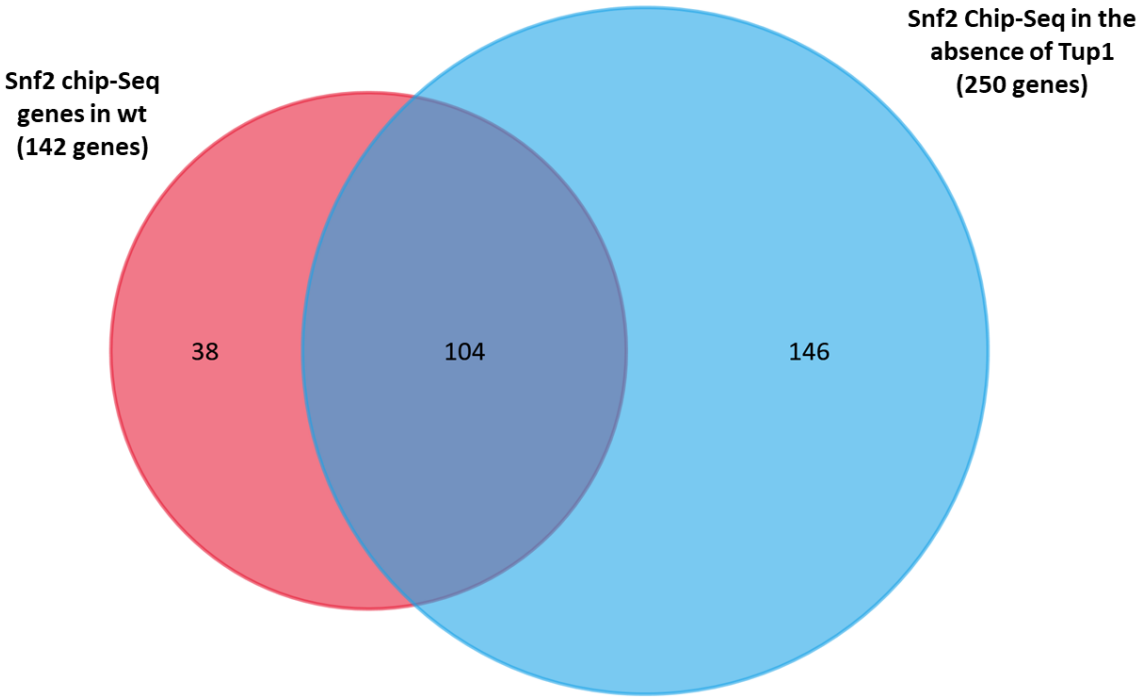

Figure 6.21 Comparison between Snf2 occupancy in the presence and absence of Tup1. Venn diagram to identify the genes specific of the Snf2 ChIP-Seq in the presence of and in the absence of Tup1. 38 genes were specific in Snf2 ChIP-Seq in wt while 146 genes were specific in Snf2 ChIP-Seq in the absence of Tup1. 104 genes were unaffected of the presence or absence of Tup1. Fun rich software was used to prepare the Venn diagram (M. Pathan *et al*. 2015).

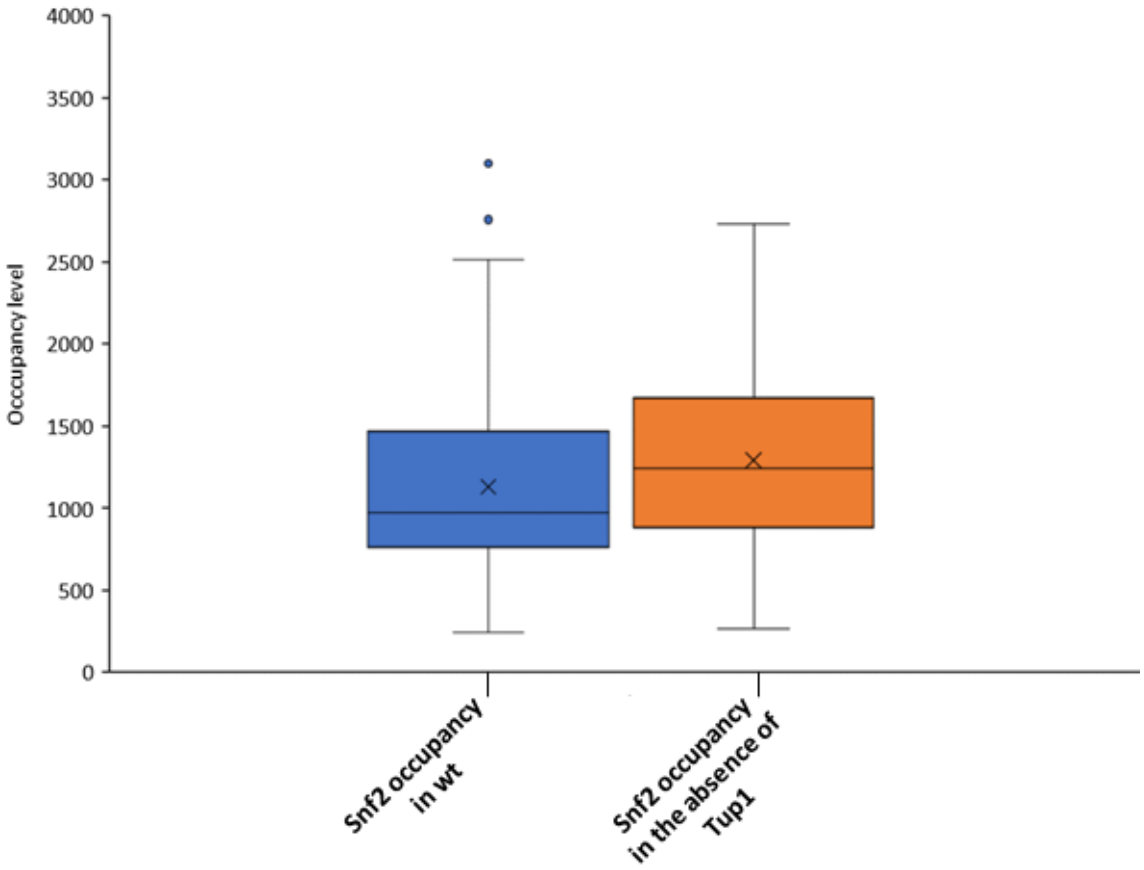

Figure 6.22 Snf2 occupancy levels in the presence and absence of Tup1 at sites where Snf2 persists. Sites at which the average peak score showing occupancy levels at the 104 sites were Snf2 is found in the presence (wt) and in the absence of Tup1 (Tup1-AA).

6.2.4.2 Tup1-Cyc8 and Swi-Snf co-regulated genes to which Snf2 is recruited in the absence of Tup1 (Model 1):

I next wanted to know whether after Tup1 anchor away, Snf2 went to the sites previously occupied by Tup1. This behaviour would be consistent with our proposed Model 1 regulation of Tup1-Cyc8 and Swi-Snf regulation of transcription. I therefore constructed a Venn diagram to compare the 146 unique sites to which Snf2 goes following Tup1 depletion with the 496 unique Tup1 binding sites (see Fig. 6.17). The results showed that Snf2 went to 102 new sites previously solely occupied by Tup1 (Fig. 6.23).

Our favoured model (Model 1) for how Swi-Snf and Tup1-Cyc8 co-regulate target genes involves such a recruitment event. Therefore, to test how many of the 102 co-regulated genes we had uncovered from the RNA-Seq analysis (see Fig. 5.33) showed evidence of Snf2 and Tup1 behaving in such a manner, these 102 co-regulated genes were compared to the 102 sites previously occupied by Tup1 to which Snf2 is recruited in its absence (Fig. 6.24).

The results showed that 17 genes fulfilled the criteria as being activated by Swi-Snf recruitment following the removal of the Tup1 repressor (Table 6.10). A screen shot from J-browse of the *FLO5* gene is shown as an example of a Swi-Snf and Tup1-Cyc8 co-regulated gene whereby Snf2 is recruited to the gene promoter in the absence of Tup1. This mutually exclusive behaviour of Tup1 and Snf2 is an example of the Model 1 type of Swi-Snf and Tup1-Cyc8 co-regulated genes (Fig. 6.25). Here we can see that only Tup1 can be detected in the wt strain which correlated with *FLO5* gene repression with no Snf2 sign detectable. However, in the absence of Tup1 following its anchor away, Snf2 can now be detected at the *FLO5* promoter of the active gene. Interestingly, the site of Snf2 occupancy at the active gene promoter almost exactly overlaps with the previous site of occupancy of Tup1. This might suggest a mechanism at these genes where Tup1 occupancy physically occludes Snf2 from binding.

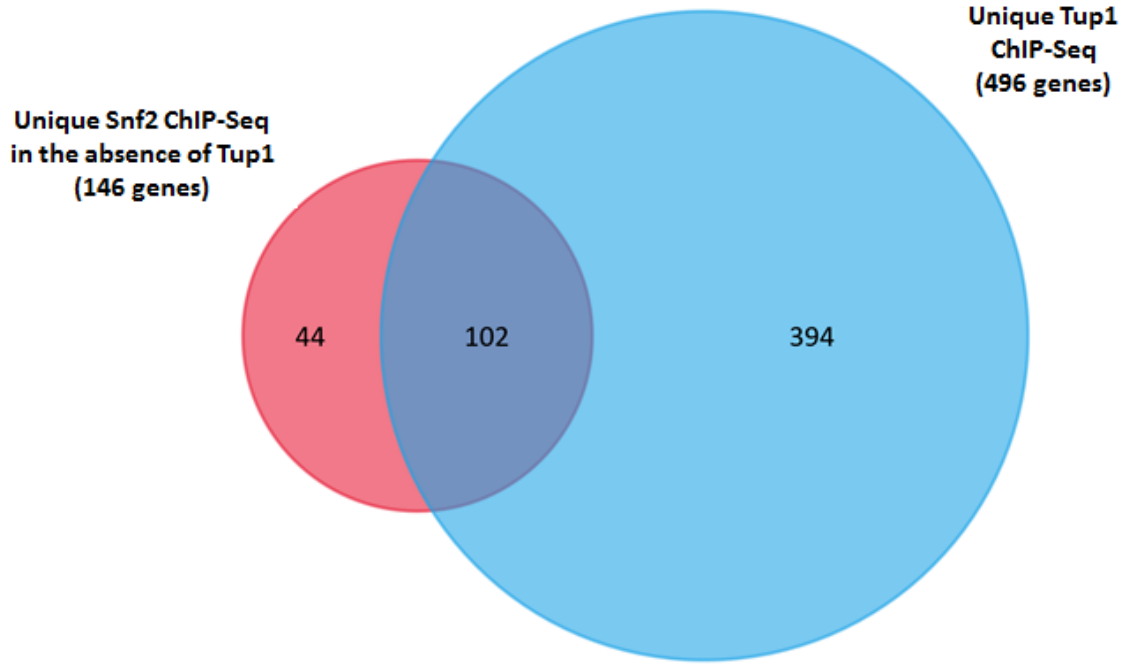

Figure 6.23 Snf2 recruitment to sites previously uniquely occupied by Tup1 following Tup1 anchor away. Venn diagram to show 102 genes. Identification the different of direct effected genes by Swi-Snf. Fun rich software was used to perform the Venn diagram (M. Pathan *et al*. 2015).

.

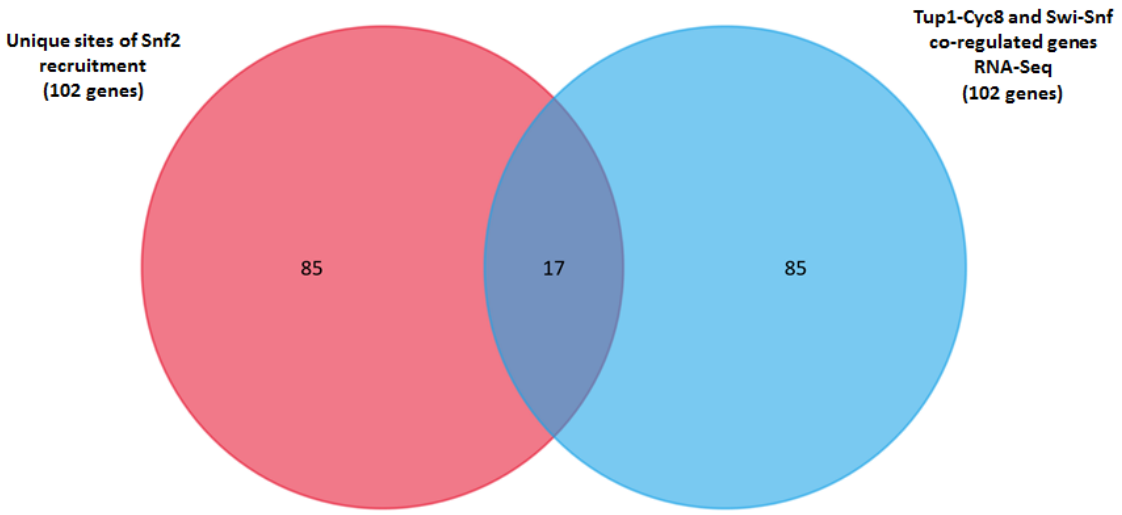

Figure 6.24 Identifying Swi-Snf and Tup1-Cyc8 co-regulated genes to which Snf2 is recruited in the absence of Tup1 (Model 1). Venn diagram to show 17 overlapped genes were directly co-regulated by Tup1-Cyc8 and Swi-Snf. Fun rich software was used to perform the Venn diagram (M. Pathan *et al*. 2015).

			Snf2 occupancy in the absence of Tup1				Tup1 occupancy			
Gene	Description	*cyc8* vs *snf2 cyc8* Fold change	start	End	Peak Score	Distance from TSS	start	End	Peak Score	Distance from TSS
ACA1	ATF/CREB activator	-2.67	242066	242258	1797.3	-661	242028	242268	13977.5	-647
AQY1	Aquaporin, spore-specific water channel	-3.57	921027	921219	1497.1	-737	921078	921318	7409.2	-662
CIN5	AP-1-like transcription factor	-2.16	383007	383199	1742.7	1317	383216	383456	17007.8	1084
DSF1	Mannitol dehydrogenase, oxidoreductase	-7.35	18808	19000	1345.1	-685	18785	19025	5600.5	-684
FLO5	Flocculation protein	-7.54	524861	525053	1278.8	-435	524810	525050	2951	-462
HSP26	Heat shock protein	-22.56	381614	381806	1516.6	-320	381383	381623	2054.6	-527
HXT13	Hexose transporter	-57.88	23676	23868	1883.1	-541	23569	23809	5838.5	-458
IME1	Meiosis-inducing protein	-4.79	606416	606608	1746.6	-861	606405	606645	22410	-874
NCA3	Beta-glucosidase-like protein, mitochondrial	-5.66	195388	195580	596.5	-611	195421	195661	2062.5	-668
PAU5	Seripauperin-5	-34.67	98866	99058	1302.2	637	98867	99107	3419	612
PHO89	Phosphate permease	-4.87	798931	799123	666.7	-505	798919	799159	2760.6	-517
PRY1	Sterol binding protein	-4.78	291218	291410	963	-540	291122	291362	2911.3	-468
TDA8	Topoisomerase I damage affected protein	-2.66	14821	15013	600.4	-1174	14715	14955	1245.4	-1092
TIR1	Cold shock-induced protein	-2.51	174730	174922	1411.3	-422	174726	174966	4267.8	-402
TIR2	Cold shock-induced protein	-2.93	347683	347875	1052.7	-829	347478	347718	2427.4	-648
YCT1	High affinity cysteine transporter	-2.56	29607	29799	662.8	-406	29539	29779	1459.6	-450
YHR022C	Uncharacterized protein	-10.34	150679	150871	799.2	-430	150693	150933	4664.4	-468

Table 6.11: The Swi-Snf and Tup1-Cyc8 co-regulated genes (model 1): The table shows 17 co-regulated genes which Snf2 is recruited in the absence of Tup1. The blue colour gradient indicates the transcription fold decrease in *snf2 cyc8* double mutants vs *cyc8*. Tup1 occupancy and Snf2 occupancy in the absence of Tup1 was indicated in the table with red colour gradient indicting the occupancy peak score.

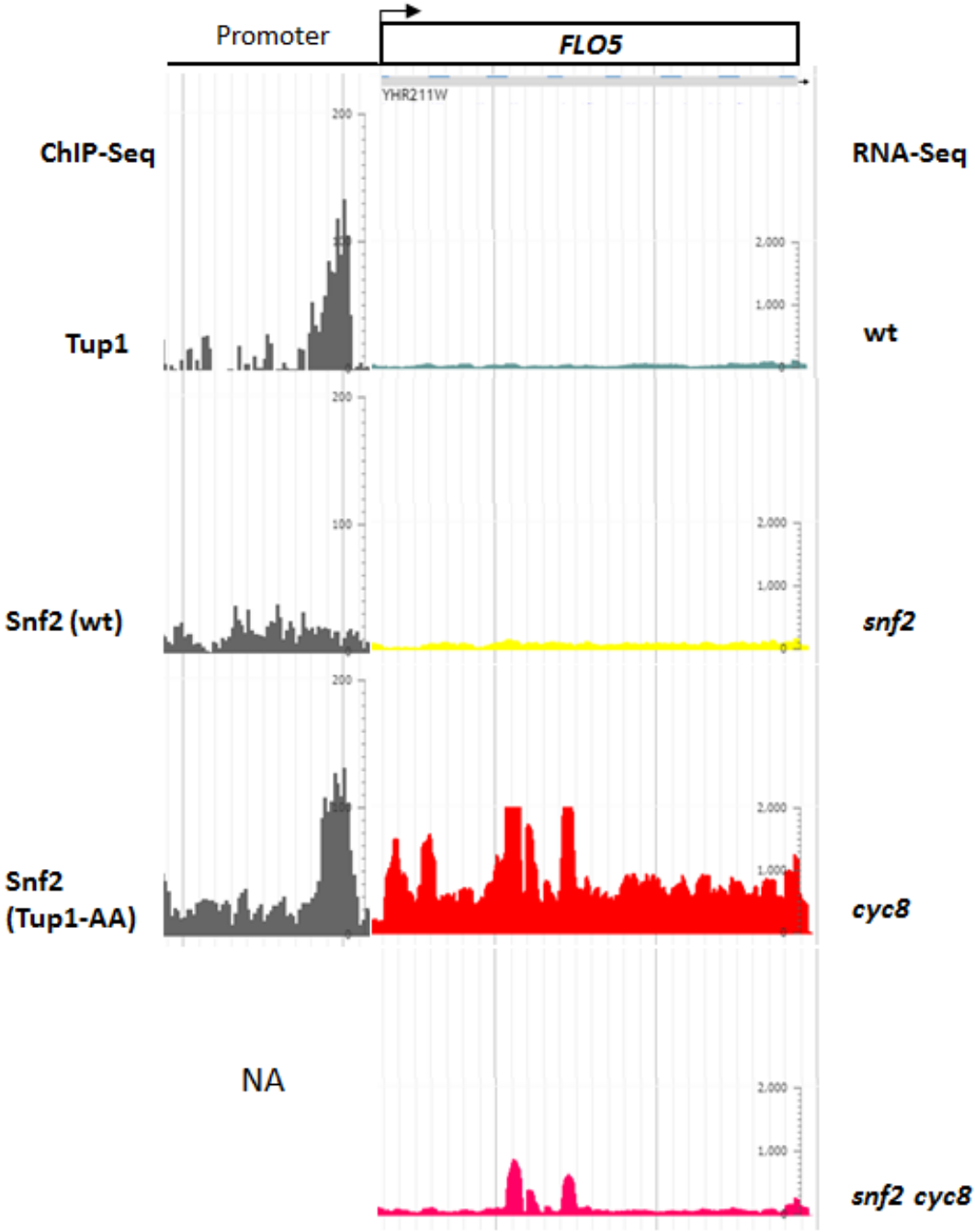

Figure 6.25 J-browse screen shot of the *FLO5* Swi-Snf and Tup1-Cyc8 co-regulated gene (Model 1) showing Tup1 and Snf2 occupancy during gene repression and activation. Screen shot from J-browse of *FLO5* gene as an example of a model 1 Swi-Snf and Tup1-Cyc8 co-regulated genes. RNA-Seq transcription data for wt, *snf2*, *cyc8* and *snf2 cyc8* mutants is shown (right side). ChIP-Seq data for Tup1 in wt and Snf2 in the presence of Tup1 (wt) and absence (Tup1-AA) is shown (lift side).

6.2.4.3 Tup1-Cyc8 and Swi-Snf co-regulated genes at which both Snf2 and Tup1 bind prior to activation (Model 2):

I next wanted to determine whether there was evidence that any of the 102 co-regulated genes that we had uncovered from the transcription analysis behaved as predicted in model 2. In this case, we would expect some of the co-regulated genes to have Tup1 and Snf2 already present at the repress gene, and that the Snf2 occupancy at these genes would persist or increase at these sites in the absence of Tup1 when the gene is derepressed.

I therefore prepared a Venn diagram of the 105 genes where Snf2 and Tup1 were both found to be present in wt (see Fig. 6.17) and the 102 co-regulated genes from the RNA-Seq analysis (see Fig. 5.33). The result showed that just 3 genes overlapped suggesting that these genes were subject to the model 2 type of co-regulation by Swi-Snf and Tup1-Cyc8 (Fig. 6.26).

Interestingly, two genes out of the three function in the cell wall (*FLO9* and *SED1),* whilst the third gene, *PDR15*, is involved in plasma membrane ATP binding (Table 6.11). The J-browse screen shot of the *FLO9* and *SED1* genes were given as examples of the genes co-regulated in this manner (Fig. 6.27 and 6.28), albeit with different transcriptional outputs.

In the wt strain, both Snf2 and Tup1 are detectable at the promoter of the repressed *FLO9* gene (Fig. 6.27). When Tup1 is anchored away, Snf2 is recruited to the *FLO9* promoter gene at levels 3-4-fold higher than before and there is a 90-fold increase in transcription in a *cyc8* mutant (Tup1-AA). In a *snf2 cyc8* double mutant, transcription is decreased 3-fold compared to the *cyc8* single mutant. Thus, at the *FLO9* gene Snf2 and Tup1 are acting to activate and repress the gene respectively, although both are present in wt when the gene is off. Snf2 levels are further enriched in the absence of Tup1, under which conditions the gene is activated.

This situation at *SED1* is different (Fig. 6.28). Here, both Snf2 and Tup1 are again present at the *SED1* promoter. However, under these wt conditions the gene is partially active. When Tup1 is removed via anchor away, Snf2 is slightly enriched at the *SED1* promoter and transcription in a *cyc8* mutant is increased 2.14-fold compared to levels in the wt.

In the *snf2 cyc8* double mutant, transcription is decreased -2.12-fold compared to the *cyc8* single mutant. Thus, although *snf2* and *cyc8* are showing positive and negative roles in transcription of *SED1* respectively, the gene is partially active even when Tup1 is present.

Importantly, Snf2 occupancy increases at all of these genes in the absence of Tup1 compared to its occupancy alongside Tup1 in wt conditions.

In summary, I have presented evidence showing the direct co-regulation of 20 genes by Swi-Snf acting as a co-activator and Tup1-Cyc8 acting as a repressor. The data also suggests that this co-regulation can occur via two mechanisms; one involving recruitment of Snf2 to sites vacated by Tup1 (Model 1), and the other involving a possible enrichment and activation of Snf2 in the absence of Tup1 at genes to which it was already bound along with Tup1 (Model 2) (Fig. 6.29).

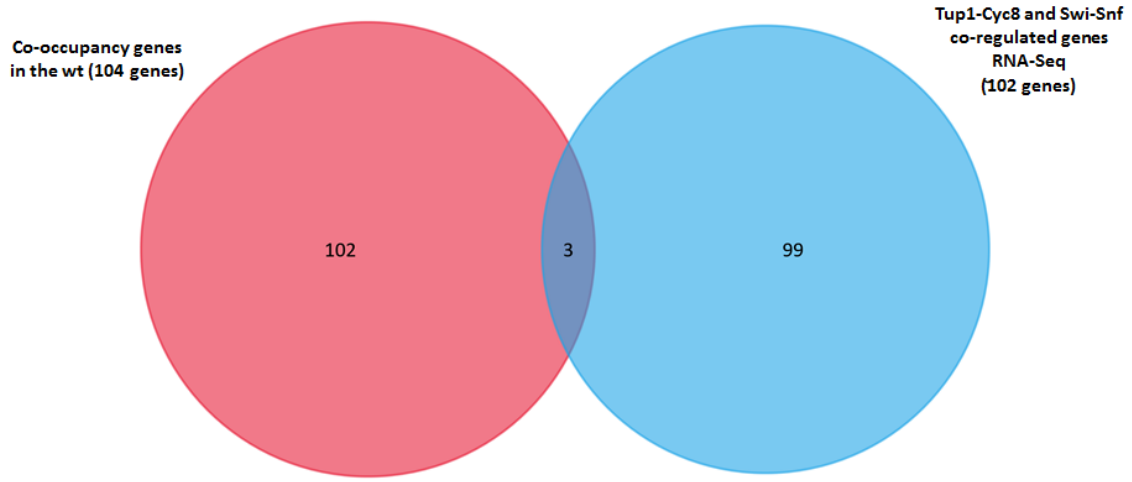

Figure 6.26 Identifying Swi-Snf and Tup1-Cyc8 co-regulated genes at which Snf2 and Tup1 are already present (Model 2). Venn diagram to show 3 overlapped genes were directly co-regulated by Tup1-Cyc8 and Swi-Snf. Fun rich software was used to perform the Venn diagram (M. Pathan *et al*. 2015).

			Snf2 occupancy in wt				Snf2 Occupancy in the absence of Tup1				Tup1 occupancy			
Gene	Description	*cyc8* vs *snf2 cyc8* Fold change	start	End	Peak Score	Distance from TSS	start	End	Peak Score	Distance from TSS	start	End	Peak Score	Distance from TSS
SED1	Cell wall protein	-2.12	599834	600004	1543.8	-874	599842	600034	2448.4	-855	599861	600101	11597.7	-812
PDR15	ATP permease	-3.18	1278737	1278907	650	-388	1278741	1278933	1232	-373	1278705	1278945	2475	-385
FLO9	Flocculation protein	-3.25	28546	28716	514.6	-663	28604	28796	2733	-732	28601	28841	20077.8	-753

Table 6.12: The Swi-Snf and Tup1-Cyc8 co-regulated genes in wt (model 2): only 3 co-regulated genes were identified in wt which Tup1-Cyc8 and Swi-Snf appear in their promoter. The gradient blue colour indicates the decrease in transcription fold change in *snf2 cyc8* double mutant's vs *cyc8*.the occupancy of Snf2 in wt, Snf2 in the absence of Tup1 and Tup1 occupancy was indicated in the table.

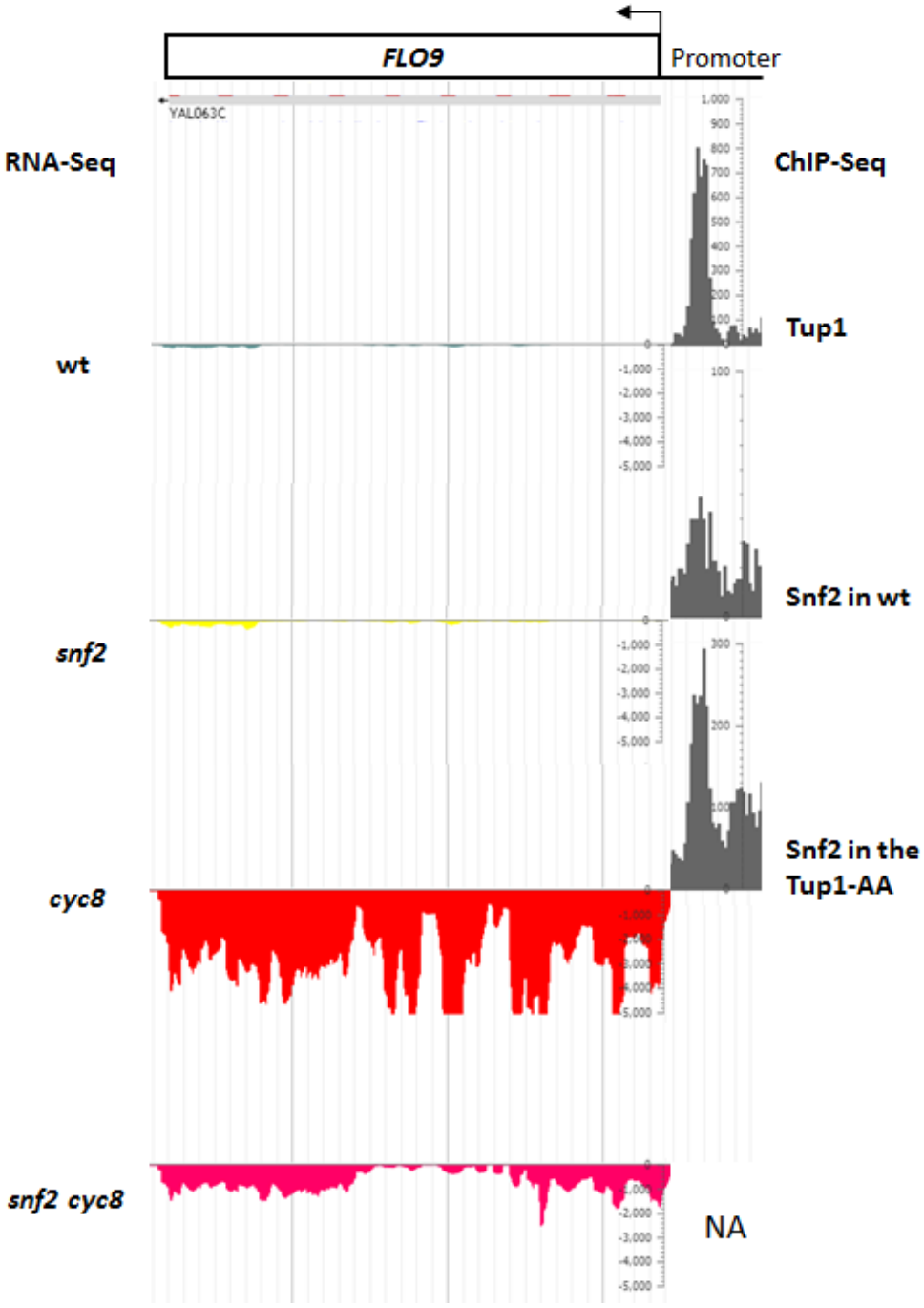

Figure 6.27 J-browse screen shot of the *FLO9* Swi-Snf and Tup1-Cyc8 co-regulated gene (Model 2) showing Tup1 and Snf2 occupancy during gene repression and activation. Screen shot from J-browse of *FLO9* gene as an example of a model 2 Swi-Snf and Tup1-Cyc8 co-regulated genes. RNA-Seq transcription data for wt, *snf2*, *cyc8* and *snf2 cyc8* mutants is shown (right side). ChIP-Seq data for Tup1 in wt and Snf2 in the presence of Tup1 (wt) and absence (Tup1-AA) is shown (lift side).

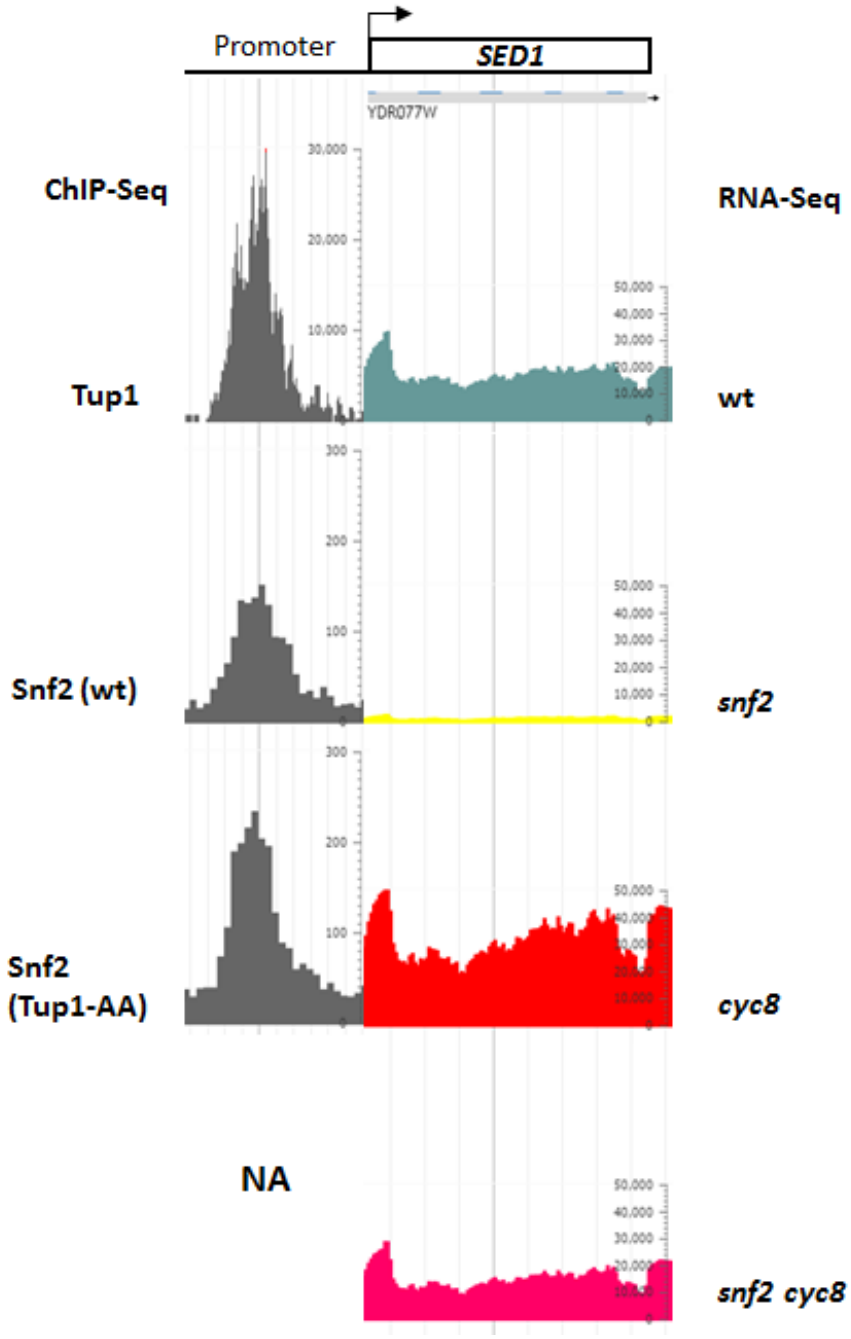

Figure 6.28 J-browse screen shot of the *SED1* Swi-Snf and Tup1-Cyc8 co-regulated gene (Model 2) showing Tup1 and Snf2 occupancy during gene repression and activation. Screen shot from J-browse of *SED1* gene as an example of a model 2 Swi-Snf and Tup1-Cyc8 co-regulated genes. RNA-Seq transcription data for wt, *snf2*, *cyc8* and *snf2 cyc8* mutants is shown (right side). ChIP-Seq data for Tup1 in wt and Snf2 in the presence of Tup1 (wt) and absence (Tup1-AA) is shown (lift side).

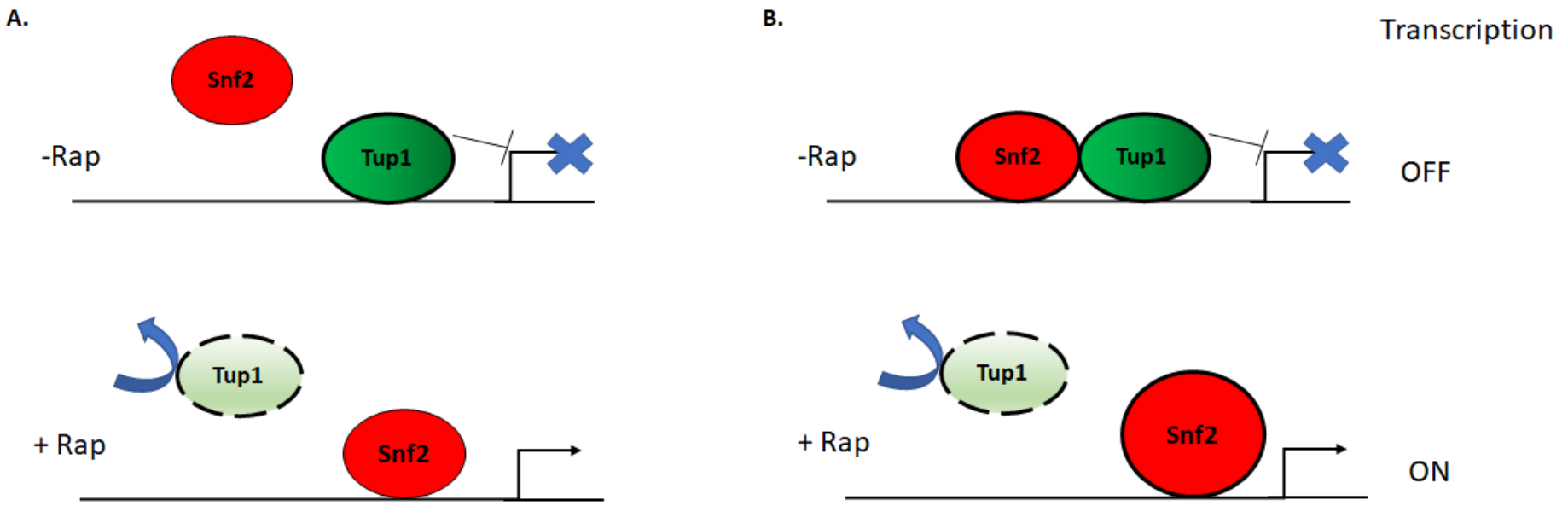

Figure 6. 29 Swi-Snf and Tup1-Cyc8 mechanism of action; models 1 and 2. (A) without rapamycin (-Rap) Snf2 was not detectable in the presence of Tup1; after the addition of rapamycin (+Rap) Snf2 is recruited to the site previously occupied by Tup1 (Model 1). (B) In the absence of rapamycin, Snf2 and Tup1 were detected at the gene; after the addition of rapamycin Tup1 is removed and Snf2 is further enriched (Model 2).

6.2.4.4 Chromosomal location of Swi-Snf occupancy and transcription of the Tup1-Cyc8 and Swi-Snf co-regulated genes at which Snf2 and Tup1 can be found:

The previous analyses culminated in the identification of 20 genes for which there is evidence for their being directly regulated by Snf2 as an activator and Tup1 as a repressor. I therefore analysed the chromosomal location of these genes (Fig. 6.30). The result showed that the 20 directly coregulated genes were spread over many of the chromosomes with 6 of these genes being located at subtelomeric regions including the *FLO9* and *FLO5* cell wall proteins, the *PHO89* phosphate transporter and *HXT13* carbohydrate transporter encoding genes.

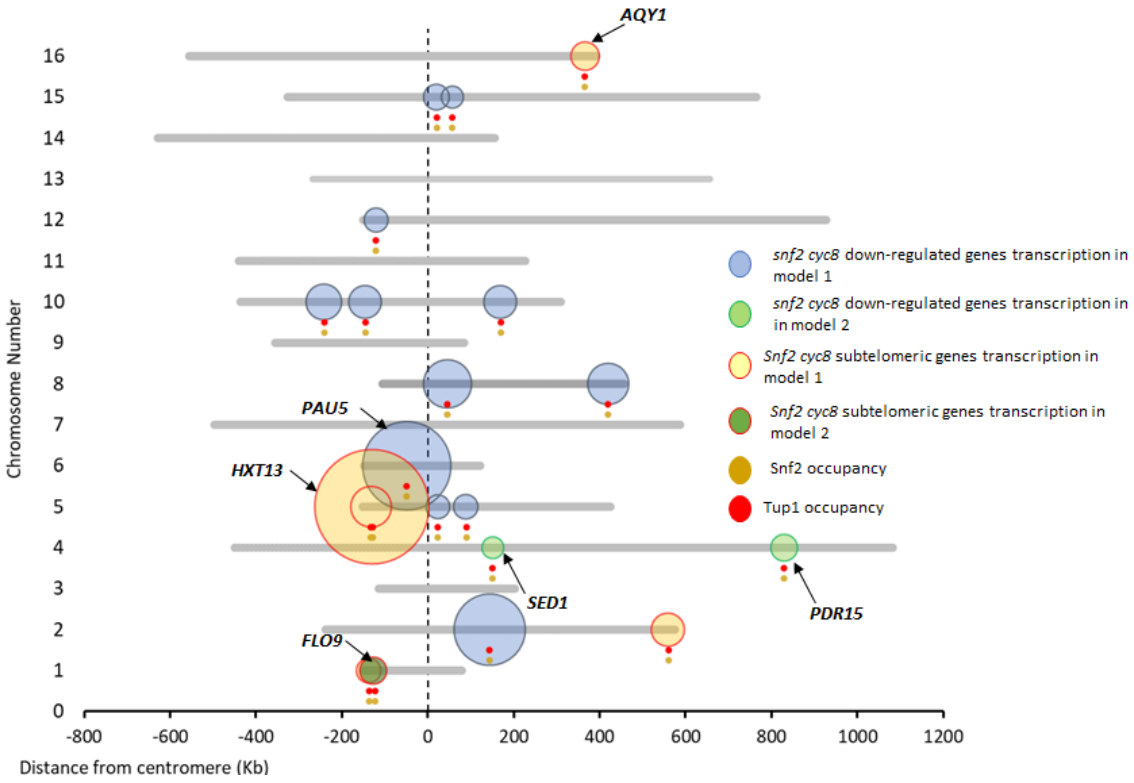

Figure 6.30 Location of Tup1-Cyc8 and Swi-Snf co-regulated genes and Tup1 and Snf2 occupancy in the presence and absence of Tup1. 'Bubble' plot showing the location of the 20 co-regulated genes in both model 1 and 2 and their fold decrease in transcription in a *snf2 cyc8* mutant vs *cyc8* mutant. Circle position reflects gene location, circle area represents the fold decrease in transcription of genes in a *snf2 cyc8* mutant relative to *cyc8*. Each line represents the chromosome number. The colour code indicated the transcription decrease for *snf2 cyc8* transcription in co-regulated genes in model 1 and 2 both separately and indicates the subtelomeric genes. the small circle colour coded under the genes indicates Tup1 and Snf2 occupancy.

6.2.4.5 Investigating the relationship between Snf2 and Tup1 with gene transcription for the 20 directly co-regulated genes:

The data suggested that 20 genes were directly co-regulated by Swi-Snf and Tup1-Cyc8. I next investigated whether there was a relationship between the distance of Snf2 binding relative to the transcription start site and the fold decrease in transcription in the *snf2 cyc8* mutant compared to the *cyc8* mutant.

However, before I started the analysis, I first examined the relative location of Tup1 and Snf2 at these genes (Table 6.8). The data showed that for the 17 genes which behaved according to the model 1 regulatory mechanism, Tup1 was located within a range of -1092 and -402 bp upstream of the TSS at the repressed gene. Following removal of Tup1 from the nucleus, Snf2 was enriched at sites between -1147 and -320 bp upstream of the active gene.

For the three model 2 genes, Tup1 and Snf2 were located within 12 to 43 bp of each other and were sited within -373 and -855 bp of the TSS at the inactive *FLO9* and *PDR15* genes, and the partially active *SED1* gene. Thus, at all of these co-regulated sites, Snf2 and Tup1 were largely found within a small window of each other and were positioned around -500 bp upstream of the gene under their control.

Subsequent plotting of the location of Tup1 versus the transcription fold change (decrease) in transcription of the *cyc8* single mutant versus the *snf2 cyc8* double mutant revealed no clear relationship (Fig 6.31). Indeed, genes at which Tup1 was located over 1000 bp up or down stream of the TSS showed similar levels of transcription fold change as the bulk of genes which had Tup1 located at promoters within 400 and 700 bp upstream of the TSS. Indeed, the gene showing the highest fold change in transcription was the *HXT13* gene which had Tup1 located 500 bp upstream of the TSS, in common with most of the Tup1 binding sites.

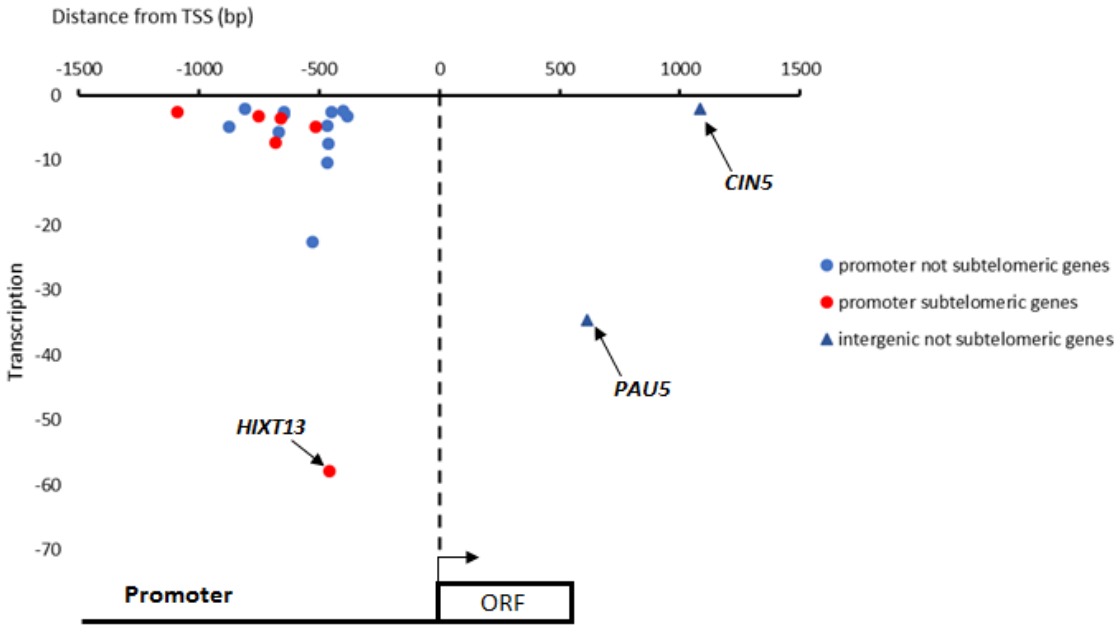

Figure 6.31 The relationship between the co-regulated genes transcription fold changes in the *cyc8* vs *snf2 cyc8* mutants and the distance of Tup1 occupancy from TSS. The *snf2 cyc8* transcription down-regulated genes were plotted against the distance of Tup1 from the transcription TSS in a scatter plot. Two chromosomal regions were identified, non subtelomeric genes in blue and subtelomeric genes in red. Two occupancy categories were defined under the two regions in Tup1 occupancy were located in promoters and intergenic region.

6.2.4.6 Investigating the relationship between promoter size and levels of gene transcription of the 20 directly co-regulated genes

I next analysed whether there was a relationship between promoter size and the levels of gene transcription in the various mutants for the 20 directly co-regulated genes. This was because I had previously hypothesised that those genes with large promoters (or upstream gene free regions) would show the greatest changes in transcription in the presence and absence of Tup1 and Snf2. Specifically, I plotted the fold decrease in transcription of the 20 genes in the *snf2 cyc8* double mutant versus the *cyc8* single mutant against the length of gene free upstream region for each gene (Fig. 6.32).

The result showed that all but one of the genes had promoter size evenly disrupted between 2200 bp and 2.4Kb in size. The genes with largest upstream gene-free region was the *TDA8* gene at 8 Kb. However, for 17 of these genes, they all shows transcription fold change of~10-fold in the *cyc8* mutant vs *snf2 cyc8*. Indeed, the *TDA8* gene with the longest promoter and the *CIN5* gene with the shorter promoter showed similar fold change in transcription as each other. conversely, the gene showed the greatest fold change in transcription in the absence of *cyc8* and *snf2* was the *HXT13* gene which had a gene- free upstream region of 2.7 Kb.

Overall, the result observed no relation between promoter size and transcription level in *snf2 cyc8* (Fig. 6.32).

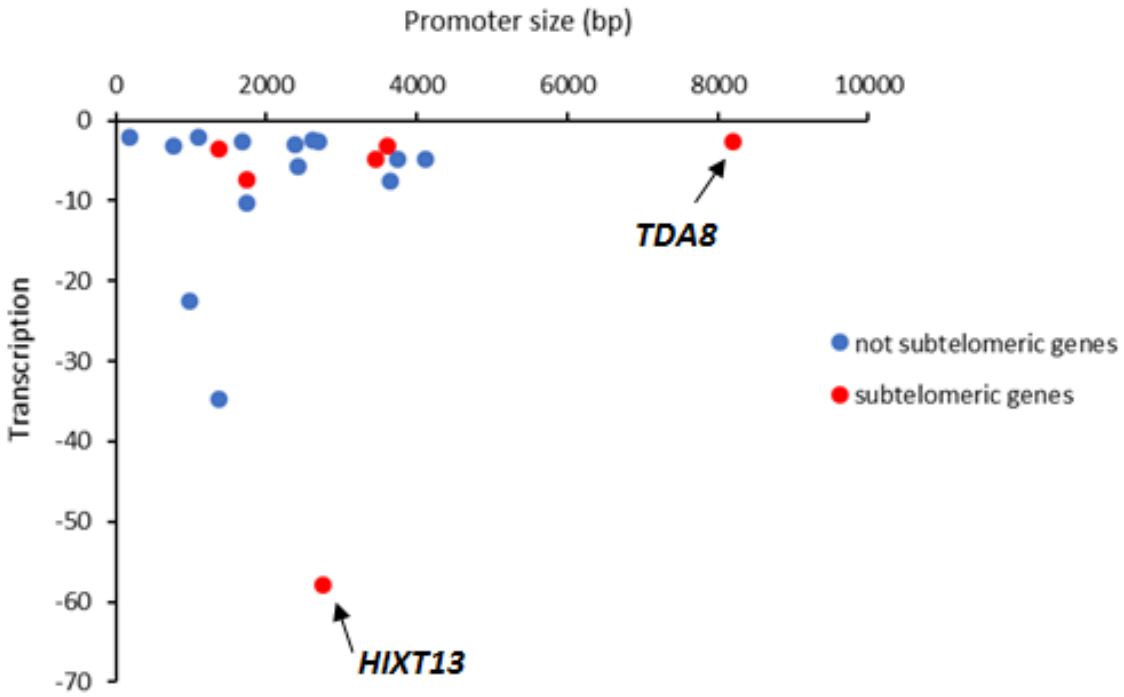

Figure 6.32 The relationship between the co-regulated genes transcription levels and promoter size. The *snf2 cyc8* transcription down-regulated genes were plotted against the promoter size in scatter plot. Two chromosomal regions were identified, non subtelomeric genes in blue and subtelomeric genes in red.

6.3 Discussion:

The data presented in chapter 5 for RNA-Seq analysis identified the set of genes that were under regulation by Swi-Snf and Tup1-Cyc8. However, the transcription data does not tell us if the transcription changes were a direct or indirect effect of the Swi-Snf and Tup1-Cyc8 chromatin remodelling complexes.

The Snf2 global ChIP-Seq data was therefore compared to the *snf2* RNA-Seq transcription data to examine the association of Snf2 at the genes down-regulated in a *snf2* mutant. Our analysis revealed that of the 278 genes down regulated in a *snf2* mutant only 27 genes had peaks of Snf2 associated with them, suggesting that these genes were under the direct control of Swi-Snf (Fig. 6.1). The low number of Snf2-dependant genes showing Snf2 occupancy might be an underestimation of the real number of genes directly regulated by Snf2 as epitope masking might have blocked detection. This blocking could be due to the rest of the Swi-Snf complex itself, or the surrounding chromatin architecture at target genes (Kidder *et al*. 2011).

Further analysis was performed to identify if there was a specific location occupied by Snf2 at target genes. However, only one gene lay in a subtelomeric region (Fig. 6.3), and the distance of the Snf2 from the TSS showed no effect on the transcription level. Interestingly, the farthest point of Snf2 from a TSS was 970 base pairs upstream of the *GAC1* gene indicating a possible ability of Swi-Snf for long range chromatin remodelling at target genes to influence transcription (Fig. 6.4).

Swi-Snf is known as a co-activator. However, the *snf2* transcription profile also revealed 208 genes that were up-regulated in the absence if *snf2* suggesting these genes required Swi-Snf as a repressor (see Fig. 5.15) and (see Table 5.4). I also found Snf2 occupancy at 19 of these genes (Fig 6.5), or 23 if the cut off for consideration was reduced (Fig. 6.6). One such gene shown to require Snf2 for repression was the *SER3* gene which is known to be regulated via a Swi-Snf dependent transcript run through event (Albers *et al*. 2003; Martens & Winston, 2002).

The genes under repression by Snf2 were located in varying places on the genome (Fig. 6.7), with no Snf2 repressed gene being found at subtelomeric regions. I also compared the distance of Snf2 from the TSS of the repressed genes with the transcription fold de-

repression in the *snf2* mutant. Intriguingly, aside from for *SER3*, the data suggested that Swi-Snf might repress more powerfully the closer it is to the TSS (Fig 6.8).

The analysis of the Tup1 occupancy data and the *cyc8* transcription profile also revealed evidence of the direct effect of the Tup1-Cyc8 complex. The Tup1 occupancy data analysed from (Wong & Struhl, 2011) showed that 601 genes were associated with Tup1. Comparing these 601 genes with the 575 genes up regulated in a *cyc8* mutant showed that 175 of these genes were associated with Tup1, suggesting that these genes were directly repressed by Tup1-Cyc8 (Fig. 6.9). Analysis of these Tup1-Cyc8 repressed genes revealed this complex is involved in the repression of many pathways in yeast such as carbohydrate transport, cell wall proteins, and many other stress response genes like the heat shock genes *SUT1* and *MGA1* (Table 6.8).

Importantly, when we mapped the 175 repressed genes which show Tup1 localization,30 (17.1%) were located at subtelomeric regions either on the left or the right of the chromosome's arms which might suggest this is an area enriched for Tup1-Cyc8 repression activity (Fig. 6.11).

At the repressed genes where Tup1 could be found, Tup1 was localized between -3000bp upstream to 2000bp downstream from the transcription start site (TSS) (Fig 6.12). It was found to be located predominantly around -500 bp in gene promoters of 146 genes but was also found at ~ 250bp ORFs of 20 genes and ~ 900 downstream intergenic regions of 9 genes.

Tup1-Cyc8 was first described as a repressor of gene transcription. However, there is evidence that Tup1-Cyc8 can function as an activator (Conlan *et al*. 1999). Our analysis of the *cyc8* transcription profile in chapter 5 showed transcription of 158 genes were down-regulated in a *cyc8* mutant which is consistent with their being activated by Tup1 (see Fig. 5.4) and (see Table 5.2). However, only 20 of these genes were found to show occupancy by Tup1 to suggest that they are direct targets for Tup1-Cyc8 (Table 6.9) (Fig. 6.13). The mechanism of how Tup1-Cyc8 could bring about gene activation is not clear. However, Tup1-Cyc8 activation of *CIT2*, a gene encoding a citrate synthase involved in the glyoxylate cycle, involves Tup1-Cyc8 binding to Rtg3, a DNA-binding transactivator of *CIT2* to turn the gene on (Conlan *et al*. 1999). The 20 genes under possible direct

activation by Tup1-Cyc8 were located at various regions across the chromosomes with only *AGP3,* which encodes and amino acid transporter, and *IRC7* which is involved in production of thiols, being located at subtelomeric regions on chromosome (Fig. 6.15). The distance of Tup1 occupancy at these genes was also compared to the transcription change of these genes in a *cyc8* mutant to reveal that transcription increased the closer Tup1 was to the TSS region (Fig 6.16).

The results also revealed that 105 genes showed occupancy by both Tup1 and Snf2 (Fig. 6.17) and (Table 6.10). However, although tempting to think otherwise, this data does not tell if Tup1-Cyc8 and Swi-Snf occupy these sites at the same time. Interestingly, one of these genes is *CYC8* which shows Tup1 and Snf2 binding upstream of the wt *CYC8* gene raising the possibility of regulation of *CYC8* transcription by Tup1 and Snf2 (Fig. 6.18). Also, found in this group of genes was *FLO9* which encodes one of the *FLO* family of flocculin genes (Soares, 2011).

The study showed that Tup1 and Snf2 were predominantly located in the promoter at a site ~500 bp upstream of the ATG (Fig 6.19 A and B). with exception of two genes were where Tup1 and Snf2 bound almost 3 kb upstream of the *GTT1* transcription start site and bound ~ 2.2 Kb downstream of the transcription stop site of the *YLR154C-G* gene. Thus, there were 85 sites for Snf2 and Tup1 found at gene promoters, whilst 18 and 3 sites (*YLR154C*-G, *ILV5* and *CHA1*) were found in ORFs and downstream intergenic regions respectively (Fig. 6.19 C).

When I analysed the Tup1 and Snf2 distance from each other at co-occupied genes, although 6 categories were identified, the majority of the genes showing occupancy by both snf2 and Tup1 (44 genes) had these proteins located between 11 and 50 bp apart (Fig. 6.20 A & B), with the majority of these sites located in promoters. Two genes, *CHA1* and *RNH203* were associated with Tup1 and Snf2 located over 500 bp apart. at *CHA1*, Tup1 and Snf2 were located 1106 bp apart with Snf2 being located in the gene promoter and Tup1 being located after the transcription stop site (Fig. 6. 20 C).

The main aim of my work was to identify those genes co-regulated by Tup1-Cyc8 as a repressor and Swi-Snf as an activator Therefore, I was most interested in correlating the co-regulated genes I had identified from the transcriptome analysis with Tup1 and Snf2

occupancy. I hypothesised that there might be two modes of co-regulation; Model 1 would involve Snf2 being recruited to target promoters when Tup1 was absent, whilst model 2 would have further enrichment of Snf2 occupancy at genes where Snf2 and Tup1 were already present.

My analysis found direct evidence for 17 genes behaving according to model 1 (Fig. 6.24), including the *FLO5* gene (Table 6.11), and 3 genes behaving according to model 2 (Fig. 6.26), including the *FLO9* gene (Table 6.12). I expect that these numbers are an underestimation of the true numbers of genes co-regulated in this way, as the *FLO1* gene which is known to be regulated according to model 1 did not show up in my analysis. This might be to do with the different ChIP protocols employed between various studies having different efficiencies in their ability to detect Tup1 (or Cyc8) at target sites. For example, studies by (Fleming *et al*. 2014; Rizzo *et al*. 2011) could detect Tup1 at the *FLO1* promoter, whilst the study by (Wong & Struhl, 2011), and which was the data I used for my analysis here, did not. In addition, although Tup1 is difficult to ChIP at the repressed *SUC2* gene, where it has been well characterised as being required for repression, it can be identified when the gene is active (unpublished observation). Thus, Tup1 in particular seems to be a difficult protein to identify using ChIP.

Two genes that were previously well characterised as being under the antagonistic control of the Swi-Snf and Tup1-Cyc8 complexes were the *SUC2* and *FLO1* genes (Fleming and Pennings 2001; Fleming and Pennings 2007, Gavin and Simpson, 1997). At these genes it was shown that an extensive region of chromatin was remodelled by the complexes upstream of these genes. I was therefore interested to investigate whether there was any relationship between the location of Snf2 and Tup1 at target genes and the levels of regulation of transcription. Specifically, I wanted to know if the distance of occupancy of either Tup1 or Snf2 might have an impact on that genes transcription, and whether the length of the promoter, or gene free upstream region, influenced regulation by Swi-Snf and Tup1-Cyc8.

When the decrease in gene transcription in the *snf2 cyc8* double mutant relative to *cyc8* transcription was compared with the distance of Snf2 and Tup1 occupancy from the TSS the result showed no obvious relationship between the *snf2 cyc8* level of transcription and the distance from TSS (Fig. 6.31). There was also no obvious relationship between

the size of the gene free region and the influence upon transcription of Snf2 and Tup1 at target genes (Fig. 6.32). This went against my original hypothesis that the length of gene free upstream region might allow greater repression of transcription by Tup1-Cyc8 by enabling tighter packaging of the genes promoter in the more extensive chromatin region. Thus, although there is an enrichment of Swi-Snf and Tup1-Cyc8 co-regulated genes in subtelomeric regions where the genes often have larger gene free upstream regions, this does not seem to have an impact upon the level of repression by Tup1 or the degree of activation by Snf2.

In summary, I have found direct evidence of genes under the antagonistic control of Snf2 (as activator) and Tup1 (as repressor) being co-regulated via two modes of action. Model one involves a mutually exclusive recruitment of Snf2 to Tup1 repressed genes, and model two involves both snf2 and tup1 being present at repressed genes, with Snf2 remaining at the active target gene in the absence of Tup1. This latter model is consistent with the work of (Wong & Struhl, 2011) in which they suggest that Tup1-Cyc8 can mask the activating domain of activator proteins to block transcription.

The next chapter investigates chromatin remodelling by Swi-Snf and Tup1-Cyc8 at these two classes of antagonistically regulated genes. A prediction would be that the model one genes might be regulated via strongly positioned nucleosomes and the model two genes would not be so impacted by nucleosome positioning.

Chapter 7

Mapping genome-wide chromatin remodelling by Tup1-Cyc8 and Swi-Snf

7.1 Introduction:

In the previous chapters, an investigation into how Tup1-Cyc8 and Swi-Snf complexes regulate genes was presented via RNA-Seq and ChIP-Seq analyses. These data have shown the number of genes that were under the antagonistic control of Swi-Snf as an activator, Tup1-Cyc8 as a repressor, and the correlated Snf2 and Tup1 occupancy at these genes.

This chapter investigates the mechanism of action of these complexes by determining the global nucleosome positioning in wt, and in strains deficient for the Swi-Snf and Tup1-Cyc8 complexes, in order to establish precisely how they remodel chromatin at target genes.

This was achieved by digesting chromatin from wt and the various mutants with Micrococcal Nuclease (MNase) to generate predominantly mono-nucleosome length DNA, which was then sequenced; a technique known as MNase-Seq.

The nucleosome is the fundamental repeating subunit of chromatin which consists of two each of the core histones H3, H4, H2A and H2B, around which 146bp of DNA is wrapped. The linker DNA connects adjacent nucleosomes. MNase is commonly used to map nucleosome positions via its endonuclease and exonuclease activities (Chereji *et al*. 2017; Kent *et al*. 1993) which cleave the internucleosomal (linker) DNA while leaving the nucleosomal DNA which is protected from digestion (Fig. 7.1) (Gutiérrez *et al*. 2017; Noll, 1974). Thus, partial digestion of chromatin with MnaseA results in the formation of a ladder pattern of the DNA with each rung of the ladder being a multiple of 146 bp length nucleosomal DNA (Fig. 7.1).

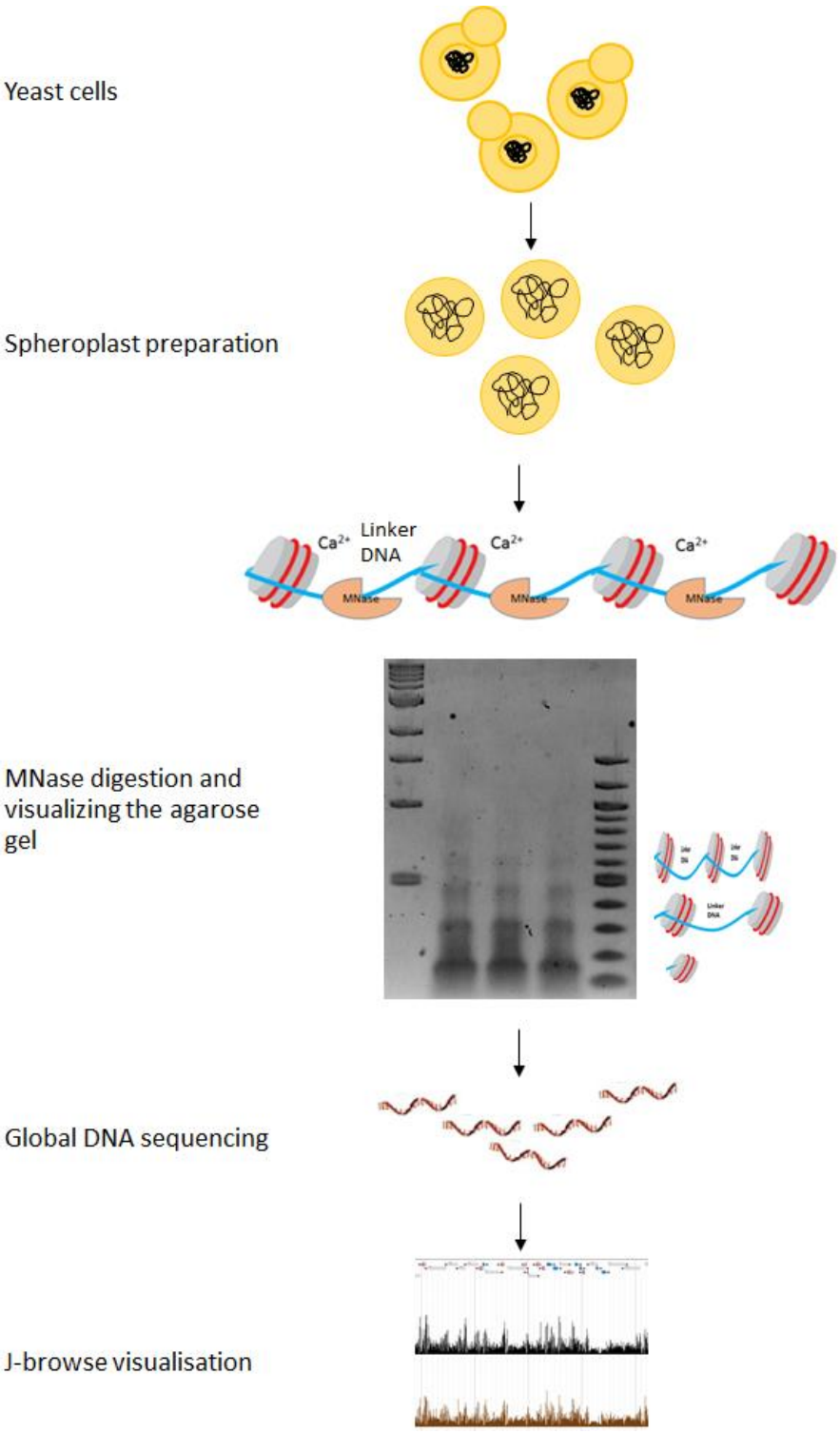

Figure 7.1 MNase-Seq technique. Spheroplasts were prepared and chromatin was digested by MNase in the presence of calcium to mono-, di- and tri- nucleosomal length fragments. The DNA was purified and sent to be sequenced. Peaks representing the number of sequence reads were mapped back to the genome and denote nucleosomal positions which were visualised in J-browse.

7.2 Results:

7.2.1 Investigating histone protein levels in Tup1-Cyc8 and Swi-Snf mutants:

Prior to investigating the mechanism of Tup1-Cyc8 and Swi-Snf chromatin remodelling by using Micrococcal Nuclease digestion and sequencing (MNase-Seq), Western blot analysis was performed to determine core histone (H3, H4, H2A, H2B) and H1 levels in the various mutants (Fig. 7.2). This was to see if there were any differences in global histone levels in the Swi-Snf or Tup1-Cyc8 mutants which might influence global nucleosome positions. The results showed that histone protein levels were largely unaffected in either the *cyc8* mutant, any of the Swi-Snf mutants or in the double mutants.

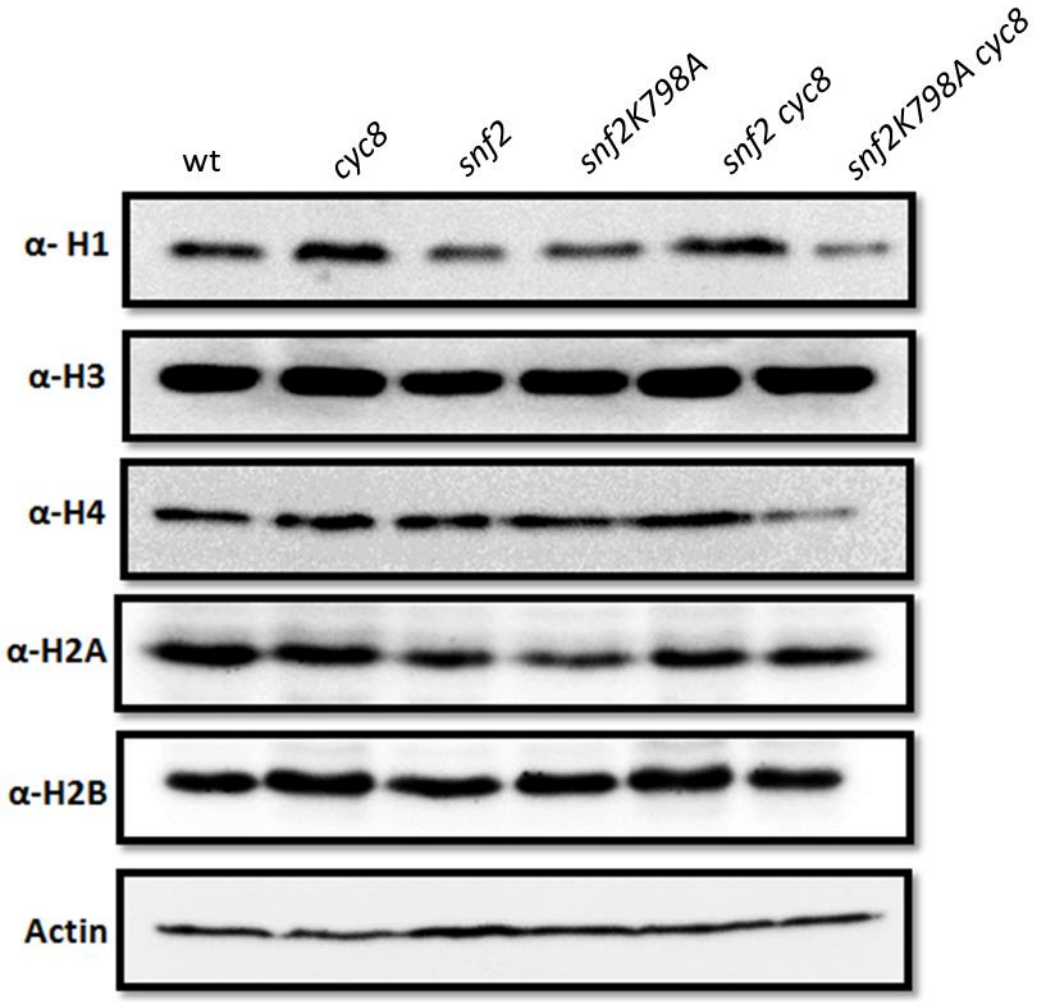

Figure 7.2 Histones protein levels in the different Tup1-Cyc8 and Swi-Snf mutants. Western blot analysis of TCA extracted protein in log phase of wild type (wt), *cyc8* and Swi-Snf complex single and double mutants. Antibodies were specific to H3, H4, H2A and H2B. β-Actin was used as a loading control. Image is representative of three independent biological replicates.

7.2.2 Micrococcal Nuclease digestion:

The general chromatin structure in each strain was next investigated by assaying digestion of their chromatin by Micrococcal Nuclease (Mnase). Nucleii were prepared from the strains indicated and subjected to an MNase digestion time-course. Differences in gross chromatin structure can be revealed by visualising differences in the rate or extent of chromatin digestion using agarose gel electrophoresis (Fig. 7.3A). Densitometry was performed by using the Imagequant software to detect the bands size and density relative to the 100bp DNA ladder (Fig. 7.3B). The results indicated that the chromatin in the *snf2* mutant digested at the same rate and to the same extent as wt, suggesting no difference in accessibility to Mnase in the *snf2* mutant. Conversely, the *cyc8* single and *snf2 cyc8* double mutants showed similarly faster digestion rates than wt, suggesting chromatin in the *cyc8* mutant background was more accessible to digestion by Mnase. In the *cyc8* and *snf2 cyc8* mutants, chromatin digestion yielded a greater enrichment of mono and di-nucleosomal length fragments after 10 min digestion than was evident for wt and *snf2* strains.

Overall, the result suggested that there was a difference in the global chromatin structure in Tup1-Cyc8 deficient strains whereby it was more open to digestion, whilst the absence of functional Swi-Snf had no effect on global chromatin structure.

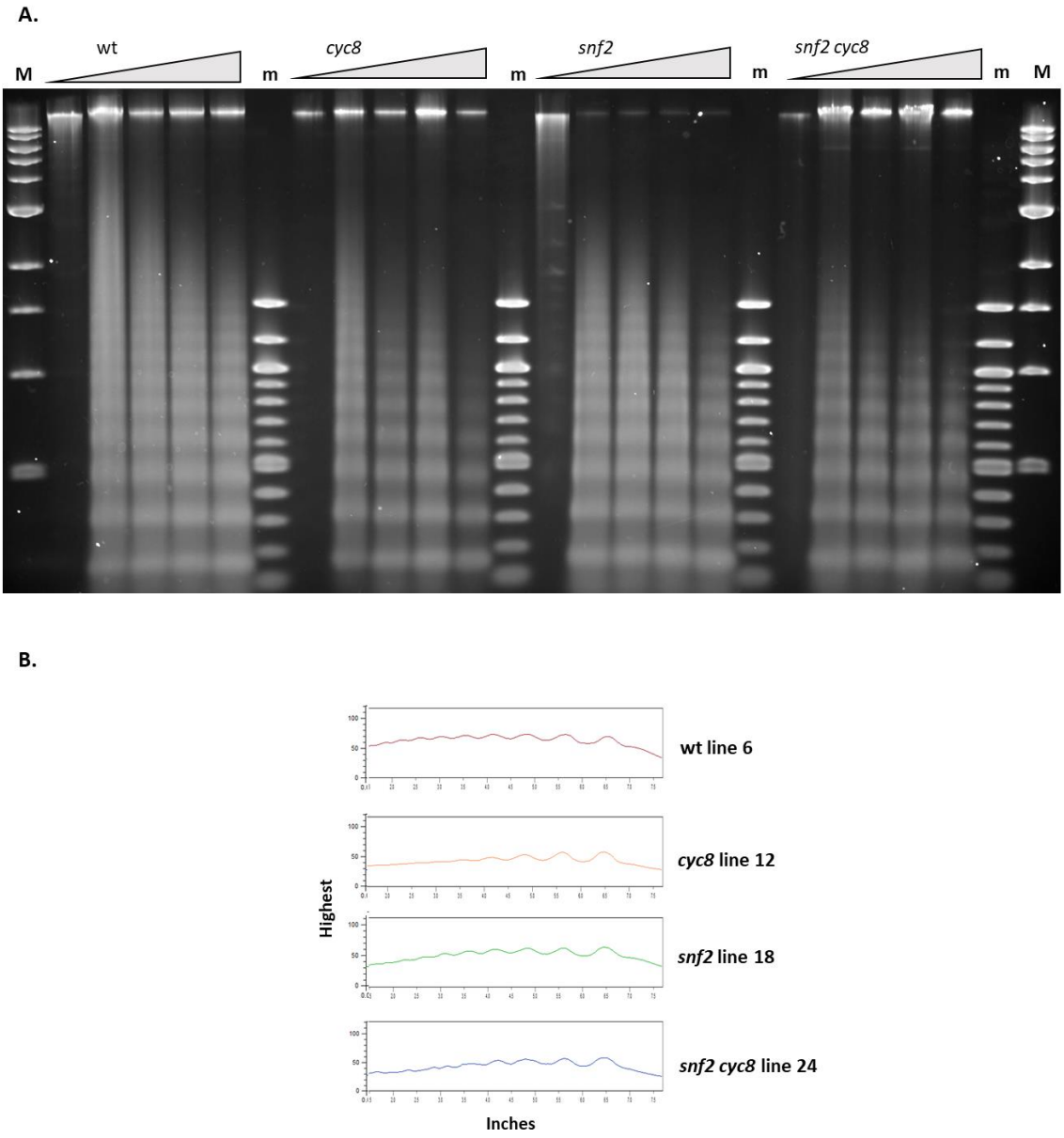

Figure 7.3 Micrococcal Nuclease Digestion. A: 1.25% agarose gel showing chromatin digestion by Micrococcal nuclease A (MNaseA) for the strains indicated. The triangle symbol indicates the time course of digestion (0, 4, 6, 8 and 10 minutes; 10U of Mnase). (M) is a 1Kb ladder, (m) is a 100bp ladder. **B:** Densitometry profiles of the final digestion time point lanes (10 min) for each strain are shown using Imagequant software analysis. Images are representative of three biological replicates.

7.2.3 Mapping global nucleosome positions by MNase-Seq:

The aim of this chapter was to examine the mechanism of Swi-Snf and Tup-Cyc8 for remodelling the chromatin by using MNase-Seq to map global nucleosome positions in wt and Snf2 and Cyc8-deficient strains. Chromatin from each strain was digested to predominantly mono- and di-nucleosomal length fragments. The DNA was purified, the extent of digestion confirmed by gel electrophoresis, and then sent to our collaborator from the University of Cardiff, Dr N. Kent, for library preparation and sequencing (Fig. 7.5 A). Chromatin from each strain was prepared in duplicate. Naked DNA was also digested by Mnase and sequenced to act as a control for MNase DNA sequence specificity (Fig. 7.5 B) (Clark, 2010; Fleming *et al*. 2014)

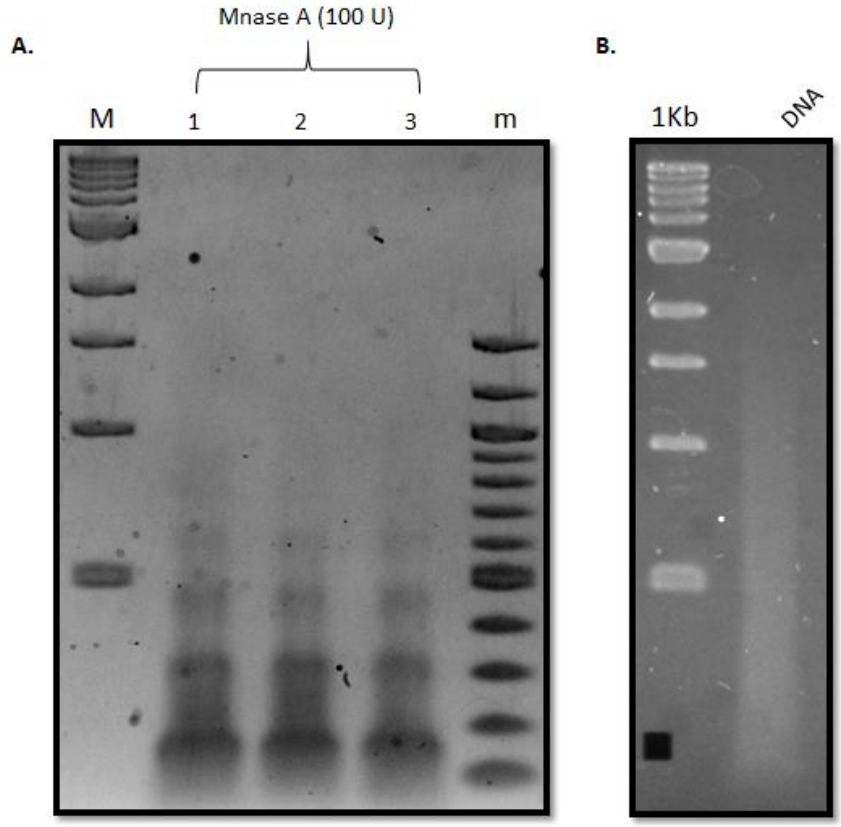

Figure 7.4 Micrococcal Nuclease Digestion (MNase) for MNase-Seq. A: 1.25% agarose gel showing chromatin digestion by micrococcal nuclease (MNase, 100U) to yield mono- di- and tri- nucleosomal length fragments. Chromatin from *snf2 cyc8* is shown as an example for the chromatin digestion. **B:** Naked DNA from wt was digested by MNase as a control. (M) is a 1Kb ladder, (m) is a 100bp ladder. Images are representative of two independent biological replicates.

7.2.4 Mnase-Seq data quality control:

Following Mnase-Seq, the quality of the duplicate data sets for each strain were compared by plotting the aligned sequence reads against each other relative to gene transcription start sites (TSS, set at '0'). As can be seen by the overlapping traces of nucleosomal peaks (Fig. 7.5 A), the data was of high quality as the R^2 values for all data sets was above 0.95. The result from Mnase-Seq of wt is shown as an example (Fig. 7.5 B). The data clearly shows the canonical nucleosome architecture found in yeast, up and downstream of the TSS, whereby the strength of the nucleosome positions decreases the greater the distance the nucleosomes are either up or downstream from the nucleosome free region (NFR) (Kent *et al*. 2011; Xi *et al*. 2011).

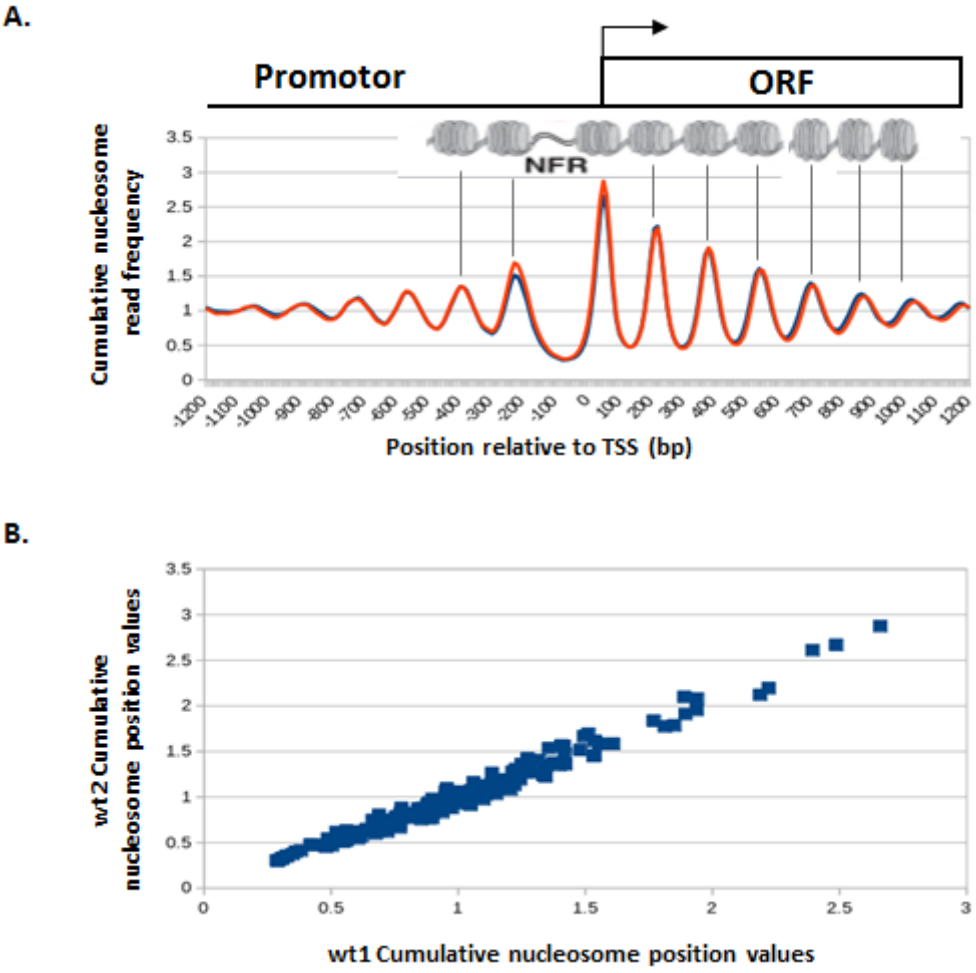

Figure 7.5 Mnase-Seq analysis data quality control. A: Distinct chromatin particle distributions were normalized and plotted relative to the transcription start site (TTS)(arrow) set at '0'bp. **B:** The data from duplicate wt chromatin digestions were plotted against each other, relative to transcription start site (TSS, '0'). NFR indicates the nucleosome free region. This data and the figure were generated by Dr. Nick Kent, Cardiff University.

7.2.5 Analysing global chromatin structure in the Snf2 and Cyc8 deficient mutants using Mnase-Seq:

In order to assess whether there were any global differences in chromatin architecture in the Snf2, Cyc8 and Snf2 and Cyc8-deficient mutants, the global sequence reads aligned relative to gene transcription start sites for each strain were plotted against each other (TSS, set at '0') (Fig. 7.6). This effectively compares the general nucleosome structure around all genes in the different strains (Fig. 7.6 A). As can be seen by the overlapping traces of nucleosomal peaks in the wt and *cyc8* strains (Fig. 7.6 B), the wt and *snf2* strains (Fig. 7.6 C), and the similar profile in the *cyc8* and *snf2 cyc8* strains (Fig. 7.6 D), the correlations between our matched samples was extremely high, suggesting that Cyc8 and Snf2 have no global effect on the nucleosome organisation. Although this result was inconsistent with the crude Mnase analysis following digestion of chromatin in nuclei shown in (Fig. 7.3), the Mnase-Seq analysis would be expected to be the more accurate as it involves sequence depth which is absent in the crude analysis. Thus, whether Snf2 and Cyc8 are present or absent, global chromatin structure as assessed by Mnase-seq, is similar to wt.

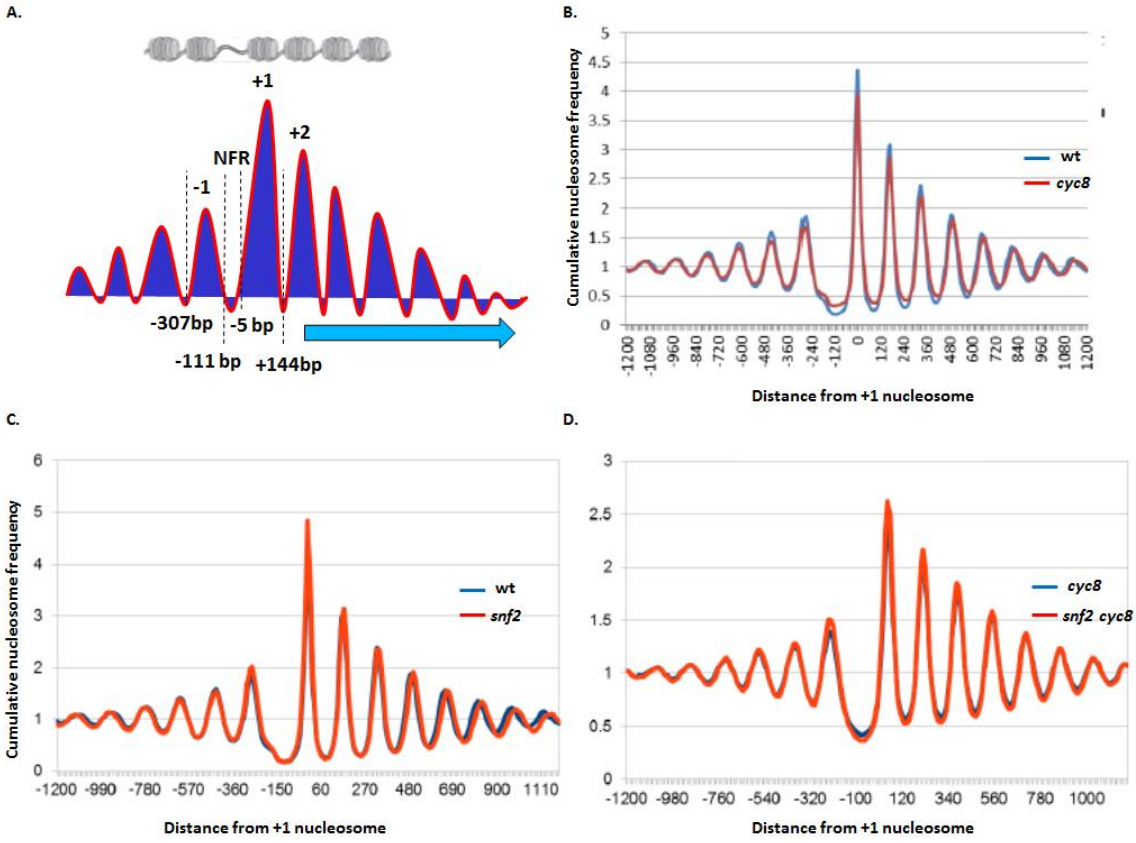

Figure 7.6 Global chromatin alignment in wt, *snf2, cyc8* and *snf2 cyc8* strains: A: The data from each strain plotted against wt from +1 nucleosome which is located between -5 to +144 bp upstream of the transcription start site (TSS). **B:** A plot of the *cyc8* data vs wt. **C:** A plot of the *snf2* data vs wt. **D:** A plot of the *snf2 cyc8* vs wt data.

7.2.6 Chromatin remodelling in Cyc8 and Snf2 deficient mutants:

Our RNA transcriptome data observed 575 (8.7% of total) genes that were upregulated in a *cyc8* mutant suggesting that Tup1-Cyc8 acts as a repressor at these genes, whilst 278 genes were downregulated in a *snf2* mutant suggesting that Swi-Snf acts as an activator of these gene's expression. Importantly, this study also identified 102 Tup1-Cyc8 and Swi-Snf co-regulated genes at which Swi-Snf was required for activation, and Tup1-Cyc8 was required for repression.

Within these co-regulated genes, this study discovered evidence for two possible models of regulation of transcription by Swi-Snf and Tup1-Cyc8 (see section 6.2.4), depending on the occupancy of Tup1 and Snf2 at the co-regulated genes. In model one, the repressed gene is occupied by Tup1, which is replaced by Snf2 when the gene's expression is active. In model two, Tup1 and Snf2 both occupy repressed genes, with gene activation following the loss of Tup1 coinciding with the retention (and often enrichment) of Snf2.

The position of nucleosomes over gene promoters can limit the accessibility of the transcription machinery to influence whether the gene is on or off (Clark, 2010). The nucleosome organisation at the two different types of co-regulated genes was therefore examined in wt, *snf2*, *cyc8,* and *snf2 cyc8* strains to determine the influence of nucleosome positioning at these genes by Swi-Snf and Tup1-Cyc8.

7.2.7 The chromatin environment at the *FLO5* ORF and upstream region: An example of a 'model 1' co-regulated gene:

In the previous chapter, it was shown how Tup1-Cyc8 and Swi-Snf act together to co-regulate genes via 2 models. Model 1 (i) involves Snf2 being recruited to their promoters when Tup1 was absent and Model 2 (ii) involves a further enrichment of Snf2 occupancy at genes where Snf2 and Tup1 were already present. Interestingly, members of the *FLO* gene family are included in these two different models; *FLO5* is a model 1 regulated gene, and *FLO9* represents model 2.

FLO5 was used as an example of a gene regulated by the antagonistic action of Swi-Snf and Tup1-Cyc8 chromatin remodelling functioning via model 1 (Fig. 7.7). At this repressed gene, Tup1 was found located at – 462 bp relative to the TSS, whilst Snf2 could not be detected at the repressed gene (Fig 7.7A, B). However, when the *FLO5* gene was strongly de-repressed in the *cyc8* mutant, Snf2 was recruited to within 27 base pairs of the site to which Tup1 was previously bound (Fig 7.7 A, B).

The overall chromatin structure of the *FLO5* ORF and upstream gene free region was next examined in the wt, and in the presence and absence of Tup1 and Snf2. Similar to the well characterised *FLO1* gene which is co-regulated by Tup1-Cyc8 and Swi-Snf (Fleming & Pennings, 2001), *FLO5* has a relatively large gene free upstream region which stretches for ~4.8 kb before the location of the next ORF. In the wt strain, in which *FLO5* is repressed, there is a strong series of peaks representing positioned nucleosomes across the entire upstream region shown (Fig 7.7 C). However, in the *cyc8* mutant, in which *FLO5* is highly de-repressed, these strong peaks are almost entirely obliterated across the entire upstream region (Fig 7.7 C, compare *cyc8* and wt). When *snf2* is additionally deleted in the *cyc8* mutant, the pattern of peaks in the double *snf2 cyc8* mutant now largely resembles the pattern seen in wt. This suggests that the disruption to chromatin seen in the *cyc8* mutant is dependent upon Snf2. Interestingly, the peaks in the *snf2* mutant are even more pronounced than in wt, even though the gene is repressed in both strains. Overall, there is a clear pattern of peaks which indicates strong nucleosomal positions at the extensive *FLO5* upstream region when the gene is off, that are significantly disrupted in a Snf2-dependent manner when the gene is on.

A. Chip-Seq

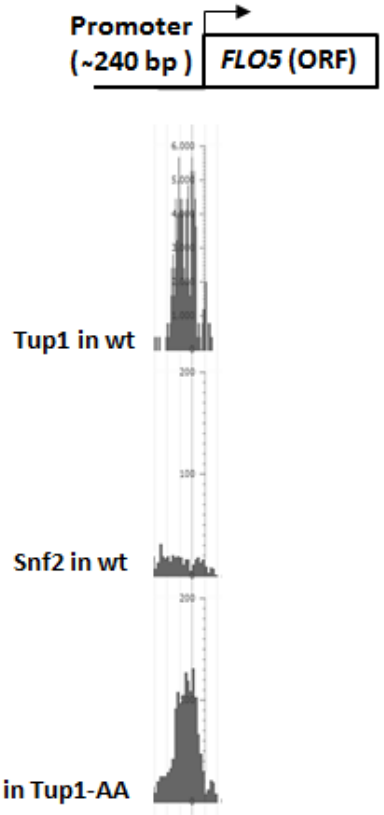

B.

FLO5	Distance From TSS (bp)	Peak score
Tup1	-462	2951
Snf2 in wt	-	-
Snf2 in Tup1-AA	-435	1278.8

B. MNase-Seq RNA-Seq

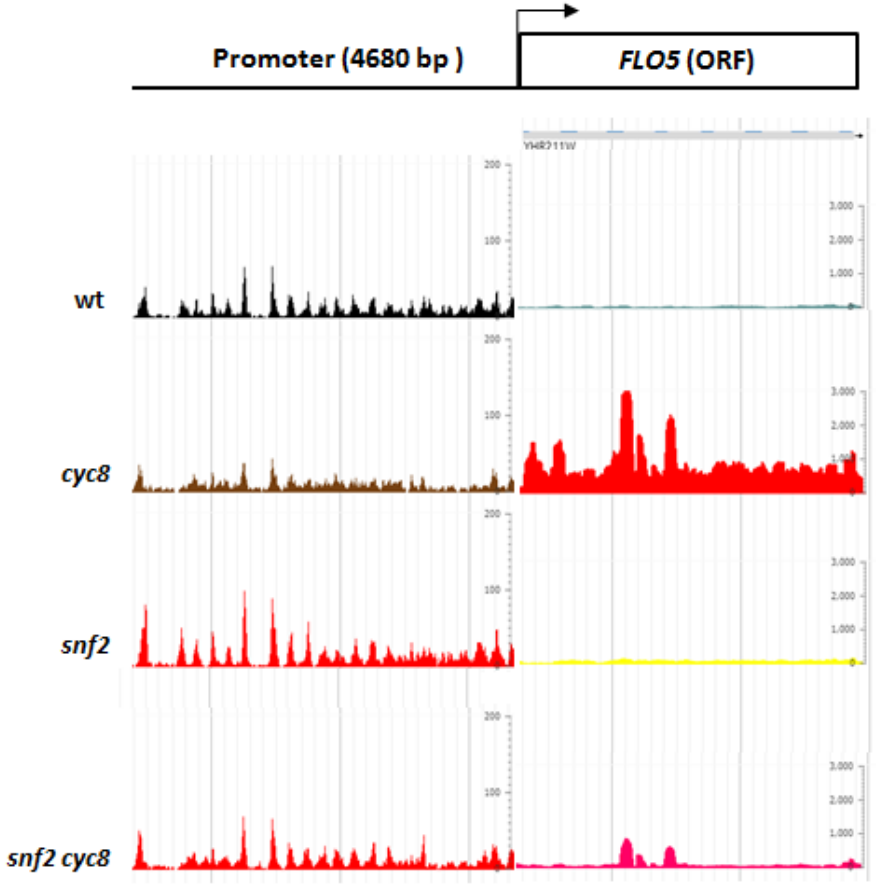

Figure 7.7 J-browse image of transcription, chromatin structure and Tup1 and Snf2 occupancy at the *FLO5* ORF and upstream region. A: ChIP-Seq profiles of Tup1 and Snf2 occupancy in the presence (wt) and absence (Tup1-AA) of Tup1 in J-browse. **B:** The level and the distance from the *FLO5* transcription start site (TSS) of Tup1 and Snf2 occupancy (in the presence (wt) and absence (Tup1-AA) of Tup1) at *FLO5*. **C:** *FLO5* transcription in the strains indicated with the peaks of MNase-Seq reads to indicate nucleosome positions at the upstream gene-free region of the *FLO5*. The arrow indicates the transcription start site (TTS).

7.2.7.1 Digital indirect end labelling analysis to show chromatin remodelling at the model 1 *FLO5* gene:

The previous figure shows the peaks according to the number of sequence reads of the DNA protected from digestion of chromatin by MnaseA, which potentially indicates nucleosome positions. It was next of interest to allocate more precisely the nucleosome positions to the MNase-seq peak profile (Fig. 7.8). To do this, the unpublished technique called 'Digital indirect end labelling (dIEL)' was used, which was devised by our collaborator, Dr Nick Kent. This technique takes into account the sequence specificity of MNaseA by comparing the chromatin MNase-seq profile with that of the MNase digested naked DNA. Specifically, this enables a nucleosome to be positioned with confidence at those sites where there is 146bp of protection (high number of nucleosome reads) in the chromatin digestion versus a site of digestion (low reads) in the naked DNA control profile. Where these criteria are met, a nucleosome can be positioned in confidence.

In the wt chromatin profile at the repressed *FLO5* gene-free upstream region, nucleosomes can be clearly allocated at the promoter and extensive upstream region. Interestingly, the nucleosomal sites beyond what might be considered the *FLO5* promoter (covering the first 1 kb upstream of the ORF) seemed to be more distinctive or 'stronger' nucleosomal positions (compare read peaks associated with the first 8 nucleosomes upstream of the ORF, with the 13 peaks further upstream) (Fig. 7.8). In the *snf2* mutant, where the *FLO5* gene is also repressed, a similar nucleosome profile to that seen in wt was evident. However, many of the peaks in the *snf2* mutant were stronger than those in wt, again suggesting stronger nucleosome positions in the *snf2* mutant chromatin compared to the wt chromatin even though *FLO5* transcription is equally repressed in both strains. In the absence of Cyc8*,* where the *FLO5* gene is highly de-repressed, very few nucleosomes could be allocated to positions with any confidence over much of the 4.7 kb upstream region. Thus, in the *cyc8* mutant, the entire gene free region upstream of *FLO5* contains severely remodelled nucleosomes. When *SNF2* was additionally deleted in the *cyc8* mutant, the double mutant nucleosomal profile reverted back to a pattern resembling the wt nucleosomal profile, albeit with a few differences around the site of previous Tup1 and Snf2 occupancy and further upstream at around -

3.7 kb. This suggests that the gross disruption of nucleosome sites seen in the *cyc8* mutant when the gene is de-repressed is a Snf2 dependent event.

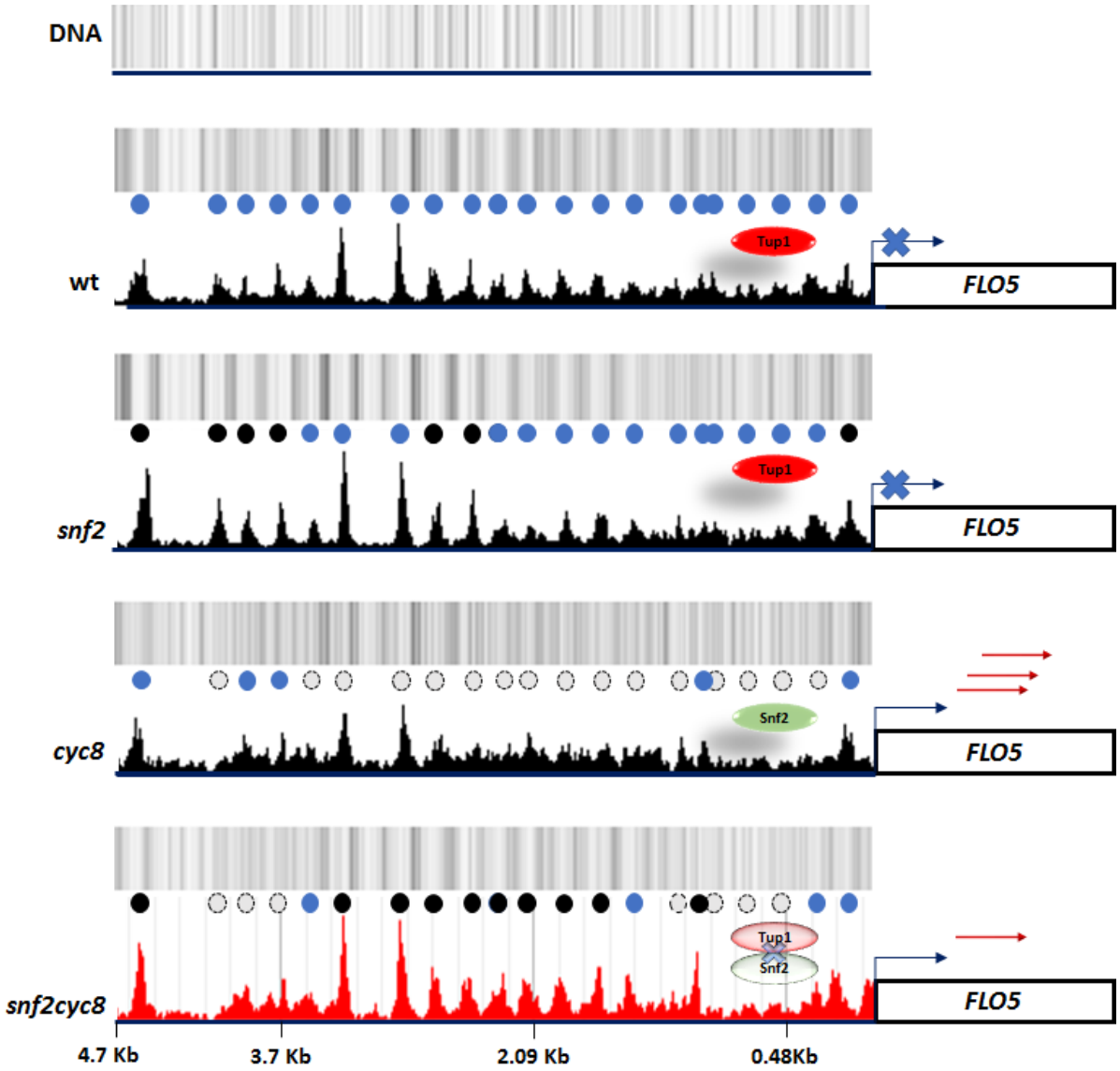
DNA
wt
Tup1
FLO5
snf2
Tup1
FLO5
cyc8
Snf2
FLO5
snf2cyc8
Tup1
Snf2
FLO5
4.7 Kb
3.7 Kb
2.09 Kb
0.48Kb

Figure 7.8 Digital Indirect End Labelling analysis to show nucleosome remodelling at the *FLO5* gene and upstream region: Digital indirect end labelling (dIEL) analysis at the *FLO5* upstream region to show nucleosome positions in the strains indicated. Mapping the region upstream of the *FLO5* gene as an example of a model 1 Swi-Snf and Tup1-Cyc8 co-regulated gene; dIEL images for naked DNA and wt, *snf2*, *cyc8* and *snf2 cyc8* chromatin are shown alongside J-browse images of MNase-seq sequencing read peaks. Blue ovals depict nucleosome positions centred according to dIEL analysis, black ovals depict where there was stronger nucleosome enrichment compared to wt. Grey dashed ovals depict 'remodelled' nucleosomes which could not be allocated according to dIEL analysis. Tup1 localisation was indicated in red and Snf2 localization in green, where appropriate.

7.2.8 The chromatin environment at the *FLO9* ORF and upstream region: An example of a 'model 2' co-regulated gene:

Chromatin remodelling at the *FLO9* gene which is an example of a gene regulated by the antagonistic action of Swi-Snf and Tup1-Cyc8 chromatin remodelling activity functioning via model 2 was next examined. In model 2 genes, both Snf2 and Tup1 occupy the wt repressed gene, whilst Snf2 is further enriched in the absence of Tup1 when the gene is active.

In wt, when *FLO9* is repressed, Tup1 was found located at – 753 bp relative to the TSS, and Snf2 was detected at -663 (Fig 7.9A, B). However, when the *FLO9* gene was strongly de-repressed in the *cyc8* mutant, Snf2 was found to be more enriched at a site within 21 base pairs of the site of previous Tup1 occupancy (Fig 7.9 A, B).

The chromatin remodelling activity was next investigated at the *FLO9* ORF and gene-free upstream region which stretches for ~7.5 kb before the next ORF. In the wt strain, in which *FLO9* is repressed, there is a strong series of peaks representing positioned nucleosomes across the entire upstream region shown (Fig 7.9 C). However, in the *cyc8* mutant in which *FLO9* is de-repressed, these peaks were almost abolished across the entire upstream region (Fig 7.9 C, compare *cyc8* and wt). When *snf2* is additionally deleted in the *cyc8* mutant, the pattern of peaks in the double *snf2 cyc8* mutant is similar to that seen in wt, except for the canonical promoter region immediately upstream of the ORF, at which the 4 peaks seen in wt are not present. This suggests that the disruption to the far upstream chromatin seen in the *cyc8* mutant is dependent upon Snf2. Interestingly, the peaks in the *snf2* mutant are even more strong than in wt, even though the gene is repressed in both strains. Overall, we can see a clear pattern of peaks which indicates strong nucleosomal positions at the extensive *FLO9* upstream region when the gene is off, that are significantly disrupted, in a largely Snf2-dependent manner, when the gene is on.

A. Chip-Seq

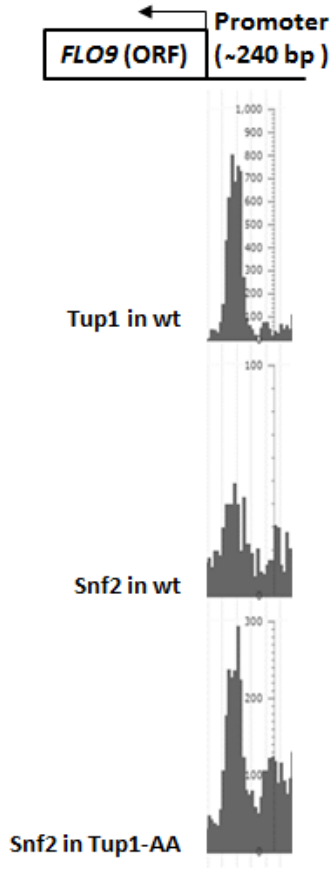

B.

FLO9	Distance From TSS (bp)	Peak score
Tup1	-753	20077.8
Snf2 in wt	-663	514.6
Snf2 in Tup1-AA	-732	2733

C. RNA-Seq MNase-Seq

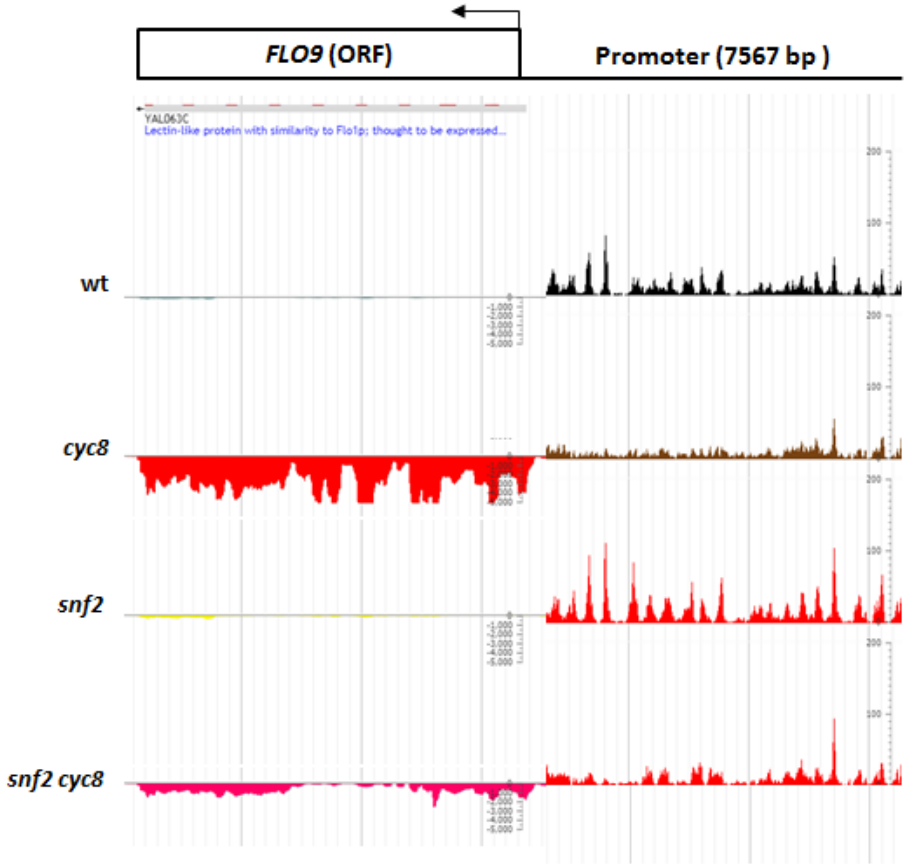

Figure 7.9 J-browse image of transcription, chromatin structure and Tup1 and Snf2 occupancy at the *FLO9* ORF and upstream region. A: ChIP-Seq profiles of Tup1 and Snf2 occupancy in the presence (wt) and absence (Tup1-AA) of Tup1 in J-browse. **B:** The level and the distance from the *FLO9* transcription start site (TSS) of Tup1 and Snf2 occupancy (in the presence (wt) and absence (Tup1-AA) of Tup1) at *FLO9*. **C:** *FLO9* transcription in the strains indicated with the peaks of MNase-Seq reads to indicate nucleosome positions at the upstream gene-free region of the *FLO9*. The arrow indicates the transcription start site (TTS).

7.2.8.1 Digital indirect end labelling analysis to show chromatin remodelling at the model 2 *FLO9* gene:

To clearly visualise the chromatin remodelling at the model 2 *FLO9* gene, the unpublished technique of 'Digital indirect end labelling (dIEL)' analysis was used, which was devised by our collaborator, Dr Nick Kent.

When *FLO9* was repressed in wt, the nucleosomes can be clearly assigned at the promoter and extensive upstream region (Fig 7.10). Interestingly, the nucleosomal sites beyond what might be considered the canonical *FLO9* promoter (covering the first 1 kb upstream of the ORF) appear to contain stronger nucleosomal positions in a manner which was similar to that of *FLO5* (compare read peaks associated with the first 10 nucleosomes upstream of the ORF, with the 7 peaks further upstream). In the *snf2* mutant at which *FLO9* is also repressed, a similar nucleosome profile to that shown in wt was evident. However, many of the nucleosomes were more distinct in the *snf2* mutant than those in wt, suggesting stronger nucleosome positions in the *snf2* mutant's chromatin compared to the wt's chromatin even though *FLO9* transcription is equally repressed in both strains.

In contrast, when *CYC8* was deleted and *FLO9* is de-repressed, very few nucleosomes could be assigned to positions with any confidence over much of the 7.5 kb upstream region. Thus, in the absence of *cyc8*, the entire gene free region upstream of *FLO9* contains strongly remodelled nucleosomes. When *SNF2* was additionally deleted in the *cyc8* mutant, the double mutant far upstream nucleosomal profile reverted to a pattern resembling the wt nucleosomal profile, whilst around the site of previous Tup1 and Snf2 occupancy and further upstream at around -3 kb and 5 Kb, the nucleosome profile was less pronounced than in wt. This suggests that the majority of the disruption of nucleosome sites seen in the *cyc8* mutant when the *FLO9* gene is de-repressed is a Snf2 dependent event.

The *GCN3* gene, which encodes the alpha subunit of translation initiation factor eIF2B, was used as a negative control of Tup1-Cyc8 and Swi-Snf activity where the nucleosomes were found to be organised at the gene promoter in wt, *snf2*, *cyc8* and *snf2 cyc8* mutants with no obvious changes evident (Fig. 7.11).

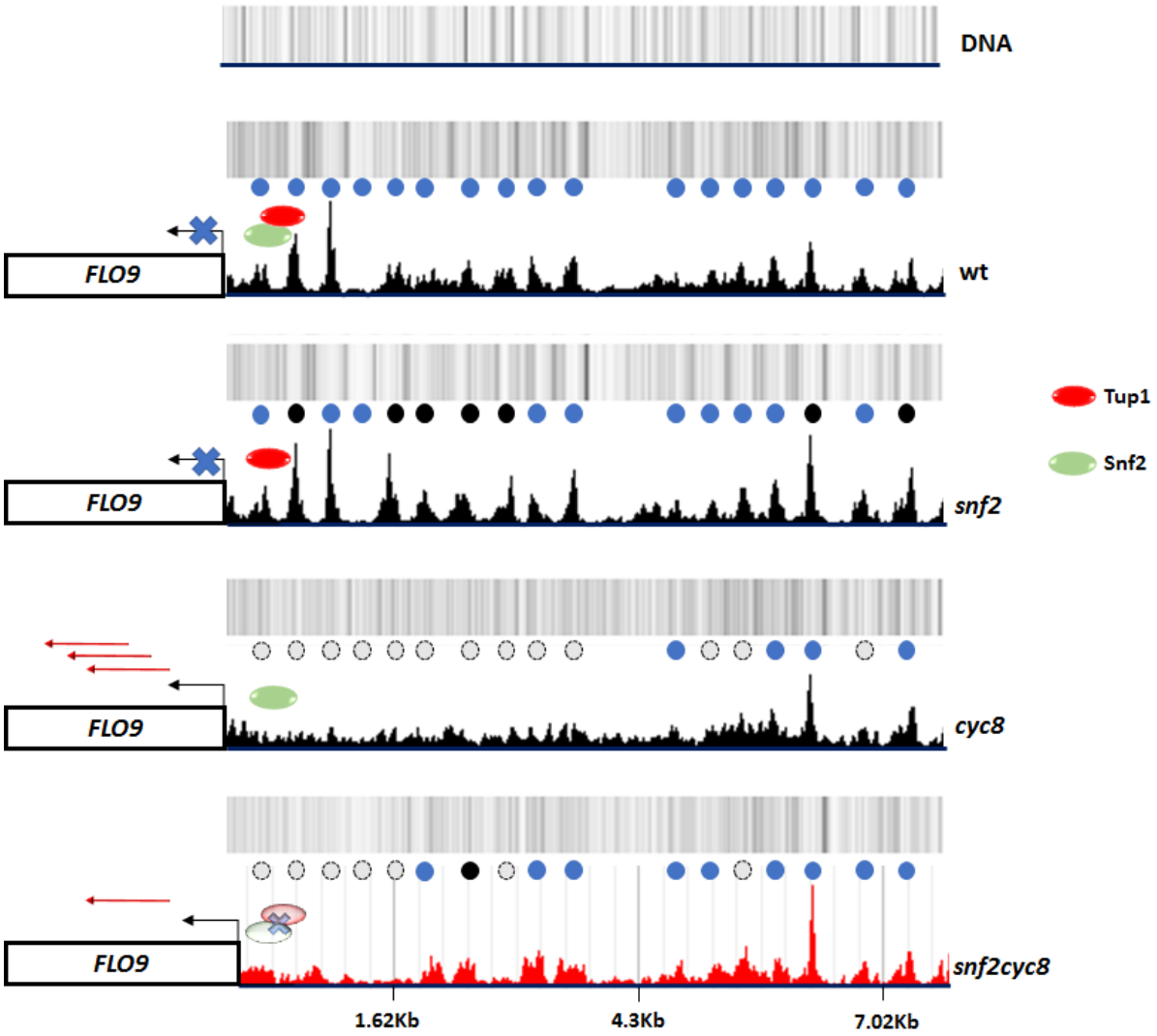
DNA
FLO9
wt
FLO9
snf2
Tup1
Snf2
FLO9
cyc8
FLO9
snf2cyc8
1.62Kb
4.3Kb
7.02Kb

Figure 7.10 Digital Indirect End Labelling analysis to show nucleosome remodelling at the *FLO9* gene and upstream region: Digital indirect end labelling (dIEL) analysis at the *FLO9* upstream region to show nucleosome positions in the strains indicated. Mapping the region upstream of the *FLO9* gene as an example of a model 1 Swi-Snf and Tup1-Cyc8 co-regulated gene, dIEL images for naked DNA and wt, *snf2*, *cyc8,* and *snf2 cyc8* chromatin are shown alongside J-browse images of MNase-Seq sequencing read peaks. Blue ovals depict nucleosome positions centred according to dIEL analysis, Black ovals depict where there was stronger nucleosome enrichment compared to wt. Grey dashed ovals depict 'remodelled' nucleosomes which could not be allocated according to dIEL analysis. Tup1 localisation was indicated in red and Snf2 localization in green, where appropriate.

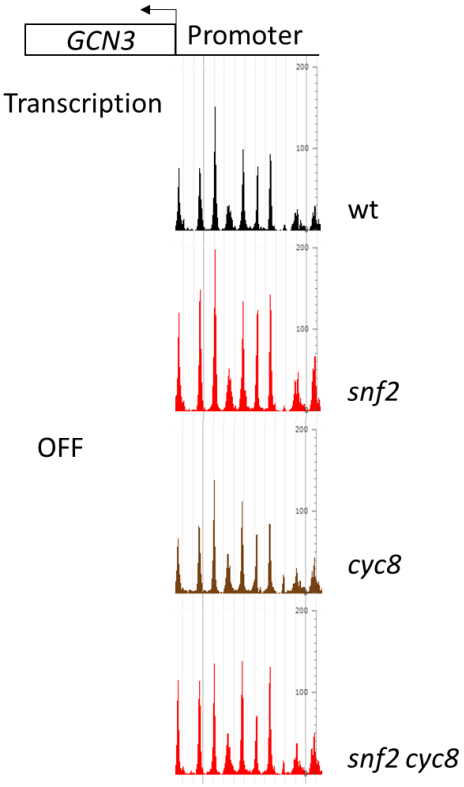

Figure 7.11 Negative control gene for nucleosome remodelling. *GCN3* gene as a negative control for the organisation of nucleosomes at a gene promoter in wt, *snf2*, *cyc8* and *snf2 cyc8* mutants.

7.2.9 Discussion:

The RNA transcriptome data in chapter 5 observed 575 (8.7%) genes which were upregulated in the *cyc8* mutant, suggesting that Tup1-Cyc8 act as a repressor in these genes. The transcriptome data also defined 278 genes that were downregulated in a *snf2* mutant, suggesting that Swi-Snf acts as an activator of these genes. This study also identified 102 Tup1- Cyc8 and Swi-Snf co-regulated genes. Chapter 6 then analysed ChIP-Seq data for the Tup1 and Snf2 proteins to correlate occupancy of these proteins with the genes identified in chapter 5 that were under their control. Thus, the genes subject to activation by Swi-Snf, and repression by Tup1-Cyc8 were identified, and it was further shown at which of these genes Tup1 and Snf2 could be found.

The nucleosome organization along gene promoters has a fundamental role in the regulation of gene expression. Previously, the chromatin-mediated co-regulation of transcription by Tup1-Cyc8 and Swi-Snf had been investigated at only a handful of genes including the *FLO1* and *SUC2* genes (Fleming & Pennings, 2001; Fleming & Pennings, 2007). In this chapter, the global nucleosome positions were mapped in wt and the *snf2*, *cyc8,* and *snf2 cyc8* mutants to uncover the antagonistic chromatin remodelling activities of the Swi-Snf and Tup1-Cyc8 complexes at their target genes. This therefore concludes the analysis to reveal which genes are subject to Swi-Snf and Tup1-Cyc8 regulation, where the complexes bind across the genome and to show what the complexes do to chromatin at the genes under their control.

Prior to mapping the nucleosome positions in the Tup1-Cyc8 and Swi-Snf complex mutants, western blot analysis of histone levels in the mutants was performed as a control to determine if there were any differences in the global levels of the nucleosome core proteins. The result observed that the core histone protein levels and H1 were unaffected in the mutants (Fig. 7.2).

The bulk chromatin structure was next analysed in the various strains by performing Micrococcal nuclease (MNase) digestion on isolated nuclei (Fig. 7.3). MnaseA digests the linker region between nucleosomes, and compares the rate, and the extent of chromatin digestion between strains, which can be used to reveal if the strains have major differences in global chromatin architecture.

The results showed that chromatin in the *cyc8* and *snf2 cyc8* mutants was more accessible to MNase digestion suggesting Tup1-Cyc8 might have a global effect on stabilising chromatin.

To define the genome-wide nucleosome maps in wt and the *cyc8*, *snf2* and *snf2 cyc8* mutants, the DNA purified from the MNase digestion of their chromatin sent was sequenced (Fig. 7.4). Initial analysis confirmed that the quality of the nucleosomal mapping data obtained was high (Fig. 7.5).

Subsequent analysis of the MNase-Seq data showed that there was no apparent difference in gross nucleosome structure around gene start sites in any of the mutants analysed (Fig. 7.6). This was in contrast to the results of the agarose gel showing bulk chromatin digestion by Mnase, which had suggested chromatin from strains containing a *cyc8* gene deletion were more sensitive to digestion, indicating a possible more 'open' chromatin structure in this mutant background. This result is not surprising as the chromatin digestion of nuclei used for the agarose gel analysis is very crude and can be influenced by errors in the efficiency of sphearoplasting used to release the nuclei, and differences in the amount of nuclei used as starting material for the digestion (Dunn & Wobbe, 1993). In addition, other studies had also shown that loss of Tup1, Cyc8 and Snf2 only affected chromatin at distinct sites, and not globally (Kaifu Chen *et al*. 2013; Dutta *et al*. 2014).

The previous chapter (chapter 6) showed direct evidence for two possible modes of action for Tup1-Cyc8 and Swi-Snf gene regulation. In model 1, Snf2 is recruited to gene promoters when Tup1 was absent. Conversely, in model 2, Snf2 occupancy is further enriched at gene promoters where Snf2 and Tup1 were already present. 17 genes were shown to behave via model 1 (see Table 6.11), while just three genes were shown to behave via model 2 (see Table 6.12). Interestingly members of the *FLO* gene family were present in each of the two types of co-regulated genes; *FLO5* was under model 1 type control, and *FLO9* was under model 2 type control. Interestingly, both genes contained large upstream regions that were gene free and which were occupied by strongly positioned nucleosome in the wt strain when the gene was off.

In the *snf2* mutant, where both genes were again repressed, the nucleosome positions across the gene promoters and extensive upstream regions were even stronger. Strikingly, in the *cyc8* mutant, in which both *FLO9* and *FLO5* are strongly de-repressed, the nucleosome positions were almost completely abolished over the entire upstream region. Finally, in the *snf2 cyc8* double mutant, where transcription was again severely reduced, many of the nucleosome peaks (but not all) were reinstated suggesting the remodelling seen in the absence of Cyc8 is due to Snf2 (Fig. 7.7).

Digital indirect end labelling analysis was applied for better visualisation of nucleosome positions at the *FLO5* and *FLO9* promoter and gene free upstream regions. The nucleosome mapping detected an array of about 21 nucleosomes organized over the *FLO5* promoter and upstream region in repressed wt strain (Fig. 7.8). In the *snf2* mutants, in which the transcription was again repressed, the nucleosomes were even more enriched in four positions between the -3.7 to -4.7Kb upstream region compared to wt. In the *cyc8* mutant 16 nucleosomes out of 21 were remodelled via the action of Swi-Snf (Fig. 7.8).

At the model 2 type *FLO9* gene, in which Snf2 and Tup1 are both present at the repressed promoter, 17 nucleosomes were found to be organised across the promoter and upstream region in wt (Fig. 7.10 wt). In the *snf2* mutant the data showed an increase in the occupancy of 4 nucleosomes between the region of -1.6 to -2.9 Kb relative to the gene start site. In the absence of *cyc8* the action of Swi-Snf was to remodel 13 of these nucleosomes over a region from the TSS to -4.3 Kb upstream

The results for the antagonistic chromatin remodelling observed at *FLO5* and *FLO9* via the activity of Tup1-Cyc8 and Swi-Snf was compatible with the published results at the *FLO1* and *SUC2* genes which also showed remodelling over large upstream regions (Fleming & Pennings, 2001; Fleming & Pennings, 2007). Thus, this study has expanded on the number of genes go-regulated by these complexes and provided in depth insights into the activities of these complexes at specific promoters.

Chapter 8

Final Discussion

8.1 Discussion:

Eukaryotic chromatin was first identified by Walther Flemming as the structure which compacted the DNA into the cell nucleus. However, many recent studies have concentrated on how the structure of chromatin regulates the transcription of the genes. Additionally, studies have shown that chromatin is essential in regulating cell development and contributing to many human cancers as well as aging (Morgan & Shilatifard, 2015; Purohit & Chaturvedi, 2017).

The are many ways that chromatin can be remodelled to alter its structure and function. This study focused on the Swi-Snf and the Tup1-Cyc8 chromatin remodelling complexes which are best known for their roles in regulating gene transcription. Swi-Snf was the first ATP-dependent chromatin remodelling complex discovered, where it can function as an activator of gene expression. Although first found in yeast, it is conserved from yeasts to human cells (Winston & Carlson, 1992). Swi-Snf has been linked to many human diseases such as cancer. It has been proposed that abnormalities in this complex are found in 20% of all human tumours, making the Swi-Snf complex a potentially very important factor in cancer biology. Mutants in the *SNF5* gene, also known as *SMARCB1* in human cells, are a defining molecular feature of childhood malignant rhabdoid tumours (Lu and Allis 2017; Sen *et al*. 2017).

Conversely, the Tup1-Cyc8 complex was the first global co-repressor of transcription identified in yeast. Tup1-Cyc8 is also conserved in flies, worms and mammals, and controls of wide variety of important genes linked to many diseases. Studies have suggested that Tup1-Cyc8 interacts with the Swi-Snf complex to regulate gene transcription (Liu and Karmarkar 2008; Payankaulam *et al*. 2010). Indeed, the antagonistic chromatin remodelling and regulation of the *SUC2* and *FLO1* genes has been reported (Fleming and Pennings 2001; Fleming and Pennings 2007). However, the total number of genes under the antagonistic control of both Tup1-Cyc8 and Swi-Snf is not known.

The aim of this study was to identify in yeast precisely which genes are co-regulated by these complexes, where these genes are located on the genome, and how the chromatin at these genes is remodelled.

8.2 The Swi-Snf complex sub-units have distinct roles:

The Swi-Snf complex contains 12 subunits, initial experiments sought to investigate which Swi-Snf subunit has the most impact on the cell by investigating whether there were different phenotypes in strains containing single deletion mutations of each subunit. Therefore, a number of phenotypic analyses were carried out to investigate the behaviour of each Swi-Snf sub unit mutant compared with wt *Saccharomyces cerevisiae*.

Five Swi-Snf subunit activities were investigated by constructing yeast mutants deficient for each subunit encoding gene. The strains used included *snf2, swi3*, *snf5*, *snf6* and *snf11* full gene deletion mutants and a *snf2K798A* mutant which contains a lysine to alanine amino acid substitution at residue 798 of Snf2 and is catalytically dead (Martens & Winston, 2002). The study observed that when the mutant cells were grown in different sources of carbohydrate, the *snf2* and *snf5* mutants had the slowest growth rate, suggesting these sub units had a greater role upon general cell health (Fig. 3.1).

The cell morphology of the mutant cells also varied. The *snf2* and *snf2K798A* mutants had cells which formed small clumps of between five and ten cells, whereas the *swi3* mutant showed a large cell morphology. Most strikingly the *snf6* and *snf11* mutants had an elongated sausage-shape cell morphology (Fig. 3.6). These data suggest differing roles of the Swi-Snf sub units upon cell wall metabolism and suggest that Snf2 plays a role in cell separation.

Analyses was also carried out to investigate the survival of the mutants under different environmental stresses. This study first investigated the cellular growth in the presence of DNA damaging reagents, whereby the cells were growing in the presence of the DNA damaging reagent, methyl methanesulfonate (MMS). By this assay, the *snf6* showed the greatest sensitivity compared to wt, while intriguingly, the other Swi-Snf mutants grew even better than wt in the presence of the drug. This result was interesting and might suggest that the DNA damage repair mechanisms in these mutants are being by-passed. A prediction of this would be that these apparently more resistant mutants would actually be accumulating more DNA damage. Such a mutant phenotype, if occurring in the same subunits in the human Swi-Snf complexes, would be good candidates for making a major contribution to cancer. When the DNA damaging reagent, hydroxy urea

(HU) was applied the cells, *swi3* showed the greatest sensitivity to this drug, followed by *snf2* (Fig. 3.7). It was then investigated how the mutants responded to caffeine, which is a cell wall damaging reagent (Kuranda *et al*., 2006). The results indicated that *snf2*, *swi3* and *snf6* were the most sensitive Swi-Snf mutants to this reagent which was consistent with the cell morphology data, and the work of others (Chai *et al*. 2005)(Fig. 3.8).

Thus, these experiments were aimed to determine which subunit of the Swi-Snf remodelling complex has the most impact on yeast cells, and to show the different phenotypes of each mutant. The results suggest that the catalytic mutant, *snf2* was the best sub unit mutant to examine further, as it was shown to have the most phenotypic impact in the experiments performed. However, I also chose to pursue the *snf2K798A* catalytic dead mutant, and the *swi3* and *snf5* mutants which also showed some interesting phenotypes.

8.3 The impact upon cell function of Swi-Snf subunit mutants with Tup1-Cyc8 deficient strains:

The main aim of this study was to investigate the impact of Swi-Snf and Tup1-Cyc8 on chromatin remodelling, and to identify the genes under the antagonistic control of these complexes. However, in Chapter 3, it was observed that the Swi-Snf subunit mutants have a different phenotype. Indeed, the results suggested that the *snf2*, *snf2K798A*, *swi3* and *snf5* mutants each showed distinct phenotypes and were each therefore worth investigating further. The Tup1-Cyc8 complex consists of four Tup1 subunits and one Cyc8 subunit, previous studies had shown that deletion of Cyc8 resulted in loss of Tup1 from the *FLO1* promoter making this gene deletion the best candidate to cripple the Tup1-Cyc8 complex (Fleming *et al*., 2014). However, in order to study the transcriptional interplay between Swi-Snf and Tup1-Cyc8, the choice of Swi-Snf sub unit to delete together with the Cyc8 gene deletion was not clear. Therefore, double mutants deficient for b *cyc8* and either *snf2*, *snf2K798A*, *swi3* or *snf5* were investigated to determine which double mutant would be best to use for the final analysis.

The best known examples of genes whose regulation is under the antagonistic mechanism of Tup1-Cyc8 as a repressor, and Swi-Snf as an activator, are the *FLO1* and

SUC2 genes (Fleming and Pennings 2007; Fleming and Pennings 2001). The transcription levels of these genes in each single, and double mutant was therefore first investigated. In the single, *snf2*, *snf2K798A*, *swi3* and *snf5* mutants it was observed that *FLO1* and *SUC2* were repressed, as expected due to the presence of the repressor Tup1-Cyc8 (Fig. 4.2). While in the *cyc8* deletion mutant, *FLO1* and *SUC2* were highly de-repressed, due to loss of the repressor and the presence of Swi-Snf as an activator (Fig. 4.2). Subsequent analysis of *FLO1* and *SUC2* gene transcription in the different double mutants (*snf2 cyc8*, *snf2K798A cyc8* and *swi3 cyc8*) showed that the Swi-Snf sub units did make different contributions to the de-repression of the genes. Surprisingly, although Snf2 and Swi3 were required for *FLO1* and *SUC2* transcription in the absence of Cyc8, Snf5 was not required as much. Indeed, the results might suggest that the remaining subunits of the Swi-Snf can remain largely functional in the absence of the Snf5 sub unit (Fig. 4.2).

It was next investigated whether the complexes regulated expression of their own, or each other's subunit encoding genes. The transcription levels of *CYC8*, *SNF2*, *SWI3* and *SNF5* were therefore examined in the various mutants (Fig. 4.3). The result indicated no difference in level of the transcription for all the genes in all mutants relative to actin, suggesting that these two complexes do not regulate each others genes, or their own genes transcription.

Swi-Snf and Tup1-Cyc8 protein levels were next investigated by Western immunoblotting in the various gene deletions to confirm that there was no regulation of each others sub unit encoding genes expression (Fig. 4.4). Surprisingly, whereas RT-qPCR suggested *CYC8* mRNA levels were unaffected compared to wt in a *swi3* mutant, Cyc8 protein levels were almost undetectable in the absence of Swi3. This result could suggest that there is a direct interaction between Swi-Snf and Tup1-Cyc8, in which the Swi3 effects the stability of the Cyc8 protein (Fig. 4.5). Alternatively, a growth defect in the Swi3 mutant might cause loss of the Cyc8 protein similar to what occurs in yeast cells after glucose depletion (unpublished data).

Either way, these results suggested that the *snf5* and *swi3* mutants would not be the best candidate mutants to use for further analysis. I therefore focussed on the mutants deficient for Snf2, which is the catalytic heart of the Swi-Snf complex (Dutta *et al*., 2017). Specifically, I chose to analyse both the Snf2 full gene deletion in which the rest of the

Swi-Snf complex becomes unstable, and the *snf2K798A* mutant which is functionally dead but where the complex remains intact (Dutta *et al*. 2017; Martens & Winston, 2002).

The next series of experiments focused on phenotypes of the *cyc8* and *snf2* single and *snf2 cyc8* double mutants. The growth rate in YPD media showed that the mutants had varying growth defects in terms of doubling time and the maximum cell density reached with the (Fig. 4.6). The microscopic analysis revealed that the *cyc8* cells were tightly compacted which correlated with their strong flocculation phenotype whereas the *snf2 cyc8* double mutants showed less aggregation. These result support the role of Swi-Snf and Tup1-Cyc8 in the transcription of *FLO1*. The level of the transcription of *SUC2* encoding an invertase was also examined (Fig. 4.13). This gene is under repression of Tup1-Cyc8 under high glucose media (2%), and it is activated by Swi-Snf under low glucose levels (0.05%) (Ozcan *et al*. 1997). The results indicated that in *cyc8* mutants the *SUC2* was highly de-repressed in high and low level of glucose, while it was repressed in the absence of *snf2*. In *snf2 cyc8* the transcription of *SUC2* was lower than that of wt. This confirmed the study that *SUC2* is also under the antagonistic mechanism of Tup1-Cyc8 and Swi-Snf (Fleming & Pennings, 2007).

Thus, these analyses indicated that the *snf2* mutants were ideal candidates for further analyses to determine (i) how many genes are under Tup1-Cyc8 and Swi-Snf control and (ii)to investigate how chromatin is remodelled at these genes.

8.4 Global transcription profile in Tup1-Cyc8 and Swi-Snf:

The Tup1-Cyc8 and the Swi-Snf complexes have been studied in detail. However, the exact number of genes these complexes co-regulate is not known. The antagonistic mechanism of Tup1-Cyc8 and Swi-Snf regulation of gene transcription has been studied in detail at just two genes. These genes are *FLO1* and *SUC2*, which are induced under certain stress condition (Lahtvee *et al*. 2011). *FLO1* is involved in cell-cell adhesion, saving the cells from external environmental stresses, and is important during the industrial fermentation process. *SUC2* is induced under glucose starvation conditions. These genes also have a unique feature in that they located at subtelomeric regions and studies have shown that the remodelling activities of Tup1-Cyc8 and Swi-Snf occur over

the gene promoters and an extensive (~5 kb) region upstream of the gene. Thus, these subtelomeric genes have been described as being subject to 'long-range' chromatin remodelling by Tup1-Cyc8 and Swi-Snf (Fleming and Pennings 2007; Fleming and Pennings 2001). This led to the hypothesis that Tup1-Cyc8 and Swi-Snf would robustly regulate other inducible sub telomeric genes via long range chromatin remodelling events at the promoter and extensive upstream regions. Indeed, it would only be at sub telomeric regions where this long-range remodelling could occur as the gene density is low in these regions compared to the relative high gene density in the rest of the *S. cerevisiae* genome.

This research aimed to identify the Tup1-Cyc8 and Swi-Snf co-regulated genes by first examining the global transcription change in the Swi-Snf catalytic subunit *snf2* full deletion mutant, the *snf2K798A* catalytically dead mutant, and also the *cyc8* mutant in order to cripple the Swi-Snf and Tup1-Cyc8 complexes respectively. To identify the co-regulated genes, this study also determined the transcription profiles in the *snf2 cyc8* and *snf2K798A cyc8* double mutants and compared them to the profiles in the single mutants. Importantly, this research also aimed to determine whether there was any difference in the regulatory ability between the *snf2* full deletion, when the complex should full apart, compared with the catalytic dead mutant, when the complex is intact but lacking the ATPase activity and inactive. This was to discover whether the remaining Swi-Snf complex subunits can regulate transcription independent of the Snf2 ATPase activity.

The results revealed that 575 genes (8.7% of all genes) were upregulated in the *cyc8* mutant by more than 2-fold, suggesting that these genes required Tup1-Cyc8 to be repressed (Fig. 5.4 and Table 5.1). Intriguingly, the data also showed that 158 genes (2.3% of all genes) were downregulated in the *cyc8* mutant by at least 2-fold, suggesting that these genes were activated by Tup1-Cyc8 (Fig. 5.4 and Table 5.2).

The Tup1-Cyc8 is best known as a repressor for genes induced in response to stress (Smith & Johnson, 2000). In yeast cells, by using gene ontology analysis, I identified a wide variety of gene families that were subject to regulation by Tup1-Cyc8 (Fig. 5.6). The most statistically significant gene family identified were those involved in drug metabolism such as gene involved in vitamin synthesis or in response to antibiotics. The

BIO gene family was an example of this, and included the *BIO2*, *BIO3* and *BIO5* genes which are involved in Biotin synthesis (Hall *et al*. 2005; Hall and Dietrich 2007). The reference strain of *S. cerevisiae* is auxotrophic for biotin and requires uptake of this vitamin from the external medium, a recent study showed that a strain of sake yeast has the ability to synthesise Biotin due to the presence of *BIO6* gene (Wu *et al*. 2005). Interestingly, evidence has shown that the *BIO3* gene was acquired by horizontally gene transfer (HGT) from bacteria (Hall *et al*. 2005; Hall and Dietrich 2007). The fact that these genes are under the repression of Tup1-Cyc8, illustrates how Tup1-Cyc8 is involved in the evolution of a biochemical pathway for one of the important vitamins for yeast (Pinon *et al*. 2005; Zempleni *et al*. 2009).

The second important term in biological processes was the category, about 60 genes involved cell wall organisation were also shown to be subject to repression by Tup1-Cyc8. An example these genes are the *FLO* gene family, which includes *FLO1*, *FLO5*, *FLO9*, *FLO10* and *FLO11*, these genes are responsible for the flocculation phenotype caused by cell-cell interaction in the presence of the Ca^{+} (Soares, 2011). The *FLO* genes are induced by stress responses to many environmental factors such oxygen and pH. These genes are also very important in industrial processes such as fermentation and for biofilm formation (Soares, 2011). The *FLO1*, *FLO9* and *FLO10* genes are all located in subtelomeric regions, making them of interest for studying how their chromatin is remodelled during activation and repression (Teunissen & Steensma, 1995). Other cell wall relevant genes such as *DAN*, *TIR, UTR* and *PAU* were also subject to repression by Cyc8 (Fig. 5.9).

Thus, many of the genes under the repression of Tup1-Cyc8 encoded products which were involved in cell wall organisation (Fig. 5.9), are important for maintaining cell shape, protecting cells from the external environment, preparation for sporulation, and for remodelling the cell wall prior to entering stationary phase (Aguilar-Uscanga & Francois, 2003).

Another large gene family repressed by Tup1-Cyc8 were those involved in carbohydrate uptake and metabolism (Fig. 5.6). The best-studied example of these is *SUC2*, which is involved in sucrose metabolism (Fleming & Pennings, 2007; Neigeborn & Carlson, 1984).

This gene is important for the organism to survive and adapt to conditions of nutrient deprivation.

Other genes of interest repressed by Tup1-Cyc8 include the *ASF1* gene which encodes a histone chaperone involved in nucleosome assembly during DNA replication and transcription (English *et al*. 2006). Thus Tup1-Cyc8 could indirectly regulate global nucleosome dynamics during transcription and DNA replication. There were also genes encoding transcription factors including *NRG1* and *NRG2*, which were repressed by Tup1-Cyc8 and which are involved in regulating transcriptional responses to carbohydrate levels. The transcriptomic data also identified *XBP1* which encodes a stationary phase-specific transcriptional repressor responsible for shutting down 15% of the genes involved in cell growth and metabolism following glucose depletion (L. Li *et al*. 2013; Miles *et al*. 2013). Therefore, Tup1-Cyc8 can also be seen to be important for preventing the inappropriate repression of genes during active cell growth by repressing the Xbp1 repressor.

These data are consistent with previously published data sets which show how Tup1-Cyc8 controls of vast variety of genes involved in many important biochemical pathways in yeast (Chen *et al*. 2013; Smith & Johnson, 2000).

Although Tup1-Cyc8 is best known as a repressor our data observed 158 genes that were repressed in the absence of *cyc8*, suggesting that Tup1-Cyc8 can also act as an activator. The gene ontology analysis was applied to these genes (Fig. 5.7). A study by (Conlan *et al*. 1999) showed that Tup1-Cyc8 can shift from mediating repression to promoting activation at a the citrate synthase *CIT2* gene. Here, Tup1-Cyc8 interacted with the Rtg3, DNA binding activator at the promoter of *CIT2* to activate transcription. Consistent with this data, out transcriptomic data revealed that this gene was down-regulated 7.4-fold in the *cyc8* mutant.

With regards Swi-Snf, the global RNA transcriptome data indicated that 278 (4.2% of total) genes were down regulated at least 2-fold in the *snf2* mutant, suggesting that these genes required Swi-Snf as an activator. On the other hand, the data also observed 208 (3.5% of total) genes were up-regulated at least 2-fold in the absence of *snf2*, suggesting that Swi-Snf was acting as a repressor at these genes.

Swi-Snf is an activator for 278 genes which were determined to be involved in many roles in the yeast cell. The gene ontology analysis of the 278 genes for which Swi-Snf is required as an activator of transcription were classified into three categories; biological process, molecular function and cellular component (Fig. 5.17).

In the biological process category, the majority of the genes activated by Swi-Snf were classified as having transmembrane transporter activity like the zinc transporter encoding *ZRT1* gene and the amino acid transporter encoding *AGP1* gene (Fig. 5.17). In the molecular function category, most of the genes were classified as having catalytic activity like the ergosterol biosynthesis gene, *ERG5*. In the molecular component category, most of the genes encoded products which were located at the plasma membrane, reflecting the previous result in the biological process category. These data were consistent with previous published data sets (Dutta *et al*. 2014,2017).

Although Swi-Snf is best known as an activator of transcription, our data observed that 208 genes were de-repressed in the *snf2* mutant, suggesting that these genes required Swi-Snf as a repressor. Many of these genes were categorised as being involved in 'metabolic processes' and included the *SER3* gene. *SER3* encodes a phosphoglycerate dehydrogenase involved in serine biosynthesis and is a known example of a gene at which Swi-Snf has been shown to directly repress its transcription (Martens & Winston, 2002).

One of the aims of this study was to identify whether Swi-Snf predominantly requires the Snf2 ATPase activity for its action, or whether the structural integrity of the complex is more important for function. Thus, the study compared the *snf2* full deletion, where the SWI-SNF complex falls apart with *snf2K798A* catalytic dead mutant, in which the complex is functionally dead, but intact (Martens & Winston, 2002). The results indicated only 55 and 25 genes were uniquely down regulated in the *snf2* and *snf2K798A* mutants, respectively (Fig. 5.27). Based on this, the results suggest that there was no obvious difference in impact upon the cell whether *snf2* was fully deleted, or just crippled for activity. Together, these data suggest that the main activity of this complex requires the ATP hydrolysation activity.

A fundamental aim of this project was to identify the co-regulated genes that were under the antagonistic control of Tup1-Cyc8 as a repressor and Swi-Snf as an activator. To identify this set of genes, the genes which were upregulated more than 2-fold in the *cyc8* mutant were compared, with the genes which were downregulated at least 2-fold in the *snf2* single and *snf2 cyc8* double mutants (Fig. 5.33). The results indicated that 102 genes were under the antagonistic control of Tup1-Cyc8 and Swi-Snf.

When the genes ontology analysis was applied to the co-regulated genes, most of the genes were categorised under the 'cell wall organisation' category (Fig. 5.36). Gene products which are localised to the cell wall, are often important in responding to environmental stimuli, and are therefore important for cell life. Some examples include the *DAN1* gene and *FLO* and *TIR* gene families which include *TIR1*, *TIR2* and *TIR3* which are expressed under anaerobic condition, and in response to cold shock. These latter genes have been shown to be repressed under aerobic conditions by Tup1-Cyc8 (Abramova *et al*. 2001).

Analysis of the location of the co-regulated genes showed that 31 of these genes (30.1%of co-regulated genes) were located at subtelomeric regions and that they were highly repressed in the *snf2 cyc8* mutant compared to the *cyc8* mutant (Fig. 5.38). This was consistent with the sub telomeric location of the *FLO1* and *SUC2* co-regulated genes which had previously been characterised (Fleming and Pennings 2007; Fleming and Pennings 2001).

When the analysis to identify the co-regulated genes was performed using the *snf2K798A* mutant instead of the *snf2* full gene deletion mutant, the data revealed 77 co-regulated genes (Fig. 5.42). When this set of 77 genes was compared to the 102 in *snf2 cyc8* co-regulated genes, the results showed that the bulk of the genes overlapped (Fig. 5.43). This suggested therefore that there was no significant difference in the co-regulated genes when using a *snf2* full gene deletion or the catalytically dead *snf2K798A* mutant for the analyses, again suggesting that Snf2 ATPase activity, rather than Swi-Snf complex integrity, is more important in determining Tup1-Cyc8 and Swi-Snf co-regulation of transcription.

One hypothesis as to why co-regulated genes were predominantly located in the sub-telomeric regions was that the Tup1-Cyc8 and Swi-Snf complexes could remodel chromatin over extensive regions, as had been seen at *SUC2* and *FLO1*, in these locations to elicit stronger transcriptional control. One prediction of this hypothesis would be that the co-regulated genes showing the most robust regulation would have much larger gene free upstream regions (or promoters) to enable this level of regulation. However, an analysis of the promoter size of each gene plotted against the fold decrease in transcription of that gene in the *snf2 cyc8* mutant revealed no relationship between promoter size and transcription (Fig. 5.41). Thus, although the locations of genes which are co-regulated by Tup1-Cyc8 and Swi-Snf are enriched in subtelomeric regions, the extent of the upstream region that is gene free in these gene sparse locations has no impact upon the level of regulation of target gene transcription by Swi-Snf and Tup1-Cyc8. The significance of the co-regulated genes being predominantly located in subtelomeric regions might therefore be due to some other chromatin feature found at these sites, such as the histone deacetylation status in these regions (Church & Fleming, 2017).

8.5. Swi-Snf and Tup1-Cyc8 occupancy at target genes:

The transcription changes observed in Tup1-Cyc8 and Swi-Snf deficient strains could be due to indirect effects of either Tup1-Cyc8 or Swi-Snf upon gene transcription. To identify the direct target genes for Tup1-Cyc8 and Swi-Snf activity I correlated the published localization data of these complexes with the genes shown to be under their joint control.

The Snf2 global ChIP-Seq data was therefore compared to the *snf2* RNA-Seq transcription data to examine the association of Snf2 at the genes downregulated in a *snf2* mutant. Our analysis revealed that out of the 278 genes downregulated in a *snf2* mutant, only 27 genes had peaks of Snf2 associated with them, suggesting that these genes were under the direct control of Swi-Snf as a co-activator (Fig. 6.1). Snf2 was located in gene promoters at all of these 27 genes.

Swi-Snf is best known as a co-activator of transcription. However, the *snf2* transcription profile also revealed 208 genes that were upregulated in the absence of *SNF2,*

suggesting these genes require Swi-Snf as a repressor (see Fig. 5.15 and Table 5.4). Snf2 occupancy was found at only 19 of these genes which were 2-fold upregulated in a *snf2* mutant, and 23 genes when the cut off for up regulation was reduced to a 1.5-fold increase (Fig. 6.6). One such gene where Snf2 was found and where it was required for repression was the *SER3* gene, which encodes a product known to be regulated via a Swi-Snf dependent transcript run-through event (Albers *et al*. 2003; Martens & Winston, 2002). Interestingly, although Snf2 was located predominantly at promoters at these 'repressed' genes, 7 genes showed Snf2 occupancy in their open reading frames (ORFs).

From the RNA-Seq data in the *cyc8* mutant, Tup1-Cyc8 was observed to be a transcriptional repressor for 575 genes. However, Tup1 occupancy was observed to be associated with only 175 of these genes suggesting that these genes were directly repressed by Tup1-Cyc8 (Fig. 6.2). At these repressed genes, Tup1 was found to be associated with 146 promoters, 20 open reading frames and 9 intergenic regions. Notable by their absence in this list of Tup1 occupancy at Tup1-Cyc8 repressed genes were the *FLO1* and *SUC2* genes.

Tup1-Cyc8 was also shown to act as an activator at 158 genes which were downregulated in *cyc8* mutants by at least 2-fold. However, just 20 of these genes showed occupancy by Tup1-Cyc8. At these Tup1 activated genes, Tup1 was again predominantly found at gene promoter regions.

Together, these data highlight that Snf2 could only be detected at around 10% of the genes which were either up or down regulated in its absence. Conversely, Tup1 could be detected at around 30% and 12% of the genes up-regulated or down-regulated in the absence of Cyc8. This low correlation of the occupancy of Snf2 and Tup1 at genes whose transcription is altered in their absence could reflect either (i) that these complexes predominantly regulate genes indirectly, or (ii) that the efficiency of ChIP for these proteins is poor and that many sites of occupancy are not detected. The poor detection could be as a result of other chromatin factors occluding the epitope to which the ChIP antibodies are directed or could reflect the transient nature of the complexes binding at target sites. For example, Swi-Snf might only transiently bind to target sites to bring about the remodelling prior to or during transcription initiation, whilst Tup1-Cyc8 might be expected to persist at repressed sites. Indeed, this would correlate with the lower

occupancy of Swi-Snf found at genes altered in its absence compared to the higher percentage of genes repressed by Tup1-Cyc8 where Tup1 was found. Further studies will have to be performed to clarify the exact number of binding sites for the complexes in question.

The ultimate aim of this study was to identify the cohort of genes directly regulated by Tup1-Cyc8 as a repressor and Swi-Snf as an activator. For this analysis we utilised the published Snf2 and Tup1 occupancy data set in a strain where Tup1 could be conditionally depleted via the anchor away technique (Wong & Struhl, 2011). This meant that we could analyse Snf2 occupancy in the presence and absence of Tup1. We predicted that there might be two models for how these co-regulated genes would be governed by Tup1 and Snf2. In model one, we predicted that Tup1 would occupy the repressed gene, which would then be replaced by Snf2 when the gene was active following depletion of Tup1. In model 2, we predicted that both Tup1 and Snf2 might be present at the repressed gene with Snf2 remaining and either increasing in occupancy or activity in the absence of Tup1. 17 genes were found to obey model 1 where Snf2 was recruited to targeted genes when Tup1 was absent, (Fig. 6.24), including the *FLO5* gene (Table 6.11). Three genes were found to obey model 2 in which both Snf2 and Tup1 are already present at the repressed gene, after which Snf2 remains (Fig. 2.26). The *FLO9* gene was found to be an example of such a gene (Table 6.12).

The data revealed that for model 1 genes, Snf2 was recruited, on average, to within ~60 base-pairs of the site of initial Tup1 occupancy suggesting a possible occlusion of Swi-Snf occupancy by Tup1-Cyc8 at repressed genes (Fig. 6.10 and 6.25). For model two genes, Tup1 and Snf2 were found within 62, 2 and 110 base pairs of each other at the repressed gene, with Snf2 remaining within 20, 15 and 70 base pairs of its initial site of occupancy when Tup1 was absent. Thus, Snf2 and Tup1 occupancy sites largely overlapped at co-regulated genes.

From studies at the Swi-Snf and Tup1-Cyc8 regulated *SUC2* and *FLO1* genes, the data had shown that these genes resided in gene sparse sub telomeric regions and had extensive gene free upstream regions over which chromatin remodelling by these complexes was observed. This led to the hypothesis that all co-regulated genes might have similar extensive gene free regions which might contribute to the strong regulation

of transcription by Tup1-Cyc8 and Swi-Snf. Conceivably, larger upstream gene free regions might allow greater packaging of the promoter into a repressive state by Tup1-Cyc8 to give robust repression.

However, my analyses showed that, although the co-regulated genes were enriched in sub telomeric regions, there was no obvious relationship between the size of the gene free region and any influence upon transcription by Snf2 and Tup1 at target genes (Fig. 6.31). Nor was there any apparent influence on how far away Snf2 and Tup1 were located from the transcription start sites. Thus, although the co-regulated genes do reside in gene sparse sub telomeric regions, the availability of that region for potential remodelling does not seem to influence how tightly repressed the gene is by Tup1-Cyc8 or how highly activated that gene is by Swi-Snf.

8.6 Nucleosome mapping at Tup1-Cyc8 and Swi-Snf co-regulated genes:

I have identified which genes are subject to co-regulation by Swi-Snf and Tup1-Cyc8 and have shown at which of these genes the Tup1 and Snf2 proteins can be located. The final analyses was to determine how these complexes actually remodel the chromatin at target genes.

Initial analyses were to investigate the impact of Snf2 and Tup1 upon global chromatin structure. I first demonstrated that histone levels in the absence of Snf2 and Tup1 were not affected (Fig. 7.2), whilst MNase digestion of bulk chromatin did suggest that chromatin in a *cyc8* mutant was more sensitive to digestion than wt chromatin (Fig. 7.3). However, subsequent global nucleosome mapping analyses by Mnase-Seq revealed that this was not the case, and that global nucleosome structure around gene transcription start sites was similar whether Snf2 and Tup1 were present or not. This suggested that Swi-Snf and Tup1-Cyc8 do not have any impact on the global chromatin architecture in cells.

However, when nucleosome arrays found around genes in the *cyc8* and *snf2* mutants were normalised, aligned and compared to wt, major differences in nucleosome structure could be seen. Specifically, when the nucleosome arrays of the genes up regulated in a *cyc8* mutant were aligned, a dramatic loss in nucleosome positioning was apparent. This indicates that Tup1-Cyc8 was acting to stabilise strongly positioned nucleosomes around transcription start sites of target genes. Conversely, in the *snf2*

mutant chromatin, the nucleosome positions were even stronger than in wt at those genes subject to Swi-Snf activation. This suggests Swi-Snf does act to remodel nucleosomes at the promoters under its positive control.

The final analysis used the technique of digital Indirect end-labelling analysis to examine chromatin structure at specific genes in the *snf2*, *cyc8* and *snf2 cyc8* mutants to offer insight into how Tup1-Cyc8 and Swi-Snf regulate chromatin at these differently targeted co-regulated genes (N. Kent, unpublished protocol). In this case we examined chromatin structure at the *FLO5* gene as an example of a Model 1 co-regulated gene in which Snf2 is enriched after Tup1 loss, and *FLO9* as an example of a model 2 co-regulated gene where Snf2 and Tup1 are both present at the promoter prior to Tup1 loss and Snf2 retention.

At the model 1 *FLO5* gene when it is repressed, there was a strong series of peaks reflecting an ordered nucleosomal organisation across the entire 4.8 kb gene free upstream region. When Snf2 was absent, there was even more pronounced peaks across this region upstream of the repressed gene suggesting a role of Cyc8 in maintaining this strongly positioned nucleosome array to repress this gene. However, when the gene was fully de-repressed in the *cyc8* mutant, these strong peaks were almost obliterated across the entire upstream region indicating that the strongly positioned nucleosomes previously present were largely disrupted when the genes was active. Importantly, in the *snf2 cyc8* double mutants, the pattern of peaks across this extensive upstream region were reinstated to resemble the pattern seen in wt (Fig. 7.5), thus showing the nucleosome disruption seen in the *cyc8* mutant is Swi-Snf dependent A similar result was evident at the model 2 *FLO9* gene. These results were consistent with chromatin remodelling observed at the *FLO1* and *SUC2* genes by traditional indirect end labelling analysis (Fleming & Pennings, 2001; Fleming & Pennings, 2007; Gavin & Simpson, 1997).

Together these data showed that we can accurately map the nucleosome positions at all of the Swi-Snf and Tup1-Cyc8 co-regulated genes to determine precisely how these complexes are remodelling chromatin to elicit gene repression and activation. However, as time permitted only the analysis of two genes by dIEL, further analysis will have to be performed to fully elucidate exactly how Swi-Snf and Tup1-Cyc8 regulate target genes (Fleming & Pennings, 2001).

8.7 Conclusion:

The work in this study has brought an insight into how the Tup1-Cyc8 and Swi-Snf chromatin remodelling complexes antagonistically regulate target genes. I have identified all of the genes subject to Swi-Snf and Tup1-Cyc8 co-regulation and have mapped Snf2 and Tup1 at these genes where they reside predominantly in gene promoters. I have demonstrated that many of the co-regulated genes subject to co-regulation are located in the sub telomeric regions and that genes at these sites are subject to the most robust regulation by Swi-Snf and Tup1-Cyc8. I have shown that there are two modes of Tup1-Cyc8 and Swi-Snf action. In model 1, Snf2 is recruited to the site previously occupied by Tup1 to activate transcription, whereas in model 2, Tup1 and Snf2 are both present at the gene prior to activation which occurs following loss of Tup1 and retention and enrichment of Snf2. In both cases, Tup1 and Snf2 are closely located within an 11-50 bp window of each other at target gene promoters. Finally, I have analysed the impact of Tup1 and Snf2 upon chromatin at nucleosomal resolution. I have shown that Snf2 and Tup1 do not influence bulk chromatin structure but do have a profound effect on the chromatin structure of genes under their control. Specifically, Cyc8 acts to stabilise chromatin over promoter regions, whilst Snf2 acts to disrupt this chromatin. At the *FLO5* and *FLO9* genes, which are examples of model 1 and model 2 types of regulated gene, I have shown that extensive antagonistic remodelling of the chromatin occurs over the promoters and regions far upstream of the transcription start site. In summary I have (i) uncovered how many genes are subject to Swi-Snf and Tup1-Cyc8 co-regulation, (ii) identified the sites of occupancy of Tup1 and Snf2 at these target genes, and (iii) mapped their chromatin remodelling activities at nucleosome resolution at the co-regulated genes. This study has expanded on the repertoire of genes whose expression is subject to regulation by these complexes and provided valuable new insight into their mechanism of chromatin remodelling at these genes.

References

Abramova, N E, Cohen, B. D., Sertil, O., Kapoor, R., Davies, K. J., & Lowry, C. V. (2001). Regulatory mechanisms controlling expression of the *DAN*/*TIR* mannoprotein genes during anaerobic remodeling of the cell wall in *Saccharomyces cerevisiae*. *Genetics*, *157*(3), 1169–1177.

Aguilar-Uscanga, B., & Francois, J. M. (2003). A study of the yeast cell wall composition and structure in response to growth conditions and mode of cultivation. *Letters in Applied Microbiology*, *37*(3), 268–274.

Albers, E., Laizé, V., Blomberg, A., Hohmann, S., & Gustafsson, L. (2003). *Ser3p (Yer081wp) and Ser33p (Yil074cp) are phosphoglycerate dehydrogenases in Saccharomyces cerevisiae Downloaded from*. JBC Papers in Press.

Allfrey, V. G., Faulkner, R., & Mirsky, A. E. (1964). Acetylation and methylation of histones and their possible role in the regulation of RNA synthesis. *Proceedings of the National Academy of Sciences*, *51*(5), 786-794.

Andrews, A. J., & Luger, K. (2011). Nucleosome Structure(s) and Stability: Variations on a Theme. *Annual Review of Biophysics*, *40*(1), 99–117.

Barton, A. B., Su, Y., Lamb, J., Barber, D., & Kaback, D. B. (2003). A function for subtelomeric DNA in *Saccharomyces cerevisiae*. *Genetics*, *165*(2), 929–934.

Becker, D. M., & Lundblad, V. (2001). Introduction of DNA into Yeast Cells. In *Current Protocols in Molecular Biology* (pp. 13.7.1-13.7.10). Hoboken, NJ, USA: John Wiley & Sons, Inc.

Becker, P. B., & Hörz, W. (2002). ATP-Dependent Nucleosome Remodeling. *Annual Review of Biochemistry*, *71*(1), 247–273.

Becker, P. B., & Workman, J. L. (2013). Nucleosome remodeling and epigenetics. *Cold Spring Harbor Perspectives in Biology*, *5*(9), a017905.

Berger, S. L. (2001). An embarrassment of niches: the many covalent modifications of histones in transcriptional regulation. *Oncogene*, *20*(24), 3007–3013.

Bookout, A. L., Cummins, C. L., Mangelsdorf, D. J., Pesola, J. M., & Kramer, M. F. (2006). High-Throughput Real-Time Quantitative Reverse Transcription PCR. In *Current Protocols in Molecular Biology* (pp. 15.8.1-15.8.28). Hoboken, NJ, USA: John Wiley & Sons, Inc.

Bradbury, E. M. (2002). Chromatin structure and dynamics: state-of-the-art. *Molecular Cell*, *10*(1), 13–19.

Breitenbach-Schmitt, I., Heinisch, J., Schmitt, H. D., & Zimmermann, F. K. (1984). Yeast mutants without phosphofructokinase activity can still perform glycolysis and alcoholic fermentation. *MGG Molecular & General Genetics*, *195*(3), 530–535.

Brown, C. A., Murray, A. W., & Verstrepen, K. J. (2010). Rapid expansion and functional divergence of subtelomeric gene families in yeasts. *Current Biology : CB*, *20*(10), 895–903.

Cairns, B. R. (1998). Chromatin remodeling machines: similar motors, ulterior motives. *Trends in Biochemical Sciences*, *23*(1), 20–25.

Caro, L. H. P., Tettelin, H., Vossen, J. H., Ram, A. F. J., Van Den Ende, H., & Klis, F. M. (1997). In silicio identification of glycosyl-phosphatidylinositol-anchored plasma-membrane and cell wall proteins of*Saccharomyces cerevisiae*. *Yeast*, *13*(15), 1477–1489.

Chai, B., Huang, J., Cairns, B. R., & Laurent, B. C. (2005). Distinct roles for the RSC and Swi/Snf ATP-dependent chromatin remodelers in DNA double-strand break repair. *Genes & Development*, *19*(14), 1656–1661.

Chai, Bob, Huang, J., Cairns, B. R., & Laurent, B. C. (2005). Distinct roles for the RSC and Swi/Snf ATP-dependent chromatin remodelers in DNA double-strand break repair. *Genes & Development*, *19*(14), 1656–1661. https://doi.org/10.1101/gad.1273105

Chen, J. (2016). The cell-cycle arrest and apoptotic functions of p53 in tumor initiation and progression. *Cold Spring Harbor Perspectives in Medicine*, *6*(3).

Chen, K., Wilson, M. A., Hirsch, C., Watson, A., Liang, S., Lu, Y., … Dent, S. Y. R. (2013). Stabilization of the promoter nucleosomes in nucleosome-free regions by the yeast Cyc8-Tup1 corepressor. *Genome Research*, *23*(2), 312–322.

Chen, K., Wilson, M. A., Hirsch, C., Watson, A., Liang, S., Lu, Y., ... & Dent, S. Y. (2013). Stabilization of the promoter nucleosomes in nucleosome-free regions by the yeast Cyc8–Tup1 corepressor. *Genome research*, *23*(2), 312-322.

Chereji, R. V., Ocampo, J., & Clark, D. J. (2017). MNase-Sensitive Complexes in Yeast: Nucleosomes and Non-histone Barriers. *Molecular Cell*, *65*(3), 565-577.e3.

Cherry, J., Adler, C., Ball, C., Chervitz, S. A., Dwight, S. S., Hester, E. T., … Botstein, D. (1998). SGD: *Saccharomyces* Genome Database. *Nucleic Acids Research*, *26*(1), 73–79.

Church, M. C., & Fleming, A. B. (2018). A role for histone acetylation in regulating transcription elongation. *Transcription*, *9*(4), 225-232.

Church, M., Smith, K. C., Alhussain, M. M., Pennings, S., & Fleming, A. B. (2017). Sas3 and Ada2(Gcn5)-dependent histone H3 acetylation is required for transcription elongation at the de-repressed *FLO1* gene. *Nucleic Acids Research*, *72*(8), gkx028.

Clapier, C. R., & Cairns, B. R. (2009). The Biology of Chromatin Remodeling Complexes. *Annual Review of Biochemistry*, *78*(1), 273–304.

Clapier, C. R., Iwasa, J., Cairns, B. R., & Peterson, C. L. (2017). Mechanisms of action and regulation of ATP-dependent chromatin-remodelling complexes. *Nature Reviews Molecular Cell Biology*, *18*(7), 407–422.

Clark, D. J. (2010). Nucleosome positioning, nucleosome spacing and the nucleosome code. *Journal of Biomolecular Structure & Dynamics*, *27*(6), 781–793.

Cohn, M., Liti, G., & Barton, D. B. (2006). Telomeres in fungi. In *Comparative Genomics* (pp. 101-130). Springer, Berlin, Heidelberg.

Collart, M. A., & Oliviero, S. (2001). Preparation of Yeast RNA. In *Current Protocols in Molecular Biology* (Vol. Chapter 13, p. Unit13.12). Hoboken, NJ, USA: John Wiley & Sons, Inc.

Conlan, R. S., Gounalaki, N., Hatzis, P., & Tzamarias, D. (1999). The Tup1-Cyc8 Protein Complex Can Shift from a Transcriptional Co-repressor to a Transcriptional Co-activator. *Journal of Biological Chemistry*, *274*(1), 205–210.

Cooper, G.M. (2000). Chromosomes and Chromatin. The Cell: A Molecular Approach. 2nd edition. Sunderland (MA).

Curcio, M. J., Lutz, S., & Lesage, P. (2015). The Ty1 LTR-Retrotransposon of Budding Yeast, *Saccharomyces cerevisiae*. In *Mobile DNA III* (Vol. 3, pp. 927–964). American Society of Microbiology.

David, L., Huber, W., Granovskaia, M., Toedling, J., Palm, C. J., Bofkin, L., … Steinmetz, L. M. (2006). A high-resolution map of transcription in the yeast genome. *Proceedings of the National Academy of Sciences*, *103*(14), 5320–5325.

Deed, R. C., Fedrizzi, B., & Gardner, R. C. (2017). *Saccharomyces cerevisiae* FLO1 Gene Demonstrates Genetic Linkage to Increased Fermentation Rate at Low Temperatures. *G3 (Bethesda, Md.)*, *7*(3), 1039–1048.

Dever, T. E., Kinzy, T. G., & Pavitt, G. D. (2016). Mechanism and Regulation of Protein Synthesis in *Saccharomyces cerevisiae*. *Genetics*, *203*(1), 65–107.

Dunn, B., & Wobbe, C. R. (1993). Preparation of Protein Extracts from Yeast. *Current Protocols in Molecular Biology*, *23*(1), 13.13.1-13.13.9.

Dutta, A., Gogol, M., Kim, J.-H., Smolle, M., Venkatesh, S., Gilmore, J., … Workman, J. L. (2014). Swi/Snf dynamics on stress-responsive genes is governed by competitive bromodomain interactions. *Genes & Development*, *28*(20), 2314–2330.

Dutta, A., Sardiu, M., Gogol, M., Gilmore, J., Zhang, D., Florens, L., … Workman, J. L. (2017). Composition and Function of Mutant Swi/Snf Complexes. *Cell Reports*, *18*(9), 2124–2134.

English, C. M., Adkins, M. W., Carson, J. J., Churchill, M. E. A., & Tyler, J. K. (2006). Structural Basis for the Histone Chaperone Activity of Asf1. *Cell*, *127*(3), 495–508.

Fan, X., Lamarre-Vincent, N., Wang, Q., & Struhl, K. (2008). Extensive chromatin fragmentation improves enrichment of protein binding sites in chromatin immunoprecipitation experiments. *Nucleic Acids Research*, *36*(19), e125–e125.

Fleming, A B, & Pennings, S. (2001). Antagonistic remodelling by Swi-Snf and Tup1-Ssn6 of an extensive chromatin region forms the background for FLO1 gene regulation. *The EMBO Journal*, *20*(18), 5219–5231.

Fleming, Alastair B., Beggs, S., Church, M., Tsukihashi, Y., & Pennings, S. (2014). The yeast Cyc8–Tup1 complex cooperates with Hda1p and Rpd3p histone deacetylases to robustly repress transcription of the subtelomeric *FLO1* gene. *Biochimica et Biophysica Acta (BBA) - Gene Regulatory Mechanisms*, *1839*(11), 1242–1255.

Fleming, Alastair B, & Pennings, S. (2007). Tup1-Ssn6 and Swi-Snf remodelling activities influence long-range chromatin organization upstream of the yeast *SUC2* gene. *Nucleic Acids Research*, *35*(16), 5520–5531.

Fragiadakis, G. S., Tzamarias, D., & Alexandraki, D. (2004). Nhp6 facilitates Aft1 binding and Ssn6 recruitment, both essential for FRE2 transcriptional activation. *The EMBO Journal*, *23*(2), 333–342.

Galili, T. (2015). dendextend: An R package for visualizing, adjusting and comparing trees of hierarchical clustering. *Bioinformatics*, *31*(22), 3718–3720.

Galili, T., O'Callaghan, A., Sidi, J., & Sievert, C. (2018). heatmaply: An R package for creating interactive cluster heatmaps for online publishing. *Bioinformatics*, *34*(9), 1600–1602.

Gallagher, S., Winston, S. E., Fuller, S. A., & Hurrell (tank transfer systems; rev, J. G. R. (2008). Immunoblotting and Immunodetection. In *Current Protocols in Molecular Biology* (pp. 10.8.1-10.8.28). Hoboken, NJ, USA: John Wiley & Sons, Inc.

Gavin, I. M., & Simpson, R. T. (1997). Interplay of yeast global transcriptional regulators Ssn6p-Tup1p and Swi-Snf and their effect on chromatin structure. *The EMBO Journal*, *16*(20), 6263–6271.

Georgieva, M., Roguev, A., Balashev, K., Zlatanova, J., & Miloshev, G. (2012). Hho1p, the linker histone of *Saccharomyces cerevisiae*, is important for the proper chromatin organization in vivo. *Biochimica et Biophysica Acta*, *1819*(5), 366–374.

Georgieva, M., Staneva, D., Uzunova, K., Efremov, T., Balashev, K., Harata, M., & Miloshev, G. (2015). The linker histone in *Saccharomyces cerevisiae* interacts with actin-related protein 4 and both regulate chromatin structure and cellular morphology. *The International Journal of Biochemistry & Cell Biology*, *59*, 182–192.

Gounalaki, N., Tzamarias, D., & Vlassi, M. (2000). Identification of residues in the TPR domain of Ssn6 responsible for interaction with the Tup1 protein. *FEBS Letters*, *473*(1), 37–41.

Grewal, S. I. S., & Jia, S. (2007). Heterochromatin revisited. *Nature Reviews Genetics*, *8*(1), 35–46.

Gutiérrez, G., Millán-Zambrano, G., Medina, D. A., Jordán-Pla, A., Pérez-Ortín, J. E., Peñate, X., & Chávez, S. (2017). Subtracting the sequence bias from partially digested MNase-seq data reveals a general contribution of TFIIS to nucleosome positioning. *Epigenetics & Chromatin*, *10*(1), 58.

Hall, C., Brachat, S., & Dietrich, F. S. (2005). Contribution of horizontal gene transfer to the evolution of *Saccharomyces cerevisiae*. *Eukaryotic Cell*, *4*(6), 1102–1115.

Hall, C., & Dietrich, F. S. (2007). The reacquisition of biotin prototrophy in *Saccharomyces cerevisiae* involved horizontal gene transfer, gene duplication and gene clustering. *Genetics*, *177*(4), 2293–2307.

Hani, J., & Feldmann, H. (1998). tRNA genes and retroelements in the yeast genome. *Nucleic Acids Research*, *26*(3), 689.

Haruki, H., Nishikawa, J., & Laemmli, U. K. (2008). The Anchor-Away Technique: Rapid, Conditional Establishment of Yeast Mutant Phenotypes. *Molecular Cell*, *31*(6), 925–932.

Hazelwood, L. A., Daran, J.-M., van Maris, A. J. A., Pronk, J. T., & Dickinson, J. R. (2008). The Ehrlich pathway for fusel alcohol production: a century of research on *Saccharomyces cerevisiae* metabolism. *Applied and Environmental Microbiology*, *74*(8), 2259–2266.

Hellauer, K., Sirard, E., & Turcotte, B. (2001). Decreased Expression of Specific Genes in Yeast Cells Lacking Histone H1. *Journal of Biological Chemistry*, *276*(17), 13587–13592.

Hepp, M. I., Smolle, M., Gidi, C., Amigo, R., Valenzuela, N., Arriagada, A., … Gutiérrez, J. L. (2017). Role of Nhp6 and Hmo1 in SWI/SNF occupancy and nucleosome landscape at gene regulatory regions. *Biochimica et Biophysica Acta (BBA) - Gene Regulatory Mechanisms*, *1860*(3), 316–326.

Hewish, D. R., & Burgoyne, L. A. (1973). Chromatin sub-structure. The digestion of chromatin DNA at regularly spaced sites by a nuclear deoxyribonuclease. *Biochemical and Biophysical Research Communications*, *52*(2), 504–510.

Hocher, A., Ruault, M., Kaferle, P., Descrimes, M., Garnier, M., Morillon, A., & Taddei, A. (2018). Expanding heterochromatin reveals discrete subtelomeric domains delimited by chromatin landscape transitions. *Genome Research*, *28*(12), 1867–1881.

Hoffman, C. S., & Winston, F. (1987). *A ten-minute DNA preparation from yeast efficiently releases autonomous plasmids for transformaion of Escherichia coli*. *Gene* (Vol. 57).

Illumina. (2012). *TruSeq ChIP Sample Preparation Guide 15023092 B*.

Jiménez, G., Paroush, Z., & Ish-Horowicz, D. (1997). Groucho acts as a corepressor for a subset of negative regulators, including Hairy and Engrailed. *Genes & Development*, *11*(22), 3072–3082.

Johnston, M. (1987). A model fungal gene regulatory mechanism: the *GAL* genes of *Saccharomyces cerevisiae*. *Microbiological Reviews*, *51*(4), 458–476.

Keleher, C. A., Redd, M. J., Schultz, J., Carlson, M., & Johnson, A. D. (1992). Ssn6-Tup1 is a general repressor of transcription in yeast. *Cell*, *68*(4), 709–719.

Kent, N A, Bird, L. E., & Mellor, J. (1993). Chromatin analysis in yeast using NP-40 permeabilised sphaeroplasts. *Nucleic Acids Research*, *21*(19), 4653–4654.

Kent, N A, & Mellor, J. (1995). Chromatin structure snap-shots: rapid nuclease digestion of chromatin in yeast. *Nucleic Acids Research*, *23*(18), 3786–3787.

Kent, Nicholas A, Adams, S., Moorhouse, A., & Paszkiewicz, K. (2011). Chromatin particle spectrum analysis: a method for comparative chromatin structure analysis using paired-end mode next-generation DNA sequencing. *Nucleic Acids Research*, *39*(5), e26.

Kidder, B. L., Hu, G., & Zhao, K. (2011). ChIP-Seq: technical considerations for obtaining high-quality data. *Nature Immunology*, *12*(10), 918–922.

Kim, J.-H., Saraf, A., Florens, L., Washburn, M., & Workman, J. L. (2010). Gcn5 regulates the dissociation of SWI/SNF from chromatin by acetylation of Swi2/Snf2. *Genes & Development*, *24*(24), 2766–2771.

Kingston, R. E., & Narlikar, G. J. (1999). ATP-dependent remodeling and acetylation as regulators of chromatin fluidity. *Genes & Development*, *13*(18), 2339–2352.

Koç, A., Wheeler, L. J., Mathews, C. K., & Merrill, G. F. (2004). Hydroxyurea arrests DNA replication by a mechanism that preserves basal dNTP pools. *The Journal of Biological Chemistry*, *279*(1), 223–230.

Köhler, A., & Hurt, E. (2007). Exporting RNA from the nucleus to the cytoplasm. *Nature Reviews Molecular Cell Biology*.

Korber, P., & Hörz, W. (2004). *In Vitro* Assembly of the Characteristic Chromatin Organization at the Yeast *PHO5* Promoter by a Replication-independent Extract System. *Journal of Biological Chemistry*, *279*(33), 35113–35120.

Kornberg, R. D. (1974). Chromatin structure: a repeating unit of histones and DNA. *Science (New York, N.Y.)*, *184*(4139), 868–871.

Kouzarides, T. (2007). Chromatin Modifications and Their Function. *Cell*, *128*(4), 693–705.

Kuranda, K., Leberre, V., Sokol, S., Palamarczyk, G., & Francois, J. (2006). Investigating the caffeine effects in the yeast *Saccharomyces cerevisiae* brings new insights into the connection between TOR, PKC and Ras/cAMP signalling pathways. *Molecular Microbiology*, *61*(5), 1147–1166.

Lahtvee, P.-J., Kumar, R., Hallström, B. M., & Nielsen, J. (2016). Adaptation to different types of stress converge on mitochondrial metabolism. *Molecular Biology of the Cell*, *27*(15), 2505–2514.

Laurent, B. C., Treich, I., & Carlson, M. (1993). The yeast SNF2/SWI2 protein has DNA-stimulated ATPase activity required for transcriptional activation. *Genes & Development*, *7*(4), 583–591.

Lee, K. K., & Workman, J. L. (2007). Histone acetyltransferase complexes: one size doesn't fit all. *Nature Reviews Molecular Cell Biology*, *8*(4), 284–295.

León-Medina, P. M. De, Elizondo-González, R., Damas-Buenrostro, L. C., Geertman, J.-M., Broek, M. Van den, Galán-Wong, L. J., … Pereyra-Alférez, B. (2016). Genome annotation of a Saccharomyces sp. lager brewer's yeast. *Genomics Data*, *9*, 25.

Levin, D. E. (2005). Cell wall integrity signaling in *Saccharomyces cerevisiae*. *Microbiology and Molecular Biology Reviews: MMBR*, *69*(2), 262–291.

Li, B., Carey, M., & Workman, J. L. (2007). The Role of Chromatin during Transcription. *Cell*, *128*(4), 707–719.

Li, H. (2013). *Aligning sequence reads, clone sequences and assembly contigs with BWA-MEM*.

Li, L., Miles, S., Melville, Z., Prasad, A., Bradley, G., & Breeden, L. L. (2013). Key events during the transition from rapid growth to quiescence in budding yeast require posttranscriptional regulators. *Molecular Biology of the Cell*, *24*(23), 3697.

Liu, H., Styles, C. A., & Fink, G. R. (1996). *Saccharomyces cerevisiae* S288C has a mutation in *FLO8*, a gene required for filamentous growth. *Genetics*, *144*(3), 967–978.

Liu, Z., & Karmarkar, V. (2008). Groucho/Tup1 family co-repressors in plant development. *Trends in Plant Science*, *13*(3), 137–144.

Lohr, D. (1997). Nucleosome Transactions on the Promoters of the Yeast *GAL* and *PHO* Genes. *Journal of Biological Chemistry*, *272*(43), 26795–26798.

Louis, E. J., Becker, M. M. (2014). *Subtelomeres*. Springer.

Lu, C., David Allis, C., & Genet Author manuscript, N. (2017). SWI/SNF Complex in Cancer: "Remodeling" Mechanisms Uncovered HHS Public Access Author manuscript, *49*(2), 178–179.

Lundin, C., North, M., Erixon, K., Walters, K., Jenssen, D., Goldman, A. S. H., & Helleday, T. (2005). Methyl methanesulfonate (MMS) produces heat-labile DNA damage but no detectable in vivo DNA double-strand breaks. *Nucleic Acids Research*, *33*(12), 3799–3811.

Luo, J., Sun, X., Cormack, B. P., & Boeke, J. D. (2018). Karyotype engineering by chromosome fusion leads to reproductive isolation in yeast. *Nature*, *560*(7718), 392–396.

Luo, Z., & van Vuuren, H. J. J. (2009). Functional analyses of *PAU* genes in *Saccharomyces cerevisiae*. *Microbiology*, *155*(12), 4036–4049.

Malave, T. M., & Dent, S. Y. (2006). Transcriptional repression by Tup1–Ssn6. *Biochemistry and cell biology*, *84*(4), 437-443.

Martens, J. A., & Winston, F. (2002). Evidence that Swi/Snf directly represses transcription in *S. cerevisiae*. *Genes & Development*, *16*(17), 2231–2236.

Mefford, H. C., & Trask, B. J. (2002). The complex structure and dynamic evolution of human subtelomeres. *Nature Reviews Genetics*.

Mell, J. C., & Burgess, S. M. (2001). Yeast as a model genetic organism. *e LS*.

Metsalu, T., & Vilo, J. (2015). ClustVis: a web tool for visualizing clustering of multivariate data using Principal Component Analysis and heatmap. *Nucleic Acids Research*, *43*(W1), W566–W570.

Mi, H., Huang, X., Muruganujan, A., Tang, H., Mills, C., Kang, D., & Thomas, P. D. (2017). PANTHER version 11: expanded annotation data from Gene Ontology and Reactome pathways, and data analysis tool enhancements. *Nucleic Acids Research*, *45*(D1), D183–D189.

Miles, S., Li, L., Davison, J., & Breeden, L. L. (2013). Xbp1 directs global repression of budding yeast transcription during the transition to quiescence and is important for the longevity and reversibility of the quiescent state. *PLoS Genetics*, *9*(10), e1003854.

Mitra, D., Parnell, E. J., Landon, J. W., Yu, Y., & Stillman, D. J. (2006). SWI/SNF Binding to the *HO* Promoter Requires Histone Acetylation and Stimulates TATA-Binding Protein Recruitment. *Molecular and Cellular Biology*, *26*(11), 4095–4110.

Mohrmann, L., & Verrijzer, C. P. (2005). Composition and functional specificity of SWI2/SNF2 class chromatin remodeling complexes. *Biochimica et Biophysica Acta (BBA) - Gene Structure and Expression*, *1681*(2–3), 59–73.

Monahan, B. J., Villén, J., Marguerat, S., Bähler, J., Gygi, S. P., & Winston, F. (2008). Fission yeast SWI/SNF and RSC complexes show compositional and functional differences from budding yeast. *Nature Structural & Molecular Biology*, *15*(8), 873–880.

Morgan, M. A., & Shilatifard, A. (2015). Chromatin signatures of cancer. *Genes & Development*, *29*(3), 238–249.

Muchardt, C., & Yaniv, M. (1999). ATP-dependent chromatin remodelling: SWI/SNF and Co. are on the job. *Journal of Molecular Biology*, *293*(2), 187–198.

Mukai, Y., Matsuo, E., Roth, S. Y., & Harashima, S. (1999). Conservation of histone binding and transcriptional repressor functions in a *Schizosaccharomyces pombe* Tup1p homolog. *Molecular and Cellular Biology*, *19*(12), 8461–8468.

Narlikar, G. J., Fan, H.-Y., & Kingston, R. E. (2002). Cooperation between complexes that regulate chromatin structure and transcription. *Cell*, *108*(4), 475–487.

Nechaev, S., & Adelman, K. (2011). Pol II waiting in the starting gates: Regulating the transition from transcription initiation into productive elongation. *Biochimica et Biophysica Acta (BBA) - Gene Regulatory Mechanisms*, *1809*(1), 34–45.

Neigeborn, L., & Carlson, M. (1984). Genes affecting the regulation of *SUC2* gene expression by glucose repression in *Saccharomyces cerevisiae*. *Genetics*, *108*(4), 845–858.

Neuaia, P., & Oliver Laiipes, A. J. (1968). *Comparative Study of the Properties of the Purified Internal and External Invertases from Yeast*. *Journal of Biological Chemistry*, *243*(7), 1573-1577.

Noll, M. (1974). Subunit structure of chromatin. *Nature*, *251*(5472), 249–251.

Oezcan, S. A. B. I. R. E., VALLIER, L. G., FLICK, J. S., CARLSON, M., & JOHNSTON, M. (1997). Expression of the *SUC2* gene of Saccharomyces cerevisiae is induced by low levels of glucose. *Yeast*, *13*(2), 127-137.

Olins, A. L., & Olins, D. E. (1974). Spheroid chromatin units (v bodies). *Science (New York, N.Y.)*, *183*(4122), 330–332.

Ozcan, S., & Johnston, M. (1995). Three different regulatory mechanisms enable yeast hexose transporter (*HXT*) genes to be induced by different levels of glucose. *Molecular and Cellular Biology*, *15*(3), 1564–1572.

Ozcan, S., Vallier, L. G., Flick, J. S., Carlson, M., & Johnston, M. (1997). Expression of the *SUC2* gene of *Saccharomyces cerevisiae* is induced by low levels of glucose. *Yeast (Chichester, England)*, *13*(2), 127–137.

Parnell, E. J., & Stillman, D. J. (2011). Shields up: the Tup1-Cyc8 repressor complex blocks coactivator recruitment. *Genes & Development*, *25*(23), 2429–2435.

Pathan, E. K., Ghormade, V., & Deshpande, M. V. (2017). Selection of reference genes for quantitative real-time RT-PCR assays in different morphological forms of dimorphic zygomycetous fungus Benjaminiella poitrasii. *PLoS ONE*, *12*(6), e0179454.

Pathan, M., Keerthikumar, S., Ang, C.-S., Gangoda, L., Quek, C. Y. J., Williamson, N. A., … Mathivanan, S. (2015). FunRich: An open access standalone functional enrichment and interaction network analysis tool. *PROTEOMICS*, *15*(15), 2597–2601.

Payankaulam, S., Li, L. M., & Arnosti, D. N. (2010). Transcriptional repression: conserved and evolved features. *Current Biology : CB*, *20*(17), R764-71.

Peterson, C. L., Dingwall, A., & Scott, M. P. (1994). Five SWI/SNF gene products are components of a large multisubunit complex required for transcriptional enhancement. *Proceedings of the National Academy of Sciences of the United States of America*, *91*(8),

Pinon, V., Ravanel, S., Douce, R., & Alban, C. (2005). Biotin synthesis in plants. The first committed step of the pathway is catalyzed by a cytosolic 7-keto-8-aminopelargonic acid synthase. *Plant Physiology*, *139*(4), 1666–1676.

Purohit, J. S., & Chaturvedi, M. M. (2017). Chromatin and Aging. In *Topics in Biomedical Gerontology* (pp. 205–241). Singapore: Springer Singapore.

Rando, O. J., & Winston, F. (2012). Chromatin and Transcription in Yeast. *Genetics*, *190*(2).

Reid, J. L., Iyer, V. R., Brown, P. O., & Struhl, K. (2000). Coordinate Regulation of Yeast Ribosomal Protein Genes Is Associated with Targeted Recruitment of Esa1 Histone Acetylase. *Molecular Cell*, *6*(6), 1297–1307.

Reinke, H., Gregory, P. D., & Hörz, W. (2001). A Transient Histone Hyperacetylation Signal Marks Nucleosomes for Remodeling at the *PHO8* Promoter In Vivo. *Molecular Cell*, *7*(3), 529–538.

Rizzo, J. M., Mieczkowski, P. A., & Buck, M. J. (2011). Tup1 stabilizes promoter nucleosome positioning and occupancy at transcriptionally plastic genes. *Nucleic Acids Research*, *39*(20), 8803–8819.

Roberts, C. W. M., & Orkin, S. H. (2004). The SWI/SNF complex — chromatin and cancer. *Nature Reviews Cancer*, *4*(2), 133–142.

Sekinger, E. A., Moqtaderi, Z., & Struhl, K. (2005). Intrinsic Histone-DNA Interactions and Low Nucleosome Density Are Important for Preferential Accessibility of Promoter Regions in Yeast. *Molecular Cell*, *18*(6), 735–748.

Sellick, C. A., Campbell, R. N., & Reece, R. J. (2008). Chapter 3 Galactose Metabolism in Yeast-Structure and Regulation of the Leloir Pathway Enzymes and the Genes Encoding Them. *International Review of Cell and Molecular Biology*.

Sen, P., Vivas, P., Dechassa, M. L., Mooney, A. M., Poirier, M. G., & Bartholomew, B. (2013). The SnAC Domain of SWI/SNF Is a Histone Anchor Required for Remodeling. *Molecular and Cellular Biology*, *33*(2), 360–370.

Sen, Payel, Luo, J., Hada, A., Hailu, S. G., Dechassa, M. L., Persinger, J., … Bartholomew, B. (2017). Loss of Snf5 Induces Formation of an Aberrant SWI/SNF Complex. *Cell Reports*, *18*(9), 2135–2147.

Sertil, O., Kapoor, R., Cohen, B. D., Abramova, N., & Lowry, C. V. (2003). Synergistic repression of anaerobic genes by Mot3 and Rox1 in *Saccharomyces cerevisiae*. *Nucleic Acids Research*, *31*(20), 5831–5837.

Sertil, Odeniel, Vemula, A., Salmon, S. L., Morse, R. H., & Lowry, C. V. (2007). Direct role for the Rpd3 complex in transcriptional induction of the anaerobic *DAN*/*TIR* genes in yeast. *Molecular and Cellular Biology*, *27*(6), 2037–2047.

Sewack, G. F., Ellis, T. W., & Hansen, U. (2001). Binding of TATA Binding Protein to a Naturally Positioned Nucleosome Is Facilitated by Histone Acetylation. *Molecular and Cellular Biology*, *21*(4), 1404–1415.

Shilatifard, A. (2006). Chromatin Modifications by Methylation and Ubiquitination: Implications in the Regulation of Gene Expression. *Annual Review of Biochemistry*, *75*(1), 243–269.

Shivaswamy, S., & Iyer, V. R. (2008). Stress-dependent dynamics of global chromatin remodeling in yeast: dual role for SWI/SNF in the heat shock stress response. *Molecular and Cellular Biology*, *28*(7), 2221–2234.

Smith, R. L., & Johnson, A. D. (2000). Turning genes off by Ssn6–Tup1: a conserved system of transcriptional repression in eukaryotes. *Trends in Biochemical Sciences*, *25*(7), 325–330.

Smolle, M., & Workman, J. L. (2013). Transcription-associated histone modifications and cryptic transcription. *Biochimica et Biophysica Acta (BBA) - Gene Regulatory Mechanisms*, *1829*(1), 84–97. https://doi.org/10.1016/J.BBAGRM.2012.08.008

Soares, E. V. (2011). Flocculation in *Saccharomyces cerevisiae*: a review. *Journal of Applied Microbiology*, *110*(1), 1–18.

Stewart, G. G. (2009). The Horace Brown Medal Lecture: Forty Years of Brewing Research. *Journal of the Institute of Brewing*, *115*(1), 3–29.

Stillman, D. J. (2010). Nhp6: A small but powerful effector of chromatin structure in *Saccharomyces cerevisiae*. *Biochimica et Biophysica Acta (BBA) - Gene Regulatory Mechanisms*, *1799*(1), 175–180.

Sudarsanam, P., Iyer, V. R., Brown, P. O., & Winston, F. (2000). Whole-genome expression analysis of snf/swi mutants of *Saccharomyces cerevisiae*. *Proceedings of the National Academy of Sciences*, *97*(7), 3364–3369.

Sudarsanam, P., & Winston, F. (2000). The Swi/Snf family nucleosome-remodeling complexes and transcriptional control. *Trends in Genetics: TIG*, *16*(8), 345–351.

Szerlong, H., Saha, A., & Cairns, B. R. (2003). The nuclear actin-related proteins Arp7 and Arp9: a dimeric module that cooperates with architectural proteins for chromatin remodeling. *The EMBO Journal*, *22*(12), 3175–3187.

Szymanski, E. P., & Kerscher, O. (2013). Budding yeast protein extraction and purification for the study of function, interactions, and post-translational modifications. *Journal of Visualized Experiments: JoVE*, (80), e50921.

Tanaka, N., & Mukai, Y. (2015). Yeast Cyc8p and Tup1p proteins function as coactivators for transcription of Stp1/2p-dependent amino acid transporter genes. *Biochemical and Biophysical Research Communications*, *468*(1–2), 32–38.

Tashiro, S., Nishihara, Y., Kugou, K., Ohta, K., & Kanoh, J. (2017). NAR Breakthrough Article Subtelomeres constitute a safeguard for gene expression and chromosome homeostasis. *Nucleic Acids Research*, *45*(18), 10333–10349.

Taussig, R., & Carlson, M. (1983). Nucleotide sequence of the yeast *SUC2* gene for invertase. *Nucleic Acids Research*, *11*(6), 1943–1954.

Teunissen, A. W., & Steensma, H. Y. (1995). Review: the dominant flocculation genes of *Saccharomyces cerevisiae* constitute a new subtelomeric gene family. *Yeast (Chichester, England)*, *11*(11), 1001–1013.

Thoma, F., Koller, T., & Klug, A. (1979). Involvement of histone H1 in the organization of the nucleosome and of the salt-dependent superstructures of chromatin. *The Journal of Cell Biology*, *83*(2).

Treitel, M. A., & Carlson, M. (1995). Repression by SSN6-TUP1 is directed by MIG1, a repressor/activator protein. *Proceedings of the National Academy of Sciences of the United States of America*, *92*(8), 3132–3136.

Turner, B. M. (2001). *Chromatin and gene regulation: molecular mechanisms in epigenetics* (pp. 1–284). John Wiley & Sons.

Van Mulders, S. E., Christianen, E., Saerens, S. M. G., Daenen, L., Verbelen, P. J., Willaert, R., … Delvaux, F. R. (2009). Phenotypic diversity of Flo protein family-mediated adhesion in *Saccharomyces cerevisiae*. *FEMS Yeast Research*, *9*(2), 178–190.

Varanasi, U. S., Klis, M., Mikesell, P. B., & Trumbly, R. J. (1996). The Cyc8 (Ssn6)-Tup1 corepressor complex is composed of one Cyc8 and four Tup1 subunits. *Molecular and Cellular Biology*, *16*(12), 6707–6714. https://doi.org/10.1128/MCB.16.12.6707

Von der Haar, T. (2008). A quantitative estimation of the global translational activity in logarithmically growing yeast cells. *BMC Systems Biology*, *2*, 87.

Wang, W., Xue, Y., Zhou, S., Kuo, A., Cairns, B. R., & Crabtree, G. R. (1996). Diversity and specialization of mammalian SWI/SNF complexes. *Genes & Development*, *10*(17), 2117–2130.

Wickham, H. (2016). *ggplot2: elegant graphics for data analysis*. Springer.

Winston, F., & Carlson, M. (1992). Yeast SNF/SWI transcriptional activators and the SPT/SIN chromatin connection. *Trends in Genetics: TIG*, *8*(11), 387–391.

Wolf, J. B. W. (2013). P R I M E R Principles of transcriptome analysis and gene expression quantification: an RNA-seq tutorial.

Wong, K. H., & Struhl, K. (2011). The Cyc8-Tup1 complex inhibits transcription primarily by masking the activation domain of the recruiting protein. *Genes & Development*, *25*(23), 2525–2539.

Wu, H., Ito, K., & Shimoi, H. (2005). Identification and Characterization of a Novel Biotin Biosynthesis Gene in *Saccharomyces cerevisiae*. *Applied and Environmental Microbiology*, *71*(11), 6845.

Xi, Y., Yao, J., Chen, R., Li, W., & He, X. (2011). Nucleosome fragility reveals novel functional states of chromatin and poises genes for activation. *Genome Research*, *21*(5), 718–724.

Yen, K., Vinayachandran, V., Batta, K., Koerber, R. T., & Pugh, B. F. (2012). Genome-wide Nucleosome Specificity and Directionality of Chromatin Remodelers. *Cell*, *149*(7), 1461–1473.

Zempleni, J., Wijeratne, S. S. K., & Hassan, Y. I. (2009). Biotin. *BioFactors (Oxford, England)*, *35*(1), 36–46.

Zhang, Z., & Reese, J. C. (2005). Molecular Genetic Analysis of the Yeast Repressor Rfx1/Crt1 Reveals a Novel Two-Step Regulatory Mechanism. *Molecular and Cellular Biology*, *25*(17), 7399–7411.